MOLECULAR IMAGING AGENTS FOR UROKINASE PLASMINOGEN ACTIVATOR

THE SYNTHESIS AND EVALUATION OF SMALL MOLECULE INHIBITORS AS MOLECULAR IMAGING AGENTS FOR UROKINASE PLASMINOGEN ACTIVATOR

By

SILVIA A. ALBU, M.Sc.

A Thesis
Submitted to the School of Graduate Studies
in Partial Fulfillment of the Requirements for the Degree
Doctor of Philosophy

McMaster University

DOCTOR OF PHILOSOPHY (2014)
(Chemical Biology)

McMaster University
Hamilton, Ontario

TITLE: The Synthesis and Evaluation of Small Molecule Inhibitors as Molecular Imaging Agents for Urokinase Plasminogen Activator

AUTHOR: Silvia A. Albu
M.Sc. (Coventry University, UK)

SUPERVISORS: Professor John F. Valliant
Professor Alfredo Capretta

NUMBER OF PAGES: xvi, 218, cvii

Abstract

Urokinase-type plasminogen activator (uPA) protein is a serine protease of the trypsin family that is overexpressed by tumors cells seeking to metastasize. Molecular imaging methods using molecular imaging probe designed to target uPA could provide a method for the detection of aggressive cancers and monitoring response to treatment. Four classes of high affinity uPA inhibitors, three which were reversible and one irreversible, were used as platforms to develop radiolabeled probes for uPA. Based on structure-activity relationships, lead compounds were modified to allow for the introduction of a radiohalogen (radioiodine) at different sites in the corresponding molecules. Suitable synthetic strategies were developed to create libraries of iodinated phenyl guanidine, peptide, naphtamidine and phosphonate derivatives. For the phenylguanidines colorimetric assays showed the product had micromolar affinity while for the peptide derivatives low nanomolar affinity for the iodinated analogue was observed (1.4 nM to 2.53 nM). Unfortunately quantitative biodistribution studies showed low tumour uptake (<0.5% ID/g). More promising results were obtained for the irreversible iodinated phosphonated derivative which had an affinity of 2.1 nM. This reagent showed 1.95% ID/g tumour uptake and lower blood uptake *in vivo* which demonstrates advantageous properties over existing uPA probes in terms of tumour-to-blood ratios.

A complementary development was also achieved in that the first example of a ^{125}I-labelled tetrazine was prepared. This new reagent can be used in pre-targeted strategies that utilize bioorthogonal coupling between stained trans-cyclooctene (TCO)

and tetrazines. The product was prepared using a concomitant oxidation iodo-destannylation reaction and the product isolated in 80% radiochemical yield. The reaction with transcycloctene proceeded rapidly to produce various isomers which were fully characterized through NMR analysis of the non-radioactive analogues.

Acknowledgments

I would like to sincerely thank my supervisors Dr. John Valliant and Dr. Fred Capretta for their guidance and support throughout the course of my Ph.D. Upon my first arrival to Canada, Dr. Capretta was one of the first people I met. He offered me a position in his lab and provided me with immense support. Dr. Valliant nourished my love for research by teaching me to design new experiments and providing me with the means to accomplish them. I am deeply thankful for their valuable insight, encouragement and guidance into my research.

I would also like to extend my thanks to Emelia Awuah, Salma Al-Karmi and Patricia Edem, all of which supported me and entertained good scientific discussions. Having spent a great amount of time with them during my Ph.D, I have developed valuable friendships that I am sure will persist for future years to come. Additionally, I would like to thank Dr. Kirk Green for technical advice and being very helpful in providing me with related analytical advice on my project.

Last but not least, I would like to thank my family. My husband Mihai and my son Gabriel must be thanked for their encouraging words and emotional support. I cannot thank you enough.

TABLE OF CONTENTS

LIST OF FIGURES

LIST OF SCHEMES

LIST OF TABLES

List of Abbreviations

A	
Ac_2O	Acetic anhydride
AcOH	Acetic acid
ACN	Acetonitrile
ATF	Amino-terminal fragment
B	
B/F	Bound-to-free ratio
B_{max}	Binding site concentration
BM	Basement membrane
Boc	*Tert*-butyloxycarbonyl
Boc_2O	Di-*tert*-butyl dicarbonate
Bq	Becquerel
C	
Cbz	Benzyloxycarbonyl
CD-loop	Connecting helices C and D
Ci	Curie
CI	Chemical ionization
CT	Computed tomography
Cy	Cyanine
D	
DBDMH	1,3–dibromo-5,5-dimethylhydantoin
DCC	*N*,*N*′-Dicyclohexylcarbodiimide
DCM	Dichloromethane
DIPEA	*N*,*N*-Diisopropylethylamine
DMF	*N*,*N*-Dimethylformamide
DMSO	Dimethyl sulfoxide
DNA	Deoxyribonucleic acid
DOTA	1,4,7,10-tetraazacyclododecane-*N*,*N*′,*N*″,*N*‴-tetraacetic acid
DTPA	Diethylentriamene pentaacetatic acid
E	
ECM	Extracellular matrix
EDC	N-(3-Dimethylaminopropyl)-N′-ethylcarbodiimide hydrochloride
ELISA	Enzyme-linked immunosorbent assay
ES	Electrospray
ESA	Effective specific activity
EtOAc	Ethyl acetate
F	
^{18}F-FAZA	^{18}F-fluoroazomycin arabinoside
^{18}F-FDG	^{18}F-fluorodeoxyglucose
^{18}F-FLT	^{18}F-3-fluoro-3-deoxy-thymidine

^{18}F-FMIZO	^{18}F-fluoromisonidazole
Fmoc	Fluorenylmethyloxycarbonyl
FRET	Fluorescence energy transfer mechanism.
fXa	Factor Xa
G	
GFD	Growth factor–like sub-domain
H	
HATU	1-[Bis(dimethylamino)methylene]-1H-1,2,3-triazolo[4,5-b]pyridinium 3-oxid hexafluorophosphate)
HOBt	Hydroxybenzotriazole
HPLC	High-performance liquid chromatography
I	
IC_{50}	Concentration of an inhibitor where the response (or binding) is reduced by half
%ID/g	Percent injected dose per gram of tissue
IO	Iron oxide
K	
K_a	Association constant
K_d	Dissociation constant
K_i	Inhibition constant
L	
LC-MS	Liquid chromatography–mass spectrometry
LiHMDS	Lithium bis(trimethylsilyl)amide
M	
MeOD	Deuterated methanol
MeOH	Methanol
MIBG	*Meta*-iodobenzyl-guanidine
MI	Molecular imaging
MMPs	Matrix metalloproteinases
MRI	Magnetic resonance imaging
N	
N	Avogadro's number
NIR	Near infrared
NMP	*N*-Methyl-2-pyrrolidone
NMR	Nuclear magnetic resonance
P	
p.i.	Post injection
PA	1,3,5,7-tetramethyl-2,4,8-trioxa-(2,4-dimethoxyphenyl)-6-phosphaadamantane
PAI	Plasminogen activator inhibitors
PA-Ph	1,3,5,7-Tetramethyl-2,4,8-trioxa-6-phenyl-6-phospha-adamantane

PBS	Phosphate buffered saline
PEG	Polyethylene glycol
PET	Positron emission tomography
PyBop	Benzotriazol-1-yloxy)tripyrrolidinophosphonium hexafluorophosphate
R	
RECIST	Response evaluation criteria in solid tumors
S	
S-2444	Pyro-Glu-Gly-Arg-*p*-nitroanilide
SA	Specific radioactivity
SAAC	Single amino-acid chelate
SCID	Severe combined immunodeficiency
siRNA	Small interfering ribonucleic acid
SPE	Solid-phase extraction
SPECT	Single photon emission computed tomography
SPhos	2-Dicyclohexylphosphino-2′,6′-dimethoxybiphenyl
T	
T/NT	Target-to-non-target ratio
$t_{1/2}$	Half-life of the radionuclide
TBTU	*O*-(Benzotriazol-1-yl)-*N,N,N′,N′*-tetramethyluronium Tetrafluoroborate
TCO	*Trans*-cyclooctenes
Tf_2O	Triflic anhydride
THF	*Tetrahydrofuran*
TFA	Trifluoroacetic acid
TFAA	Trifluoroacetic anhydride
TIMP2	Tissue inhibitor of metalloproteinases
TLC	Thin layer chromatography
TMS	Trimethylsilyl
tPA	Tissue-type plasminogen activator
U	
uPA	Urokinase plasminogen activator
uPAR	Urokinase plasminogen activator receptor
US	Ultrasound
W	
W	Atomic mass
X	
XPhos	2-Dicyclohexylphosphino-2′,4′,6′-triisopropylbiphenyl

Chapter 1 – Introduction

1.1. Molecular Imaging

Molecular imaging[1] (MI) methods have revolutionized the way clinicians and researchers visualize biochemical processes and targets. MI has the capacity to provide anatomical information (visualization of internal structures) as well as functional data (quantification of physiological and pathological processes).[2,3] Among the most commonly used imaging techniques in the clinic are ultrasound (US) imaging, computed tomography (CT) and magnetic resonance imaging (MRI). While for MI, the dominant methods are optical and nuclear imaging.

US applies high frequency sound waves to generate an image via a pulse echo effect.[2,4] It is a low cost technique routinely used in hospitals and provides a resolution of 1-2 mm at depths of penetration longer than a few centimeters. CT employs ionising radiation (X-rays) that is attenuated differently depending on the density and the composition of the tissue, allowing for contrast between anatomical features.[2,4] The technique shows a spatial resolution of 0.5 - 1 mm in clinical applications. MRI is based on the signals observed from protons in different environments.[5] The concentration of water protons and biological molecules (such as proteins, lipids, etc.) will vary in different tissues. When a radio wave frequency is applied, the magnetic vector returns to its resting state over the T1 (longitudinal) relaxation time while the axial spin to returns to equilibrium over the T2 (transverse) relaxation time. Different relaxation times correspond to different tissues which are used to create the MRI image.[5] While MRI generates images with spatial resolution of 25 - 100 μM,[1] targeted MRI contrast agents

are used in high concentration therefore raising toxicity concerns and limiting the types of physiological processes and targets that can be monitored.

Optical imaging techniques are based on photon absorption and scattering differences in various tissues. They offer high sensitivity of signal detection and short imaging times, but they have low tissue penetration, which limits their use for whole body clinical imaging.[6] In contrast, nuclear imaging methods such as positron emission tomography (PET) or single photon emission computed tomography (SPECT) allow for the detection of nano to femto-molar concentrations of radiotracers without issues relating to depth of penetration and without perturbing the biological pathways being studied. These techniques form the basis for the present thesis and are described in greater detail below.

1.2. SPECT

SPECT uses rotating gamma cameras that contain an appropriate type of detector to acquire signals from gamma emitting radionuclides.[7] Emission are collimated in a lead block containing 30000-60000 small holes with a diameter of 0.8-1.5 mm allowing for localization of the decay events and only photons orthogonal to the crystal face to hit the detector. Rotating cameras are used to generate 3D images.[8]

The gamma emitting radionuclides that are most widely used in SPECT are technetium-99m, iodine-123, indium-111, and iodine-131.[6] Gamma ray energy emitted from the radionuclide employed should be of a sufficient energy so as to emerge from the body and be detected by the camera, but low enough to not affect the resolution of the images and minimize the dose to the patient.[8]

1.3. PET

PET cameras detect pairs of gamma rays emitted indirectly by positron-emitting radionuclides using a ring of detectors surrounding the patient. After the initial decay, the emitted positrons undergoes an annihilation process with electrons, which results in the formation of two photons with high energy (511 keV) oriented at approximately 180° from each other.[9] In PET, these photons are detected as a coincident (simultaneous) event, and their source is localized and reconstructed as a cross-sectional image. Since the positrons emitted from the nucleus must loose their kinetic energy before annihilation, the resolution of PET instrument is approximately 3-5 mm.[8]

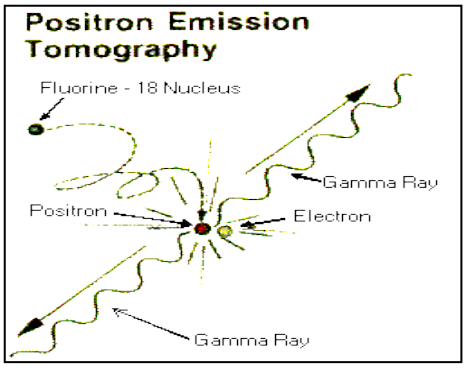

Figure 1.1. Schematic representation of positron decay and annihilation.[8]

Common PET radioisotopes include oxygen-15, carbon-11, nitrogen-13, and fluorine-18[10] and these have been incorporated in numerous imaging agents.[11] ^{18}F-fluorodeoxyglucose (^{18}F-FDG), for example, is a radiolabelled glucose analogue and is the most widely used PET agent. In tumours, the cellular metabolism is increased and an elevated expression of the insulin independent glucose transporters and hexokinase triggers ^{18}F-FDG uptake, where the product is trapped in cells following phosphorylation.[3] Other common oncology PET agents include ^{18}F-fluoroazomycin

arabinoside (^{18}F-FAZA)[12] and ^{18}F-fluoromisonidazole (^{18}F-FMIZO)[13], which are used to measure hypoxia in tumours and ^{18}F-fluoro-L-dihydroxyphenylalanine (^{18}F-fluoro-L-DOPA) which targets the activity and provides information on dopaminergic systems.[14] Another well established PET agent is ^{18}F-3-fluoro-3-deoxy-thymidine (^{18}F-FLT) which is used to measure the activity of thymidine kinase-1 and DNA synthesis associated with cellular proliferation.[13]

While both SPECT and PET are powerful techniques, SPECT imaging hardware is less expensive than the equipment associated with PET. Nevertheless PET is attractive because of the ease of quantification and the higher resolution that can be obtained on clinical scanners.[6] With respect to evaluating novel radiopharmaceuticals, such as is the topic of this thesis, the trend in preclinical (and clinical) scanners is to combine PET and SPECT with an anatomical method such as CT to provide anatomical references for the functional imaging data arising from the nuclear methods.[15]

1.4. Radioactive Isotopes of Iodine (^{123}I, ^{124}I, ^{125}I, ^{131}I)

There are 35 isotopes of iodine but the most useful for nuclear medicine are ^{123}I, ^{124}I, ^{125}I and ^{131}I.[16] Drugs, monoclonal antibodies, enzymes, peptides are routinely labelled with these isotopes and used for *in vitro* assays, biodistribution studies, quantitative imaging and targeted radionuclide therapy.[17]

^{131}I is the most commonly used isotope of iodine[18] where it is a β and γ emitter with a half-life of 8.07 days. ^{131}I is relatively inexpensive and widely available where the use of the isotope for diagnosis is decreasing because the emission of a β^- particle increases

exposure of patients to radioactivity.[16] ^{123}I is being used in its place as it emits γ radiation of an energy that minimizes dose (E_γ = 159 keV). Iodine-123 is produced using a cyclotron, has an ideal half-life of 13.2 hours and can be safely administered to patients. The most common radiotracers derived from this isotope are sodium iodine-123 (used for thyroid disorders) and *meta*-iodobenzyl-guanidine (MIBG, used for imaging neuroendocrine tumours and heart failure).[16,19]

^{124}I has not been used routinely for clinical studies because it possesses a complex decay scheme having multiple high-energy gamma rays. Despite the high cost of the isotope, ^{124}I has been used for PET imaging as its half-life of 4.18 days allows for quantitative imaging with molecules displaying slow pharmacokinetics (such as antibodies).[20]

^{125}I does not have an adequate γ emission energy for clinical imaging and its half-life is undesirably long (60.14 days).[16,17] However iodine-125 is widely used in prostate cancer therapy (Brachytherapy) and to label proteins for biochemical assays. ^{125}I is also relatively inexpensive and therefore an attractive isotope for probe development where it can be used to develop radiochemical methods and perform *in vitro* screening and quantitative biodistribution studies.[17]

1.5. Considerations for the Development of Target-Specific Radiotracers

A number of factors must be considered when selecting a target for MI. The target must be overexpressed and directly association with the disease of interest while having limited expression in other tissues undergoing normal physiology.[21] Furthermore, changes in the target's activity or expression must influence clinical decision-making. Typical

targets include receptors, enzymes, transport proteins and hormones whose over-expression is an indication of the presence, stage or probability of progression of a disease.[21] Radiotracers act as delivery vehicles to transport the radionuclide to the target of interest where selectivity is achieved using small molecules, peptides, proteins and antibodies.[21] Irrespective of class, vectors must possess a high affinity for the target, should not saturate the binding sites or perturb any biochemical processes related to the disease under study. The ideal radiotracer should accumulate in the target quickly and clear from non-target sites thereby providing a high signal-to-noise ratio.[21] Each of these considerations is discussed in detail below.

1.5.1. Location of the Target

The location of the target of interest is an important factor to consider when designing MI probes.[22] In the case of intracellular receptors, the radiotracer has to pass through the cell membrane in order to bind the target of interest. If diffusion across a cell membrane is not facilitated by specific transporters or carriers, the net flux is directly proportional to the diffusion coefficient and the partition coefficient.[22] Passive diffusion depends on molecular size, volume and solubility in lipids. Decreased size (<400–600 Da) and volume of the radiotracer help with facilitated transport across the cell membrane. Extracellular receptors are more accessible to MI probes as they do not have to cross the cell membrane. However, imaging intracellular targets provides the opportunity to enhance radioactivity uptake via repetitive trapping.

1.5.2 Lipophilicity of the Radiotracer

A critical feature that requires optimization is lipophilicity. Since cell membranes consist of a lipid bilayer, highly lipophilic radiotracers have higher passive transport across the cell membrane. At the same time, high lipophilicity can increase nonspecific binding to other proteins and result in a poor signal to noise ratio. High nonspecific binding will result in a low free fraction of the radiotracer that can be delivered to the target.[22] *Log P* represents the partition coefficient in the water/octanol and molecules with values between 2 and 3.5 are deemed optimal for intracellular targets as they balance out the issues associated with nonspecific binding and cell membrane permeability.[22]

1.5.3. Affinity of the Radiotracer

Fast dissociation rates from non-targeted tissues and slow dissociation rates from the target is a key trait for any radiotracer.[22] For receptor targeted agents, the concentration of typical receptors lies between 10^{-9}-10^{-13} moles per gram of tissue.[23] At these levels, radiotracers must have high affinity, usually in the low nanomolar range, in order to obtain a clinical useful signal to noise ratio. In the scenario where the radiotracer exhibits low binding affinity, the tracer will rapidly wash out from the binding site, resulting in low uptake and high off target binding.[23]

The radiotracer affinity depends on the density of the binding sites[91] and the association constant (K_a in nM^{-1}). K_d is expressed as the reciprocal of association constant K_a (K_d in nM). In a typical biomolecular reaction ($A + B \rightarrow AB$), the following formulae apply:[24]

$$K_a = \frac{[AB]}{[A][B]}\ (nM^{-1}) \qquad \text{Eq. 1.1. a}$$

$$K_d = \frac{[A][B]}{[AB]}\ (nM) \qquad \text{Eq. 1.1. b}$$

A bound-to-free (B/F) ratio was initially proposed for *in vitro* analysis of receptor binding and later translated to radiotracers, where B represents the concentration of bound radiotracer and F represents free concentration of radiotracer. The B/F ratio is interpreted as an estimate of the target-to-non-target (T/NT) ratio.[25,26] Higher receptor concentration and a smaller K_d or a higher K_a, will result in a higher B/F ratio (Eq. 1.2.), where B_{max} is the binding site concentration and K_d is the equilibrium dissociation constant of the radiotracer for the binding site.

$$\frac{B}{F} = B * \left(-\frac{1}{K_d}\right) + \frac{B_{max}}{K_d} \qquad \text{Eq. 1.2.}$$

From Eq. 1.2., it can be seen that as the amount of bound radiotracer trends towards zero, the ratio of B/F reaches the highest value of B_{max}/K_d.[26] Conversely, the B/F ratio that trends towards zero will provide a B_{max} value for the bound radiotracer. Ideally, only 5% of the available binding sites should be occupied by the radiotracer to avoid perturbing the system under investigation.[7] For a reversible radiotracer, the binding potential B/F (Eq. 1.3.) represents an approximate target to non target ratio *in vivo.*[26,27]

$$\frac{B}{F} = \frac{B_{max}}{K_d} \qquad \text{Eq. 1.3.}$$

For a high K_d of the radiotracer, the off-rate from the binding site will be in the same range as for the nonspecific binding and will not provide any significant differentiation of the disease or the process of interest. A low K_d implies a slow off-rate and, therefore

indicates that the behaviour of the radiotracer *in vivo* is a function of diffusion rather than the radiotracer affinity. Based on previous work, the optimal K_d range lies between 10 pM and 10 nM.[26] In order to differentiate between specific and not specific binding, a 4-fold excess of radioactivity should be accumulated in the tumour compared to the surrounding tissues and a ratio of $B_{max}/K_d > 10$ should be obtained.[27] As mentioned previously, B_{max}/K_d is suitable for evaluation of *in vitro* systems but can be confounded *in vivo* where other properties such as blood residence time, nonspecific binding, metabolism and heterogeneity of the target (discussed below) come in to play.[28]

1.5.4. Selectivity / Specificity and Blood Residence Time

The T/NT ratio will be lower if the radiotracer does not possess selectivity for the target. As a result, good selectivity of the radiotracer for the target of interest is crucial in helping to diminish additional sources of background radioactivity and to improve the contrast between the desired target and the adjacent tissues. Specificity is determined by performing blocking experiments using nonradioactive competitive binding ligands that have a well defined affinity for the target of interest. Along with specificity, selectivity which is the ability to discriminate between closely related populations (proteins, receptors, genes, etc), is also critical in achieving the desired contrast.

The blood residence time of the radiotracer should be relatively short to avoid nonspecific binding with plasma proteins, but long enough to ensure that the agent reaches the target. Rapid dissociation from blood proteins are vital in order to maximize the available free radiotracer in the vascular system which will effectively diffuse to the target of interest.[26]

1.5.5. Metabolic Stability

The metabolic stability of the radiotracer is important as neither PET nor SPECT can distinguish between the signals originating from the parent radiotracer or associated radiolabelled metabolites. Knowledge of the nature of metabolite or metabolism of the parent vector will provide a basis for choosing the position of the radioisotope on the ligand. The metabolic stability of a newly created radioligand should ideally be tested in plasma and liver homogenates or it can be assessed by analyzing blood samples during preclinical studies.[29,30]

1.5.6. Specific Radioactivity

Specific radioactivity (SA)[16] is defined as the amount of radioactivity per unit mass of a radiolabelled compound and is expressed by the Eq. 1.4.

$$S_{max} = \frac{N}{3.7 * 10^{10}} * \frac{\lambda}{W} \qquad \text{Eq. 1.4.}$$

where: N is Avogadro's number, W is atomic mass, $\lambda = \frac{\ln 2}{t_{1/2}}$, $t_{1/2}$ is half-life of the radionuclide.

Specific radioactivity is important as it can influence the extent of accumulation of the radioactivity in the target. Contamination of the radiotracer with a nonradioactive competitor can result in blocking of the binding sites and subsequent reduced or negligible uptake and potentially pharmacokinetic and toxic effects.[29] High specific activity is typically desired and requires minimizing contamination from other isotopes.

Effective specific activity (ESA) is defined as the mass or molar quantity of a single radiotracer species relative to the total mass or molar quantity of the radiotracer and non-radioactive compound(s) that have similar biochemical properties.[31] Removing unlabelled ligand is crucial as it can compete with the radiotracer for the available sites.[32] The most commonly used technique for achieving high ESA is high-performance liquid chromatography (HPLC) purification although solid-phase labeling strategies and soluble supports have been used in place of HPLC. In solid-phase labeling, the precursor is attached to an insoluble support in such a way that it will be released into solution upon reaction with the radionuclide while the unreacted material remains bound to the support.[33] Fluorous soluble supports have also been used effectively to produce radiotracers with high effective specific activity using solid phase extraction (SPE) to isolate pure products.[34]

1.5.7. Choice of Radionuclide

The choice of the radionuclide should be made by taking into account the pharmacokinetic properties of the targeting vector, the associated nuclear properties of the radionuclide, the desired detection method, the radiation dose, and the feasibility of radiochemical synthesis.[30] In devising a radiosynthetic scheme, the radionuclide should ideally be incorporated in the final step and the reaction times should reflect the half-life of the radionuclide.[26,30] The synthesis of the non-radioactive analogue of the target probe is necessary as it provides a standard by which the radioactive compound can be analyzed and quantified using standard analytical methods. Furthermore, the “cold” compound can be utilized to determine toxicology prior to human imaging studies.

1.5.8. Optimization of the Radiotracer

It is important to bear in mind that the issues discussed above are important for the initial stages of probe development *in vitro* but are not a guarantee of success in the translation to *in vivo* systems. There are several ways that a specific radiotracer can be modified in order to achieve more desirable *in vivo* properties. For example, the introduction of lyphophilic or hydrophilic moieties can affect the *log P* associated with the radiotracer and improve its pharmacokinetic profile. Biodistriubution studies are required to develop important structure activity relationships that can aid in tracer refinement and for the improvement of the affinity and selectivity.[28]

1.6. Imaging Tumour Aggressiveness / Metastatic Potential: Rationale and Value

Significant efforts have been directed towards the understanding of the biology associated with cancer proliferation and metastasis.[35] Cancer is a complex disease governed by multiple pathways, and MI can be used to provide meaningful information on disease stages and different propagation mechanisms.[35] Traditionally, the use of anatomic imaging methods such as computed tomography (CT) can evaluate cancers based on tumor size, shape and density. This information is important when determining a cancer patient's response to treatment[36,37] via the Response Evaluation Criteria in Solid Tumors (RECIST) protocol, for example. However, this RECIST evaluation is limited as it assumes spherical growth of tumours, provides no guidance for non-solid tumours, offers limited information about the disease progression, and suffers from the difficulties associated with evaluation of sub-centimeter tumours.[38] Determination of metabolic and

physiological changes can provide additional information that will improve outcomes for patients.

MI methods that can help to visualize specific biological pathways and targets can also provide unique information about the tumour microenvironment. Such methods are playing an increasingly important role in managing cancer patients at all stages of treatment.[38] For example, early detection of cancer increases the treatment effectiveness and ultimately the survival rate for patients. Agents that can identify those patients at greatest risk for metastasis by detecting particularly aggressive tumours can impact management influencing the choice of treatment option and dose. MI can also be used to predict response to a particular anti-cancer treatment and in this way, identify the best therapy option.[36] The ability to monitor response to a certain treatment makes it possible to quickly intervene when a patient exhibits resistance to therapy. While primary tumours often respond to chemotherapy, radiotherapy and/or surgery, metastases represent the main cause of death in cancer patients.[36,39] Efforts in developing and improving imaging techniques for visualizing metastases and metastatic potential are a key goal of the field of MI.

1.7. Molecular Imaging of Extracellular Cancer Proteases

Proteases, also referred to as peptidases or proteinases, are enzymes that catalyze the hydrolysis or cleavage of peptide bonds at a specific site. These enzymes are classified into six categories according to their mechanism of action and include serine-, threonine-, cysteine-, aspartate- and glutamic-proteases as well as metalloprotease.[40] These proteases are involved in a variety of physiological processes including wound healing, tissue

remodeling and homeostasis. Overexpression of these enzymes in early cancer stages has been associated with the degradation of the extracellular environment surrounding tumour cells resulting, ultimately, in metastasis.[41] Detecting and monitoring the level of protease activity represent an approach for the early detection of aggressive cancers.

MI of tumour-associated proteases is attractive for a number of reasons:[42,43]

- Extracellular proteinases including the matrix metalloproteinases (MMPs), cathepsin B, and urokinase plasminogen activator (uPA) have modest expression during normal physiological function and are overexpressed in a limited number of disease processes.
- Extracellular proteases are secreted at the surface of the extracellular matrix, thus making them more accessible to substrates from the bloodstream.
- The activity of a proteinase can enhance signal amplification over time due to its ability to promote cleavage of multiple substrate molecules.

Of the various extracellular cancer proteases, cathepsin B, MMPs, and uPA have been studied extensively.[44] MMPs are Zn-dependent endopeptidases that degrade components of the extracellular matrix.[44] This class of protease has received much attention in terms of inhibitor development and represents a biologically interesting group of targets for cancer imaging. MMP2 and MMP9 are the most characterized from this class.[45]

There are eleven classes of cathepsin cysteine proteases that include types B, D, S, K and L. Cathepsin D and cathepsin B (lysosomal) are involved in the degradation of the basement membrane while cathepsin S is a papain protease that is overexpressed in lung cancer.[46] Attempts have been made to use MRI, PET or SPECT[42,45,47] to image proteases

as a means to provide information concerning the potential invasiveness of malignant lesions.[48] A review of these approaches is provided below.

1.7.1. Optical Imaging of Extracellular Proteases

In 1999, Weissleder *et al.*[49] developed a near infrared probe (NIR) for imaging the overexpression of proteases. The probe design was based on a polymer of poly-L-lysine and methoxy-polyethylene glycol (PEG) succinate containing multiple copies of Cy5.5 fluorophores linked by a cleavable sequence specifically recognized by the enzyme. The location of the fluorophores in the construct quenches the optical signal *via* a fluorescence energy transfer (FRET) mechanism. Upon cleavage by cathepsin B, the fluorophores are separated and fluorescence is no longer quenched, resulting in the detection of an optical signal. This approach has been applied to monitor cathepsin B activity in a mouse breast cancer model and showed a 30-fold increase in fluorescence in the tumour compared to normal tissues. Proteases from the same family including cathepsin D[50] and S[51] were also studied using developed optical probes, but these studies were limited to *in vitro* tests. The same activatable-based probe used for cathepsin B was extended to the MMP class with the Cy5.5 dye used as the reporter.[52]

In another study, gold nanoparticles[53] were used to develop MMP9 probes by acting as ultra-efficient quenchers to improve the resolution and florescence quenching effectiveness. Work by Lee *et al.*[53] allowed for multiple Cy5.5 dye units to be attached to an MMP cleavable peptide and then loaded onto a gold nanoparticle surface. Upon intratumoral injection in mice bearing squamous tumors, an amplification of the NIRF probe was detected and a 7-fold increase in the target to non-target fluorescence signal

was observed at 240 minutes. The authors concluded that intravenously injected gold nanoparticles probes did not display amplified NIRF signals in the tumor when compared with the intratumoural injection. This was likely due to poor localization of the large size particles.[53]

An alternative imaging agent design was developed by Jiang *et al.*[54] which takes advantage of cell penetrating-polycationic peptide sequences. As shown in Figure 1.2., the construct involves a polycationic peptide modified with a fluorophore linked through an MMP2-cleavable linker to anionic peptides. With the intact construct, delivery into the cell will not take place as the polycationic peptides are charge neutralized. In the presence of MMP2, the polycationic peptide is released and taken up by the tumour cell. This approach was used to study laryngeal tumors and showed a contrast of 3.4 - 6.5 between target and nontarget tissues. The authors suggest that this same strategy is also suitable for the delivery of radiotracers, drugs or quantum dots for selective release and internalization at tumour sites.[54]

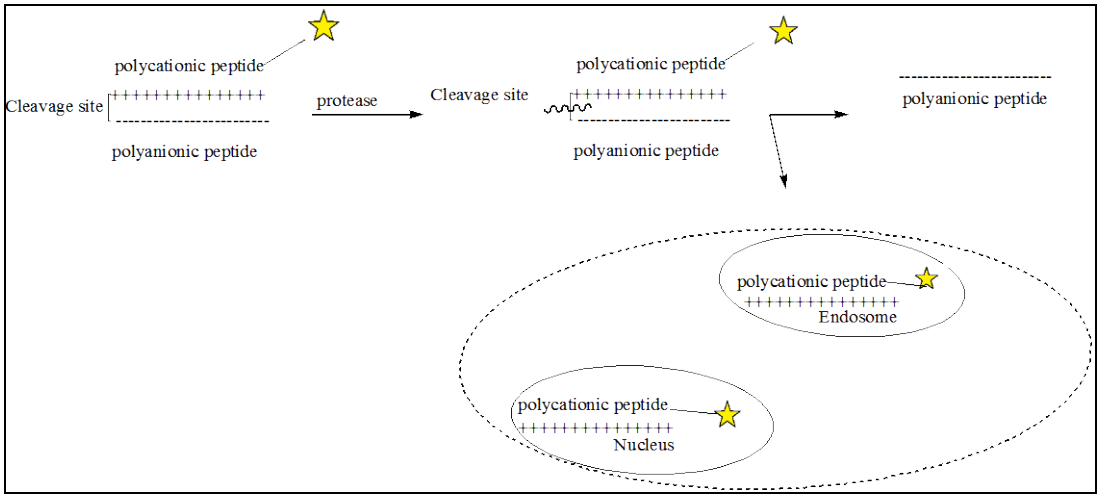

Figure 1.2. Schematic diagram of activatable cell penetrating peptides.[54]

1.7.2. Molecular Imaging of Extracellular Cancer Proteases using Magnetic Resonance Imaging Techniques

MRI contrast agents[55] based on Gd^{3+} and iron oxide nanoparticles[56] were used to study MMP2 and MMP7.[57] The strategy (illustrated in Figure 1.3.) is based on a "solubility switch" mechanism wherein the probe consists of a Gd chelate complex (in orange), a peptide fragment that can be selectively cleaved by the protease (in yellow) and a hydrophilic fragment attached to the N terminus of the peptide.[57]

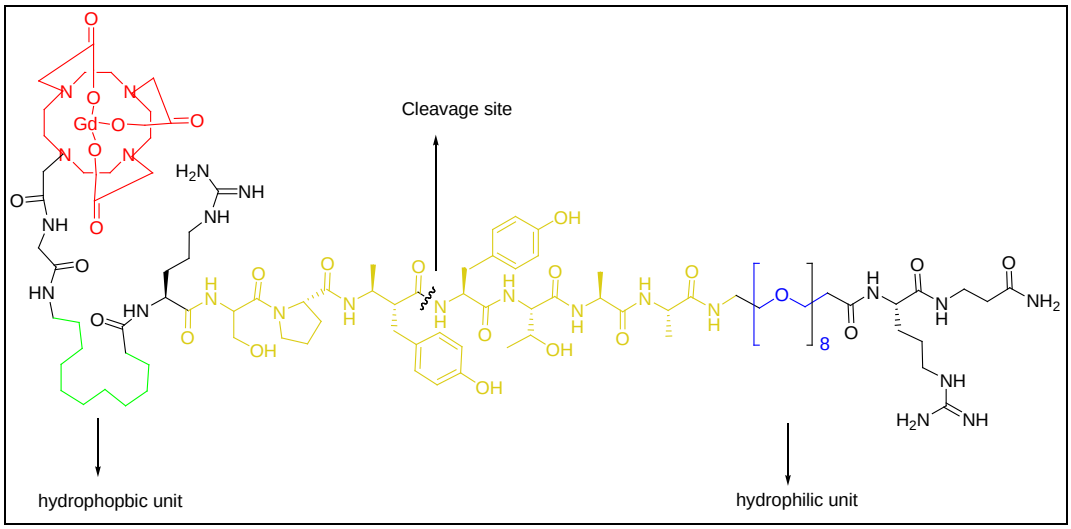

Figure 1.3. Solubility-Switchable Contrast Agent for Magnetic Resonance Imaging.[57]

This hydrophilic fragment incorporates a PEG unit (in blue) which ensures probe solubility and longer circulation time in order to reach the tumour site.[57] Upon cleavage by the protease, the chelate fragment (which incorporates a short alkyl moiety shown in green) becomes less hydrophilic thereby remains localized at the imaging site. Preclinical imaging results showed good tumour contrast.

1.7.3. Molecular Imaging of Extracellular Cancer Proteases using Nuclear Imaging Techniques

Several radiolabeled probes for proteases have also been developed. One approach[58] involved labeling tissue inhibitors of metalloproteinases (TIMP-2), the endogenous inhibitor of MMPs, with ^{111}In. *In vitro* data showed that the construct retained full inhibitory activity in a fluorometric binding assay. However, when tested in human kaposi sarcoma tumours, the compound showed high non-specific binding and uptake in non-target tissues.[59] An alternative imaging strategy involving the radiolabelling of synthetic inhibitors of MMP (Figure 1.4.)[60-64] was also developed. Unfortunately, these compounds were not able to adequately visualize preclinical tumour models despite possessing a high affinity for the target *in vitro.*[65]

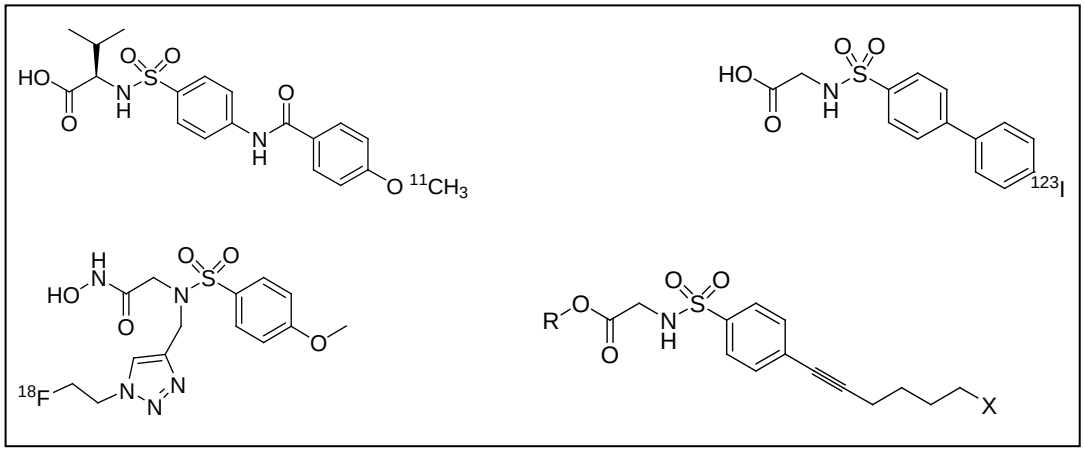

Figure 1.4. Representative MMP targeted radiotracers. (X = ^{18}F)

1.8. The Urokinase Plasminogen Activator System

The urokinase plasminogen activator system is a family of serine proteases that consists of the urokinase-type plasminogen activator (uPA), the plasminogen activator

inhibitors (PAI's), the tissue-type plasminogen activator (tPA) and the uPA receptor (uPAR).[66] It has been widely documented that the urokinase plasminogen activator system is involved in many types of cancers,[66] represents an interesting target for MI probe development and is the focus of the present thesis.

1.8.1. Urokinase-type Plasminogen Activator (uPA)

uPA is a serine protease of the trypsin family.[66-68] The protein is secreted as a single-chain 53 kD zymogen (pro-urokinase) by multiple cells types, such as endothelial cells, smooth muscle cells, macrophages, fibroblasts, tumour cells or adjacent stroma. uPA is activated upon binding to its receptor uPAR, through cleavage of the Lys158-Ile159 bond to produce the active two-chain form and ultimately results in the generation of plasmin from inactive zymogen plasminogen.[66-68]

The uPA protein is made up of 411 amino acids and has two main domains:[66-68]

- an amino-terminal ATF (amino acids 1-135) contains the growth factor–like sub-domain (GFD; amino acids 1-43) responsible for the binding of uPA with its receptor uPAR, and the Kringle sub-domain (amino acids 47-135)
- a carboxy-terminal domain which contains the serine protease catalytic site (amino acids 136-411)

Tumour overexpression of uPA starts an extracellular proteolytic cascade which allows tumours cells to destroys barriers such as the extracellular matrix (ECM) and basement membrane (BM) and foster migration.[66] This process plays a major role in physiological events, including angiogenesis, movement of immune cells into inflammatory sites and wound healing but also has a decisive role in numerous diseases

associated with tissue remodeling such as aortic aneurisms, multiple sclerosis, diabetic retinopathy, arthritis along with tumour invasion and metastasis.[69] Compared with normal tissue, many tumours cells have the capacity to produce elevated levels of proteolytic enzymes. Therefore a high level of uPA can be used as an indicator for poor prognosis for cancer patients.[70,71]

In 2007, the American Society of Clinical Oncology reviewed thirteen categories of breast tumor markers and uPA was recommended for monitoring cancer and prediction of recurrence risk.[72] A 300 mg sample of fresh or frozen breast cancer tissue could be used for prognosis in patients diagnosed with node-negative breast cancers. Data analysis from 8,377 breast cancer patients showed the correlation between overexpression of uPA and PAI-1 and the cancer prognosis during the 79 month follow-up evaluation. Although enzyme-linked immunosorbent assay (ELISA) and imunohistochemistry are routinely used to evaluate uPA overexpression, these methods do not provide information on the sources of expression consequently several *in vivo* MI studies have been described.[70,71]

As will be described in Section1.10, uPA was selected as a target around which to develop a new MI probe. The strategy involved building novel probes by modification of a number of known uPA inhibitors which show high affinity and selectivity to the target. As a result, reviews detailing known uPA inhibitors (Section 1.8.2) and the imaging of uPA using various modalities (Section 1.9) are presented below.

1.8.2. uPA Inhibitors: Approaches and Design Considerations

Two main approaches have been described in the literature for inhibiting uPA.[73] Peptides and peptidomimetics that target the N terminal GFD have been used successfully

as uPAR antagonists blocking the ligation of uPA to its receptor uPAR.[73] The second approach uses small molecule inhibitors to target the serine protease domain and interfere with the proteolytic activity of uPA. This in turn has been shown to greatly decrease tumour growth and inhibit metastasis.[41,73]

It should be noted that several homologous enzymes such as trypsin, tryptase, factor Xa, thrombin, and tissue type plasminogen tPA posses similar active site features present in uPA and, as a result, selective uPA inhibitors need to effectively discriminate between closely related trypsin-like serine proteases.[74,75] In nature, endogenous substrates discriminate among structurally similar serine proteases via the combination of interactions at a series of sites named S3, S2, S1, S1', S2'and S3' which will bind the substrate peptide side chains P3, P2, P1, P1', P2' and P3' (Figure 1.5.).[74]

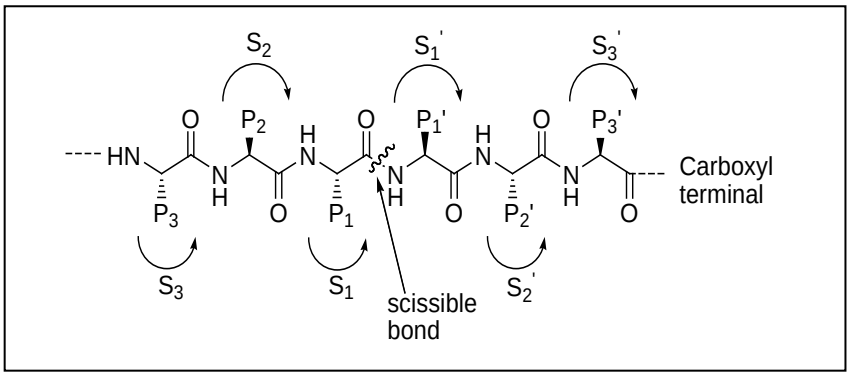

Figure 1.5. Nomenclature for protease substrate cleavage[41,74] P_n, P3, P2, P1, P1′, P2′, P3′, P_n', for the amino acid side chains of a peptide substrate. S_n, S3, S2, S1, S1′, S2′, S3′, S_n' for the corresponding binding sites in the protease active site.

The S1 site of each trypsin-like serine protease is unique as a result of the protein sequence and structure and these differences are exploited for selective inhibition. Examination of the active site of uPA, for example, reveals that the main binding groove of uPA, S1, contains a serine (Ser190), which hampers the binding of hydrophobic

moieties that are usually found in inhibitors of thrombin10 and FactorXa.[75,76] Studies also revealed the existence of a shallow subsite S1 β located near the S1 pocket and this more distal pocket has been explored in the design of selective uPA inhibitors.[77,78]

The binding groove of uPA contains an aspartate residue (Asp189), which interacts with an arginine (Arg560) of plasminogen. Most of the reported uPA inhibitors contain guanidine or amidine functionalities, which mimic the basic side-chain of arginine. These positively charged functionalities make hydrogen-bonded salt bridges with Asp 189 present in the active site of uPA.

1.8.2.1. Reversible uPA inhibitors of the serine protease domain

In 1987, studies revealed that the diuretic drug amiloride is a weak but selective inhibitor of uPA (K_i = 7 μM).[79] This compound has no inhibitory activity against tPA or plasmin.

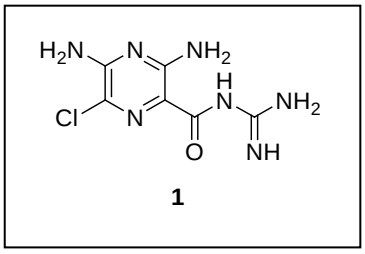

Figure 1.6. uPA inhibitor-diuretic drug amiloride.[79]

Indeed, various substituted phenylguanidines[80] (of the general type (**2**) shown in Figure 1.7.) are reported to possess μM inhibition potency with good selectivity against plasmin, thrombin, fXa, tPA and uPA ($K_i > 10^3$). The most potent compound in the series is (**3**) which has a K_i of 2.5 μM.

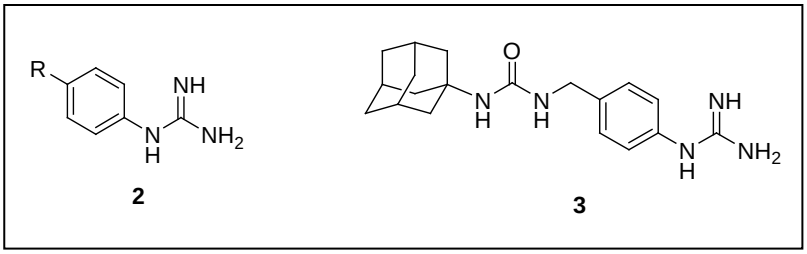

Figure 1.7. uPA inhibitors – Phenylguanidines.[80]

The amidinophenylalanine-type uPA inhibitor (WX-UK1) (**4**) and its prodrug were developed by Wilex Inc.[81] and a clinical study in 25 cancer patients was completed. The combination therapy with capecitabine was safe and well tolerated. The reported K_i value for this compound is 0.41 nM; however, the specificity of this compound with respect to other related proteases is moderate.

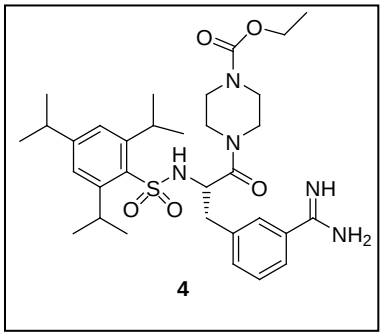

Figure 1.8. uPA inhibitor (WX-UK1).[81]

Wendt[77,78] reported a series of naphthyl amidines as uPA inhibitors (compounds (**5**), (**6**), (**7**) in Figure 1.9.). These inhibitors exploit the binding to the $S1_\beta$ pocket of uPA where K_i values ranged from 0.6 nM to 40 nM.

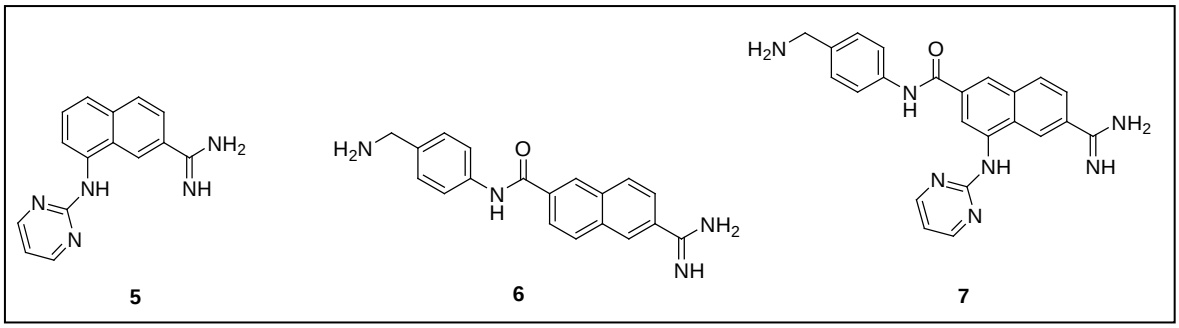

Figure 1.9. uPA inhibitors – Naphthyl amidines.[77,78]

The most potent of a series of 4-substituted benzothiophene-2-carboxamidines[82] has a benzodioxolanylethenyl side chain (B263, compound (**9**)) and posses an IC_{50} value against uPA of 0.07 μM. B623 and its parent B428 (**8**) were tested against a variety of serine proteases as tPA, plasmin, on chymotrypsin, elastase, kallikrein, thrombin, and trypsin and showed that neither of the two compounds had significant inhibitory effects against competitive targets.

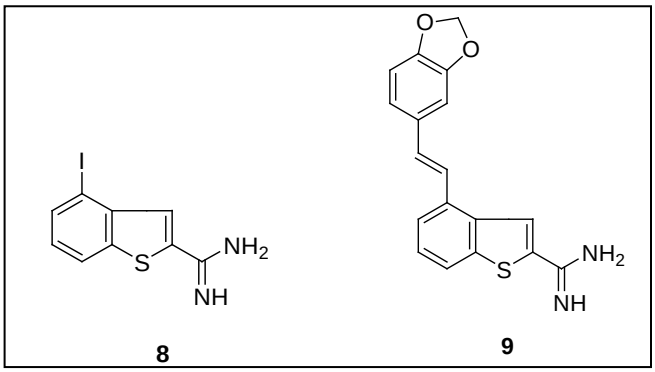

Figure 1.10. uPA inhibitors - Benzothiophene-2-carboxamidines.[82]

2-Pyridinylguanidine[83] (**10**) is a selective inhibitor of uPA while showing only moderate affinity for tPA or plasmin. The potency of this compound is increased by the presence of a 5-halo substituent and the introduction of various substituents at the 3 position of the pyridine ring (one example is compound (**11**)).[84]

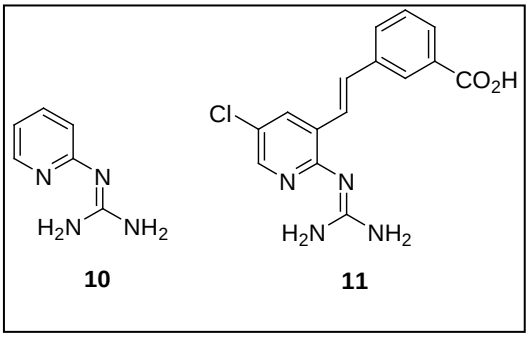

Figure 1.11. uPA inhibitors -2-Pyridinylguanidine.[84]

Modification of 1-isoquinolinylguanidine template by introduction of *m*-benzoic acid at the 7 position of the isoquinoline ring leads to the potent and selective inhibitor (**12**) (K_i = 27 nM).[85] Further increase in potency and selectivity was achieved by adding a series of sulphonamide fragments at the 7 position of the isoquinoline ring. One example, compound (**13**), shows a K_i = 10 nM against uPA.[85]

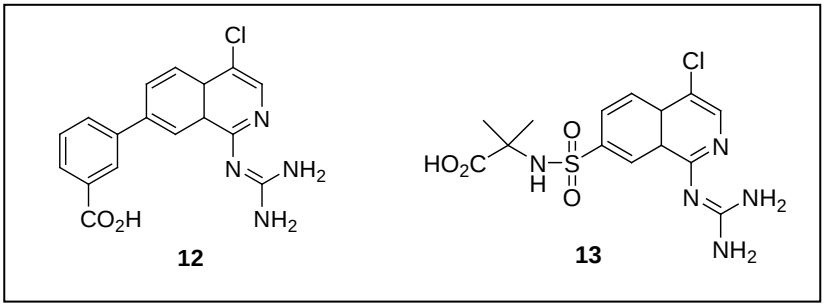

Figure 1.12. uPA inhibitors – Isoquinolinylguanidine derivatives.[85]

Substitution of the phenyl ring on the parent benzimidazole compound (**14**) generated compound (**15**) which has a K_i = 400 nM against uPA.[86] Swapping the benzimidazole with an indole resulted in a more potent inhibitor (**16**) (K_i = 8 nM) that displays selective inhibition of uPA over other related serine protease (tPA: K_i = 35 nM, factor Xa: K_i = 78 nM, plasmin: K_i = 100 nM, trypsin: K_i = 130 nM, thrombin: K_i = 320 nM).[87]

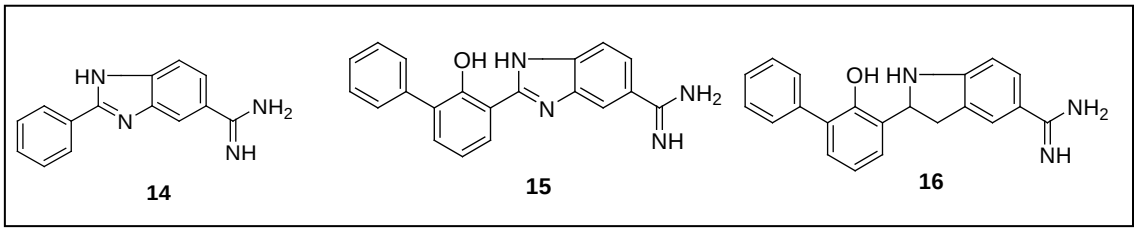

Figure 1.13. uPA inhibitors – Benzimidazole derivatives.[86,87]

Amidine-based, peptide-derived inhibitors were designed based on Arg mimetics, where the phenyl group interacts with S1 subsite. The peptide (**17**) and its guanidine derivative (**18**) show inhibitory activities in the low nM range.[88,89]

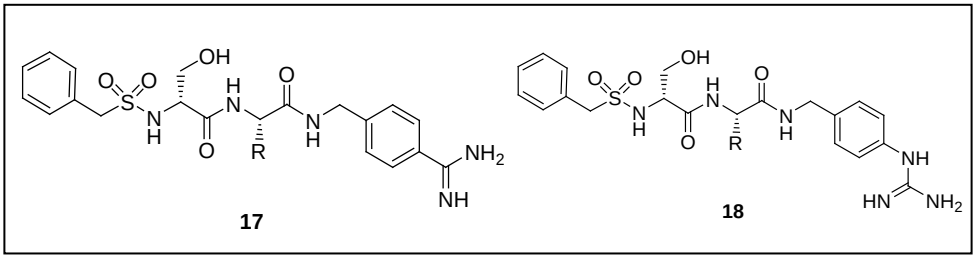

Figure 1.14. Dipeptide based inhibitors.[88,89]

1.8.2.2. Irreversible uPA Inhibitors of the Serine Protease Domain.

Based on the *Z*-D-Ser-Ala-Arg sequence reported by Tamura *et al.*,[90] Joossens *et al.*[91] were able to prepare a collection of selective and potent diphenyl phosphonate inhibitors. One representative example from these series is compound (**19**) that showed an IC_{50} against uPA at 4 nM while inhibition of tPA showed an IC_{50} of 0.28 μM.

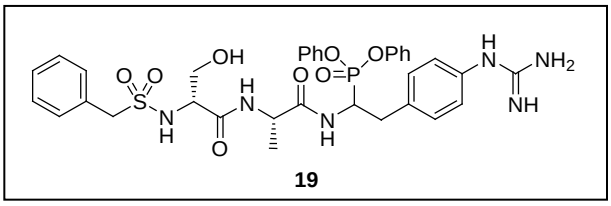

19

Figure 1.15. uPA inhibitors - Diphenyl phosphonate peptide.[91]

The cyclopeptide[92] (**20**) inhibited uPA selectively and irreversibly with a K_i of 41 nM), while no inhibition was observed for plasmin, tPA or thrombin.

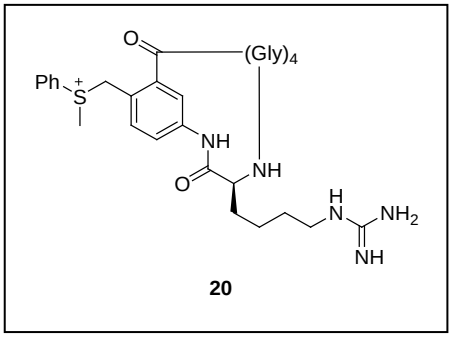

20

Figure 1.16. Cyclopeptide uPA inhibitor.[92]

1.9. uPA and molecular imaging

1.9.1 Molecular Agents based on the Amino Terminal Fragment of uPA (ATF)

The ATF of uPA consists of 135 amino acids and was the first peptide discovered that targets uPAR with high affinity. ATF includes the GFD and has been shown to compete with uPA for the uPAR receptor.[93] The peptide has been used for MRI, NIR imaging and drug delivery studies.[94]

Reports have described the radiolabelling of the ATF with ^{125}I and the *in vivo* biodistribution studies carried out using severe combined immunodeficiency (SCID) mice bearing MDA-MB-231 human breast cancer tumor xenografts.[95] These results were

compared with those of the uPAR probe, ^{111}In-1,4,7,10-tetraazacyclododecane-N,N',N'',N'''-tetraacetic acid (DOTA)-AE120, a radiolabeled peptide antagonist. The biodistribution profile of the ^{125}I ATF reveals that the highest tumour uptake was at 1h post injection (p.i. at 4.60 ± 0.63 %ID/g) which slowly decreased after 4h p.i. (3.09 ± 0.29% ID/g). Slow elimination of ^{125}I ATF from the blood is observed with 7.75 ±1.00% ID/g at 1h p.i. and 3.41 ± 0.86 remaining in blood at 4h p.i. However, the tumour uptake of ^{125}I ATF was superior when compared with that of ^{111}In-DOTA-AE120 as it showed a maximum tumour uptake of 1.48 ± 0.28% ID/g at 1h p.i. and a blood uptake of 1.48 ± 0.28% ID/g at 1h p.i. ^{125}I-ATF exhibited greater binding to MDA-MB-231 cells when endogenous uPA was removed by acid stripping or when the endogenous expression of uPA diminished using specific siRNA's. These experiments suggest that expression of endogenous uPA could obstruct the available uPAR sites and reduce or prevent the binding of ligands and/or inhibitors.[95]

Table 1.1. In vivo biodistribution (n = 3, mean %ID/g ± SD) of ^{125}I-ATF in SCID mice bearing MDA-MB-231 human breast cancer tumor xenografts at 1, 4, and 24h.[95]

Organ	1 h	4 h	24 h	24 h (blocked)
blood	7.75 ±1.00	3.41 ± 0.86	0.26 ± 0.06	0.60 ± 0.69
heart	2.56 ± 0.12	1.19 ± 0.16	0.08 ± 0.02	0.06 ± 0.01
lung	5.39 ± 0.35	2.67 ± 0.51	0.16 ± 0.05	0.17 ± 0.02
liver	3.01 ± 0.45	1.81 ± 0.42	0.25 ± 0.06	0.23 ± 0.02
spleen	2.92 ± 0.39	1.72 ± 0.35	0.09 ± 0.02	0.10 ± 0.03
intestines	3.27 ± 0.40	2.53 ± 0.28	0.16 ± 0.03	0.13 ± 0.02
kidney	16.72 ± 1.59	4.65 ± 0.84	0.88 ± 0.21	0.81 ± 0.09
muscle	1.21 ± 0.08	0.61 ± 0.10	0.03 ± 0.01	0.02 ± 0.01
bone	1.55 ± 0.13	0.87 ± 0.11	0.04 ± 0.01	0.03 ± 0.001
pancreas	3.98 ± 0.77	2.18 ± 0.65	0.06 ± 0.03	0.05 ± 0.01
tumor	4.60 ± 0.63	3.09 ± 0.29	0.29 ± 0.06	0.19 ± 0.05

The GFD of the ATF served as a starting point for the development of related uPAR binding peptides. Among these peptides is cyclo19,31[D-Cys(19)]uPA which was radiolabeled with ^{99m}Tc using a single amino-acid chelate (SAAC) labeling strategy. Unfortunately the ^{99m}Tc-labeled cyclo19,31[D-Cys(19)]uPA exhibited a 30-fold decrease in binding affinity to uPAR after conjugation with the SAAC.[96]

The ATF of uPA was also used to create MRI based ligands which target uPAR. Yang *et al.*[97] characterized mouse ATF conjugated-iron oxide which showed a specific uptake and internalization in 4T1 mouse mammary tumors. Despite this, several groups have reported species specificity and a reduced affinity of mouse ATF to human uPAR.[98] The findings reported by Yang *et al.* [97] suggest cross-reactivity with human uPAR expressing tumour cells. In the same study, an optical probe consisting of Cy5.5 conjugated to the ATF-IO nanoparticles was used for validation of the paramagnetic nanoparticle.

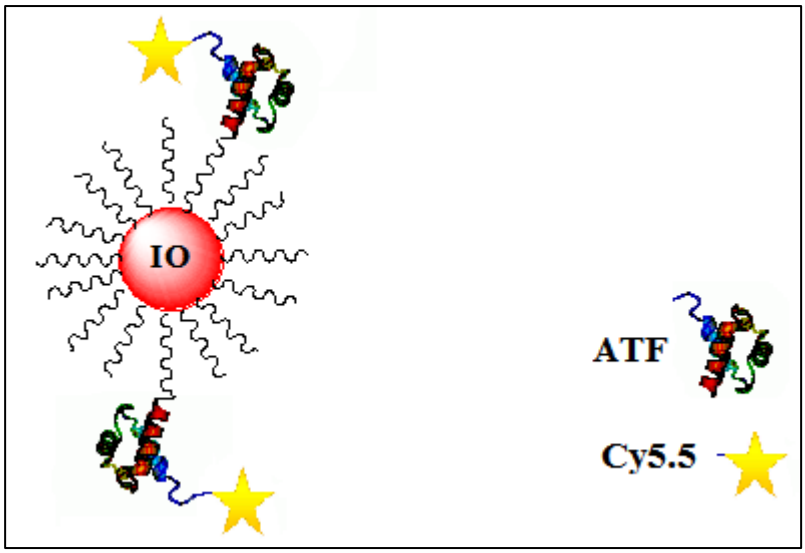

Figure 1.17. Characteristics of ATF-IO nanoparticles.[97]

A dual NIR and MRI construct derived from ATF was reported by Abdalla *et al.*[99] and used for the imaging of uPAR. The paramagnetic iron oxide nanoparticles were coated with Cy5.5. Noscapine (a plant derived anti-tumour alkaloid) was loaded onto the uPAR-targeted nanoparticles and was triggered to release in response to the acidic tumour environment (pH 4-5), while remaining intact under physiological pH. The efficiency of the Noscapine loaded uPAR-targeted nanoparticles was evaluated in human PC-3 prostate cancer cells using optical imaging and MRI. The results showed 6-fold stronger inhibitory effect on PC-3 growth compared to free noscapine.[99]

1.9.2. Molecular imaging for uPA

1.9.2.1. Optical imaging probes for uPA

Law *et al.*[100] examined uPA activity *in vivo* using a near-infrared reporter. The probe is made up of multiple copies of a peptide sequence, GGSGRSANAKC-NH_2, that are selectively recognized and cleaved by uPA. These peptide sequences are anchored at the C terminus of an L-lysine copolymer and capped with a Cy.5.5 dye conjugated at the N terminus. Initially, the proximity of the adjacent Cy5.5 moieties to each other results in a quenching of fluorescence via a FRET mechanism. When uPA selectively cleaves the peptide, the Cy5.5 fragments are released and a fluorescence signal is obtained. The efficiency of the probe was tested in HT-1080 fibrosarcoma bearing mice using HT-29 colon adenocarcinoma bearing mice as the negative control. Unfortunately, the reported fluorescence intensity of HT-1080 tumor was similar to that of the negative HT-29 control tumor.[100]

During the writing of this thesis a report was published where an optical probe and ^{18}F probe were prepared using an irreversibile phosphonate[101] as a targeting vector (see Figure 1.18.). In the presence of serine moiety in the active site of the protease, the side chain hydroxyl reacts at the phosphorous releasing a phenolic moiety and forming a covalent bond with the protein. Unfortunately, the biodistribution results showed a poor T/NT ratio (see chapter 5 for additional details).

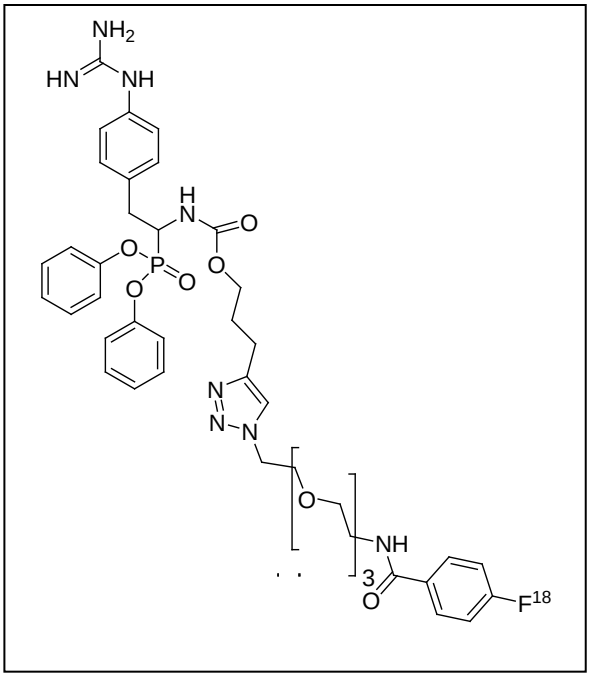

Figure 1.18. Phosponate inhibitors as MI agents.

1.9.2.2. Nuclear Imaging Probes for uPA

The endogenous uPA inhibitor, human plasminogen activator inhibitor type-2 (PAI-2, serpinB2), is a recombinant protein which selectively binds membrane-bound uPA and is internalized upon binding.[102,103] PAI-2 includes a CD-loop consisting of 33 amino acids which does not play a role in uPA inhibition. Truncation of the CD-loop from PAI-2

produces a 44 KDa fragment known as ΔCDloop which maintains uPA binding properties.[101,102] PAI-2 and ΔCDloop were investigated as potential radioimaging probes and subjected to radiolabeling *via* the incorporation of isotopes such us ^{213}Bi, ^{125}I, ^{123}I, and ^{99m}Tc.[71,104,105] In a recent study, the wild type PAI-2 and its shorter fragment ΔCDloop were radiolabeled with ^{123}I and ^{99m}Tc. Radiolabeling with ^{123}I was accomplished in two ways. The first involved conjugation *via* an amide using an *N*-succinimidyl 3-trimethylstannyl benzoate prosthetic group. The second labeling strategy involved direct radiolabeling of tyrosine moiety. Radiolabeling with ^{99m}Tc was performed using a diethylentriamene pentaacetatic acid (DTPA) chelate conjugated to PAI-2. The biodistribution profiles of the probes were examined in a mouse model bearing PC-3 human prostate cancer cell line and revealed that none of these radiolabeled ligands showed significant accumulation in the tumour (1-1.6% tumour uptake). Instead, these modified ligands displayed substantial accumulation in non-target organs. The tyrosine labeled ^{123}I-PAI-2 was more prone to deiodination as observed with increased thyroid uptake compared with the ^{123}I-PAI-2 benzoate derivative. Both ligands exhibited rapid renal excretion and a similar profile was displayed by ^{123}I ΔCDloop PAI-2 which accumulated in the bladder in 5 to 10 minutes post injection and was eliminated even faster from the body, in comparison to the radiolabeled wild type PAI-2. These ligands were further modified with varying PEG chains in an attempt to increase tumour uptake, avoid liver accumulation and prolong blood residency time. These modifications, however, showed little improvement in the pharmacokinetics and target uptake.

Consequently, radiolabeled PAI-2 and related constructs were unable to achieve the desired contrast required for tumour visualization.[104]

The use of ^{213}Bi –PAI-2 constructs allows for the development of targeted alpha therapy, wherein the targeting vector selectively bind to the uPA on the surface of cancer cells and delivers a radioisotope that emits deadly alpha radiation to the tumour.[71,105] While no biodistribution data was provided for the ^{213}Bi-PAI-2 system, its use on several types of cancer (ovarian, breast, pancreatic, and prostatic) showed delay to total inhibition of cancer cell growth.[71,105]

Recently [106] two antibodies 3C6 and 2G10 where radiolabeled with ^{111}In and ^{177}Lu and successfully used to detect over expression of uPAR. The therapeutic form reduced tumour burden in several breast cancer mouse models validating the importance of the target. Antibodies labeled in the classical approach have the distinct disadvantage that they require long circulation times which complicates their use clinically. A small molecule based MI probe for uPAR would overcome this issue and building on the antibody data could represent a new type of tracer for visualizing metastatic potential.

1.10. Objectives

MI probes that provide information on the metastatic potential of tumours has been a long sought after goal as the resultant images could be used to direct patients towards appropriate therapy or “active surveillance”. Unfortunately, developing an agent for assessing metastatic potential has proven to be a challenging task.

While there has been active work on developing MI probes for specifically targeting uPAR and uPA using different imaging techniques, no truly effective small molecule

agent has been identified or translated to human use. If an effective probe could be identified it would allow for better management of cancer patients by providing a non-invasive means of assessing metastatic potential, drug resistance and stage of the disease.

Motivated by the potential impact of such a probe, the goal of the present thesis was to develop new methods for the synthesis of MI probes that target uPA. The approach focused on utilizing isotopes of iodine as they can be used with PET and SPECT cameras and for Auger and β^- therapy applications.

Traditionally, once a lead compound has been identified, a radionuclide-bearing functional group is added. Unfortunately, introducing the radioisotope often decreases affinity and/or selectivity, rendering the lead compound useless. The approach developed in the present thesis involves the generation of compound libraries in which every member contains a stable-isotope analogue of the radionuclide of interest. Any "hits" that arise from screening will have already taken into account any impact imparted by the label. These hits can then be converted to their radiolabelled analogues and their performance in animals or cell lines assessed.

Four families of uPA inhibitors were prepared and screened for uPA binding. Chapter 2 describes the use of phenyl guanidines as a model compounds for the development of key synthetic methods and assay protocols. Chapter 3 involved the development and evaluation of naphthamidine-based probes. Chapter 4 extends our study to a family of unique dipeptides that target uPA and their development and assessment as MI probes. Chapter 5 looks at irreversible inhibitors based on a phosphonate series that help to address some of the *in vivo* issues identified in the previous chapters. Finally,

Chapter 6 describes the development of a new labelling pretargeted approach based on a tetrazine cycloaddition protocol while the Conclusions and Future Work are outlined in Chapter 7.

1.11. References

(1) James, M. L.; Gambhir, S. S. *Physiol Rev* **2012**, *92*, 897.
(2) Glunde, K.; Pathak, A. P.; Bhujwalla, Z. M. *Trends Mol Med.* **2007**, *13*, 287.
(3) Barentsz, J.; Takahashi, S.; Oyen, W.; Mus, R.; De Mulder, P.; Reznek, R.; Oudkerk, M.; Mali, W. *JCO.* **2006**, *24*, 3234.
(4) Kherlopian, A.; Song, T.; Duan, Q.; Neimark, M.; Po, M.; Gohagan, J.; Laine, A. *BMC Syst. Biol.* **2008**, *2*, 74.
(5) Henderson, R. G. *J. R. Soc. Med.* **1983**, *76*, 206.
(6) Dzik-Jurasz, A. S. K. *Br. J. Radiol.* **2003**, *76*, S98.
(7) Hamilton, D.; Springer: New York, NY, 2004.
(8) Bailey, D. L.; Adamson, K. L. *Curr. Pharm. Des.* **2003**, *9*, 903.
(9) Cherry, S. R. *J. Clin. Pharmacol.* **2001**, *41*, 482.
(10) Van de Wiele, C.; Lahorte, C.; Oyen, W.; Boerman, O.; Goethals, I.; Slegers, G.; Dierckx, R. A. *Int. J. Radiat. Oncol., Biol., Phys.* **2003**, *55*, 5.
(11) Pantaleo, M. A.; Nannini, M.; Maleddu, A.; Fanti, S.; Ambrosini, V.; Nanni, C.; Boschi, S.; Biasco, G. *Cancer Treat Rev.* **2008**, *34*, 103.
(12) Souvatzoglou, M.; Grosu, A. L.; Röper, B.; Krause, B. J.; Beck, R.; Reischl, G.; Picchio, M.; Machulla, H. J.; Wester, H. J.; Piert, M. *Eur. J. Nucl. Med. Mol. Imaging.* **2007**, *34*, 1566.
(13) Been, L.; Suurmeijer, A. H.; Cobben, D. P.; Jager, P.; Hoekstra, H.; Elsinga, P. *Eur. J. Nucl. Med. Mol. Imaging.* **2004**, *31*, 1659.
(14) Barrio, J. R.; Huang, S. C.; Melega, W. P.; Yu, D. C.; Hoffman, J. M.; Schneider, J. S.; Satyamurthy, N.; Mazziotta, J. C.; Phelps, M. E. *J. Neurosci. Res.* **1990**, *27*, 487.
(15) Cherry, S. R. *Semin. Nucl. Med.* **2009**, *39*, 348.
(16) Adam, M. J.; Wilbur, D. S. *Chem. Soc. Rev.* **2005**, *34*, 153.
(17) Seevers, R. H.; Counsell, R. E. *Chem. Rev.* **1982**, *82*, 575.
(18) Kwak, Y.; Jiang, W.; Dassama, L. M. K.; Park, K.; Bell, C. B.; Liu, L. V.; Wong, S. D.; Saito, M.; Kobayashi, Y.; Kitao, S.; Seto, M.; Yoda, Y.; Alp, E. E.; Zhao, J.; Bollinger, J. M.; Krebs, C.; Solomon, E. I. *J. Am. Chem. Soc.* **2013**.

(19) Binderup, T.; Knigge, U.; Loft, A.; Mortensen, J.; Pfeifer, A.; Federspiel, B.; Hansen, C. P.; Højgaard, L.; Kjaer, A. *J. Nucl. Med.* **2010**, *51*, 704.
(20) Pentlow, K. S.; Graham, M. C.; Lambrecht, R. M.; Daghighian, F.; Bacharach, S. L.; Bendriem, B.; Finn, R. D.; Jordan, K.; Kalaigian, H.; Karp, J. S.; Robeson, W. R.; Larson, S. M. *J. Nucl. Med.* **1996**, *37*, 1557.
(21) Wester, H.-J. *Clin. Cancer Res.* **2007**, *13*, 3470.
(22) Eckelman, W. C. *Nucl. Med. Biol.* **1998**, *25*, 169.
(23) Liu, S.; Edwards, D. S. *Chem. Rev.* **1999**, *99*, 2235.
(24) Hulme, E. C.; Trevethick, M. A. *Br. J. Pharmacol.* **2010**, *161*, 1219.
(25) Eckelman, W. C.; Reba, R. C.; Gibson, R. E.; Rzeszotarski, W. J.; Vieras, F.; Mazaitis, J. K.; Francis, B. *J. Nucl. Med.* **1979**, *20*, 350.
(26) Patel, S.; Gibson, R. *Nucl. Med. Biol.* **2008**, *35*, 805.
(27) Eckelman, W. C.; Kilbourn, M. R.; Mathis, C. A. *Nucl. Med. Biol.* **2006**, *33*, 449.
(28) Eckelman, W. C.; Kilbourn, M. R.; Mathis, C. A. *Nucl. Med. Biol.* **2009**, *36*, 235.
(29) Ametamey, S. M.; Honer, M.; Schubiger, P. A. *Chem. Rev.* **2008**, *108*, 1501.
(30) Eckelman, W. C.; Mathis, C. A. *Nucl. Med. Biol.* **2006**, *33*, 161.
(31) Vanessa Gómez-Vallejo, V. G., Jacek Koziorowski and Jordi Llop *Specific Activity of 11C-Labelled Radiotracers: A Big Challenge for PET Chemists, Positron Emission Tomography - Current Clinical and Research Aspects*, 2012.
(32) Chopra, A.; Shan, L.; Eckelman, W. C.; Leung, K.; Menkens, A. E. *Nucl. Med. Biol.* **2011**, *38*, 1079.
(33) Hunter, D. H.; Zhu, X. *J. Labelled Comp. Radiopharm* **1999**, *42*, 653.
(34) Donovan, A.; Forbes, J.; Dorff, P.; Schaffer, P.; Babich, J.; Valliant, J. F. *J. Am. Chem. Soc.* **2006**, *128*, 3536.
(35) Fass, L. *Mol. Oncol.* **2008**, *2*, 115.
(36) Mankoff, D. A.; O'Sullivan, F.; Barlow, W. E.; Krohn, K. A. *Acad. Radiol.* **2007**, *14*, 398.
(37) Eisenhauer, E. A.; Therasse, P.; Bogaerts, J.; Schwartz, L. H.; Sargent, D.; Ford, R.; Dancey, J.; Arbuck, S.; Gwyther, S.; Mooney, M.; Rubinstein, L.; Shankar, L.; Dodd, L.; Kaplan, R.; Lacombe, D.; Verweij, J. *Eur. J. Cancer* **2009**, *45*, 228.
(38) Wahl, R. L.; Jacene, H.; Kasamon, Y.; Lodge, M. A. *J. Nucl. Med.* **2009**, *50*, 122S.
(39) Chaffer, C. L.; Weinberg, R. A. *Science* **2011**, *331*, 1559.
(40) Rawlings, N. D.; Tolle, D. P.; Barrett, A. J. *Nucleic Acids Res.* **2004**, *32*, D160.
(41) Lee, M.; Fridman, R.; Mobashery, S. *Chem. Soc. Rev.* **2004**, *33*, 401.
(42) McIntyre, J. O.; Matrisian, L. M. *J. Cell. Biochem.* **2003**, *90*, 1087.
(43) Koblinski, J. E.; Ahram, M.; Sloane, B. F. *Clin. Chim. Acta* **2000**, *291*, 113.
(44) Kessenbrock, K.; Plaks, V.; Werb, Z. *Cell* **2010**, *141*, 52.

(45) Yang, Y.; Hong, H.; Zhang, Y.; Cai, W. *Cancer Growth and Metastasis* **2009**, *2*, 13.
(46) Mohamed, M. M.; Sloane, B. F. *Nat Rev Cancer* **2006**, *6*, 764.
(47) Glunde, K.; Pathak, A. P.; Bhujwalla, Z. M. *Trends Mol. Med.* **2007**, *13*, 287.
(48) Allgayer, H. *Eur. J. Cancer* **2006**, *42*, 811.
(49) Weissleder, R.; Tung, C.-H.; Mahmood, U.; Bogdanov, A. *Nat Biotech* **1999**, *17*, 375.
(50) Tung, C.-H.; Bredow, S.; Mahmood, U.; Weissleder, R. *Bioconjugate Chem.* **1999**, *10*, 892.
(51) Galande, A. K.; Hilderbrand, S. A.; Weissleder, R.; Tung, C.-H. *J. Med. Chem.* **2006**, *49*, 4715.
(52) Bremer, C.; Bredow, S.; Mahmood, U.; Weissleder, R.; Tung, C.-H. *Radiology* **2001**, *221*, 523.
(53) Lee, S.; Cha, E.-J.; Park, K.; Lee, S.-Y.; Hong, J.-K.; Sun, I.-C.; Kim, S. Y.; Choi, K.; Kwon, I. C.; Kim, K.; Ahn, C.-H. *Angew. Chem.* **2008**, *120*, 2846.
(54) Jiang, T.; Olson, E. S.; Nguyen, Q. T.; Roy, M.; Jennings, P. A.; Tsien, R. Y. *Proc. Natl. Acad. Sci. U.S.A.* **2004**, *101*, 17867.
(55) de Roos, A.; Doornbos, J.; Baleriaux, D.; Bloem, H. L.; Falke, T. H. *Magnetic resonance annual* **1988**, 113.
(56) Thorek, D. L.; Chen, A. K.; Czupryna, J.; Tsourkas, A. *Ann. Biomed. Eng*. **2006**, *34*, 23.
(57) Jastrzębska, B.; Lebel, R. j.; Therriault, H. l. n.; McIntyre, J. O.; Escher, E.; Guérin, B.; Paquette, B.; Neugebauer, W. A.; Lepage, M. *J. Med. Chem.* **2009**, *52*, 1576.
(58) Giersing, B. K.; Rae, M. T.; CarballidoBrea, M.; Williamson, R. A.; Blower, P. J. *Bioconjugate Chem.* **2001**, *12*, 964.
(59) Kulasegaram, R.; Giersing, B.; Page, C. J.; Blower, P. J.; Williamson, R. A.; Peters, B. S.; O'Doherty, M. J.; Kulasegaram, R.; Giersing, B.; Page, C. J.; Blower, P. J.; Williamson, R. A.; Peters, B. S.; O'Doherty, M. J. *Eur J Nucl Med.* **2001**, *28*, 756.
(60) Wagner, S.; Breyholz, H.-J.; Höltke, C.; Faust, A.; Schober, O.; Schäfers, M.; Kopka, K. *Appl. Radiat. Isot.* **2009**, *67*, 606.
(61) Fei, X.; Zheng, Q.-H.; Liu, X.; Wang, J.-Q.; Sun, H. B.; Mock, B. H.; Stone, K. L.; Miller, K. D.; Sledge, G. W.; Hutchins, G. D. *Bioorg. Med. Chem. Lett.* **2003**, *13*, 2217.
(62) Li, Y.; Ting, R.; Harwig, C. W.; auf dem Keller, U.; Bellac, C. L.; Lange, P. F.; Inkster, J. A. H.; Schaffer, P.; Adam, M. J.; Ruth, T. J.; Overall, C. M.; Perrin, D. M. *MedChemComm* **2011**, *2*, 942.

(63) Oltenfreiter, R.; Staelens, L.; Lejeune, A.; Dumont, F.; Frankenne, F.; Foidart, J.-M.; Slegers, G. *Nucl. Med. Biol.* **2004**, *31*, 459.
(64) Kuhnast, B.; Bodenstein, C.; Wester, H. J.; Weber, W. *J. Labelled Comp. Radiopharm.* **2003**, *46*, 539.
(65) Matusiak, N.; van Waarde, A.; Bischoff, R.; Oltenfreiter, R.; van de Wiele, C.; Dierckx, R. A.; Elsinga, P. H. *Curr. Pharm. Des.* **2013**, *19*, 4647.
(66) Pillay, V.; Dass, C. R.; Choong, P. F. M. *Trends Biotechnol.* **2007**, *25*, 33.
(67) Crippa, M. P. *Int. J. Biochem. Cell Biol.* **2007**, *39*, 690.
(68) Dass, K.; Ahmad, A.; Azmi, A. S.; Sarkar, S. H.; Sarkar, F. H. *Cancer Treat Rev* **2008**, *34*, 122.
(69) Ulisse, S.; Baldini, E.; Sorrenti, S.; D'Armiento, M. *Curr. Cancer Drug Targets* **2009**, *9*, 32.
(70) Weigelt, B.; Peterse, J. L.; van't Veer, L. J. *Nat Rev Cancer* **2005**, *5*, 591.
(71) Look, M. P.; van Putten, W. L. J.; Duffy, M. J.; Harbeck, N.; Christensen, I. J.; Thomssen, C.; Kates, R.; Spyratos, F.; Fernö, M.; Eppenberger-Castori, S.; Sweep, C. G. J. F.; Ulm, K.; Peyrat, J.-P.; Martin, P.-M.; Magdelenat, H.; Brünner, N.; Duggan, C.; Lisboa, B. W.; Bendahl, P.-O.; Quillien, V.; Daver, A.; Ricolleau, G.; Meijer-van Gelder, M. E.; Manders, P.; Fiets, W. E.; Blankenstein, M. A.; Broët, P.; Romain, S.; Daxenbichler, G.; Windbichler, G.; Cufer, T.; Borstnar, S.; Kueng, W.; Beex, L. V. A. M.; Klijn, J. G. M.; O'Higgins, N.; Eppenberger, U.; Jänicke, F.; Schmitt, M.; Foekens, J. A. *J. Natl. Cancer Inst.* **2002**, *94*, 116.
(72) Harris, L.; Fritsche, H.; Mennel, R.; Norton, L.; Ravdin, P.; Taube, S.; Somerfield, M. R.; Hayes, D. F.; Bast, R. C. *JCO* **2007**, *25*, 5287.
(73) Rockway, T. W. *Expert Opin. Ther. Pat.* **2003**, *13*, 773.
(74) Schechter, I.; Berger, A. *Biochem. Biophys. Res. Commun.* **1967**, *27*, 157.
(75) Katz, B. A.; Mackman, R.; Luong, C.; Radika, K.; Martelli, A.; Sprengeler, P. A.; Wang, J.; Chan, H.; Wong, L. *Chem. Biol.* **2000**, *7*, 299.
(76) Katz, B. A.; Sprengeler, P. A.; Luong, C.; Verner, E.; Elrod, K.; Kirtley, M.; Janc, J.; Spencer, J. R.; Breitenbucher, J. G.; Hui, H.; McGee, D.; Allen, D.; Martelli, A.; Mackman, R. L. *Chem. Biol.* **2001**, *8*, 1107.
(77) Wendt, M. D.; Geyer, A.; McClellan, W. J.; Rockway, T. W.; Weitzberg, M.; Zhao, X.; Mantei, R.; Stewart, K.; Nienaber, V.; Klinghofer, V.; Giranda, V. L. *Bioorg. Med. Chem. Lett.* **2004**, *14*, 3063.
(78) Wendt, M. D.; Rockway, T. W.; Geyer, A.; McClellan, W.; Weitzberg, M.; Zhao, X.; Mantei, R.; Nienaber, V. L.; Stewart, K.; Klinghofer, V.; Giranda, V. L. *J. Med. Chem.* **2003**, *47*, 303.
(79) Vassalli, J.-D.; Belin, D. *FEBS Lett.* **1987**, *214*, 187.

(80) Sperl, S.; Jacob, U.; Arroyo de Prada, N.; Stürzebecher, J.; Wilhelm, O. G.; Bode, W.; Magdolen, V.; Huber, R.; Moroder, L. *Proc. Natl. Acad. Sci.* **2000**, *97*, 5113.

(81) Stürzebecher, J.; Vieweg, H.; Steinmetzer, T.; Schweinitz, A.; Stubbs, M. T.; Renatus, M.; Wikström, P. *Bioorg. Med. Chem. Lett.* **1999**, *9*, 3147.

(82) Bridges, A. J.; Lee, A.; Schwartz, C. E.; Towle, M. J.; Littlefield, B. A. *Bioorg. Med. Chem.* **1993**, *1*, 403.

(83) Barber, C. G.; Dickinson, R. P.; Horne, V. A. *Bioorg. Med. Chem. Lett.* **2002**, *12*, 181.

(84) Barber, C. G.; Dickinson, R. P.; Fish, P. V. *Bioorg. Med. Chem. Lett.* **2004**, *14*, 3227.

(85) Fish, P. V.; Barber, C. G.; Brown, D. G.; Butt, R.; Collis, M. G.; Dickinson, R. P.; Henry, B. T.; Horne, V. A.; Huggins, J. P.; King, E.; O'Gara, M.; McCleverty, D.; McIntosh, F.; Phillips, C.; Webster, R. *J. Med. Chem.* **2007**, *50*, 2341.

(86) Verner, E.; Katz, B. A.; Spencer, J. R.; Allen, D.; Hataye, J.; Hruzewicz, W.; Hui, H. C.; Kolesnikov, A.; Li, Y.; Luong, C.; Martelli, A.; Radika, K.; Rai, R.; She, M.; Shrader, W.; Sprengeler, P. A.; Trapp, S.; Wang, J.; Young, W. B.; Mackman, R. L. *J. Med. Chem.* **2001**, *44*, 2753.

(87) Mackman, R. L.; Hui, H. C.; Breitenbucher, J. G.; Katz, B. A.; Luong, C.; Martelli, A.; McGee, D.; Radika, K.; Sendzik, M.; Spencer, J. R.; Sprengeler, P. A.; Tario, J.; Verner, E.; Wang, J. *Bioorg. Med. Chem. Lett.* **2002**, *12*, 2019.

(88) Künzel, S.; Schweinitz, A.; Reißmann, S.; Stürzebecher, J.; Steinmetzer, T. *Bioorg. Med. Chem. Lett.* **2002**, *12*, 645.

(89) Zeslawska, E.; Jacob, U.; Schweinitz, A.; Coombs, G.; Bode, W.; Madison, E. *J. Mol. Biol.* **2003**, *328*, 109.

(90) Tamura, S. Y.; Weinhouse, M. I.; Roberts, C. A.; Goldman, E. A.; Masukawa, K.; Anderson, S. M.; Cohen, C. R.; Bradbury, A. E.; Bernardino, V. T.; Dixon, S. A.; Ma, M. G.; Nolan, T. G.; Brunck, T. K. *Bioorg. Med. Chem. Lett.* **2000**, *10*, 983.

(91) Joossens, J.; Van der Veken, P.; Surpateanu, G.; Lambeir, A. M.; El-Sayed, I.; Ali, O. M.; Augustyns, K.; Haemers, A. *J. Med. Chem.* **2006**, *49*, 5785.

(92) Wakselman, M.; Xie, J.; Mazaleyrat, J. P.; Boggetto, N.; Vilain, A. C.; Montagne, J. J.; Reboud-Ravaux, M. *J. Med. Chem.* **1993**, *36*, 1539.

(93) Appella, E.; Blasi, F. *Ann. N. Y. Acad. Sci.* **1987**, *511*, 192.

(94) Persson, M.; Kjaer, A. *Clin Physiol Funct Imaging.* **2013**, *33*, 329.

(95) Liu, D.; Overbey, D.; Watkinson, L.; Giblin, M. F. *Bioconjugate Chem.* **2009**, *20*, 888.

(96) Armstrong, A. F.; Lemon, J. A.; Czorny, S. K.; Singh, G.; Valliant, J. F. *Nucl. Med. Biol.* **2009**, *36*, 907.

(97) Yang, L.; Peng, X.-H.; Wang, Y. A.; Wang, X.; Cao, Z.; Ni, C.; Karna, P.; Zhang, X.; Wood, W. C.; Gao, X.; Nie, S.; Mao, H. *Clin. Cancer Res.* **2009**, *15*, 4722.

(98) Lin, L.; Gårdsvoll, H.; Huai, Q.; Huang, M.; Ploug, M. *J. Biol. Chem.* **2010**, *285*, 10982.

(99) Abdalla, M. O.; Karna, P.; Sajja, H. K.; Mao, H.; Yates, C.; Turner, T.; Aneja, R. *J. Control. Release* **2011**, *149*, 314.

(100) Law, B.; Curino, A.; Bugge, T. H.; Weissleder, R.; Tung, C.-H. *Chem. Biol.* **2004**, *11*, 99.

(101) Augustyns, K. V. D. V., Pieter. Messagie, Jonas. Joossens, Jurgen. Malbeir, Anne-Marie; A61K 49/00 (2006.01)
C07F 9/40 (2006.01) ed.; Organization, W. I. P., Ed. BE, 2012.

(102) Al-Ejeh, F.; Croucher, D.; Ranson, M. *Exp. Cell. Res.* **2004**, *297*, 259.

(103) Kruithof, E.; Baker, M.; Bunn, C. *Blood* **1995**, *86*, 4007.

(104) Ranson, M.; Berghofer, P.; Vine, K. L.; Greguric, I.; Shepherd, R.; Katsifis, A. *Nucl. Med. Biol.* **2012**, *39*, 833.

(105) Stutchbury, T. K.; Al-ejeh, F.; Stillfried, G. E.; Croucher, D. R.; Andrews, J.; Irving, D.; Links, M.; Ranson, M. *Mol. Cancer Ther.* **2007**, *6*, 203.

(106) LeBeau, AM.; Duriseti, S.; Murphy, ST.; Pepin, F.; Hann, B.; Gray, JW.; van Brocklin, HF.; Craik, CS. *Cancer Res.* **2013**, *73*, 207.

Chapter 2 – Derivatization of Phenylguanidine-based Inhibitors for Use as uPA Imaging Agents

2.1. Introduction

A series of compounds bearing a phenylguanidine moiety[1] have been investigated as reversible uPA inhibitors.[2] For example, phenylguanidine (**1**) has been reported[3,4] to inhibit uPA with a K_i of 20 μM, while benzamidine (**2**) displayed a similar K_i of 19 μM and a lower selectivity towards other serine proteases. Several different spacers and linkers such as acyl, sulphonyl, urethane and ureido group have been attached to the phenylguanidine group in an attempt to enhance potency. Derivatives of (4-aminomethyl) phenylguanidine (**4**), (**5**), and (**7**) were found to bind uPA in micromolar range with a high specificity while analogue (**3**) and the sulphonyl derivative (**6**) lost inhibitory activity.[2]

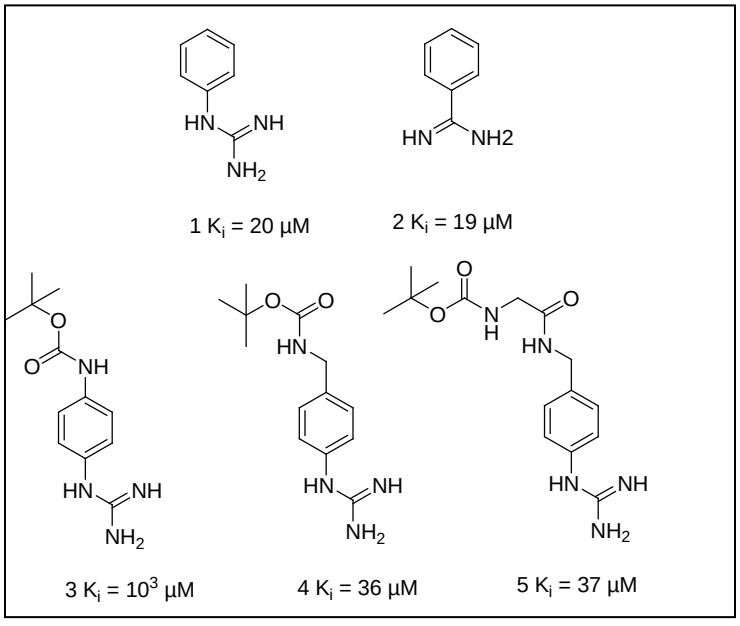

Silvia Albu synthesized all compounds, while the screening was performed by Dr. Lemon

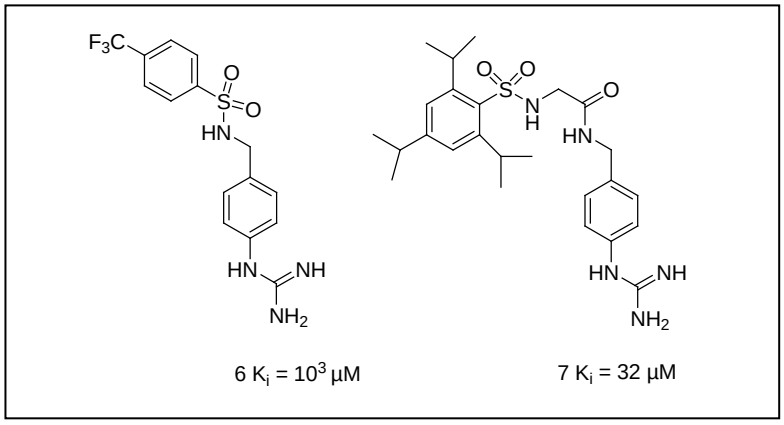

Figure 2.1. Optimization of hydrophobic moiety.[2]

The chemical space related to 4-(*N*-Boc-aminomethyl) phenylguanidine (**4**) was further explored. The hydrophobic moiety was optimized and the most potent compound from the series was found to be 4-(*N*-adamantyloxycarbonyl-aminomethyl-) phenylguanidine (**9** with a K_i = 2.4 µM). Selectivity for uPA was maintained while inhibition of plasmin, thrombin, fXa, or trypsin was undetectable at concentrations up to 1.0 mM.

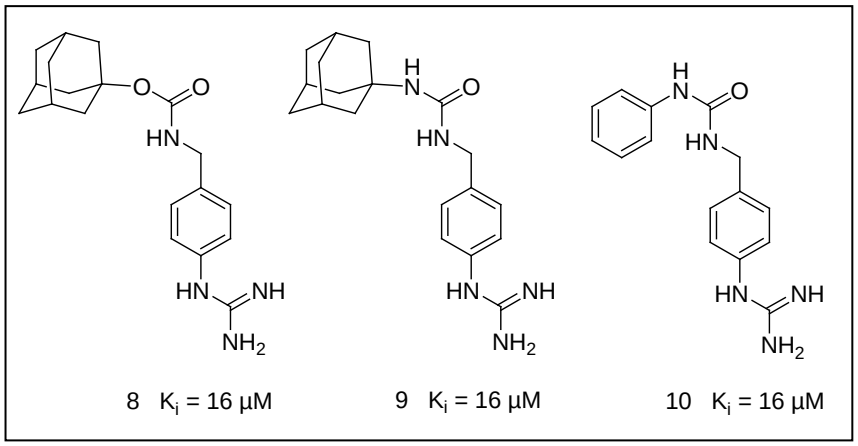

Figure 2.2. Optimization of the spacer group.[2]

The authors concluded that nature of the spacer affects uPA inhibition to a much greater extent than does the nature of the hydrophobic residue.[2] The nitrogen and the carbonyl oxygen of the urethane group were reported to be involved in hydrogen-bonding interactions with uPA. Replacement of the urethane moiety with the ureido group led to an improved potency due to an additional hydrogen bonding group.

The synthesis of the phenylguanidine inhibitors is outlined in Figure 2.3.[2] Protection of the alkylamino group as *tert*-butyloxycarbonyl (Boc) (to give (**12**)) or benzyloxycarbonyl (Cbz) derivative was to be selective due to its higher reactivity as compared to the aniline moiety. Introduction of the guanidinyl fragment (to give (**14**)) was achieved using *N*, *N*9-dibenzyloxycarbonyl-*N*O-triflylguanidine (**13**). Treatment with trifluoroacetic acid (TFA) allowed for orthogonal deprotection and the formation of (4-aminomethyl) phenyl-2, 3-di-Z-guanidine (**15**). Reaction with the various isocyanates (of the general formula (**16**)) and deprotection of the Cbz groups *via* hydrogenation over Pd/C allowed for preparation of the inhibitors (of the general structure (**18**)). Unfortunately, no experimental details for any of these transformations were provided in the paper.[2]

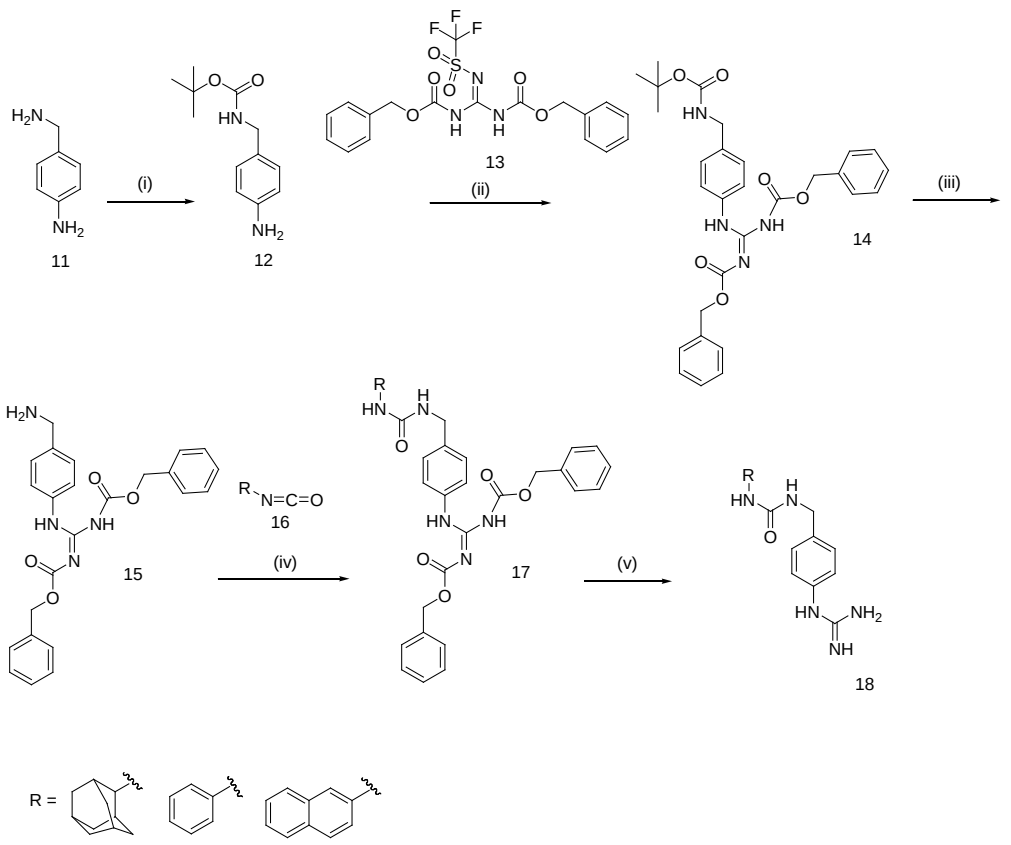

Figure 2.3. Reported phenylguanidine derivative synthesis. Reagents: (i) Boc_2O; (ii) Compound (**13**); (iii) TFA/DCM; (iv) RNCO; (v) H_2, Pd/C.

2.2. Objectives

The phenylguanidine compounds represented a useful model system to begin with to develop a MI probe for uPA. As has been previously discussed, several iodine radionuclides are used clinically for PET (^{124}I) and SPECT (^{123}I, ^{131}I). The goal was to develop a practical synthesis that allowed for the incorporation of iodine isotopes into the phenylguanidine derivatives and determination of the effect of the halogen has on uPA binding. With the present phenylguanidine system, there are a number of potential sites

for iodine incorporation including halogenation of the benzene ring (**19**) or as part of the substituent on the urea moiety (**18**) (Figure 2.4.). Our efforts focused on the former approach where the resulting iodinated phenylguanidines were screened for activity against uPA.

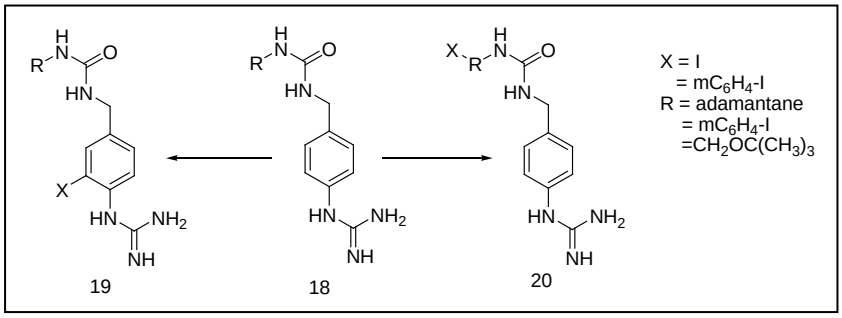

Figure 2.4. Proposed phenylguanidine derivatives.

In this way, these phenylguanidine compounds will allow us to develop robust synthetic methods for halogen and guanidinylation incorporation needed for other systems to be described elsewhere in the thesis. In addition, the relatively short syntheses needed for this series quickly provided compounds for the development of a suitable uPA binding assay.

2.3. Synthesis of iodinated of phenylguanidine inhibitors

A synthetic route suitable for the introduction of iodine into the phenyl ring of the

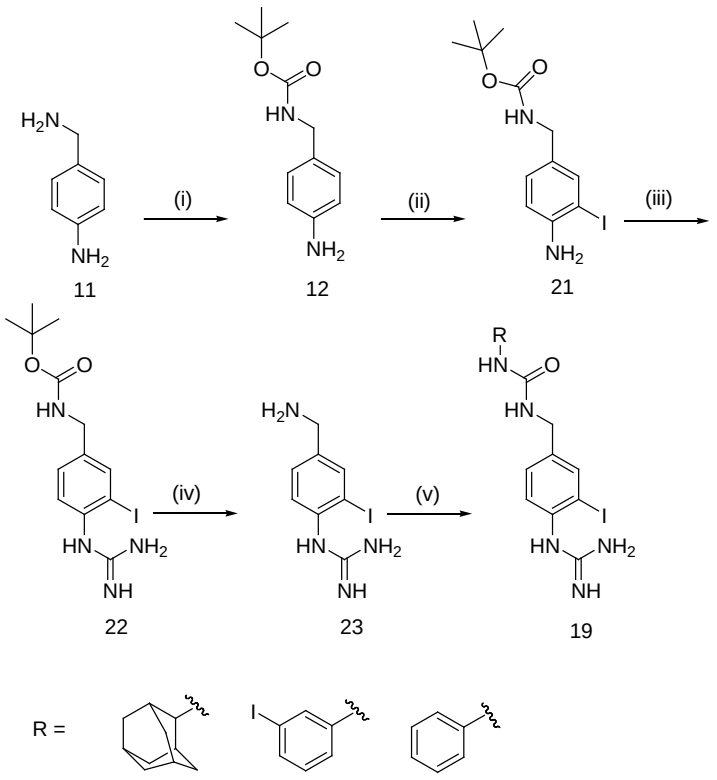

Figure 2.5. General synthesis of phenylguanidine library. Reagents: (i) Boc_2O, DCM; (ii) I_2 $CaCO_3$, MeOH; (iii) guanidination; (iv) TFA/DCM; (v) RNCO.

phenylguanidine scaffold is presented in Figure 2.5. Commercially available 4-aminobenzylamine (compound (**11**)) was selectively (Boc-) protected to give compound (**12**) using the approach described by Sperl *et al.*[2] in 65% yield. Subsequent iodination of the aromatic ring group (to give compound (**21**)) was achieved using I_2 in methanol in the presence of $CaCO_3$.

With compound (**21**) in hand, efforts turned to the introduction of the guandinyl moiety. In principle, guanidines can be synthesized by reaction of an amine with any one a series of electrophilic reagents including *S*-alkylisothioureas, protected thiourea derivatives[5-7] and pyrazole-1-carboxamidine derivatives.[8] In our case, however, the presence of the iodine substituent greatly deactivated the aniline. Initially, the published procedure for the guanidination of this class of inhibitors called for the use of *N*, *N′*-di-Cbz-*N″*-trifluoromethanesulfonyl-guanidine (**13**).[9] The reagent is not commercially available and was prepared *via* the synthesis presented in Figure 2.6. Protection of guanidine hydrochloride using Cbz-Cl generated *N*, *N′*-di-Cbz-guanidine (**24**) which could then be sulfonated using trific anhydride and sodium hydride to give the desired reagent (**13**). Unfortunately, when compound (**22**) was treated with (**13**), the desired product (**19**) was not formed and starting material was recovered.

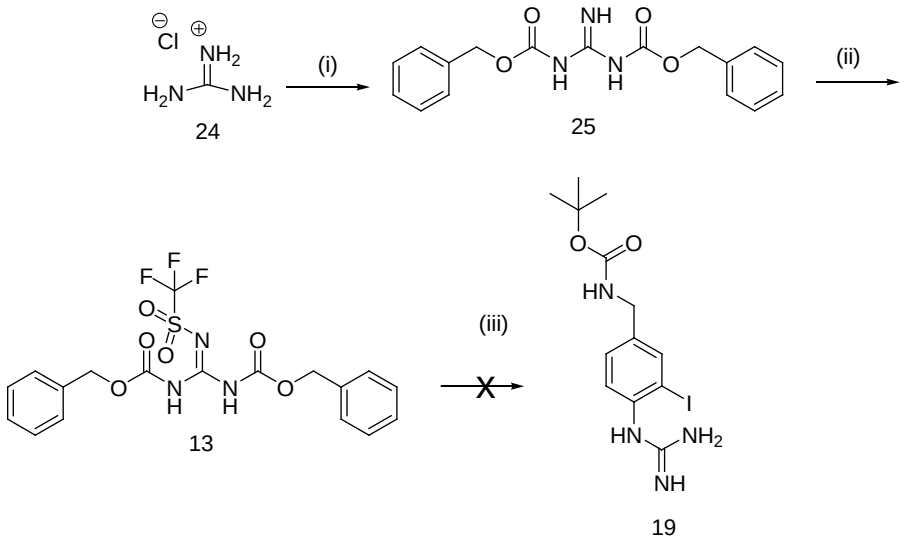

Figure 2.6. General synthesis of *N*, *N′*-di-Cbz-*N″*-trifluoromethanesulfonyl-guanidine. Reagents: (i) CbzCl, NaOH, DCM; (ii) Tf_2O, NaH, DCM; (iii) Compound (21) guanidination.

Thiourea (**26**) and isothiourea have been used previously in conjunction with mercury (II) chloride ($HgCl_2$)[10] or 2-chloro-1-methylpyridinium iodide (**27**, Mukaiyama`s reagent)[5-7] to affect guanidinylation. The guanidinylation of compound (**21**) was attempted using thiourea in the presence of both reagents and NEt_3 in a number of different solvents (such as DCM, methanol and DMF) but the reactions were unsuccessful. At higher temperatures decomposition of the starting material was observed.

Activation of S-methylisothiourea with an electron withdrawing group has been shown to improve reaction efficiency.[1] Combining S-methylisothiourea hemisulfate (**28**) with benzyl chloroformate gave the known N,N'-bis(benzyloxycarbony1)-S-methylisothiourea (**29**).[1] Unfortunately, treatment of amine (**15**) with (**29**) failed to give the desired guandinium compound. Use of another guanidinylation reagent, 1*H*-pyrazole-carboxamidine (**30**),[8] was also not successful.

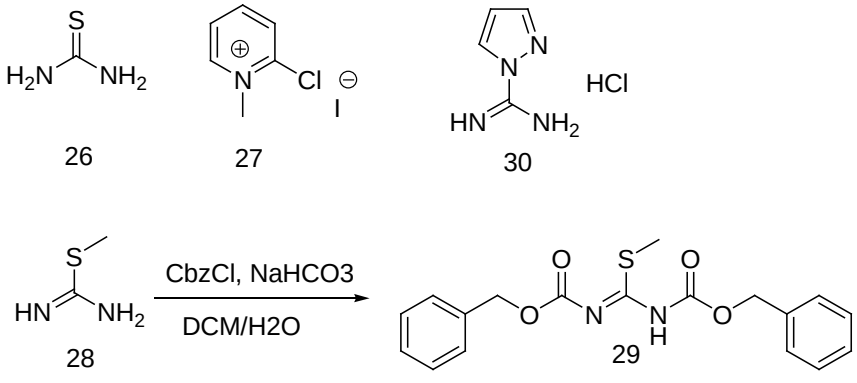

Figure 2.7. Guanidination reagents[1].

Summary of the reactions conditions attempted are described in Table 2.1.

Table 2.1. Conditions used in the attempted guanidination reactions.

Reagent	**Base**	**Additive**	**Solvent**	**Time/Temp**
N,N′ Di-Cbz-N″-Trifluoromethanesulfonyl-Guanidine (**13**) 1Eq, 0.3Eq, 3Eq	1eq, Et_3N	none	DCM	rt, 24h
				reflux, 24h
				mw, 80°C, 20min
	1eq, Et_3N	none	DMF	rt, 24h
				150 °C, 24h
	1eq, Et_3N	none	$CHCl_3$	Reflux, 48h
	none	none	DCM	Reflux, 48h
	0.3eq, Et_3N	none	DCM	Reflux, 48h
	3eq, Et_3N	none	DCM	Reflux, 48h
S-Methylisothiourea Sulfate (**28**) 1Eq, 0.3Eq, 3Eq	1eq, Et_3N	none	DCM	Reflux, 48h
	1eq, Et_3N	$HgCl_2$	DMF	80 °C, 24h mw, 80°C,120°C, 20min
	none	none	EtOH	
N,N′-di-benzyloxycarbonyl-S-methylisothioureea(**29**) 1Eq, 0.3Eq, 3Eq	1eq, Et_3N	$HgCl_2$	DMF	80 °C, 24h mw, 80°C,120°C, 20min
	3eq, Et_3N	$HgCl_2$	DMF	120°C, 20 min
Thiourea (**26**) 1Eq, 0.3Eq, 3Eq	1eq, DIPEA	Mukaiama's reagent	DCM	Reflux, 24h.
	1eq, Et_3N	Mukaiama's reagent	DMF	120 °C, 24h
	none	none	DCM	Reflux, 24h
4-benzyl-3,5-dimethyl-1*H*-pyrazole-1-carboxamidine (**30**)	3eq, Et_3N	no	DMF MeCN	mw, 90 °C, 20min 60
FmocNCS	none	none	DCM	rt ,12h

Ultimately, a successful approach involved the treatment of (**21**) with an etheral solution of HCl followed immediately by reaction with melted cyanamide. This method gave the desired guanidine (**22**) in 35% overall yield (Figure 2.8.). The low yield was attributed to the partial deprotection of the Boc group followed by guanidination of the benzylamine.

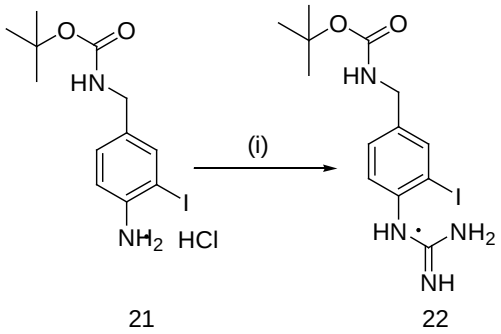

Figure 2.8. (i) Guanidination using cyanamide.

With scaffold (**22**) in hand, a general synthetic protocol for access to substituted ureas was developed (Figure 2.9.) in an effort to generate a library of iodinated guanidine compounds. Deprotection of the Boc-guanidino-intermediate was achieved using 95% TFA. The resultant salt was neutralized and used in the reaction with various isocyanates to prepare the final products with a general formula of (**19**). The chromatographic isolation was challenging due to the presence of the guanidine group and overall yields using this approach were low (5-15%).

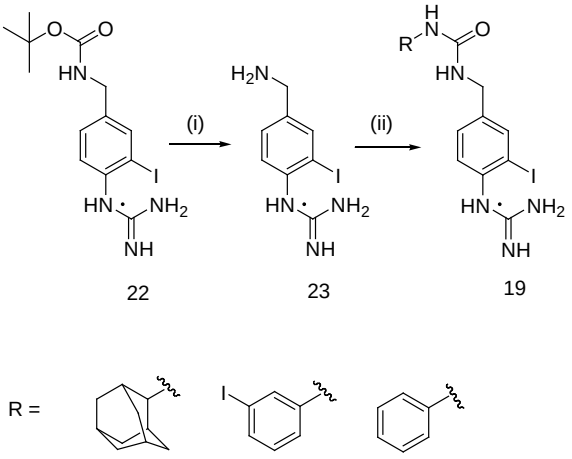

Figure 2.9. First synthetic route to iodinated phenylguanidine library: (i) TFA, DCM; (ii) RNCO, DCM.

As a result of the low yields, a second synthetic route (outlined in Figure 2.10.) in which the order of the two steps were reversed, allowed for the preparation of the target library (compounds with the general formula of (**19**)) in good yields. Deprotection of Boc 4-amino-3-iodobenzylamine (**21**) followed by selective coupling of the resultant phenylamine (**31**) with a series of isocyanates generated the phenylureas (**32**). Installation of the guanidine, to give compounds of the general formula (**19**), was achieved using the cyanamide protocol described above. The synthesized derivatives are presented in Table 2.2. The authenticity of the compounds was confirmed by NMR and HRMS. For compounds were iodine was inserted in the phenylguanidine ring (**21**, **22**, **31**, **36**, **37**, **38**, **39**, **40**) the ^{1}H NMR showed a characteristic trisubstituted pattern associated with the aromatic rings. A doublet with a coupling constant in the range between 1-2 Hz for the meta coupling, a doublet of doublet with coupling constants revelling an ortho coupling (7-8 Hz) and a meta coupling (1-2 Hz) and another doublet with an ortho coupling. The

Boc protected derivatives (**4**, **12**, **21**, **22**) where easily recognized from the singlet which integrated as 9H around 1.5 ppm and the adamantane group (**9**, **36**, **37**, **39**) showed a series of multiplets in the aliphatic region.

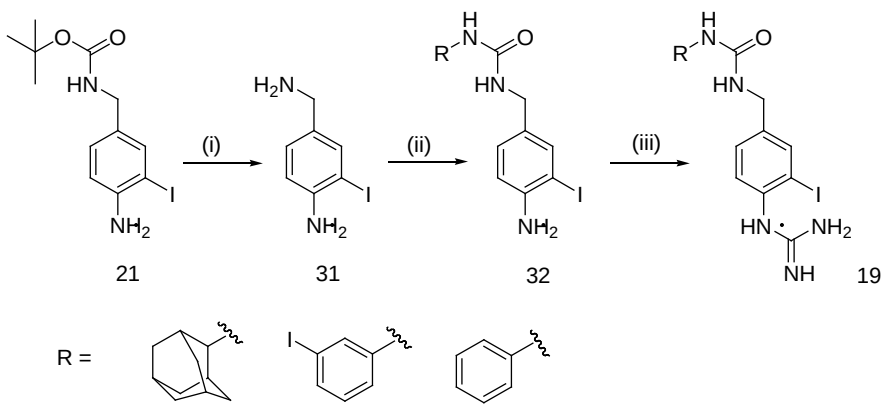

Figure 2.10. Second synthetic route to iodinated phenylguanidine library. (i)TFA,DCM; (ii) RNCO, DCM; (iii) HCl ether, cyanamide;

The analogous noniodinated compounds served as positive controls in the colorimetric assay and were synthesized using the series of reactions outlined in Figure 2.11. The structures of the noniodinated derivatives are presented in Table 2.2.

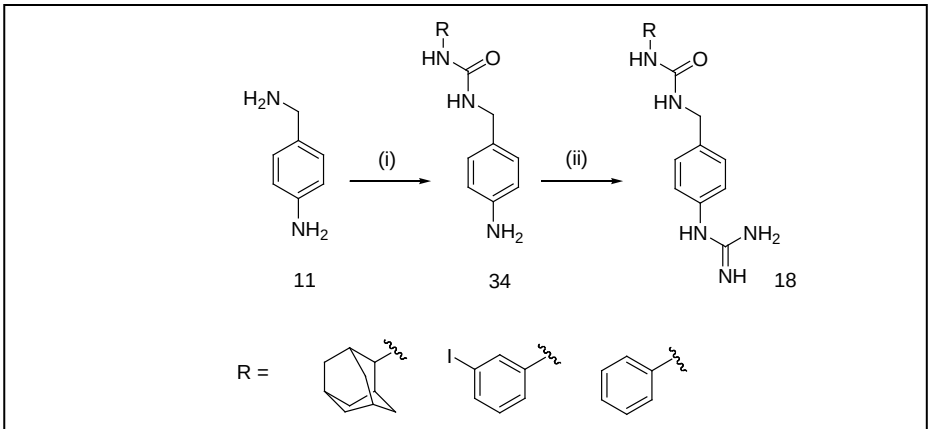

Figure 2.11. Synthetic route to noniodinated phenylguanidine.

Table 2.2. Synthesized phenylamine and phenylguanidine derivatives.

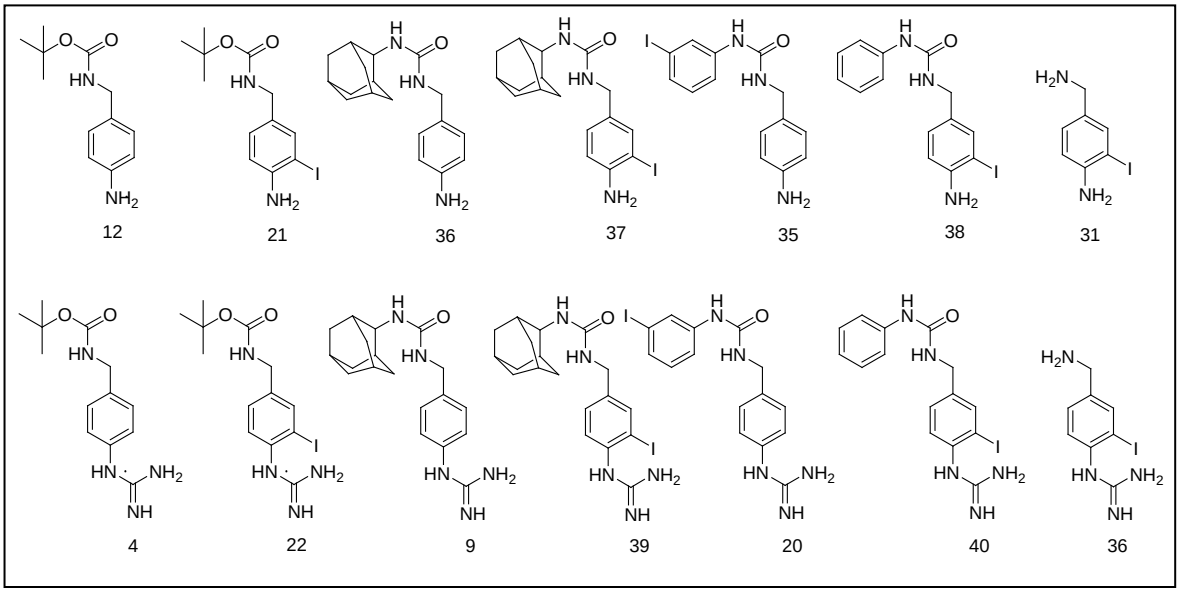

2.4. Biological evaluation of phenylguanidine inhibitors

Compounds (**4**, **22**, **9**, **39**, **20**, **40**, **36**) were evaluated using a known colorimetric binding assay and the results are presented in Table 2.3. uPA cleaves the chromogenic substrate pyro-Glu-Gly-Arg-*p*-nitroanilide (S-2444), to produce *p*-nitroaniline, whose concentration can be measured by monitoring at 405 nm. IC_{50} values were calculated from percent inhibition plotted against compound concentration and K_i was determined using the reported K_m value of 90 μM and equation Eq. 2.1.

$$K_i = IC_{50} / ((1 + ([S]/K_m)) \qquad (Eq.\ 2.1.)$$

The lead adamantane compound (**9**) and its iodinated analogue (**39**) were shown to have comparable binding affinities with IC_{50} = 43.6 μM and IC_{50} = 51.7 μM, respectively. The Boc iodinated derivative (**22**) was found to be less potent than its non-iodinated analogue

(**4**). Interestingly, the phenyl iodinated compound (**40**) was roughly two fold more potent than compound (**20**) where the iodine was placed in the benzyl ring. The binding affinity decreased considerably for iodinated derivative (**36**), which lacked the substituent on the amino group. Overall, however, given their IC_{50} values in the high μM range, these compounds are clearly not suitable candidates for development into uPA molecular imaging agent where IC_{50} values should be below 0.01 μM.

T**able 2.3.** IC_{50} values and K_i values for phenylguanidine uPA inhibitors.

Compound	**IC_{50} (μM)**	**K_i (μM)**
(**9**)	43.6	14.5
(**39**)	51.7	17.2
(**4**)	93.3	31.1
(**22**)	783.2	261.1
(**20**)	143.3	47.7
(**40)**	60.6	20.2
(**36**)	2076.0	692.0

2.5. Experimental

4-((Tert-butyloxycarbonyl)amino)benzylamine (12)

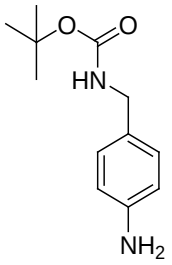

The synthesis was adapted from a procedure by Lee and coworkers. [11]

4-Aminobenzylamine (122 mg, 1.0 mmol) dissolved in DCM (10 ml), treated with di-*tert*-butyl dicarbonate (218 mg, 1 mmol) and stirred overnight. The solvent was evaporated under a reduced vacuum and the crude product purified by flash chromatography on silica gel (using a gradient (0–80% EtOAc in hexane) to provide 190 mg of a yellow solid (85% yield). Characterization data matched the data in the literature.[11]

^{1}H NMR (200 MHz, $CDCl_3$): 7.27 (s, 1H), 7.07 (d, J = 7.8 Hz, 2H), 6.79 (d, J = 7.8 Hz, 2H), 4.01 (d, J = 14.1Hz, 2H), 3.33 (s, 2H), 1.38 (s, 9H);

^{13}C NMR (50 MHz, $CDCl_3$): 155.9, 145.8, 129.0, 115.2, 79.4, 44.9, 28.6;

CI-HRMS: Calculated for $C_{12}H_{19}N_2O_2$ $[M]^+$: 223.1861. Found: 223.1860.

4-((tert-butyloxycarbonyl)-amino)-3-iodobenzylamine (21)

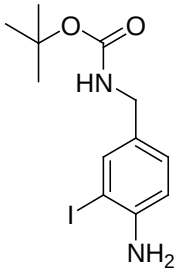

The synthesis was adapted from a procedure by Carson and coworkers [12].

4-((*tert*-Butyloxycarbonyl)amino)benzylamine (59 mg, 0.26 mmol) was treated with I_2 (135 mg, 0.53 mmol), $CaCO_3$ (33 mg, 0.33mmol), and MeOH (1 mL) and the mixture was stirred at 70°C for 16h. The reaction was then cooled to room temperature and the solvent was removed under vacuum. Saturated aqueous sodium bisulfite (10 ml) was added and extracted with ethyl acetate (3x10 ml). The crude product was purified multiple times (4) by flash chromatography on silica gel with gradient (0–80% EtOAc in hexane) to give 60 mg of a yellow sticky solid (43% yield). Characterization data matched the data in the literature.[12]

^{1}H NMR (600 MHz, $CDCl_3$): 7.54 (d, *J* = 1.8 Hz, 2H), 7.06 (dd, *J* = 8.1 Hz, *J* = 1.8 Hz 2H), 6.68 (d, *J* = 8.1 Hz, 2H), 4.16 (d, *J* = 14.1 Hz, 2H), 1.45 (s, 9H);

CI: Calculated for $C_{12}H_{17}IN_2O_2$ $[M]^+$: 349.1. Found: 349.1.

N-,N, Di-Cbz-Guanidine (25)

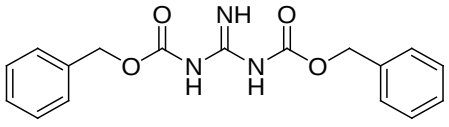

The synthesis was adapted from a procedure by Feichtinger and coworkers. [9]

To stirred solution of guanidine hydrochloride (382 mg, 4 mmol) in 80 ml diphasic mixture 1:1 DCM/0.2 M aqueous sodium hydroxide solution cooled to a 0^{O}C was added benzyloxy-carbonyl chloride (1.71 ml, 12 mmol). The mixture was stirred for 24h at 0°C and which time the aqueous layer was extracted with DCM (3x 30ml) then dried over magnesium sulphate. The solvent was removed under reduced pressure. The crude product was recrystallized from methanol to provide 984 mg (62%) yield. Characterization data matched the data in the literature.[9]

^{1}H NMR (200 MHz, DMSO): 7.01 (d, 2H,) 6.65 (d, 2H), 4.04 (s, 2H), 1.38 (s, 9H);

CI Calculated for $C_{17}H_{17}N_3O_4$ $[M]^+$: 327.3. Found: 327.1.

N, N' Di-Cbz-N''-Trifluoromethanesulfonyl-Guanidine (13)

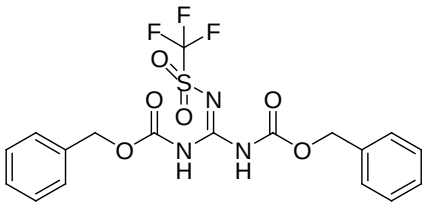

The synthesis was adapted from a procedure by Feichtinger and coworkers.[9]

To a 0°C cold solution of N-,N'-di-Cbz-guanidine (165 mg, 0.5 mmol) in anhydrous chlorobenzene (5 ml) sodium hydride (40 mg, 60% dispersion in mineral oil) was added. After stirring for 1h at 0°C, the mixture was cooled to -45°C and triflic anhydride (0.082 ml, 0.5 mmol) is added. The resulting mixture was stirred overnight at room temperature. The solvent was removed under reduced pressure and the residue dissolved in a mixture of ethyl acetate (100 ml) and 2M aqueous sodium bisulfate (25 ml). The organic layer was separated and washed with brine and dried over magnesium sulphate. After filtration

the solvent was removed under reduced pressure and the crude product was purified by flash chromatography on silica gel (gradient 0–100% eluent DCM/ethyl ether) to provide a transparent solid 125 mg (55%). Characterization data matched the data in the literature.[9]

^{1}H NMR (200 MHz, DMSO): 11.01 (brs, 2H), 7.48 (m, 10H), 5.20 (s, 4H);

CI-HRMS: Calculated for $C_{13}H_{17}F_3N_3O_6S$ $[M]^+$:459.0633. Found: 459.0631.

N, N'-di-benzyloxycarbonyl-S-methylisothioureea (29)

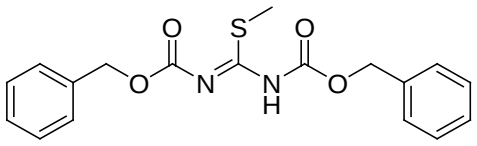

The synthesis was adapted from a procedure by Wang and coworkers.[13]

To a solution of S-methylthioureea (1.00g, 3.6mmol) in 40 ml diphasic mixture 1:1 DCM/saturated sodium bicarbonate aqueos solution is added benzyloxycarbonyl chloride (2 ml, 14.4 mmol). The mixture was stirred for 24h at room temperature. The aqueos layer was extracted with DCM (2 x 30 ml) dried over magnesium sulfate. The solvent was removed under reduced pressure. The product was purified by flash chromatography on silica gel (eluent DCM) providing 600 mg (47% yield). Characterization data matched the data in the literature.[13]

^{1}H NMR (200 MHz, DMSO): 11.91 (s, 1H) 7.42 (s, 10H), 5.24 (s, 4H), 2.46 (s, 3H);

CI Calculated for $C_{18}H_{19}N_2O_4S$ $[M]^+$:359.1 Found: 359.4.

4-Amino-3-iodobenzylamine (31)

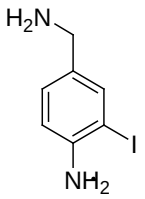

The synthesis was adapted from a procedure by Carson and coworkers.[12]

4-((Tert-butyloxycarbonyl)-amino)-3-iodobenzylamine (**21)** (174 mg, 0.5 mmol) was treated with TFA (0.4 mL) for 10 min at room temperature. TFA was removed under a flow of N_2. 4-amino-3-iodobenzylamine TFA salt was neutralized with saturated aq. NaOH and extracted with DCM (3 x 20 ml). The solvent was removed under reduced pressure and provided 105 mg of the desired compound (85%) yield which was used without further purification. Characterization data matched the data in the literature.[12]

^{1}H NMR (200 MHz, MeOD): 8.12 (s, 2H), 7.35 (d, *J* = 1.8 Hz, 1H), 7.11 (dd, *J* = 8.4 Hz, *J* = 1.8 Hz, 1H), 7.00 (d, *J* = 8.4 Hz, 1H), 3.95 (d, *J* = 5.2 Hz, 1H);

ES-HRMS: Calculated for $C_7H_9I\,N_2$ $[M]^+$:248.0. Found: 248.0.

General procedure (amine)

A solution of 4-amino-3-iodobenzylamine or 4-Amino-3-benzylamine (1 mmol) in 2.5 ml acetone was treated with different isocyanates (1 mmol) and stirred for 16h at room temperature. Solvent was removed under reduced pressure. The products were purified by flash chromatography on silica gel (gradient 0–100% eluent hexane/EtOAc).

The following derivatives have been synthesized:

N-(2-Iodo-phenyl)-N'-(4-benzylamine)-urea (35)

251 mg of a light yellow powder was obtained (68%).

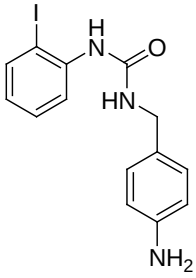

^{1}H NMR (200 MHz, MeOD): 7.88 (m, 2H), 7.29 (m, 2H), 7.06 (d, *J* = 8.4 Hz, 2H), 6.98 (dd, *J* = 8.4 Hz, *J* = 3.4 Hz, 1H), 6.70 (d, *J* = 8.4 Hz, 2H), 4.23 (s, 2H);

^{13}C NMR (50 MHz, MeOD): 152.1, 147.3, 140.5, 137.3, 128.7, 121.1, 117.7, 114.2, 82.9, 41.6;

ES-HRMS: Calculated for $C_{14}H_{15}IN_3O$ $[M]^+$: 368.0260. Found: 368.0281.

N-(-1-Adamantyl)-N'-(3-benzylamine)-urea (36)

240 mg of a light yellow powder was obtained (80%).

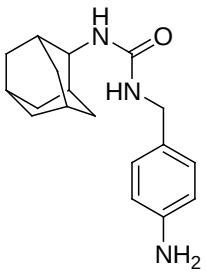

^{1}H NMR (200.33 MHz, $CDCl_3$): 7.01 (d, *J* = 8.2 Hz, 2H), 6.63 (d, *J* = 8.2 Hz, 2H), 4.13 (s, 2H), 2.04 (brs, 3H), 1.93 (brs, 6H), 1.60 (brs, 6H);

^{13}C NMR (600 MHz): 156.9, 147.2, 128.0, 113.9, 49.3, 42.3, 36.0, 35.9, 29.0, 28.8, 28.7;

ES-HRMS: Calculated for $C_{18}H_{26}N_3O$ $[M]^+$: 342.2076. Found: 342.2073.

N-(1-Adamantyl)-N'-(3-iodobenzylamine)-urea (37)

354 mg of a yellow powder was obtained (83%).

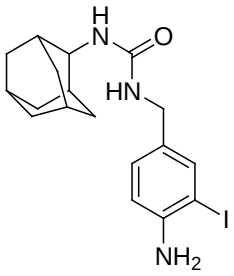

^{1}H NMR (600 MHz, $CDCl_3$): 7.54 (d, *J* =1.6 Hz, 1H), 7.06 (dd, *J* = 8.1 Hz, *J* = 1.6 Hz, 2H), 6.68 (d, *J* = 8.1 Hz, 2H), 4.14 (d, *J* = 5.0 Hz, 2H), 2.05 (s, 3H), 1.94 (s, 6H), 1.66 (s, 6H), 1.61 (s, 3H);

^{13}C NMR (150 MHz, MeOD): 157.0, 146.0, 138.1, 131.2, 129.1, 114.8, 84.1, 51.1, 43.3, 42.6, 36.5, 29.7;

ES-HRMS: Calculated for $C_{18}H_{25}IN_3O$ $[M]^+$: 426.1042. Found: 426.1047.

N-Phenyl-N'-(3-Iodo-4-benzylamine)-urea (38)

299 mg of a yellow powder was obtained (81%).

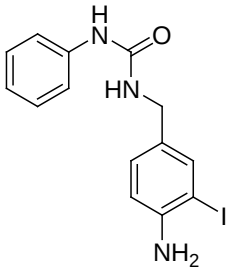

^{1}H NMR (200 MHz, DMSO): 8.48 (s, 1H), 7.48 (d, *J* = 1.2 Hz, 1H), 7.35 (dd, *J* = 8.4 Hz, *J* = 1.2 Hz 1H), 7.29 (m, 1H), 7.20 (m, 2H), 7.01 (d, *J* = 8.4 Hz, 1H), 6.87 (m, 1H), 4.09 (s, 2H);

^{13}C NMR (150 MHz, MeOD): 155.1, 147.3, 140.4, 137.3, 128.6, 128.5, 121.0, 117.6, 114.1, 82.9, 41.6;

ES-HRMS: Calculated for $C_{14}H_{15}IN_3O$ $[M]^+$: 368.0260. Found: 368.0251.

General procedure for guanidinylation:

Amine hydrochloride (1 mmol) was added to a melted cyanamide (10 mmol). The solution was stirred for 30 min to 2 hours at 90°C and then water (10 ml) was added. The solution was cooled to room temperature and washed with ethyl ether (10 ml). The organic phase was cooled in an ice water bath and treated with 10 M aq. NaOH (10 mL) and left in the fridge for 18h to crystallize. The resulting crystals were collected by filtration and washed with water. Drying in vacuo gave the desired products.

4-(tert-butyloxycarbonyl)-amino-4-benzylguanidine (4)

167 mg of a light yellow powder was obtained (63%).

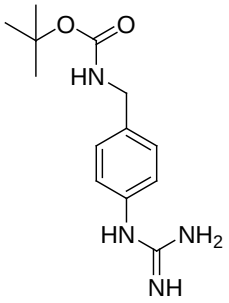

^{1}H NMR (600 MHz, DMSO): 7.01 (d, *J* = 7.9 Hz, 2H), 6.65 (d, *J* = 7.9 Hz, 2H), 4.04 (s, 2H), 1.38 (s, 9H);

^{13}C NMR (150 MHz, DMSO): 155.7, 152.4, 147.6, 132.2, 127.6, 122.6, 77.5, 43.0, 28.7;

ES-HRMS: Calculated for $C_{13}H_{21}N_4O_2$ $[M]^+$: 265.1665. Found: 265.1644.

N-(1- Adamantyl)-N′-(4-benzylguanidine)-urea (9)

286 mg of a light yellow powder was obtained (83%).

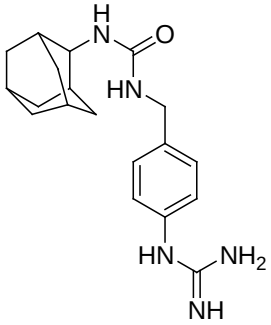

^{1}H NMR (600 MHz, MeOD): 7.21 (d, *J* = 8.1Hz, 2H), 6.94 (d, *J* = 8.1Hz, 2H), 4.20 (s, 2H), 2.04 (s, 3H), 1.97 (s, 6H), 1.70 (s, 6H);

^{13}C NMR (150 MHz, MeOD): 165.3, 160.1, 156.8, 136.7, 129.2, 125.4, 119.9, 51.5, 48.6, 44.0, 43.5, 37.6, 37.2, 31.0;

ES-HRMS: Calculated for $C_{19}H_{28}N_5O$ $[M]^+$: 342.2294. Found: 342.2286.

N-(2-iodophenyl)-N′-(4-benzylguanidine)-urea (20)

320 mg of a light yellow powder was obtained (78%).

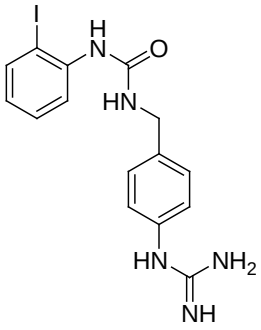

^{1}H NMR (200 MHz, MeOD): 7.88 (m, 2H), 7.29 (m, 2H), 7.06 (d, *J* = 8.4 Hz, 2H), 6.98 (dd, *J* = 8.4 Hz, *J* = 3.4 Hz, 1H), 6.70 (d, *J* = 8.4 Hz, 2H), 4.23 (s, 2H);

^{13}C NMR (150 MHz, DMSO): 175.1, 163.2, 155.7, 130.4, 128.6, 127.8, 125.4, 122.4, 118.7, 116.6, 42.1;

ES-HRMS: Calculated for $C_{15}H_{17}IN_5O$ $[M]^+$: 410.0478. Found: 410.0423.

4-((tert-butyloxycarbonyl)-amino)-3-iodobenzylguanidine (22)

258 mg of a yellow powder was obtained (66%).

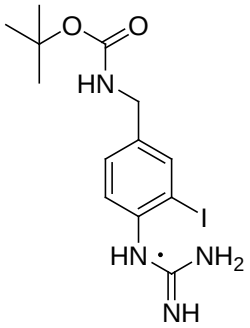

^{1}H NMR (600 MHz, MeOD): 7.78 (d, *J* = 1.8 Hz, 1H), 7.26 (dd, *J* = 8.2 Hz, *J* = 1.8 Hz, 1H), 7.04 (d, *J* = 1.8 Hz, 1H), 4.16 (s, 2H,), 1.45 (d, 1H);

^{13}C NMR (600 MHz, DMSO): 155.7. 151.2, 138.4, 137.5, 134.3, 128.1, 125.4, 122.8, 118.8, 95.2, 79.2, 42.9, 27.9;

ES-HRMS: Calculated for $C_{13}H_{20}IN_4O_2$ $[M]^+$:391.0631. Found: 391.0609.

4-amino-3-iodobenzylguanidine (36)

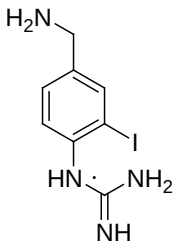

4-((Tert-butyloxycarbonyl)-amino)-3-iodobenzylguanidine (**22**) (195 mg, 0.5 mmol) treated with TFA (0.4 mL) for 10 min at room temperature. The excess of TFA was removed under nitrogen, 4-amino-3-iodobenzylamine TFA salt was, neutralized with saturated aq. NaOH (20 ml) and extracted with large amount of DCM 300-500 ml. The solvent was removed under reduced pressure and provided 62 mg of the desired compound as a yellow powder (42%).

^{1}H NMR (600 MHz, MeOD): 8.12 (d, *J* = 1.8 Hz, 1H) 7.58 (dd, *J* = 8.4 Hz, *J* = 1.8 Hz, 1H), 7.45 (d, *J* = 8.4 Hz, 1H), 4.14 (s, 2H);

^{13}C NMR (600 MHz, MeOD): 162.6. 158.1, 141.8, 138.8, 136.9, 100.2, 42.8;

ES-HRMS: Calculated for $C_8H_{12}IN_4$ $[M]^+$: 291.0107. Found: 291.0114.

N-(-1-Adamantyl)-N′-(3-iodobenzylguanidine)-urea (39)

280 mg of a yellow powder was obtained (60%).

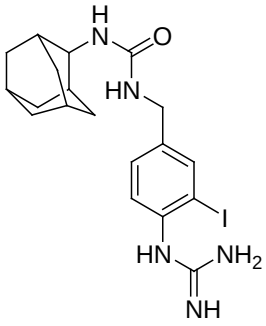

^{1}H NMR (600 MHz, MeOD): 7.73 (d, *J* = 1.6, 1H), 7.19 (dd, *J* = 8.0, *J* = 1.6, 1H), 6.93 (d, *J* = 8.0, 1H), 4.17 (s, 2H), 2.05 (s, 3H), 1.98 (s, 6H), 1.70 (s, 6H);

^{13}C NMR (150 MHz, MeOD): 160.0, 156.3, 149.2, 138.9, 129.9, 125.9, 97.7, 66.9, 51.3, 43.4, 43.2, 37.5, 31.0;

ES-HRMS: Calculated for $C_{19}H_{27}IN_5O$ $[M]^+$: 468.1260. Found: 468.1286.

N-phenyl-N′-(3-iodo-4-benzylguanidine)-urea (40)

273 mg of a light yellow powder was obtained (66%).

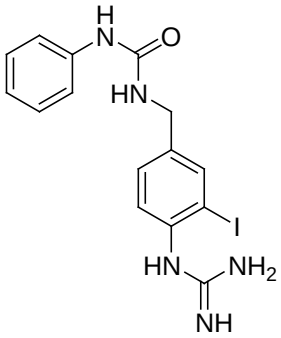

^{1}H NMR (600 MHz, MeOD): 7.83 (m, 1H), 7.36 (dd, *J* = 8.6, *J* = 1.6 Hz, 1H), 7.29 (m, 1H), 7.24 (m, 1H), 7.01 (m, 1H), 6.96 (m, 1H), 4.31 (s, 2H);

^{13}C NMR (150 MHz, DMSO):162.8, 155.1, 152.2, 151.0, 140.4, 137.0, 133.9, 128.6, 122.5, 121.0, 118.3, 117.6, 96.7, 41.5;

ES-HRMS: Calculated for $C_{15}H_{17}IN_5O$ $[M]^+$: 410.0478. Found: 410.0460.

Biological evaluation of phenylguanidine inhibitors

High molecular weight human uPA from urine, 3000 IU/vial (Calbiochem, 672081) and Chromogenic urokinase substrate pyro-Glu-Gly-Arg-*p*-nitroanilide (S-2444), 25 mg/vial. (Quadratech, 820357) were used for the colorimetric assay. The enzyme was reconstituted in H_2O to give 30000 IU/ and stored in the freezer -18°C and the Chromogenic substrate was as well reconstituted in H_2O to give 3 mM stock solution and stored at 4°C. uPA assay buffer consist of 75 mMTris, pH 8.1, 50 mM NaCl. IC_{50} and K_i values for compounds were determined based on incubation of 33 IU/mL uPA with 0.18 mM S-2444 (substrate) and various compounds concentrations in a final assay volume of 200 µL. The enzyme and the compounds were preincubated for 15 min at 37°C. The substrate was subsequently added to all wells and further incubated for 30 min at the same temperature. Upon addition of the substrate the course of the hydrolysis reaction was monitored by measuring the formation of *p*-nitroaniline. Absorbance was read at 405 nM and a background, time zero measurement was taken prior to the addition of the substrate, and measurements were continued for the following 30 min.

2.6. References:

(1) Bergeron, R. J.; McManis, J. S. *J. Org. Chem.* **1987**, *52*, 1700.
(2) Sperl, S.; Jacob, U.; Arroyo de Prada, N.; Stürzebecher, J.; Wilhelm, O. G.; Bode, W.; Magdolen, V.; Huber, R.; Moroder, L. *Proc. Natl. Acad. Sci.U.S.A.***2000**, *97*, 5113.
(3) Yang, H.; Henkin, J.; Kim, K. H.; Greer, J. *J. Med. Chem.* **1990**, *33*, 2956.
(4) Lee, M.; Fridman, R.; Mobashery, S. *Chem. Soc. Rev.* **2004**, *33*, 401.

(5) Nagashima, S.; Akamatsu, S.; Kawaminami, E.; Kawazoe, S.; Ogami, T.; Matsumoto, Y.; Okada, M.; Suzuki, K. I.; Tsukamoto, S. I. *Chem. Pharm. Bull.* **2001**, *49*, 1420.
(6) Vaidyanathan, G.; Shankar, S.; Affleck, D. J.; Alston, K.; Norman, J.; Welsh, P.; LeGrand, H.; Zalutsky, M. R. *Bioorg. Med. Chem* **2004**, *12*, 1649.
(7) Yong, Y. F.; Kowalski, J. A.; Lipton, M. A. *J. Org. Chem.* **1997**, *62*, 1540.
(8) Bernatowicz, M. S.; Wu, Y.; Matsueda, G. R. *J. Org. Chem.* **1992**, *57*, 2497.
(9) Feichtinger, K.; Zapf, C.; Sings, H. L.; Goodman, M. *J. Org. Chem.* **1998**, *63*, 3804.
(10) Kim, K. S.; Qian, L. *Tetrahedron Lett.* **1993**, *34*, 7677.
(11) Lee, J.; Lee, J.; Kang, M.; Shin, M.; Kim, J.-M.; Kang, S.-U.; Lim, J.-O.; Choi, H.-K.; Suh, Y.-G.; Park, H.-G.; Oh, U.; Kim, H.-D.; Park, Y.-H.; Ha, H.-J.; Kim, Y.-H.; Toth, A.; Wang, Y.; Tran, R.; Pearce, L. V.; Lundberg, D. J.; Blumberg, P. M. *J. Med. Chem.* **2003**, *46*, 3116.
(12) Carson, K. G.; Flynn, D. L.; Harriman, G. C. B.; Kolz, C. N.; Pham, L.; Roth, B. D.; Solomon, M. E.; Song, Y.; Sun, K. L.; Trivedi, B. K.; Google Patents: 2002.
(13) Wang, X.; Thottathil, J. *Tetrahedron: Asymmetry* **2000**, *11*, 3665.

Chapter 3 - Development of Naphthamidine-based Inhibitors as Imaging Agents of uPA

3.1. Introduction

A variety of naphthamidine-based uPA inhibitors have been reported and tested for their inhibitory potency against urokinase and related serine proteases.[1-4] Initial studies were based on the 2-naphthamidine scaffold (**1**) which showed good affinity for urokinase when compared with other aromatic amidines but modest specificity towards competitive proteases. The amidine group in the naphthamidine interacts with uPA through a salt bridge to the Asp189. Further study revealed that the S2, S4 and S3 subsites of trypsin-like serine protease could be exploited in the design of the associated inhibitors[3,5,6] for increased selectivity between targets. Thr97A and Leu97B present in urokinase are responsible for the small size of S4. Similarly, the bulky His99 reduces the size of S2.[7] The small size of the S2 and S4 sites in urokinase when compared with other trypsin-like serine proteases imposes several restrictions that have been exploited in the design small molecule inhibitors.[3]

Substitution at position 6 in the naphthamidine scaffold provides contact with the S1 site[3] of uPA. For example, naphthamidine derivative (**3**) bearing a phenyl amide in the 6-position displayed a significant improvement in inhibitory potency with a K_i = 0.631 μM compared with the unsubstituted naphthamidine.[3] The amide NH plays a key role in water-mediated hydrogen bonding to Ser214 while the amide carbonyl makes contact

Silvia Albu synthesized all compounds.

with Gln192.[3] The phenyl group accesses His57, and this interaction is probably responsible for the increased affinity. N-methylation resulted in inhibitor (**4**) which losses binding affinity due to steric factors. The most selective and potent inhibitor was shown to be the p-aminophenyl compound (**5**). The improved potency is a result of a salt bridge interaction between the Asp60A and amino group along with an extension into the S1 site.[3] While derivative (**6**) is even more potent, it loses selectivity against other related proteases.

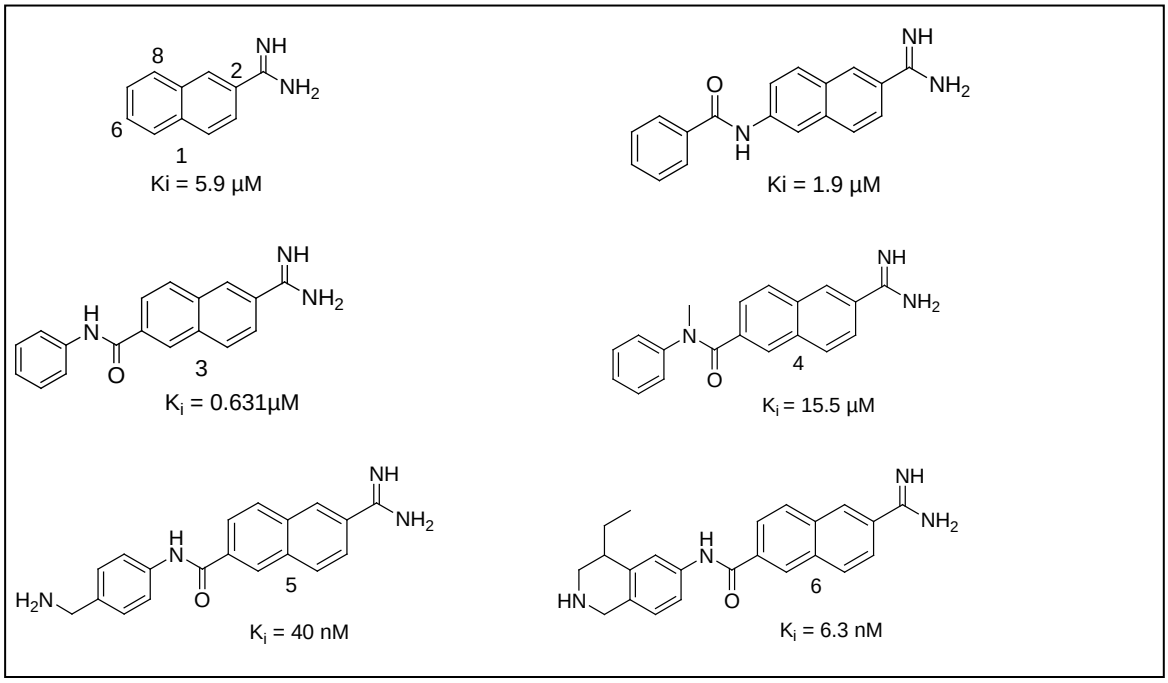

Figure 3.1. Inhibition profiles of 6 substituted 2-naphthamidine. For compound (**1**), numbers around the aromatic core indicate the different positions of substitution.

A study[1,4] on substitution at the 8-position of the naphthamidine core with various NH-linked aromatic rings and carbamates identified compound (**7**) as the most potent inhibitor from the series displaying a K_i = 35 nM. By appending an aminopyrimidine moiety at the 8-position, the S1 β binding pocket of uPA active site is accessed and the

binding affinity is greatly improved.[4] A significant increase in potency was observed by developing compounds with substitution at both the 6- and 8-sites[4,8] that take advantage of the cumulative effect in the binding affinities. Introduction of a phenyl amide substituent at position 6 and an aminopirymidyne at position 8 resulted in inhibitor (**8**) which posses a K_i = 2 nM and good selectivity against various proteases. Replacing the phenyl group with *p*-aminophenyl generates compound (**9**) that has even greater affinity in the picomolar range (K_i = 0.6 nM).[4]

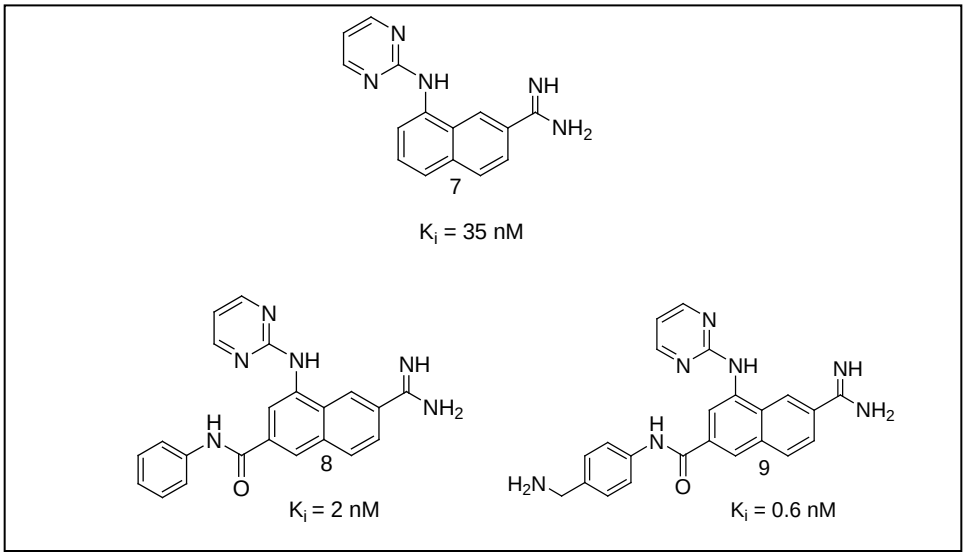

Figure 3.2. Inhibition profiles of 6,8-substituted 2-naphthamidines.

3.2. Objectives

The focus of the research described in this chapter was to develop a synthetic route that allows for the incorporation of an iodine into potent naphthamidine compounds (**5**), (**8**) and (**9**). In addition, compounds (**5**), (**8**) and (**9**) were also synthesized to serve as positive controls for *in vitro* testing. Although derivative (**5**) has a K_i = 40 nM, it was

chosen as the lead core due to its excellent selectivity for uPA against tPA, trypsin, plasmin and trombin.

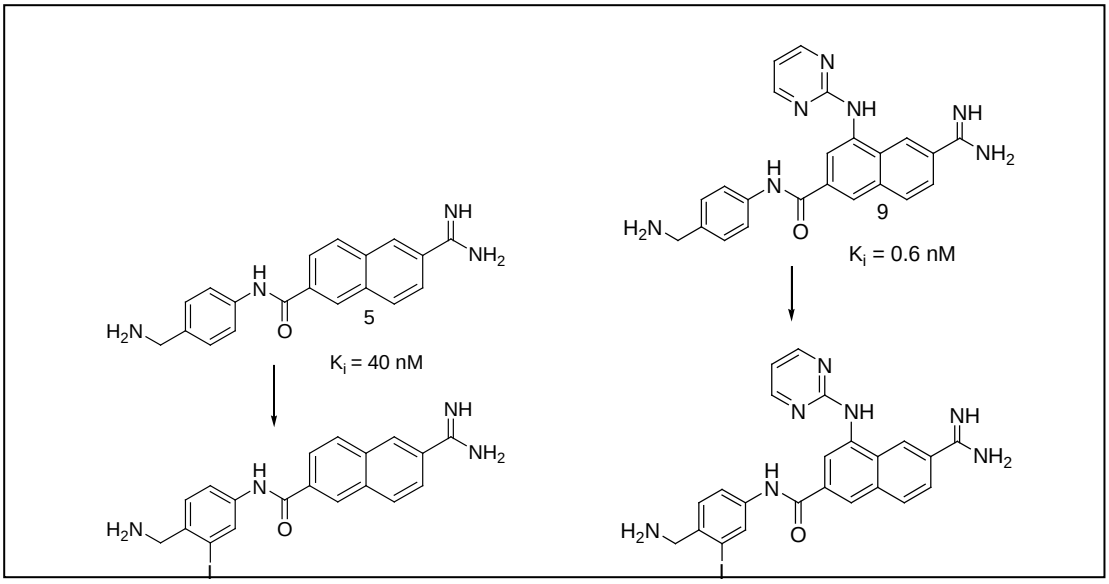

Figure 3.3. Proposed derivatization of naphthamidine inhibitors.

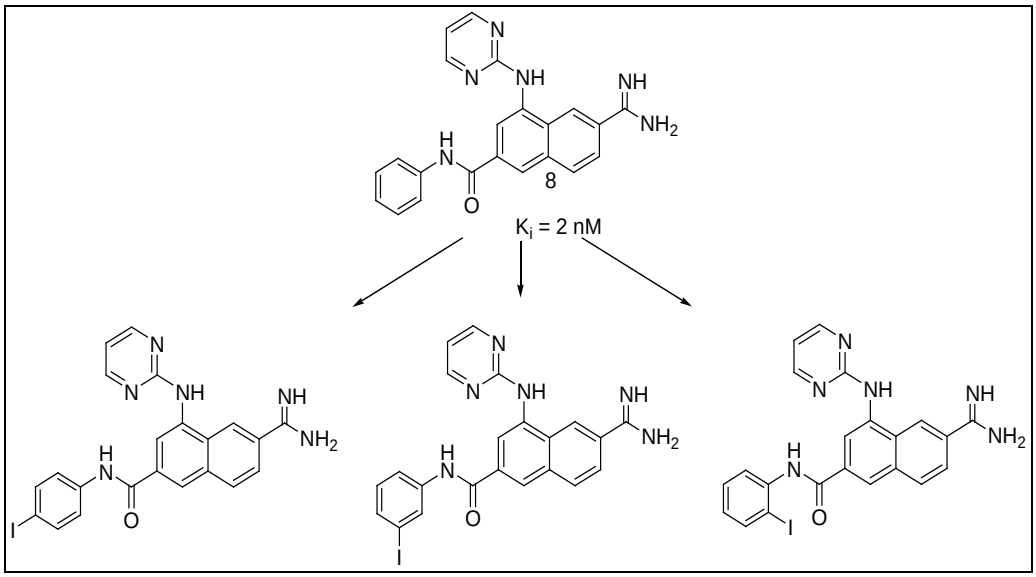

Figure 3.4. Second generation of derivatives naphthamidine inhibitors.

Prior to initiating synthetic work, the site of iodination was carefully considered. For compounds (**5**) and (**9**), introduction into the *p*-aminophenyl moiety *meta* to the amide (depicted in Figure 3.3.) was deemed the most synthetically tractable location. Similarly, for compound (**8**), substitution into the phenyl ring (as illustrated in Figure 3.4.) was chosen as the most straightforward strategy. For these targets the effects of *ortho*, *meta* and *para* substitution on binding efficiency could be investigated. Iodinated inhibitors along with their corresponding parent compound will be further evaluated for their binding affinities *in vitro*.

3.3. Synthesis of *N*-(4-(aminomethyl)phenyl)-6-carbamimidoyl-2-naphthamide

Initial efforts focused on the synthesis of compound (**5**). Despite the availability of a literature procedure,[3] its synthesis proved to be more difficult than originally envisioned. The route began with the commercially-available naphthamidine diester (**10**) which was saponified to give the mono ester using KOH. The monoacid derivative (**11**) was converted to the acid chloride (**12**) and treated subsequently with dry ammonia to yield the amide (**13**) which occurred in 86% yield. Unfortunately dehydration of the amide to its corresponding nitrile (**14**) using a TFAA/pyridine procedure described in the literature[3] was unsuccessful.

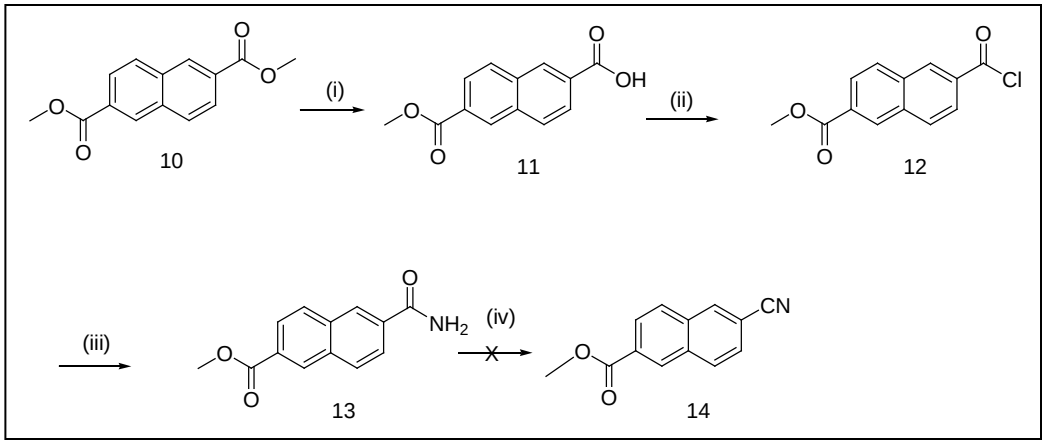

Figure 3.5. Attempted synthesis of compound (**14**). Reagents: (i) KOH, dioxane; (ii) $SOCl_2$, Toluene; (iii) dry NH_3; (iv) TFAA/pyridine; DMF.

An alternative route to nitrile (**14**) was investigated. Commercially-available (**15**) could be treated with cyanide and catalytic amount tetrakis(triphenylphosphine)-palladium(0) using microwave irradiation to promote a Pd-catalyzed cyanation. Table 3.1. summarizes the reaction parameters screened and illustrates the effect of cyanide source, solvent, reaction time and temperature on the yield of the reaction.

Table 3.1. Optimization of the reaction conditions for synthesis of (**14**).

Cyanate	**Solvent**	**Catalyst**	**Temp ^{o}C**	**Power**	**Time**	**Yield**
CuCN	DMF	$Pd[PPh_3]_4$	150	40W	10 min	6%
ZnCN	DMF	$Pd[PPh_3]_4$	150	40W	10 min	8%
CuCN	DMF	$Pd[PPh_3]_4$	165	150W	6 min	34%
ZnCN	DMF	$Pd[PPh_3]_4$	165	150W	6 min	28%
ZnCN	NMP	$Pd[PPh_3]_4$	165	150W	6 min	42%
CuCN	NMP	no catalyst	165	150W	6 min	82%

Interestingly, optimal yields were obtained in the absence of any Pd catalyst at 165° C in NMP in 6 min. (82-92% yield).[9] Saponification under basic conditions using LiOH quantitatively gave the desired cyanoacid (**16**).

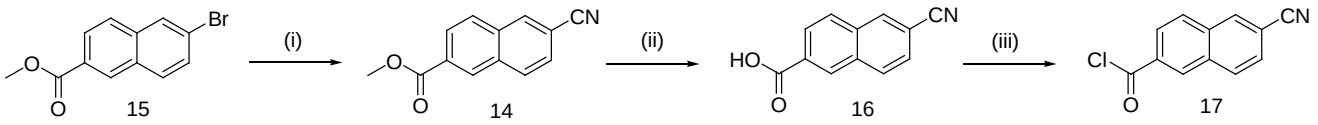

Figure 3.6. Synthesis of compound (**17**). Reagents: (i) CuCN, DMF; (ii) LiOH, THF/H_2O; (iii) oxalyl chloride.

Coupling of the protected diamine (**18**) could be performed using the acid chloride (**17**) (prepared using oxalyl chloride)[3] or HATU to activate the carboxylate of (**16**).[3] The acid chloride proved to be the more efficient coupling route allowing for the preparation of (**19**) in 62% yield.

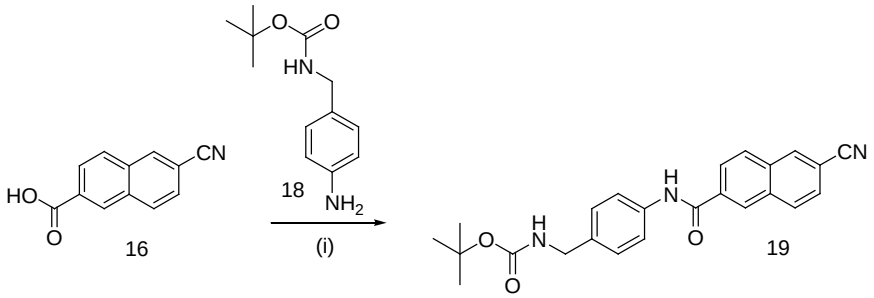

Figure 3.7. Synthesis of compound (**19**). Conditions: (i) HATU/DIPEA/DMF.

Transformation of the cyano functionality into the amidine moiety proved to be exceedingly difficult. Using the literature procedure[3] an excess of LiHMDS (5 equiv.) was combined with nitrile (**19**) in THF /hexane at room temperature for 12 h, followed by treatment with HCl. While the starting material was consumed, the desired product was

not obtained. Varying the reaction temperature or the solvent did not influence the outcome of the reaction. Efforts to isolate the protected silyl amidine were also unsuccessful.

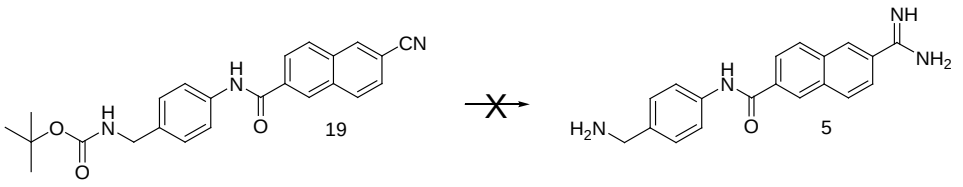

Figure 3.8. Attempted synthesis of lead compound (**5**). Reagents: (i) LiNH $(TMS)_2$, THF; (ii) 2M HCl.

Conversion of the nitrile group to its corresponding N-hydroxyamidine derivative by reaction with hydroxylamine has been described previously.[10] However, when nitrile (**19**) was treated with hydroxylamine under these conditions, an inseparable mixture was obtained.

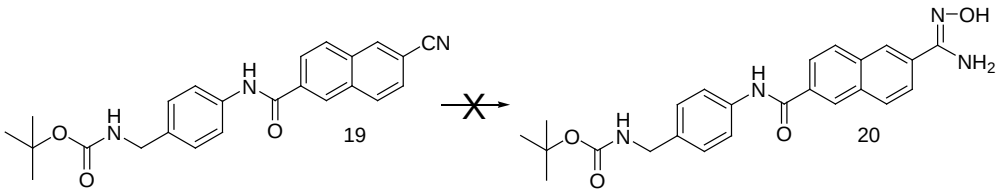

Figure 3.9. Attempted synthesis of (**20**). Reagents: (i) NH_2OH, DIPEA, EtOH.

Given the difficulties associated with the amidine formation, the overall synthetic plan was modified so as to allow for its introduction earlier in the route with amidine production being carried out on compound (**14**). The N-hydroxyamidine[10] strategy for the conversion of (**14**) to the desired derivative (**21**) (Figure 3.10.) was investigated and

several reaction parameters (time, temperature, equivalents of the reactants and different bases) were varied (summarized in Table 3.2.).

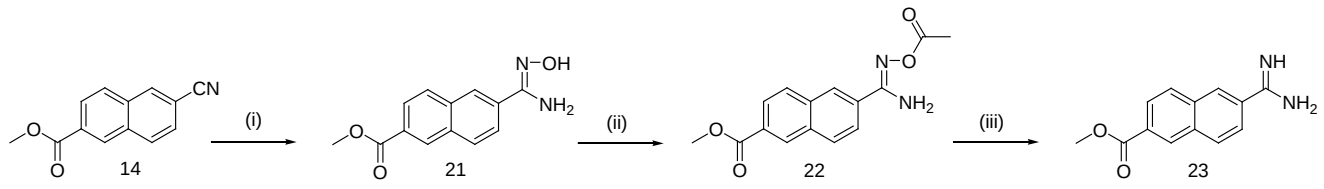

Figure 3.10. Synthesis of (**23**). Conditions: (i) NH_2OH, DIPEA, EtOH; (ii) Ac_2O,AcOH; (iii) H_2,Pd/C, MeOH/AcOH.

Ultimately, it was determined that compound (**21**) could be prepared in 72% yield using 10 equivalents of hydroxylamine in ethanol at 80^{o}C for 15 hours. Reaction with acetic anhydride gives the O-acetylamidoxime (**22**) and the labile nitrogen–oxygen bond can be easily cleaved by hydrogenation to afford the desired amidine moiety in (**23**).[10]

Table 3.2. Conditions explored for the synthesis of (**20**).

$NH_2OH.HCl$	**Base**	**Solvent**	**Temp**	**Time**	**Yield**
2eq	DIPEA	EtOH	r.t.	24 h	no
4eq	DIPEA	EtOH	r.t.	24 h	trace
10eq	DIPEA	EtOH	r.t.	24 h	18%
10eq	TEA	EtOH	r.t.	24 h	16%
2eq	NaOH	H_2O	80^{o}C	24 h	trace
10eq	DIPEA	EtOH	80^{o}C	15 h	72%

Given the complications associated with carrying out the planned coupling reactions in the presence of a free amidine moiety, the acetyl group in compound (**22**)

could act as a protecting group and be removed later in the synthesis. Efforts were directed, therefore, towards the saponification of (**22**) (Figure 3.11.) to permit introduction of the protected diamine (**18**). Several bases (including LiOH, KOH and potassium trimethylsilanolate) were investigated. The mass of the desired carboxylic acid (**24**) was observed in the crude reaction mixture but proved difficult to isolate. While a small quantity of (**24**) was purified, this approach was deemed synthetically impractical. The formation of N-hydroxyamidine (Figure 3.12.) using the acid (**16**) was attempted under the same reaction conditions as used for the N-hydroxyamidine derivative (**21**); however, no product was obtained. Attempts to saponify (**21**) were also unsuccessful. Given these complications, an alternate protecting group strategy involving (**24**) was developed.

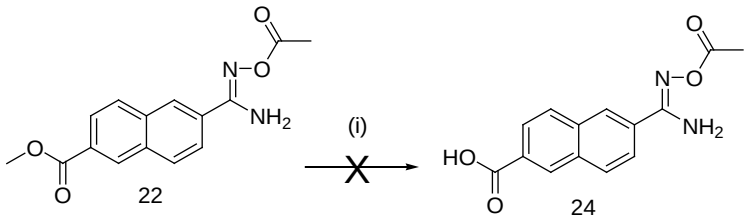

Figure 3.11. Attempted synthesis of (**24**). Conditions: (i) base.

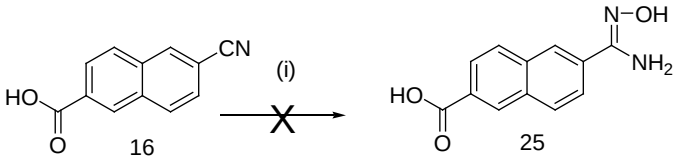

Figure 3.12. Attempted synthesis of (**25**).Reagents: (i) NH_2OH, DIPEA, EtOH.

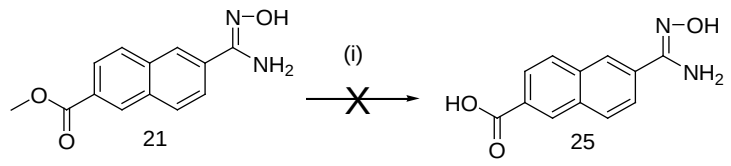

Figure 3.13. Attempted synthesis of (**25**).Reagents: (i) base.

Boc-protection of the amidine intermediate (**23**) (Figure 3.14.) was achieved using two equivalents of Boc-anhydride to give product (**26**) in 87% yield. Saponification of the Boc protected amidine intermediate provided carboxylic acid (**27**). A HATU coupling reaction with amine fragment (**18**) allowed for the production of (**28**) in low yield (18%). Finally, TFA deprotection furnished the desired product (**5**).

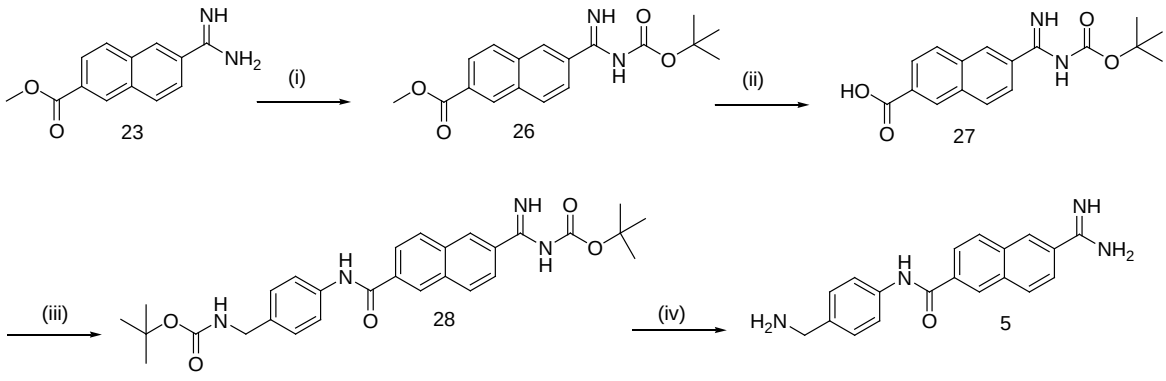

Figure 3.14. Synthesis of compound (**5**). Reagents: (i) Boc_2O, aq. sat $NaHCO_3$/THF; (ii) LiOH, H_2O/THF; (iii) compound (**18**), HATU, DIPEA, DMF; (iv) TFA/DCM.

To address the modest yield and the difficulties with coupling between fragments (**18**) and (**27**), an alternative strategy involving intermediate (**19**) was investigated. As illustrated in Figure 3.15, a thio-Pinner[4] reaction (to give (**29**)) followed by methylation of the thioamide group (to give (**30**)) and the treatment with ammonium acetate furnished

the amidine derivative (**31**). Once again, the amidine group was immediately Boc protected to facilitate purification. Upon HCl treatment, the desired amidine (**5**) was obtained. The reactions outlined using this approach proceeded in high yields, and the characterization data is consistent with literature data.[3]

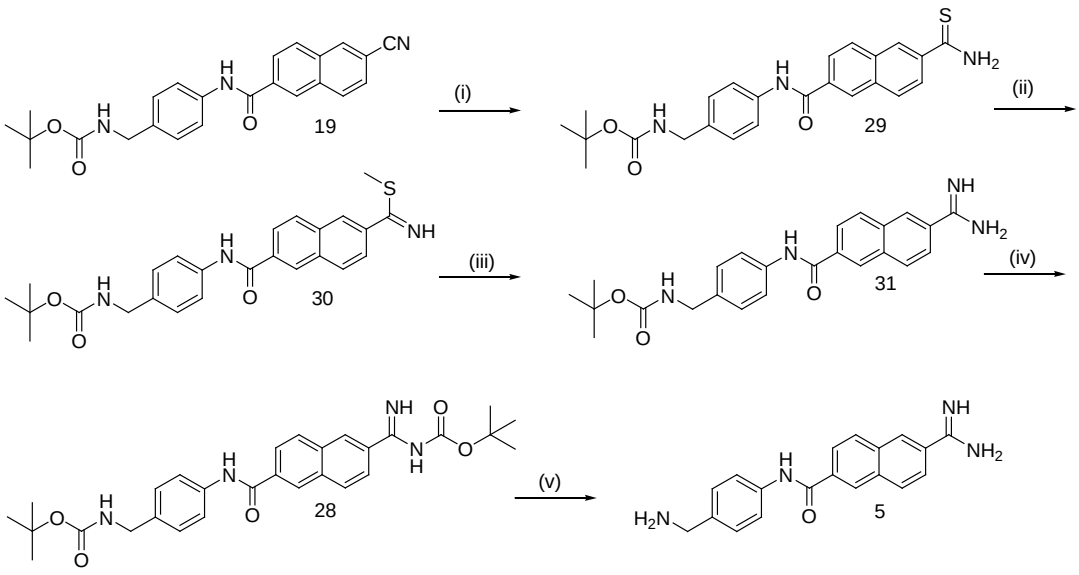

Figure 3.15. Synthesis of compound (**5**). Reagents:(i) H_2S/TEA; (ii) MeI, DCM; (iii) ammonium acetate, MeOH; (iv) Boc_2O, aq. NaOH/THF; (v) 4M HCl, dioxane.

3.4. Synthesis of iodinated analogues of 6-disubstituted-2-naphthamidine.

Taking advantage of the chemistry described above, attention was turned to the synthesis of the iodinated derivative of compound (**5**). The first site chosen for derivatization was the phenyl group. An iodinated analogue of (**18**), amine (**34**), was synthesized *via* the borane reduction of cyano compound (**32**) to give (**33**) followed by Boc protection to give (**34**) (Figure 3.16.).

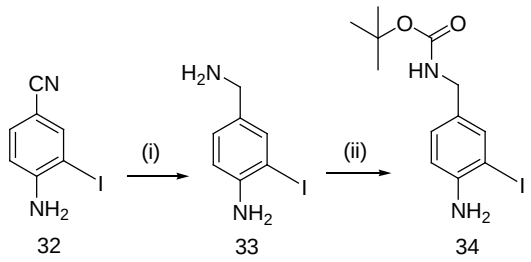

Figure 3.16. Synthesis of compound (**34**). Reagents: (i) BH_3; (ii) Boc_2O, MeOH.

Coupling the acid intermediate (**16**) with iodinated amine (**34**) using the HATU protocol developed above proceeded in a low yield (<5%). Several traditional amide bond-forming reactions were explored (including DCC/HOBt and EDC/HOBt) to generate (**35**) however, we found the most expedious route (Figure 3.18.) involved using the acyl chloride (**17**) in the presence of AgCN[11,12] to generate an acyl cyanide intermediate.

With (**35**) in hand, the synthesis (shown in Figure 3.18.) follows the same route as described for the lead compound (**5**). Note that the Boc protection step was not necessary as the final product and the desired iodinated derivative (**39**) was isolated and completely characterized. The NMR pattern indicate the presence of three sets of 1,2,4 trisubstituted benzene rings. For each set the ^{1}H NMR showed one doublet with a small coupling

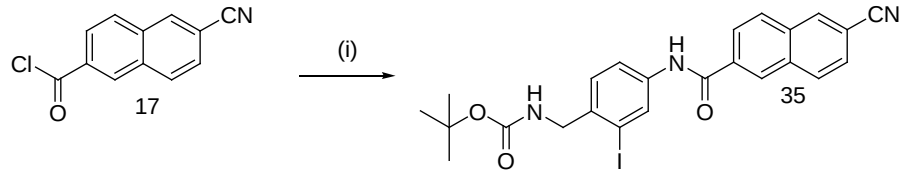

Figure 3.17. Synthesis of compound (**35**). Conditions: (i) compound (**34**), AgCN, DCM.

constant (1-2 Hz) corresponding to a meta coupling, (for 8.72 ppm the doublet was not resolved and appeared as a singlet), one doublet with a large coupling constant 8.4 Hz corresponding to an ortho coupling and a doublet of doublets.

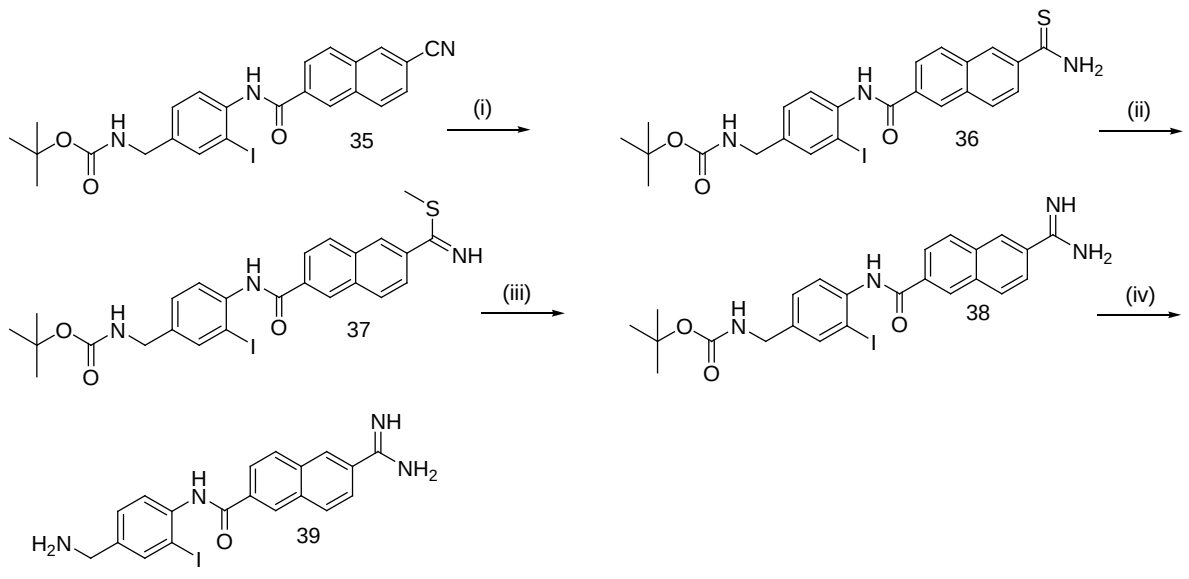

Figure 3.18. Synthesis of compound (**39**). Conditions: (i) H_2S/TEA; (ii) MeI, acetone; (iii) ammonium acetate, MeOH; (iv) 4 MHCl, dioxane.

3.5. Synthesis of 6,8-disubstituted 2-naphthamidine urokinase inhibitors

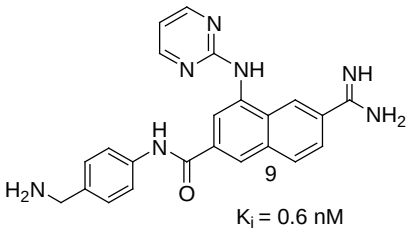

Synthesis of naphthamidine derivative (**9**) followed a literature procedure[4] (shown in Figure 3.19.) and began with the nitration (at position 8) of commercially available (**14**) using KNO_3 in concentrated H_2SO_4 to give (**40**). Hydrogenation using Pd/C in ethyl acetate selectively reduced the nitro group to the amino derivative (**41**) albeit in low yields. A palladium catalyzed amination reaction was attempted between bromopyrimidine and the amino derivative (**41**) under Buchwald conditions using BINAP as the ligand, NaO^tBu the base and toluene as the solvent. Unfortunately, just trace amounts of the desired aryl amine (**42**) were isolated despite the complete consumption of starting material.

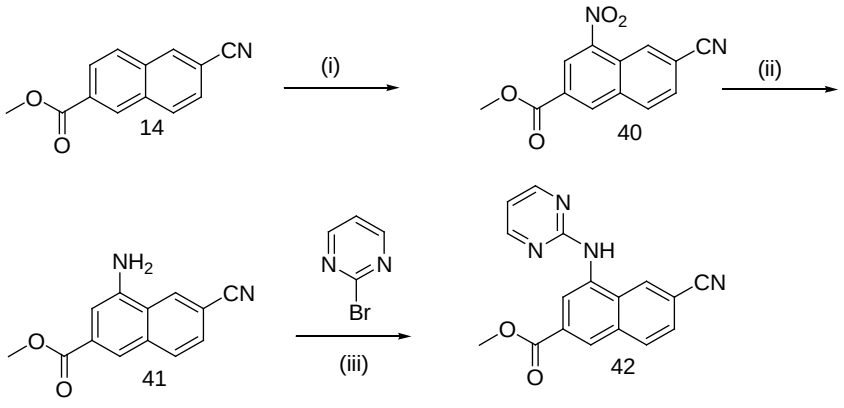

Figure 3.19. Synthesis of compound (**42**). Reagents: (i) KNO_3, H_2SO_4; (ii) H_2, 10% Pd/C, EtOAc; (iii) $Pd_2(dba)_3$, SPHOS, $CsCO_3$, THF, 120^OC.

At this point, the reactivity of the amination coupling partners was reversed by installing the halide moiety on to the naphthamidine ring and coupling with a commercially-available aminopyrimidine (Figure 3.20.) Brominaton of cyano ester[4] (**14**) was achieved using 1,3–dibromo-5,5-dimethylhydantoin.

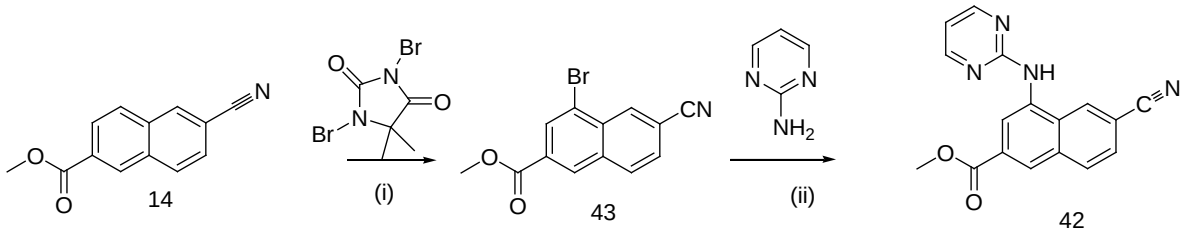

Figure 3.20. Synthesis of compound (**42**). Conditions: (i) DBDMH, DCM; (ii) $Pd_2(dba)_3$, SPHOS, $CsCO_3$, THF, 120^OC.

Several parameters were examined for the effect on the amination reaction including the Pd species, the ligand and the base (Table 3.3.). THF was used as the solvent in all cases.

Table 3.3. Optimization reactions for synthesis of (**42**).

Solvent	**Pd source**	**Ligand**	**Base**	**Yield**
THF	$Pd_2(dba)_3$	X-PHOS	NaO^tBu	10%
THF	$Pd_2(dba)_3$	S-PHOS	NaO^tBu	trace
THF	$Pd_2(dba)_3$	PA	NaO^tBu	No reaction
THF	$Pd_2(dba)_3$	X-PHOS	$CsCO_3$	18%

THF	$Pd_2(dba)_3$	S-PHOS	$CsCO_3$	48%
THF	$Pd_2(dba)_3$	PA	$CsCO_3$	No reaction
THF	$Pd(OAc)_2$	X-PHOS	$CsCO_3$	24%
THF	$Pd(OAc)_2$	S-PHOS	$CsCO_3$	36%
THF	$Pd(OAc)_2$	PA-Ph	$CsCO_3$	No reaction

After 3h at 120°C substantial amounts of starting materials remained, indicating that the excess of the amine might be poisoning the catalyst. As a result, additional aliquots of the catalyst were added as the reaction proceeded. Increasing the temperature above 120°C resulted in decomposition of the catalyst and the precipitation of palladium black. The best results were achieved using the S-PHOS ligand and $CsCO_3$ as the base in THF under microwave irradiation to provide the desired product (**42**) in 48% yield.

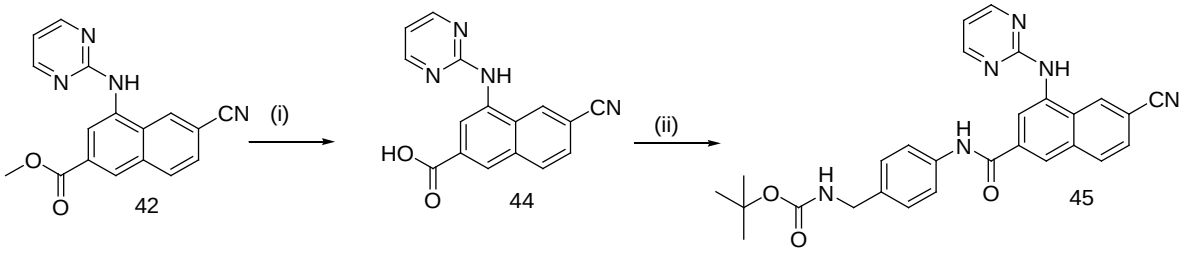

Figure 3.21. Synthesis of compound (**45**). Reagents: (i) LiOH, THF/H_2O; (ii) compound (**18**), PyBOP, DIPEA, DCM.

LiOH efficiently cleaved the methyl ester (**42**) at room temperature. However, due to its high polarity the acid (**45**) proved difficult to isolate and the coupling reaction was performed using the lithium carboxylate salt. On the basis of the result that the precursor of the naphthamidine with no aminopyrimidine moiety could be synthesized from the acid a similar approach was expected to provide the easiest access to the nitrile (**45**). However, only a trace of the desired product (**45**) was formed despite investigating several activating agents including PyBOP, DCC, HATU and TBTU.

3.6. Synthesis of iodinated analogues of 6,8-disubstituted as potential molecular imaging agents of urokinase.

The same coupling conditions used above proved inefficient for the coupling of the iodoaniline derivative (**34**) (Figure 3.22.). Clearly, the deactivating nature of the iodine substituent makes for an unreactive aniline nucleophile.

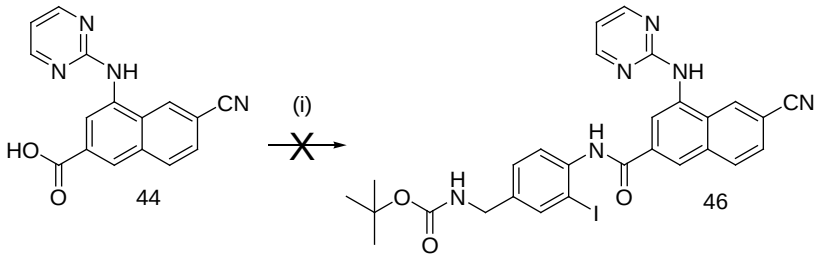

Figure 3.22. Attempted synthesis of (**46**). Reagents: (i) compound (**34**), PyBOP, DIPEA, DCM.

Overall, the 6,8-disubstituted 2-naphthamidine systems described in this section proved to be a real synthetic challenge and given the low yields of some of the key steps, this series was abandoned.

3.6.1. Synthesis of iodinated analogues of 6,8-disubstituted 2-naphthamidines

The challenges with 6,8-disubstituted 2-naphthamidine systems led to the synthesis and evaluation of the naphthamidine derivative (**8**).[4] In this case, a "stripped-down" phenyl moiety lacking the carbamate fragment was used. Synthesis of (**8**) involves coupling the previously synthesized (**42**) with aniline. However, given that aniline derivatives (**48**), (**49**) and (**50**) were likely to suffer from the same reduced nucleophilicity shown by (**35**), a coupling procedure wherein the amino group was activated was examined.

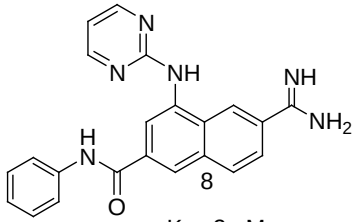

K_i = 2 nM

Formation of an aluminum amide (R_2AlNR_2) has been reported previously[13] and was used to promote amide preparation. The reagents are generated by combining amines or their HCl salts with $AlMe_3$ as depicted in Figure 3.23.

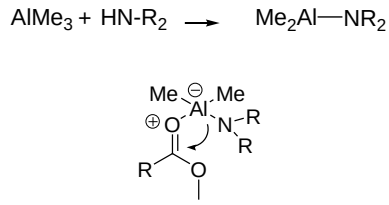

Figure 3.23. Key step in the mechanism of $AlMe_3$ mediated amide formation.

The metal center serves as a Lewis acid while delivering the nucleophilic amine moiety to the ester. In our case, $AlMe_3$ was successfully employed promoting the coupling reaction between the methyl ester (**42**) and aniline and allowing for the production of (**51**) in 73% yield. The same strategy was successfully translated to iodoaniline systems (**48**), (**49**) and (**50**) to give (**52**), (**53**), and (**54**) respectively.

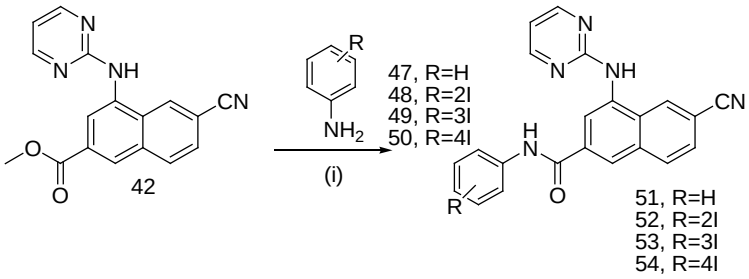

Figure 3.24. Synthesis of **51**, **52**, **53** and **54**. Conditions: (i) $AlMe_3$, DCM.

The amidine moiety was installed *via* the hydroxylamine protocol described previously to generate the corresponding amidine oxime. *O*-Acylation employing acetic anhydride in acetic acid afforded the protected hydroxylamines. Hydrogenation using a catalytic amount of palladium on activated carbon in methanol cleaved the labile nitrogen–oxygen bond and afforded the desired amidines. Isolation of the 3 aniline

derivative proved to be challenging using reverse phase LCMS while the other derivatives were successfully purified by LCMS.

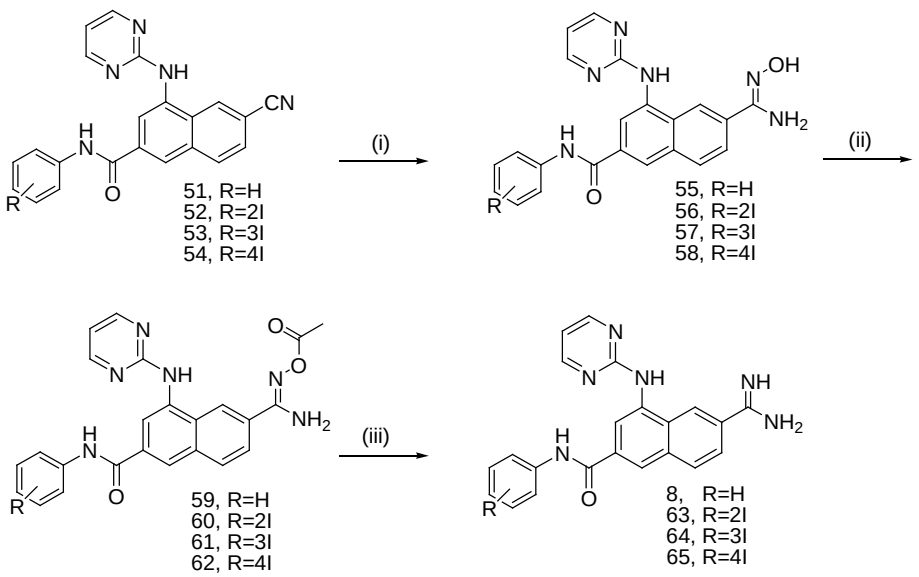

Figure 3.25. Synthesis of **8**, **63**, **64**, and **65**. Conditions: (i) NH_2OH, DIPEA, EtOH; (ii) Ac_2O, AcOH; (iii) H_2,Pd/C, MeOH/AcOH.

The authenticity of the compounds was confirmed by NMR and HRMS. For compounds where iodine was inserted in the phenyl ring (**63, 64, 65,**) the ^1H NMR showed the presence of a disubstituted aromatic ring. A set of two doublets consistent with a para substituted system with a coupling constant between 7-8 Hz (ortho coupling) was observed for derivative (**65**) while compound (**63**) showed two doublets (7-8 Hz) and two doublets of doublets (7-8 Hz and 1-2 Hz). The naphtamidine ring displayed a pattern which confirm the existence of 1, 2 ,4 trisubstituted benzene ring and two singlets (corresponding to the protons in the 7 and 9 positions). The pyrimidine ring showed an

apparent triplet from a collapsed doublet of doublets and a doublet (corresponding to the two symmetrical protons).

3.7. Summary and Future Work

At the time of writing, compounds (**39**, **63**, **65**) had not yet been screened for their binding affinity for uPA. Compounds (**5** and **8**) are being used as positive control in the colorimetric assay and the results will guide future synthetic strategies. While these compounds were waiting for screening two classes of potent inhibitors for uPA, which are described in the subsequent chapters, were identified and became the focus of the thesis.

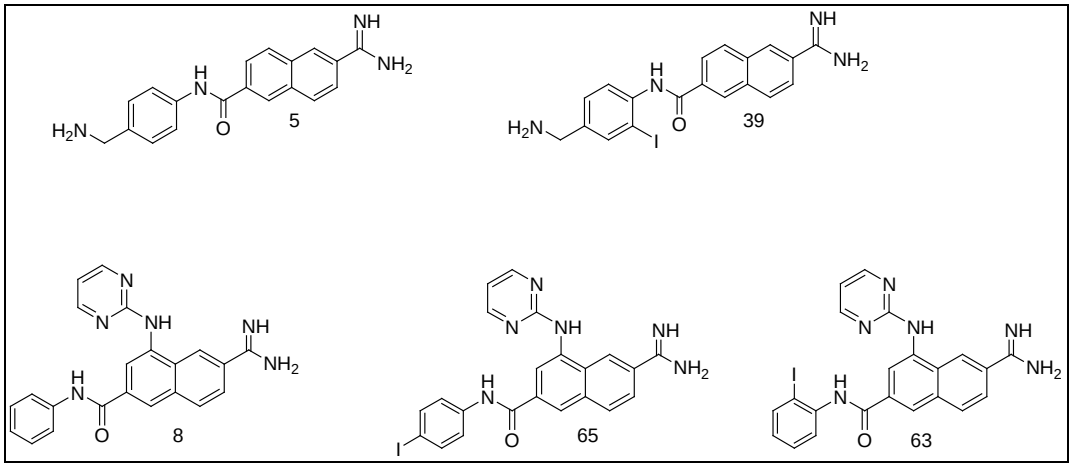

Figure 3.26. List of synthesised compounds.

3.8. Experimental procedures:

6-Carbomethoxy-2-naphthalenecarboxylic acid (11)

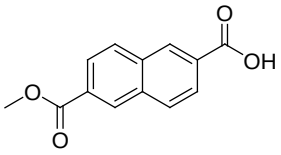

The synthesis was adapted from a procedure by Wendt and coworkers.[3]

Dimethyl 2,6-naphthalenedicarboxylate (**10**) (976 mg, 4 mmol) was dissolved in dioxane (10 mL) by heating at 80°C. A solution of KOH (224 mg, 4 mmol) in MeOH (2 mL) was dropwise added and the reaction mixture was stirred for 2h at 80°C. The reaction mixture was cooled to room temperature, filtered, and the white solid residue was rinsed with ether. The solid was then taken up in water and treated with 2 M HCl to pH 3, and a precipitate was formed which was filtered, washed with water and dried to afford 828 mg (90%) yield. Characterization data matched the data in the literature.[3]

^{1}H NMR (DMSO-*d*6) δ 13.28 (br s, 1H), 8.68 (s, 1H), 8.65 (s, 1H), 8.24 (d, 2H), 8.05 (d, 2H), 3.91(s, 3H);

ES-MS: Calculated for $C_{13}H_{21}N_4O_2$ $[M]^+$: 230.06. Found: 230.1.

6-Carbamyl-2-naphthalenecarboxylic acid, methyl ester (13)

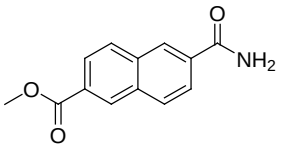

The synthesis was adapted from a procedure by Wendt and coworkers.[3]

Thionyl chloride (0.4 mL, 5.52 mmol) was added to a suspension of 6-Carbomethoxy-2-naphthalenecarboxylic acid (**11**) (303 mg, 1.3 mmol) in toluene (4 mL) followed by addition of DMAP (1 mg) and refluxed for 1h. Solvent was removed in *vacuo* and the thick precipitate, which was formed, was washed with hexanes and filtered. The solid was dissolved in CH_2Cl_2 (40 mL) at room temperature and the solution was saturated with dry ammonia gas until the product precipitate and stirred for additional 15 min. The solid was filtered, and dried under vacuum to yield 259 mg 87% of the desired product. Characterization data matched the data in the literature.[3]

^{1}H NMR 200 MHz (DMSO-*d*6) δ 8.69 (s, 1H), 8.56 (s, 1H), 8.24(s, 1H), 8.22 (d, 1H), 8.14 (d, 1H), 8.04(d, 2H), 7.60 (s, 1H), 3.94 (s, 3H);

ES-MS Calculated for $C_{13}H_{11}NO_3$ $[M]^+$: 229.21. Found: 229.9.

6-Cyano-2-naphthalenecarboxylic acid, methyl ester (14)

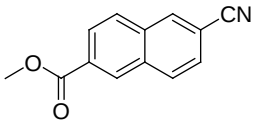

A degased suspension of 6-bromo-2-naphthalenecarboxylic acid methyl ester (**14**) (264 mg, 1 mmol) and cooper cyanate (179 mg, 2 mmol) in 3 ml NMP was placed in a microwave vial and irradiated for 6 min at 165^{o}C. The reaction mixture was diluted with H_2O and extracted with DCM. The organic layer was dried with magnesium sulfate and the crude reaction mixture was purified on silica gel gradient hexane EtOAc to yield 174 mg of the desired product (82%). Characterization data matched the data in the literature.[3]

^{1}H NMR (600 MHz, $CDCl_3$) δ 8.62 (s, 1H), 8.25 (s, 1H), 8.16 (dd, *J* = 8.6 Hz, *J* = 1.6 Hz, 1H), 8.03 (d, *J* = 8.5 Hz, 1H), 7.94 (d, *J* = 8.6 Hz, 1H), 7.66 (dd, *J* = 8.5 Hz, *J* = 1.4 Hz, 1H), 4.00 (s, 3H);

ES-MS: Calculated for $C_{13}H_9NO_2$ $[M]^+$: 211.1. Found: 211.1.

6-Cyano-2-naphthalenecarboxylic acid (16)

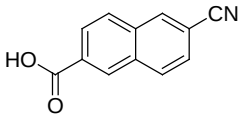

The synthesis was adapted from a procedure by Wendt and coworkers.[3]

To 6-Cyano-2-naphthalenecarboxylic Acid, Methyl Ester (**14**) (212 mg, 1 mmol) in 1:1 THF/H_2O (4 mL) was added LiOH monohydrate (209 mg, 5 mmol) and stirred for 90 min at room temperature. The reaction mixture was concentrated in *vacuo* to thick slurry, dissolved in 1 M HCl (10 mL) and extracted with EtOAc (3 x 10 mL). The organic layers were washed with brine, dried (Na_2SO_4), filtered, and concentrated to provide 178 mg (91%) of product as a white solid: Characterization data matched the data in the literature.[3]

1H NMR ($CDCl_3$): 8.73 (s, 1H), 8.31 (s, 1H), 8.24 (dd, *J* = 8.6 Hz, *J* = 1.6 Hz, 1H), 8.10 (d, *J* = 8.5 Hz, 1H), 8.03 (d, *J* = 8.6 Hz, 1H), 7.70 (dd, *J* = 8.5 Hz, *J* = 1.5 Hz, 1H);

ES HRMS Calculated for $C_{12}H_6NO_2$ $[M]^+$: 196.0399. Found: 196.0394.

6-Cyano-2-naphthalenecarbonyl chloride (17).

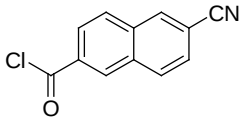

The synthesis was adapted from a procedure by Wendt and coworkers.[3]

Thionyl chloride (0.93 mL) was added dropwise to a suspension of 6-Cyano-2-naphthalenecarboxylic Acid (**16**) (197 mg, 1 mmol) in toluene (5 mL) and heated at 70°C for 18h. Extra thionyl chloride (0.5 mL) was added and heating continued for additional 4h. The reaction mixture was evaporated in vacuo, with toluene as azeotrope (3 x 10 ml toluene) to provide 181 mg (84%) of product: Characterization data matched the data in the literature.[3]

^{1}H NMR ($CDCl_3$) δ 8.78 (s, 1H), 8.31 (s, 1H), 8.19 (dd, *J* = 8.7 Hz, *J* = 1.7 Hz, 1H), 8.13 (d, *J* = 8.5 Hz, 1H), 8.02 (d, *J* = 8.7 Hz, 1H), 7.75 (dd, *J* = 8.5 Hz, *J* = 1.3 Hz, 1H);

ES-MS Calculated for $C_{12}H_6ClNO$ $[M]^+$: 215.01. Found: 215.8.

6-[*N*-(4-(tert-butoxycarbonylaminomethyl)phenyl)-carbamyl]-2-naphthalenecarbonitrile (19)

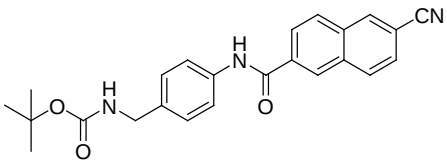

The synthesis was adapted from a procedure by Wendt and coworkers.[3] A solution of 6-cyano-2-naphthalenecarbonyl acid (**16**) (98 mg, 0.5 mmol) and *i*-Pr_2NEt (0.218 mL, 1.25 mmol) in DMF (4 mL) at 0°C was treated with HATU (191 mg, 0.4 mmol). The solution

was stirred for 30 min at 0°C, treated with 4-((tert-butyloxycarbonyl)-amino)-3-iodobenzylamine (**17**) (174 mg, 0.5 mmol), and then stirred for an additional 18h. The mixture was poured into water (40 mL), extracted with EtOAc (3 x 25 mL), washed with water and brine and dried over (Na_2SO_4). The organic layer was concentrated in *vacuo* and purified on silica gel eluting with EtOAc/hexanes to provide 36 mg (18%) of the desired product. Characterization data matched the data in the literature.[3]

^{1}H NMR (600 MHz, $CDCl_3$): 8.45 (s, 1H), 8.32 (s, 1H), 8.09 (m, 3H), 7.96 (br s, 1H), 7.74 (dd, *J* = 8.5 Hz, *J* = 1.4 Hz, 1H), 7.67 (d, *J* = 8.2 Hz, 1H), 7.35 (d, *J* = 8.0 Hz, 2H), 4.35 (d, *J* = 4.7 Hz, 2H), 1.49 (s, 9H);

ES-MS: Calculated for $C_{24}H_{27}N_4O_3$ $[M]^+$: 419.2083. Found: 419.2078.

6-[*N*-(4-(tert-butoxycarbonylaminomethyl)phenyl)-carbamyl]-2-naphthalenecarbothioic acid amide (29)

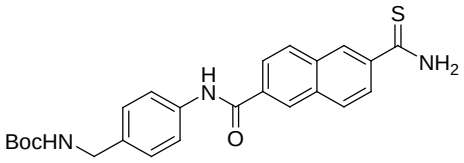

A solution of (**19**) (40 mg, 0.1 mmol) in 10:1 pyridine/Et_3N (4 mL) was treated with H_2S gas for 5 min, and the resulted green solution was stirred for 72 h. H_2O was added to the reaction mixture and the resulting yellow precipitate was collected by filtration and dried in vacuum to provide 37 mg of the title compound (85%). The reaction mixture was used without further purification.

6-[*N*-(4-(tert-butoxycarbonylaminomethyl)phenyl)-carbamyl]-2-naphthalenecarboximidothioic acid methyl ester (30).

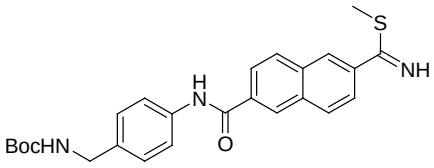

To 6-[*N*-(4-(tert-butoxycarbonylaminomethyl)phenyl)-carbamyl]-2-naphthalenecarbothioic acid amide (**29**) (43 mg, 0.1 mmol) in acetone (2 mL) was added MeI (0.15 mL) and the mixture was stirred at overnight. The reaction mixture was evaporated and used without further purification (45 mg).

6-[*N*-(4-(tert-butoxycarbonylaminomethyl)phenyl)-carbamyl]-2-naphthalenecarboxamidine (31).

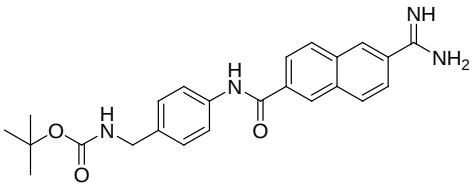

To 6-[*N*-(4-(tert-Butoxycarbonylaminomethyl)phenyl)-carbamyl]-2-naphthalenecarboximidothioic acid methyl ester (**30**) (45 mg, 0.1 mmol) in MeOH (10 mL), NH_4OAc was added (77 mg, 1 mmol), and the reaction was stirred overnight. After the evaporation of the solvent the resulting solid residue was washed with ether. The resulting precipitate was used in the next step without further purification.

Compound (28)

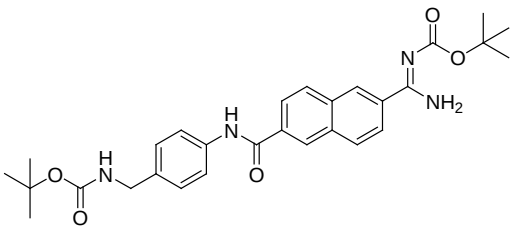

To a solution of 6-[*N*-(4-(tert-butoxycarbonylaminomethyl)phenyl)-carbamyl]-2-naphthalenecarboxamidine (**31**) (41 mg, 0.1 mmol) dissolved in THF/aq NaOH (21 mg, 0.1 mmol) of di-tert-butyl-dicarbonate was added and stirred over night. The reaction mixture was taken up in DCM and the two layers were separated. The organic phase was concentrated in *vacuo* and purified on silica gel eluting with EtOAc/hexanes to provide 20 mg (40%) of the desired product.

^{1}H NMR (600 MHz, $CDCl_3$) 8.36 (brs, 1H), 8.28 (s, 1H), 8.21(s, 1H), 7.84 (m, 2H), 7.80 (d, 1H), 7.74 (dd, 1H), 7.65 (d, 2H), 7.27 (d, 2H), 4.30 (d, 2H), 1.57 (s, 9H), 1.46 (s, 9H);

^{13}C NMR (150 MHz, $CDCl_3$): 165.2, 155.4, 136.6, 134.9, 133.5, 133.4, 133.4, 133.3, 129.1, 128.9, 127.7, 127.1, 126.7, 124.1, 123.9, 120.1, 79.6, 79.1, 43.7, 27.9, 27.7;

ES- MS Calculated for $C_{29}H_{35}N_4O_5$ $[M]^+$: 519.2. Found: 519.2.

6-[*N*-(4-(aminomethyl)phenyl)carbamyl]-2-naphthalenecarboxamidine (5)

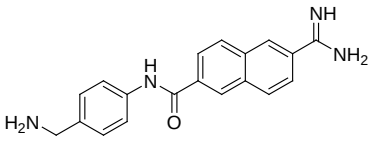

Compound (**28**) (20 mg, 0.038 mmol) was disolved in 0.2 ml acetonitrile and treated with TFA(0.4 mL) for 10 min at room temperature. The excess of TFA was removed under N_2,

then a mixture of H_2O acetonitrile was added and the compound was lyophilized and 11 mg (98%) of the desired product was obtained. Characterization data matched the data in the literature.[3]

^{1}H NMR (700 MHz, D_2O) δ: 8.45 (s, 1H), 8.43 (s, 1H), 8.21 (d, *J* = 8.4 Hz, 1H), 8.17 (d, *J* = 8.4 Hz, 1H), 8.00 (dd, *J* = 8.5 Hz, *J* = 1.8 Hz), 7.00 (dd, *J* = 8.5 Hz, *J* = 1.8 Hz), 7.66 (d, *J* = 8.4 Hz, 1H), 7.54 (d, *J* = 8.4 Hz, 1H), 4.22 (s, 2H).

^{13}C NMR (175 MHz, D_2O) δ: 168.3, 166.0, 137.2, 134.0, 133.3, 133.0, 130.0, 129.4, 129.3, 128.6, 127.6, 126.5, 124.7, 123.5, 122.3, 42.2.

ES- MS Calculated for $C_{19}H_{18}N_4O$ $[M]^+$: 319.2. Found: 319.2.

6-[*N*-(4-(tert-butoxycarbonylaminomethyl)-2-iodo-phenyl)-carbamyl]-2-naphthalenecarbonitrile (35)

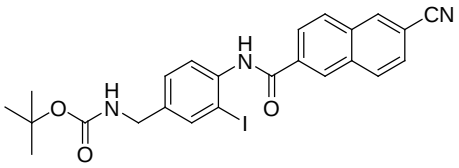

To a solution of 4-((tert-butyloxycarbonyl)-amino)-3-iodobenzylamine (60 mg, 0.15 mmol) in DCM were added 6-cyano-2-naphthalenecarbonyl chloride (64 mg, 0.3 mmol) and a suspension of AgCN (20 mg, 0.15 mmol) in acetonitrile. The suspension was stirred for 48 h filtered through Celite, concentrated in *vacuo* and purified by flash chromatography on silica gel eluting with gradient EtOAc/hexanes. The desired product (48 mg) was obtained (62%) yield.

^{1}H NMR (600 MHz, $CDCl_3$) δ: 8.52 (s, 1H), 8.40 (m, 2H), 8.32 (s, 1H), 8.13 (dd, *J* = 8.5 Hz, *J* = 1.5 Hz, 1H), 8.10 (d, *J* = 8.5 Hz, 1H), 8.05 (d, *J* = 8.5 Hz, 1H), 7.78 (s, 1H), 7.72

(dd, *J* = 8.5 Hz, *J* = 1.5 Hz, 1H), 7.36 (d, *J* = 8.2 Hz, 1H), 4.30 (d, *J* = 4.3 Hz, 1H), 1.48 (s, 9H);

^{13}C NMR (150 MHz, $CDCl_3$) δ: 164.6, 156.0, 137.8, 137.7, 137.2, 134.8, 134.2, 134.0, 133.9, 130.6, 129.7, 128.7, 128.0, 127.7, 125.4, 122.0, 118.8, 111.8, 90.7, 80.0, 43.6, 28.5;

ES-HRMS: Calculated for $C_{24}H_{23}N_3O_3I$ $[M]^+$: 528.0778. Found: 528.0784.

6-[*N*-(4-(tert-butoxycarbonylaminomethyl)-2-iodo-phenyl)-carbamyl]-2-naphthalenecarbothioic acid amide (36).

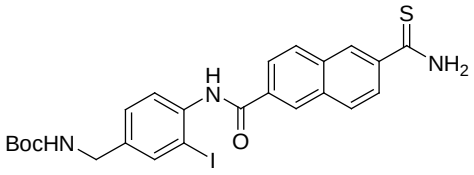

A solution of compound (**35**) (53 mg, 0.1 mmol) in 10:1 pyridine/Et_3N (8 mL) was treated with H_2S gas for 5 min, and the resulted green solution was stirred for 72 h. H_2O was added to the reaction mixture and the resulting yellow precipitate was collected by filtration. The desired product (45 mg) was obtained in 80% yield.

^{1}H NMR (600 MHz, DMSO-*d*6) δ: 10.45 (s, 1H), 10.06 (s, 1H), 8.63 (s, 1H), 8.48 (s, 1H), 8.16 (d, *J* = 8.6 Hz, 1H), 8.10 (d, *J* = 1.2 Hz, 1H), 8.09 (m, 2H), 7.80 (s, 1H), 7.48 (t, *J* = 6.3 Hz, 1H), 7.42 (d, *J* = 8.1 Hz, 1H), 7.31 (dd, *J* = 8.1 Hz, *J* = 1.2 Hz, 1H), 4.13 (d, *J* = 4.7 Hz, 2H), 1.41 (s, 9H);

^{13}C NMR (150 MHz, DMSO-*d*6): 199.8, 165.2, 155.8, 140.6, 138.4, 138.3, 137.1, 133.3, 133.1, 133.0, 129.4, 128.5, 128.3, 127.8, 127.4, 126.3, 126.0, 125.1, 98.7, 78.0, 42.3. 28.2;

ES-HRMS: Calculated for $C_{24}H_{25}N_3O_3SI$ $[M]^+$: 562.0661. Found: 562.0655.

6-[*N*-(4-(tert-butoxycarbonylaminomethyl)-2-iodo-phenyl)-carbamyl]-2-naphthalenecarboximidothioic acid methyl ester (37).

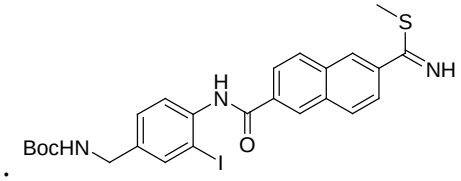

To the thioamide (**36**) (56 mg, 0.1 mol) in acetone (2 mL) was added MeI (0.15 mL) and the reaction mixture was stirred at overnight. The solvent was concentrated in *vacuo* and used without further purification. The desired product (45 mg) was obtained in 83% yield.

^{1}H NMR (600 MHz, MeOD) δ: 8.69 (s, 1H), 8.63 (s, 1H), 8.30-8.20 (m, 3H), 7.95 (dd, *J* = 8.6 Hz, *J* = 1.9 Hz, 1H), 7.89 (s, 1H), 7.56 (d, *J* = 8.0 Hz, 1H), 7.38 (dd, *J* = 8.0 Hz, *J* = 1.1 Hz, 1H), 4.23 (s, 2H), 2.95 (s, 3H), 1.41 (s, 9H);

^{13}C NMR (150 MHz,MeOD) δ: 192.8, 168.0, 158.5, 142.0, 139.2, 139.0, 136.9, 136.5, 135.2, 132.5, 132.0, 131.7, 131.6, 131.5, 131.4, 130.9, 129.3, 129.0, 128.7, 127.3, 127.2, 125.2, 125.1, 97.7, 80.4, 43.9, 28.7, 16.3;

ES-HRMS: Calculated for $C_{25}H_{27}N_3O_3SI$ $[M]^+$: 576.0818. Found: 576.0792.

6-[*N*-(4-(tert-Butoxycarbonylaminomethyl)-2-iodo-phenyl)-carbamyl]-2-naphthalenecarbonitrile (38)

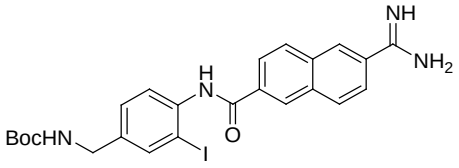

To 6-[*N*-(4-(tert-butoxycarbonylaminomethyl)-2-iodo-phenyl)-carbamyl]-2-naphthalenecarboximidothioic acid methyl ester (**37**) (57 mg, 0.1 mmol) in MeOH (10 mL), NH_4OAc was added (77 mg, 1 mmol), and the reaction was stirred overnight. After the evaporation of the solvent the resulting solid residue was washed with ether. The resulting precipitate was used without further purification.

6-[*N*-(4-(Aminomethyl)-2-iodo-phenyl)carbamyl]-2-naphthalenecarboxamidine (39)

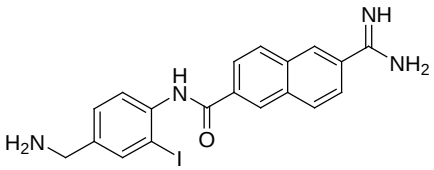

Compound (**38**) (54 mg, 0.038 mmol) was dissolved in 0.2 ml acetonittrile and treated with trifluoroacetic acid (0.4 mL) for 10 min at room temperature. The excess of TFA was removed under N_2, then a 8:1 mixture of H_2O: acetonitrile was added and the compound was lyophilized. The mixture was purified using teledyne combiflash on reverse phase C18 column using a gradient of water/ acetonitrile. The desired product (22 mg) was obtained in 50 % yield.

^{1}H NMR (600 MHz, MeOD) δ: 8.72 (s, 1H), 8.54 (d, *J* = 1.2 Hz, 1H), 8.30 (d, *J* = 8.4 Hz, 1H), 8.25 (d, *J* = 8.4 Hz, 1H), 8.22 (dd, *J* = 8.4 Hz, *J* = 1.8 Hz, 1H), 8.12 (d, *J* = 1.8 Hz,

1H), 7.90 (dd, *J* = 8,4 Hz, *J* = 1.8 Hz, 1H), 7.73 (d, *J* = 8.4 Hz, 1H), 7.58 (dd, *J* = 8.4 Hz, *J* = 1.8 Hz, 1H), 4.15 (s, 2H);

^{13}C NMR (150 MHz,MeOD) δ: 168.4, 168.2, 141.6, 141.1, 136.3, 135.7, 135.3, 135.0, 131.7, 131.1, 130.9, 130.4, 129.4, 129.0, 128.9, 127.0, 125.3, 98.0, 44.0;

ES-HRMS: Calculated for $C_{19}H_{18}N_4OI$ $[M]^+$: 445.0525. Found: 445.0514.

6-(N-hydroxycarbamimidoyl)-naphthalene-2-carboxylic acid methyl ester (21)

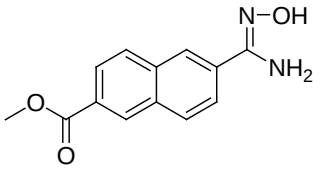

6-cyano-2-naphthalenecarboxylic acid, methyl ester (**14**) (197 mg, 1 mmol) was dissolved in EtOH (20 mL). $H_2NOH{\cdot}HCl$ (695 mg, 10 mmol) and diisopropylethylamine (3.6 ml, 20 mmol) were added and the reaction mixture was heated to reflux for 15 h. The solvent was removed under reduced pressure. Chloroform (10 ml) was added to the residue and then removed in *vacuo*. The resulting solid was purified by flash chromatography using a gradient EtOAc–hexane – 0.1 % acetic acid to give the desired product 185 mg (76%).

^{1}H NMR (600 MHz, DMSOd_6) δ: 9.92 (s, 1H), 8.10 (d, *J* = 8.6 Hz, 1H), 8.03 (d, *J* = 8.6 Hz, 1H), 8.01 (dd, *J* = 8.6 Hz, *J* = 1.6 Hz, 1H), 7.93 (dd, *J* = 8.6 Hz, *J* = 1.6 Hz, 1H), 5.99 (s, 2H), 3.32 (s, 3H);

^{13}C NMR (150 MHz, DMSOd_6) δ: 166.3, 150.3, 134.8, 133.2, 132.2, 130.2, 129.0, 128.8, 127.2, 125.2, 124.3, 124.0, 52.3;

ES-HRMS: Calculated for $C_{13}H_{12}N_2O_3$ $[M]^+$: 244.0848. Found: 244.0830.

6-Carbamimidoyl-naphthalene-2-carboxylic acid (25)

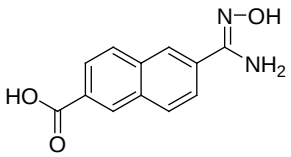

To 6-Cyano-2-naphthalenecarboxylic acid, methyl ester (**21**) (122 mg, 0.5 mmol) in 1:1 THF/H_2O (4 mL) LiOH/H_2O (102 mg, 2.5 mmol) was added and the solution stirred for 90 min. The reaction mixture was concentrated in *vacuo* to 1/3 of the initial volume. 1M HCl was added (10 mL) and extracted with EtOAc (3 x 25 mL). The combined organic extracts were washed with brine, dried (Na_2SO_4), filtered, and concentrated to provide 14 mg (12%) of product as a white solid:

^{1}H NMR (600 MHz, DMSOd_6) δ: 8.69 (s, 1H), 8.48 (s, 1H), 8.29 (d, J = 8.6 Hz, 1H), 8.14 (d, J = 8.6 Hz, 1H), 8.08 (dd, J = 8.6 Hz, J = 1.4 Hz, 1H), 7.86 (dd, J = 8.6 Hz, J = 1.4 Hz, 1H);

^{13}C NMR (150 MHz, DMSOd_6) δ: 167.0, 133.8, 133.7, 130.2, 130.0, 129.2, 128.3, 126.4, 124.6;

ES-HRMS: Calculated for $C_{13}H_{13}N_2O_3$ $[M]^+$: 245.0926. Found: 245.0927.

6-Acetyloxyamidine-2-naphthalenecarboxylic Acid, Methyl Ester (22)

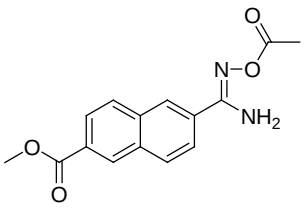

The hydroxy amidine (**21**) (122 mg, 0.5 mmol) was dissolved in acetic acid (10 mL) and treated with Ac_2O (0.472 ml, 5 mmol) at room temperature. The reaction mixture was stirred for 30 min at room temperature and the solvent was removed under reduced pressure with toluene as an azeotrope. The residue was dissolved in EtOAc and washed with $NaHCO_3$ (aq. sat.). The organic layer was dried with Na_2SO_4 and concentrated in *vacuo* from toluene three times to afford the N protected hydroxyamidine. The crude product was purified by flash chromatography gradient EtOAc–hexane –1% acetic acid to afford 108 mg (76%).

^{1}H NMR (600 MHz,DMSOd_6) δ: 8.67 (s, 1H), 8.40 (s, 1H), 8.20 (d, J = 8.7 Hz, 1H), 8.11 (d, J = 8.7 Hz, 1H), 8.04 (dd, J_1 = 1.6 Hz, J_2 = 8.7 Hz, 1H), 7.91 (dd, J_1 = 1.6 Hz, J_2 = 8.7 Hz, 1H), 7.00 (s, 2H), 3.93 (s, 3H), 2.17 (s, 3H);

^{13}C NMR (150 MHz, DMSOd_6) δ: 168.4, 166.2, 156.0, 134.4, 132.9, 131.5, 130.2, 129.4, 129.1, 127.9, 126.3, 125.4, 125.0, 52.3, 19.8;

ES-HRMS: Calculated for $C_{15}H_{15}N_2O_4$ $[M]^+$: 287.1034. Found: 287.1032.

6-Carbamimidoyl-naphthalene-2-carboxylic acid methyl ester (23)

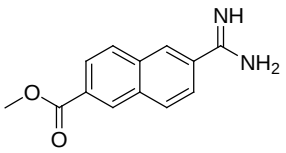

The acetylated hydroxy amidine (**21**) (143 mg, 0.5 mmol) was dissolved in acetic acid (10 mL) followed by addition of 10 mg Pd/C 10%. The suspension was hydrogentated at atmosphere pressure by saturation of the solution with H_2 gas and stirred at room temperature overnight. The reaction mixture was purged with Ar and filtered on celite. The solvent was removed in *vacuo* with toluene as azeotrope and was used without further purification.

^{1}H NMR (600 MHz,DMSOd_6) δ: 8.74 (d, *J* = 1.4 Hz, 1H), 8.49 (s, 1H), 8.32 (d, *J* = 8.4 Hz, 1H), 8.17 (d, *J* = 8.7 Hz, 1H), 8.01 (dd, *J* = 8.4 Hz, *J* = 1.4 Hz, 1H), 7.91 (dd, *J* = 8.4 Hz, *J* = 1.4 Hz, 1H), 3.94 (s, 3H);

^{13}C NMR (150 MHz, DMSOd_6) δ: 166.0, 165.4, 133.9, 133.7, 130.3, 130.0, 129.6, 128.9, 128.0, 126.0, 124.8, 52.5;

ES-HRMS: Calculated for $C_{13}H_{12}N_2O_2$ $[M]^+$: 229.0977. Found: 229.0976.

Compound (26)

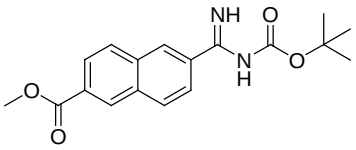

Saturated NaOH in water (20 mL) was added to a stirred suspension of naphthamidine hydrochloride (**23**) (114 mg, 0.5 mmol) in THF (20 mL), and di-*tert*butyldicarbonate (218

mg, 1 mmol) was added immediately after. After 1 h the reaction mixture was taken up with ethyl acetate and two phases was separated. The organic phase was washed with saturated NaCl solution, dried (Na_2SO4), and evaporated *in vacuo*. Flash chromatography on silica gel hexane 1:1 ethyl acetate furnished 101 mg 64% of the desired product.

^{1}H NMR (600 MHz,$CDCl_3$) δ: 8.63 (s, 1H), 8.33 (s, 1H), 8.14 (dd, *J* = 8.6 Hz, *J* = 1.6 Hz, 1H), 8.05 (s, 1H), 8.03 (d, *J* = 8.6 Hz, 1H), 7.99 (d, *J* = 8.6 Hz, 1H), 7.90 (dd, *J* = 8.6 Hz, *J* = 1.6 Hz, 1H), 4.00 (s, 3H), 1.55 (s, 9H);

^{13}C NMR (150 MHz, $CDCl_3$) δ: 166.9, 165.3, 149.6, 134.7, 134.5, 132.9, 130.8, 130.4, 129.8, 129.5, 128.2, 126.6, 124.6, 83.3, 52.6, 28.2;

CI-MS: Calculated for $C_{18}H_{21}N_2O_4$ $[M]^+$: 329.1. Found: 329.1.

Compound (27)

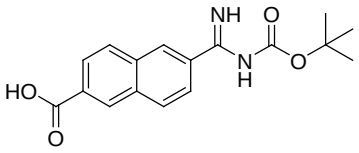

Compound (**26**) (164 mg, 0.5 mmol) in 1:1 THF/H2O (4 mL) followed by addition of LiOH (190 mg, 0.45 mmol). After 90 min at room temperature another 3 ml of THF was added, and the organic phase was separated. 1 M HCl (1 mL) etheral solution was added immediately to the organic phase and passed through a small pad of silica The product was eluted using 1:3 v/v methanol acetone. The residue was concentrated in *vacuo* and used without further purification.

Methyl 6-cyano-4-nitro-2-naphthoate (40)

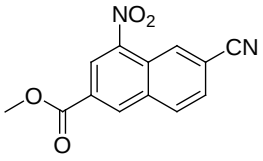

The synthesis was adapted from a procedure by Wendt and coworkers.[4]

Potassium nitrate (202 mg, 2 mmol) was slowly added at 0°C to a solution of 6-cyano-2-naphthalenecarboxylic acid methyl ester (**14**) (422 mg, 2 mmol) dissolved in concentrated sulphuric acid (5 mL). After the reaction mixture became dark brown it was stirred for 15 minutes and poured into ice-water. The precipitate was collected by filtration, washed with water and recrystallized from ethyl acetate and ethanol. A pale yellow powder 158 mg (62%) was obtained. Characterization data matched the data in the literature.[4]

^{1}H NMR (600 MHz, $CDCl_3$) δ: 9.07 (s, 1H), 8.94 (s, 1H), 8.90 (s, 1H), 8.21 (d, *J* = 8.4 Hz, 1H), 7.86 (d, *J* = 8.4 Hz, 1H), 4.06 (s, 3H);

^{13}C NMR (150 MHz, $CDCl_3$) δ: 164.5, 146.6, 136.6, 134.9, 131.5, 129.8, 129.6, 129.0, 126.2, 125.4, 118.0, 115.5, 53.4;

CI-HRMS: Calculated for $C_{13}H_8N_2O_4$ $[M]^+$: 256.0477. Found: 256.0484.

Methyl 4-amino-6-cyano-2-naphthoate (41).

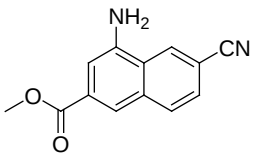

The synthesis was adapted from a procedure by Wendt and coworkers.[4]

Hydrogen gas was passed for 5 minutes through a solution of methyl 6-cyano-4-nitro-2-naphthoate **(40)** (348 mg, 1.36 mmol), 10% Pd/C (35 mg) in a mixture of THF (10 mL) and ethyl acetate (12 mL). The reaction mixture was stirred at room temperature for 16 h and filtered through celite and silica gel and washed with ethyl acetate. The solvents were evaporated in *vacuo* and the resulting solid was washed with ether (20 mL) to afford 27 mg of the desired product 12% yield. Characterization data matched the data in the literature.[4]

^{1}H NMR (600 MHz, $CDCl_3$): 8.28 (s, 1H), 8.09 (s, 1H), 7.98 (d, J = 8.5 Hz, 1H), 7.64 (dd, J = 8.5Hz, J = 0.9Hz, 1H), 7.53 (s, 1H), 3.98 (s, 3H);

^{13}C NMR (150 MHz, $CDCl_3$) δ: 166.8, 135.1, 131.3, 131.1, 127.7, 127.2, 125.2, 124.8, 121.6, 119.2, 110.9, 110.4, 52.7;

ES-HRMS: Calculated for $C_{13}H_{10}N_2O_2$ $[M]^+$: 226.0742. Found: 226.0752.

4-Bromo-6 cyano-2- naphthalenecarboxylic acid, methyl ester (43)

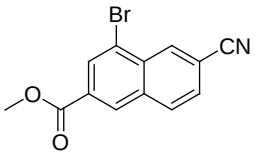

The synthesis was adapted from a procedure by Wendt and coworkers.[4] 6-Cyano-2-naphthalenecarboxylic acid, methyl ester (**14**) (211 mg, 1 mmol) was dissolved in dicloromethane (1 ml) followed by addition of bromodimethylhydantoin (285 mg, 1 mmol) and trifluoromethanesulfonic acid (0.088 ml, 1 mmol). The reaction mixture was stirred in darkness for 18 hours, and poured into saturated $NaHSO_3$. Na_2CO_3 was added until the pH was less than 7, and extracted with ethyl acetate. The organic solvents were

washed with brine, dried with Na_2SO_4, filtered and concentrated in *vacuo*. The desired product was purified on silica gel using a gradient of hexane and ethyl acetate. Characterization data matched the data in the literature.[4]

^{1}H NMR (600 MHz, $CDCl_3$): 8.68 (s, 1H), 8.59 (s, 1H), 8.47 (s, 1H), 8.07 (d, *J* = 8.4 Hz, 1H), 7.75 (dd, *J* = 8.4 Hz, *J* = 1.2 Hz, 1H), 4.02 (s, 3H);

^{13}C NMR(150 MHz, $CDCl_3$): 165.4, 135.0, 133.5, 133.4, 131.3, 131.1, 130.9, 130.5, 128.2, 123.6, 118.5, 113.3, 53.0;

ES-MS: Calculated for $C_{13}H_9NO_2Br$ $[M]^+$:289.1 Found:289.1.

4-Bromo-6 cyano-2- naphthalenecarboxylic acid (48)

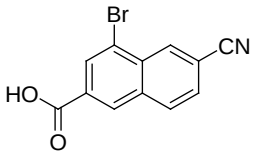

To 4-bromo-6 cyano-2- naphthalenecarboxylic acid, methyl ester **43** (144 mg, 0.5 mmol) in 1:1 THF/H_2O (4 mL) LiOH/H_2O (102 mg, 2.5 mmol) was added and stirred for 90 min. The reaction mixture was concentrated in *vacuo* and the resulting lithium carboxylate salt was used without further purification.

2-Nitrile-6-methylester-8-N-(2-pyrimidine)-naphtalene (42)

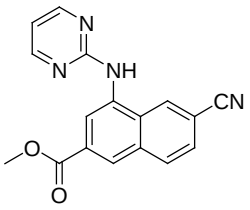

An oven-dried microwave vial was charged under argon with 4-bromo-6 cyano-2-naphthalenecarboxylic acid, methyl ester **(43)** (115 mg, 0.4 mmol), 2-dicyclohexylphosphino-2′,6′-dimethoxybiphenyl (16 mg, 0.04 mmol), tris(dibenzylideneacetone)dipalladium(0) (11 mg, 0.02 mmol), $CsCO_3$(260 mg, 0.8 mmol), 2-aminopyrimidine (75 mg, 0.8 mmol) and THF (2ml). The reaction mixture was heated in a microwave at 165^{o}C, (150W) for 10 min. The crude reaction was filtered through a pad of Celite and washed with EtOAc. The filtrate was evaporated under reduced pressure and the crude product was purified by flash chromatography on silica gel gradient hexane ethyl acetate to afford 58 mg product (48%) yield. Characterization data matched the data in the literature.[4]

^{1}H NMR (600 MHz, $CDCl_3$): 8.62 (s, 1H), 8.46-8.45(m, 4H), 8.08 (d, J = 8.5 Hz, 1H), 7.69 (dd, J = 8.5 Hz, J = 1.4 Hz, 1H), 7.38 (brs, 1H), 6.82 (t, J = 4.8 Hz, 1H), 4.00 (s, 3H);

^{13}C NMR (150 MHz, $CDCl_3$): 166.5, 161.1, 158.6, 135.7, 135.0, 131.4, 130.8, 130.0, 128.7, 127.4, 121.1, 119.0, 113.8, 111.7, 52.8;

ES-MS: Calculated for $C_{17}H_{13}N_4O_2$ $[M]^+$: 305.1 Found: 305.1.

General procedure for the coupling with iodoaniline

To a 0ºC cooled suspension of iodoaniline (219 mg, 1 mmol) in CH_2Cl_2 (5 mL) a solution of $AlMe_3$ (0.5 ml, 1 mmol, of a 2.0 M in toluene) was added dropwise. The reaction mixture was stirred for 30 minutes at room temperature followed by the addition of (152 mg, 0.5 mmol) x, and the stirring was continued for additional 30 minutes. The reaction was quenched with 5% aq HCl (20 mL). The organic layer was removed in *vacuo* and the crude reaction mixture was purified on silica (CombiFlashTeledyne Isco) using a gradient of 100-0% hexane /ethylacetate .

Compound 54

Compound **54** was obtained in 71% yield (350 mg)

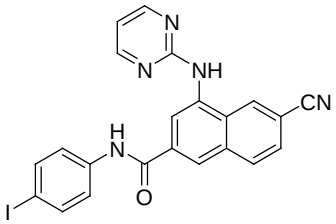

^{1}H NMR (600 MHz,DMSO): 10.62 (s, 1H), 9.87 (s, 1H), 8.74 (s, 1H), 8.49 (d, *J* = 4.8 Hz, 2H), 8.45 (s, 1H), 8.41 (s, 1H), 8.27 (d, *J* = 8.5 Hz, 1H), 7.89 (d, *J* = 8.5 Hz, 1H), 7.72 (d, *J* = 8.7 Hz, 2H), 7.66 (d, *J* = 8.7 Hz, 2H), 6.91 (t, *J* = 4.8 Hz, 1H);

^{13}C NMR (150 MHz, $CDCl_3$): 165.2, 161.0, 158.3, 138.9, 137.4, 136.7, 135.1, 134.5, 130.8, 130.0, 128.0, 127.0, 123.4, 122.5, 119.7, 119.0, 113.3, 109.4, 87.7, 54.9;

ES-HRMS: Calculated for $C_{22}H_{15}N_5OI$ $[M]^+$:492.0327 Found: 492.0321.

General procedure for amidine synthesis.

To a solution of cyano compound (**13a**), (**13b**) or (**13c**) (123 mg, 0.25 mmol) in EtOH (10 mL) (174 mg, 2.5 mmol) $H_2NOH{\cdot}HCl$ was added followed by the addition

diisopropylethylamine (0.7ml, 5 mmol). The reaction mixture was stirred at 80^{o}C for 2 h and the solvent was removed in *vacuo* and coevaporated with $CHCl_3$ three times to give hydroxy amidine (**14a**), (**14b**) or (**14c**). Ac_2O (0.765 ml, 7.5 mmol) was added to the crude hydroxy amidine dissolved in acetic acid (5 mL) and stirred for 30 min at room temperature. Toluene was used as azeotrope and solvent was removed in *vacuo*. The residue was taken up three more times in toluene and removed in *vacuo* then dissolved in EtOAc and washed with $NaHCO_3$ (aq., sat.). The organic layer was dried and concentrated under reduced pressure. Pd/C (10mg, 100 wt %), and it was added to a solution of the acetylated hydroxy amidine in MeOH (10 mL) followed by hydrogenation at atmosphere pressure for 30 min using H_2. The reaction was flushed with Ar and Pd/C was removed by filtration through a pad of celite, which was rinsed with MeOH–AcOH 10:1. The residue was taken up three more times in toluene and removed in *vacuo*. The products were isolated using LC-MC in 23% (29 mg) yield for compound (**64**) and 11 % (14mg) for compound (**66**) respectively.

Compound 66

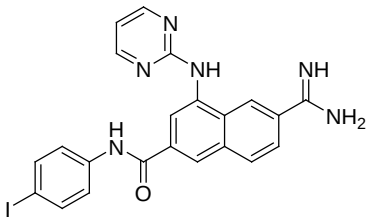

^{1}H NMR (600 MHz,DMSO): 10.62 (s, 1H), 9.76 (s, 1H), 9.43 (s, 1H), 9.12 (s, 1H), 8.80 (s, 2H), 8.54 (d, *J* = 1.2 Hz, 1H), 8.53 (d, *J* = 4.8 Hz, 2H), 8.40 (s, 1H), 8.41 (s, 1H), 8.30 (d, *J* = 8.6 Hz, 1H), 7.90 (dd, *J* = 8.6 Hz, *J*= 1.6 Hz, 1H), 7.72 (d, *J* = 8.7 Hz, 2H), 7.66 (d, *J* = 8.7 Hz, 2H), 6.94 (t, *J* = 4.8 Hz, 1H);

^{13}C NMR (150 MHz, $CDCl_3$): 165.5, 165.4, 160.8, 158.3, 138.9, 137.4, 137.1, 135.1, 134.9, 130.1, 127.3, 126.1, 125.0, 124.4, 122.8, 122.5, 118.6, 113.4, 87.7;

ES-HRMS: Calculated for $C_{22}H_{18}N_6OI$ $[M]^+$: 509.0606. Found: 509.0587.

Compound 64

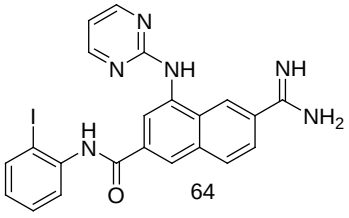

64

^{1}H NMR (600 MHz,DMSO): 10.62 (s, 1H), 9.76 (s, 1H), 9.45 (s, 1H), 9.12 (s, 1H), 8.81 (s, 1H), 8.62 (s, 1H), 8.54 (d, *J* = 4.8 Hz, 1H), 8.47 (s, 1H), 8.30 (d, *J* = 8.6 Hz, 1H), 7.97 (dd, *J* = 8.2 Hz, *J* = 1.3 Hz, 1H), 7.92 (dd, *J* = 8.6 Hz, *J* = 1.6 Hz, 1H),7.53-7.46(m, 2H), 7.10-7.08(m, 1H), 6.94 (t, *J* = 4.8 Hz, 1H);

^{13}C NMR (150 MHz, $CDCl_3$): 165.5, 160.8, 158.3, 139.7, 139.0, 137.2, 135.2, 134.4, 130.1, 128.9, 128.4, 127.5, 126.2, 125.1, 124.5, 122.9, 118.7, 113.4, 98.5;

ES-HRMS: Calculated for $C_{22}H_{18}N_6OI$ $[M]^+$: 509.0524. Found: 509.0547.

3.9. References:

(1) Nienaber, V. L.; Davidson, D.; Edalji, R.; Giranda, V. L.; Klinghofer, V.; Henkin, J.; Magdalinos, P.; Mantei, R.; Merrick, S.; Severin, J. M.; Smith, R. A.; Stewart, K.; Walter, K.; Wang, J.; Wendt, M.; Weitzberg, M.; Zhao, X.; Rockway, T. *Structure (London, England : 1993)* **2000**, *8*, 553.

(2) Klinghofer, V.; Stewart, K.; McGonigal, T.; Smith, R.; Sarthy, A.; Nienaber, V.; Butler, C.; Dorwin, S.; Richardson, P.; Weitzberg, M.; Wendt, M.; Rockway, T.; Zhao, X.; Hulkower, K. I.; Giranda, V. L. *Biochemistry* **2001**, *40*, 9125.

(3) Wendt, M. D.; Rockway, T. W.; Geyer, A.; McClellan, W.; Weitzberg, M.; Zhao, X.; Mantei, R.; Nienaber, V. L.; Stewart, K.; Klinghofer, V.; Giranda, V. L. *J. Med. Chem.* **2003**, *47*, 303.

(4) Wendt, M. D.; Geyer, A.; McClellan, W. J.; Rockway, T. W.; Weitzberg, M.; Zhao, X.; Mantei, R.; Stewart, K.; Nienaber, V.; Klinghofer, V.; Giranda, V. L. *Bioorg. Med. Chem. Lett.* **2004**, *14*, 3063.

(5) Maignan, S.; Mikol, V. *Curr. Top. Med. Chem.* **2001**, *1*, 161.

(6) Rai, R.; Sprengeler, P. A.; Elrod, K. C.; Young, W. B. *Curr. Med. Chem.* **2001**, *8*, 101.

(7) Spraggon, G.; Phillips, C.; Nowak, U. K.; Ponting, C. P.; Saunders, D.; Dobson, C. M.; Stuart, D. I.; Jones, E. Y. *Structure (London, England : 1993)* **1995**, *3*, 681.

(8) Rockway, T. W.; Nienaber, V.; Giranda, V. L. *Curr. Pharm. Des.* **2002**, *8*, 2541.

(9) Moneo, Á.; Carvalho, M. F. N. N.; Telo, J. P. *J. Phys. Org. Chem.* **2012**, *25*, 559.

(10) Ishihara, T.; Seki, N.; Hirayama, F.; Orita, M.; Koshio, H.; Taniuchi, Y.; Sakai-Moritani, Y.; Iwatsuki, Y.; Kaku, S.; Kawasaki, T.; Matsumoto, Y.; Tsukamoto, S.-i. *Bioorg. Med. Chem.* **2007**, *15*, 4175.

(11) Kofink, C. C.; Blank, B.; Pagano, S.; Gotz, N.; Knochel, P. *Chem. Commun.* **2007**, 1954.

(12) Sukata, K. *Reaction of aromatic acyl chlorides with potassium or sodium cyanide impregnated onto amberlite XAD resins. Efficient synthesis of aromatic acyl cyanides*; Chemical Society of Japan: Tokyo, JAPAN, **1987**; Vol. 60.
(13) Correa, A.; Tellitu, I.; Domínguez, E.; SanMartin, R. *Org. Lett.* **2006**, *8*, 4811.

Chapter 4 - Synthesis and Evaluation of Guanidinyl Dipeptides as Imaging Agents of Urokinase Plasminogen Activator

4.1. Overview

A promising class of uPA inhibitors have been described in literature[1-4] based on a dipeptidyl scaffold. The peptides consist of four residues (P4–P3–P2–P1) where P1 is either an aryl amidino group or aryl guanidine group at the C terminus; P2 and P3 are aminoacids; and P4 is a substituted aryl sulfonamide at the N terminus. Several aryl groups such as phenyl, 2-pyridyl, 3-pyridyl, and 2-thiophenyl were incorporated and have been explored in the optimization of the P1 position[2] with a phenylguanidine showing a relatively high affinity for uPA (K_i = 14 nm and K_i = 2 nM for (**i**) and (**ii**), respectively).[3,4]

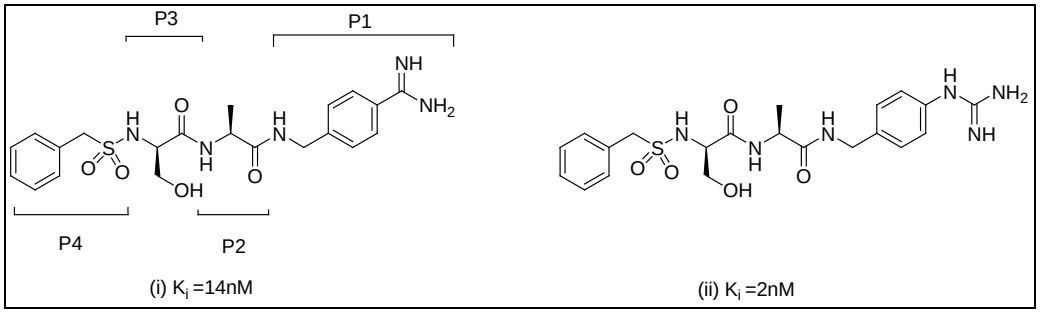

Figure 4.1. Replacement of the P1 benzamidine group in (**i**) with a phenylguanidine group shown in (**ii**) resulted in an increased affinity for uPA.[5]

It has been shown that D-serine used at P3 position greatly improved the inhibitory potency.[4] The pharmacokinetic behaviour of compound (**i**) revealed that it has a fast hepatobiliary elimination and is rapidly cleared from the blood of rats with a

The synthesis, the initial radiolabelling and the initial screening procedures were performed by Silvia Albu. Subsequent labelling and screening was done by Alyssa Vitto while in-vivo biodistribution studies were completed by Alyssa Vitto and Nancy Janzen.

halflife shorter than 20 min.[4] Modifying the benzene sulfonic ring at P4 in compound (**iii**) by substituting it with a carboxylic group in *para* and *meta* position (Figure 4.2.) resulted in the elongation of $t_{1/2}$ to between 1.3 and 2 h. Unfortunately these compounds resulted in a 3–5-fold loss in inhibitory potency towards uPA.[4]

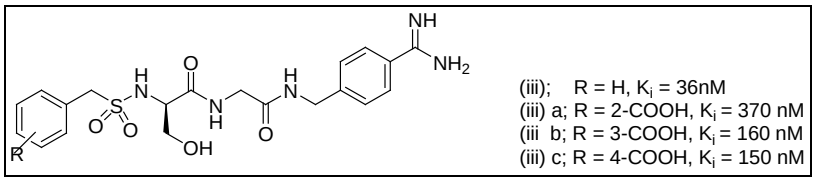

Figure 4.2. Optimization of the aryl sulfonamide at P4 resulted in a decrease in uPA binding potency.[4]

A further optimization study was conducted on compound (**i**) (Figure 4.3.) involving replacement of the alanine residue at the P2 position with polar or charged amino acids such as Ser, Glu, Lys, and Arg resulting in longer circulation time while maintaining binding affinity. Inhibitor (**i.a**) was further evaluated in *vivo* for its efficacy towards experimental lung metastases formation of human fibrosarcoma in nude mice. The compounds showed a strong antimetastatic efficacy with a significantly prolonged survival of mice.[4]

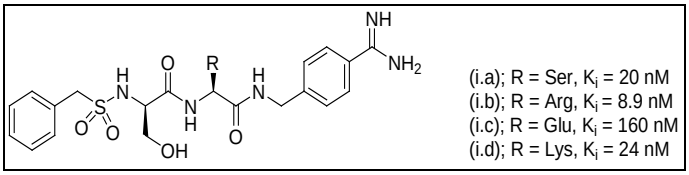

Figure 4.3. Series of derivatives developed while optimizing binding at the P2 position.[4]

Peptide (**ii**) represents an attractive lead for the development of molecular probes as its affinity for uPA is in the low nanomolar range and it can be readily modified at multiple sites (Figure 4.4.). Once again, site selection for radionuclide incorporation was carefully considered. Three positions were chosen (Figure 4.4): iodine incorporated in the

benzene sulfonyl ring (derivative **ii.a**); derivatization of the phenyl guanidine ring (derivative **ii.f**); and tyrosine iodination at P2 position (**ii.e**). In addition, we examined a number of substituions at P2 position by substituting alanine with charged or polar amino acids (**ii.b**, **ii.c** and **ii.d**) in order to modify of the pharmacokinetic properties. The following chapter is presented in the form of a manuscript describing the synthesis, radiolabeling in *vitro* and in *vivo* studies of these potent guanylated dipepetides.

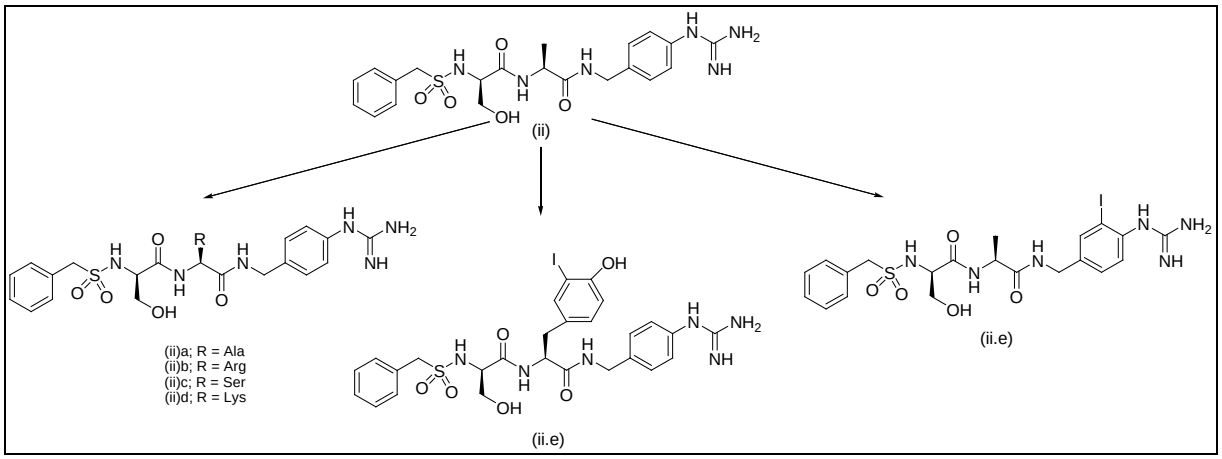

Figure 4.4. Target peptides derivatives.

4.2. Synthesis and Evaluation of Iodinated Guanidinyl Dipeptides as Molecular Imaging Probes for Urokinase Plasminogen Activator (uPA)

Silvia Albu, Alyssa Vito, Nancy Janzen, Alfredo Capretta, John F. Valliant.

Department of Chemistry and Chemical Biology, McMaster University, Hamilton, Ontario, Canada, L8S 4M1

4.2.1. Introduction

Early diagnosis has been shown to be a major determinant in the effective treatment of cancer where information about aggressiveness helps to identify patients at greatest risks.[6] As such, finding molecular imaging probes capable of selectively targeting agressive tumours has been a key goal in nuclear medicine. Urokinase plasminogen activator (uPA) is a particularly attractive target because the serine protease is universally associated with aggressive cancers where the enzyme catalyzes the activation of plasminogen into plasmin *via* cleavage of a specific arginine-valine moiety.[6] The uPA system is primarily associated with the leading edge of migrating cancer cells, which ultimately results in tumour matrix and basement membrane dissolution; prerequisites for tumour invasion and metastasis.

Cancer proteomic studies identified uPA and uPAR (uPA receptor) as being intimately involved in cancer intravasation. In a study of 8,377 breast cancer patients, levels of uPA and its inhibitor PAI-1 were among the best prognostic markers of disease free survival next to lymph-node status.[7] In patients with lymph-node negative tumours, levels of uPA/PAI-1 were strong predictors of metastasis and a high uPA/PAI-1 ratios is associated with 6-fold higher risk of relapse. Additional clinical studies have shown that the overexpression of uPAR is associated with a high incidence of disease recurrence or death.[8] Increased expression of the uPA/uPAR system, which has been found in many malignancies including breast and prostate cancers, is consistently correlated with the presence of distal metastases, invasive phenotypes and poor prognosis.[6]

There are a number of optical probes that have been developed for uPA [9] but only a limited number of radiolabeled compounds. The endogenous uPA inhibitor, human plasminogen activator inhibitor type-2 (PAI-2, serpinB2)[10,11] and the ΔCDloop fragment were labeled with a range of isotopes including ^{213}Bi, ^{125}I, ^{123}I, and ^{99m}Tc but showed low tumour uptake.[12,13,14] It should be noted however, that the alpha emitting therapeutic agent ^{213}Bi –PAI-2[13,14] did cause a notable delay in cancer cell growth.[13,14] More recently an optical and ^{18}F probe for uPA were prepared using an irreversibile phosphonate inhibitor[14,1515151515] as a targeting vector.[15,16] Unfortunately the PET agent showed modest T/NT ratio in tumour bearing mice.

There are a number of uPA inhibitors that have been reported that could serve as platforms for developing molecular imaging probes. A dipeptide system[1,2,3,4] consisting of D-serine / L-alanine capped at the N-terminus with a benzylsulphonamide and at the C-terminus with a 4-(aminomethyl)-phenylguanidine moiety have been reported to bind uPA with a K_i value of 2 nM.[3] The system also lends itself to the substitution of polar amino acids in place of alanine or serine which can be used to tune pharmacokinetic properties.[4] Herein we report the preparation and screening of a series of radioiodinated analogues where iodine was chosen as the isotope of interest since a single construct can be used to create positron emission tomography (PET) (^{124}I),[17] single photon emission computed tomography (SPECT) (^{123}I) and radiotherapy (^{131}I) agents.[18]

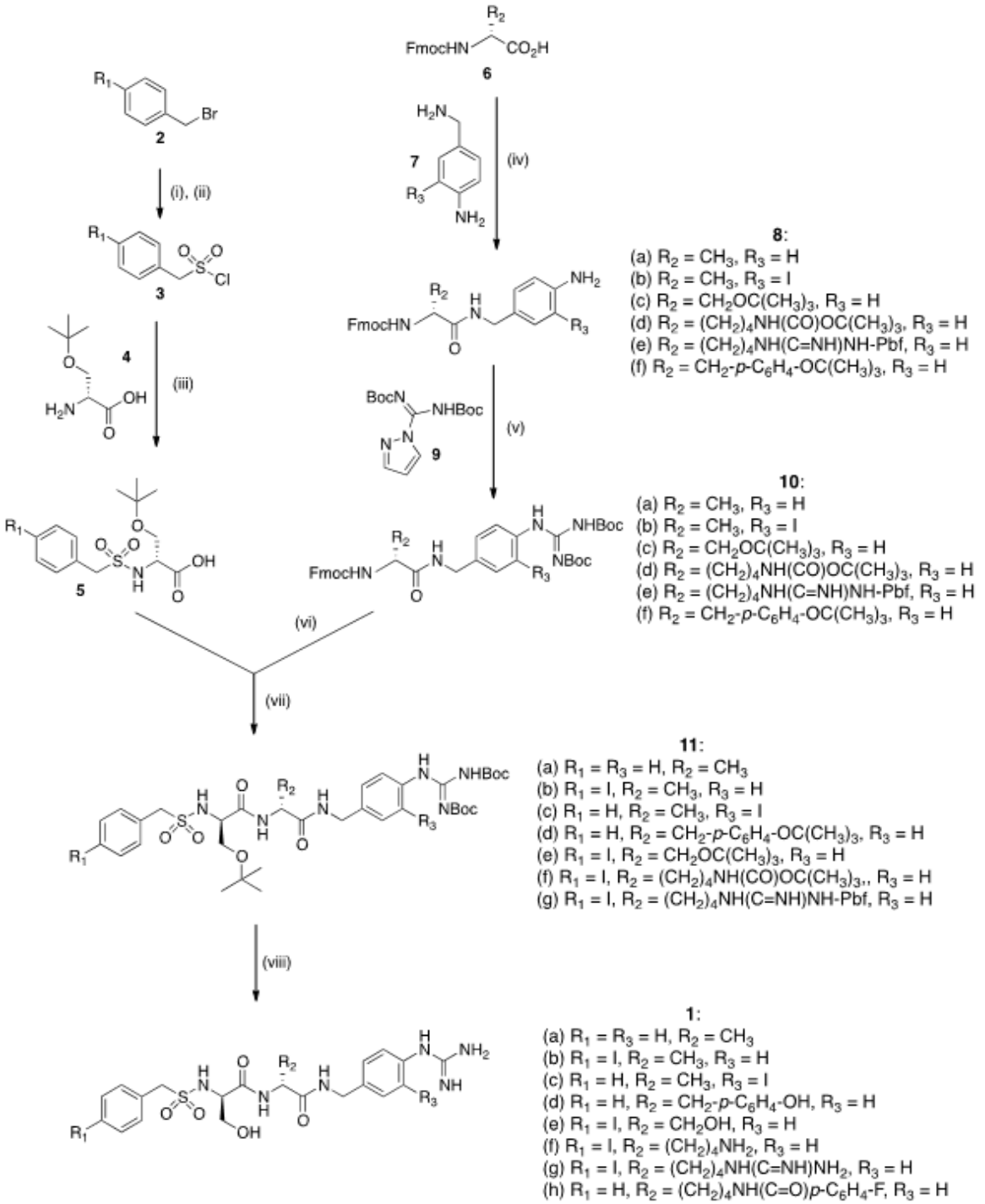

Scheme 4.1. Synthesis of iodinated peptide library. Reagents: (i) Na_2SO_3, acetone-water (1:1); (ii) $POCl_3$, ACN; (iii) TMS-Cl, TEA, DCM; (iv) PyBOP; DIPEA; DMF; (v) MeOH; (vi) diethylamine, DCM; (vii) PyBOP; DIPEA; DMF; (viii) TFA, H_2O, TIPS.

4.2.2. Results and Discussions

A modified synthesis of the alanine / serine dipeptide was developed to allow for the incorporation of iodine (Scheme 4.1.) into the peptide backbone. Treatment of benzylbromide (**2**, R_1 = H) with sodium sulfite yielded the sodium salt of phenylmethanesulfonate that could be readily converted into the corresponding sulfonylchloride ((**3**), R_1 = H) with $POCl_3$. Coupling to O-^{t}butyl protected D-serine (**4**) yielded (**5**) (R_1 = H) in 76% yield. Concurrently, Fmoc-protected L-alanine ((**6**)**,** R_2 = CH_3) was selectively ligated to 4-amino-benzylamine ((**7**), R_3 = H) to give (**8**) (R_2 = CH_3, R_3=H). Introduction of the guanidinyl moiety was achieved using *tert*-butyl (1*H*-pyrazol-1-yl) methanediylidenedicarbamate (**9**) where the deprotected product was ultimately coupled to the derivatized serine ((**5**), R_1 = H). Deprotection of the serine and guanidinyl moieties afforded the desired uPA inhibitor (**1a**).

With this synthetic route in hand, halogenated derivatives of the lead compound were readily generated. In the L-alanine / D-serine series, introduction of 4-iodobenzylbromide ((**2**), R_1 = I) into the synthetic scheme allowed for the synthesis of (**1b**) while use of 3-iodo-4-aminobenzyl amine ((**7**), R_3 = I) generated (**1c**). Furthermore, the versatility of the synthetic approach allowed for the use of a protected L-serine, L-lysine, L-arginine and L-tyrosine *in lieu* of L-alanine (to give synthons (**10c**) through (**10f**), respectively) and, ultimately, the synthesis of compounds (**1d**) through (**1g**). The structures of the above synthesized compounds were confirmd by ^{1}H and ^{13}C NMR, HPLC and high resolution MS.

4.2.3. Biological Evaluation of Guanidinylated Dipetides

Compounds (**1a**) through (**1h**) were evaluated for their inhibitory activity against uPA in a colourimetric enzyme assay using Bio-Phen CS-61 (substrate (Aniara, A2209061).[19] Each inhibitor, at various concentrations, was incubated on a 96-well microtitre plate with 50 µL of 694.4 nM stock of uPA (EMD Chemicals Millipore, 672081) for 15 min at 37°C. Upon addition of the substrate, the course of the hydrolysis reaction was monitored by formation of *p*-nitroaniline at 405 nm and 37ºC for 30 min. The reaction rates obtained in the presence of compounds (**1a**) through (**1g**) were compared to those seen with substrate alone and the percent inhibition was calculated. Reported K_m (90 µM) and percent inhibition were used for K_i calculations. All K_i and IC_{50} values were calculated based on the assay being run three times (n=3) in triplicate with the exception of (**1c**), which was only run once (n=1) in triplicate. The results are presented in Table 4.1.

Table 4.1. Inhibitor structures and affinities

Compound		K_i (nM)	95% CI	IC_{50} (nM)	95% CI	r^2	Std Error
1a	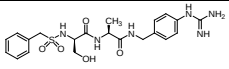	6.7	6.09 – 7.41	23.5	21.3 – 25.9	0.996	1.05
1b	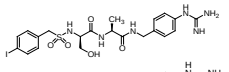	1.4	1.16 – 1.59	4.7	4.05 – 5.56	0.989	1.08
1c	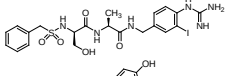	253	99.1 – 646	759	297 – 1940	0.939	2.56
1d	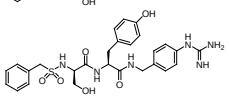	47.9	34.6 – 66.3	168	121 – 232	0.940	1.18
1e	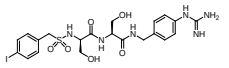	6.1	5.12 – 7.28	21.3	17.9 – 25.5	0.987	1.09

1f	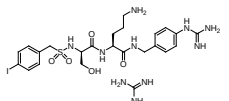	1.6	1.22 – 2.18	5.7	4.25 – 7.63	0.930	1.16
1g	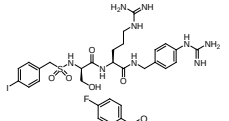	2.6	2.33 – 2.89	9.1	8.14 – 10.1	0.990	1.06
1h	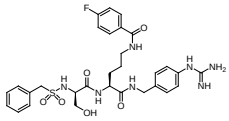	20.4	16.7 – 25.0	71.5	58.6 – 87.4	0.988	1.10

Compound (**1a**) was previously prepared and tested using the enzyme activity assay described by Zeslawska *et al.*,[3] who reported a K_i value of 2 nM. Under the conditions of the assay described above,[20] we obtained a K_i value of 6.7 nM. The iodinated derivatives were shown to have comparable *in vitro* activities with K_i values in the low nanomolar range. The binding affinity decreased considerably for iodinated analoque (**1c**), containing the iodide *meta* to the guanidine group. Substitution of the alanine at the P2 position with the tyrosine (compound (**1d**)) also yielded a less potent derivative.

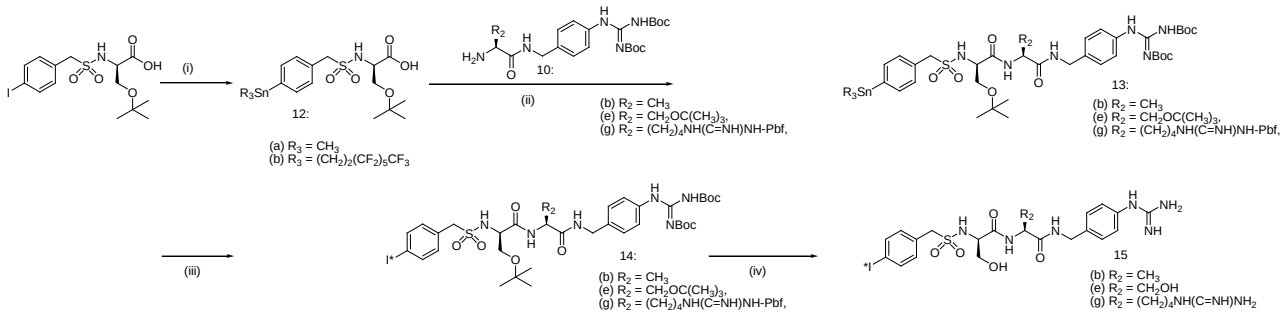

Scheme 4.2. Synthesis of radio-iodinated peptide library. Reagents: (i)$R_3Sn\text{-}SnR_3$,R = CH_3, R = $CH_2(CH_2CF_2)_5CF_3$, PdOAc, PA-Ph, THF; (ii) PyBop, DIPEA, DMF; (iii) $Na^{125}I$, Iodogen, MeOH/5% AcOH; (iv) TFA/CAN.

4.2.4. Synthesis of Radiolabelled Derivatives

Having identified (**1b**)**,** (**1e**) and (**1g**) as the most potent leads, the preparation of the

radiolabeled analogues was undertaken. The synthesis (Scheme 4.2.) takes advantage of the previously developed protocol involving the Pd-catalyzed stannylation of the aryl iodide followed by destannylation / iodination with either ^{123}I or ^{125}I.[21] In this way, (*R*)-3-(*tert*-butoxy)-2-((4-iodophenyl)methylsulfonamido)propanoic acid ((**5**), R_1= I) was stannylated with either tris(1*H*,1*H*,2*H*,2*H*-perfluorooctyl)tin hydride or hexamethyldistannane and a Pd / 1,3,5,7-tetramethyl-2,4,8-trioxa-(2,4-dimethoxyphenyl)-6-phosphaadamantane[22,23] complex to give (**11**). Fmoc deprotection of the guanidinylated amino acids (**10**) was followed by coupling with (**11**) to give the stannylated dipeptides (**13**). Stannylation using tris(1*H*,1*H*,2*H*,2*H*-perfluorooctyl)tin hydride proceed in a 23% yield while the hexamethyldistannane give (**13e**) in 49 % and (**13g**) in 59% yield. Note that the alkylstannanes were used in cases where isolation of the fluorous precursors was not possible due to the presence of impurities in the product. The ^1H NMR showed the presence of the methylene protons on tin for both (**13e**) and (**13g**) as a singlet at 0.27 ppm while compound (**13b**) showed two multiples corresponding to the $(CH_2\text{-}CH_2)_3$ in the aliphatic region at 1.33 and 2.40 ppm.

Radiolabeled compounds were prepared by the treatment of (**13b**, **13e** and **13g**) with IodoGen (1,3,4,6-tetrachloro-3R,6R-diphenylglycouril) and either $Na^{123}I$ or $Na^{125}I$. In the case of (**14b**), a fluorous tin derivative, purification was carried out conveniently using a fluorous SPE cartridge[21] while HPLC was employed for purification of (**14e**) and (**14g**). After TFA deprotection, HPLC analysis of each compound was performed with co-injection of the corresponding non-radioactive analogues to verify successful destannylation/iodination and TFA deprotection (Figures 4.5. – 4.7.).

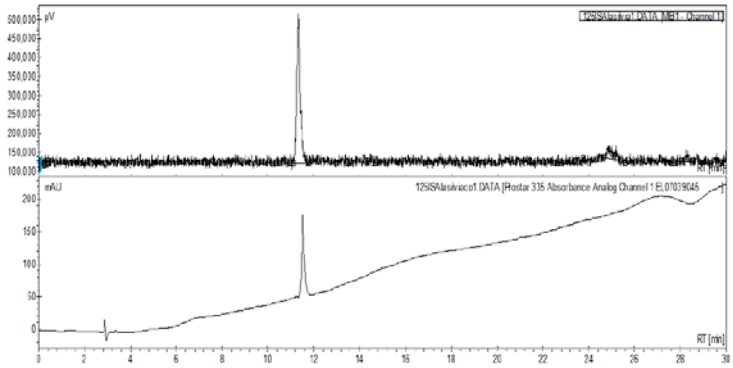

Figure 4.5. UV and γ-HPLC chromatograms (HPLC Method A) of (**15b**) co-injected with the nonradioactive standard.

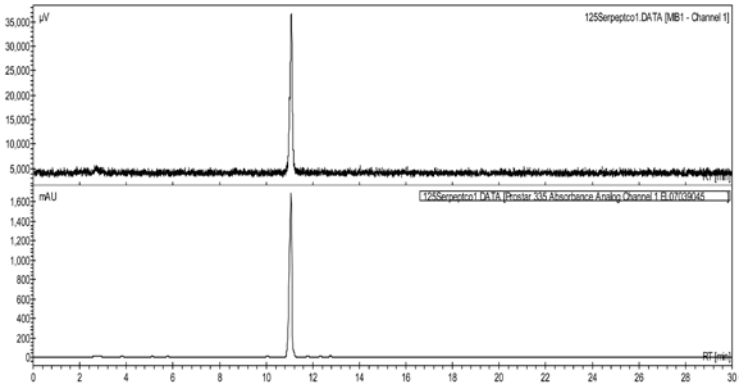

Figure 4.6. UV and γ-HPLC chromatograms (HPLC Method A) of (1**5e**) co-injected with the nonradioactive standard.

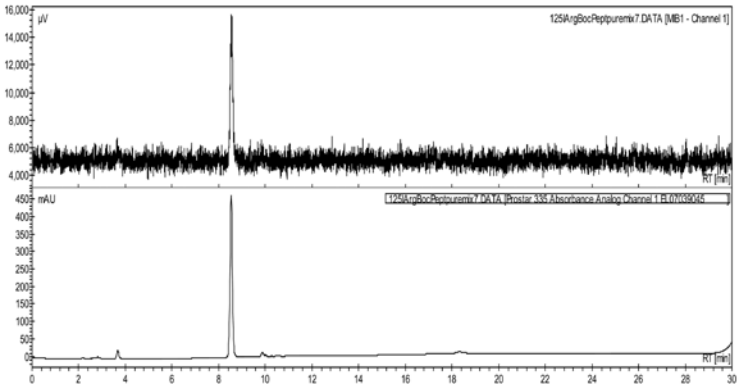

Figure 4.7. UV and γ-HPLC chromatograms (HPLC Method A) of (**15g**) co-injected with the nonradioactive standard.

4.2.5. *In Vivo* Biodistribution Studies

In vivo biodistribution studies were performed on the three lead compounds using CD1 female nude mice (3-4 weeks old) bearing tumours derived from MDA-MB-231, HT-1080 and HT-29 cells.[13] Tumour bearing mice were administered 185-370 kBq of (**15b**), (**15e**) or (**15g**) *via* a tail vein injection groups of mice (n = 3) were sacrificed and the tumors and organs isolated by dissection and counted and data reported as percent injected dose per gram (%ID/g) (Figures 4.8. – 4.10.).

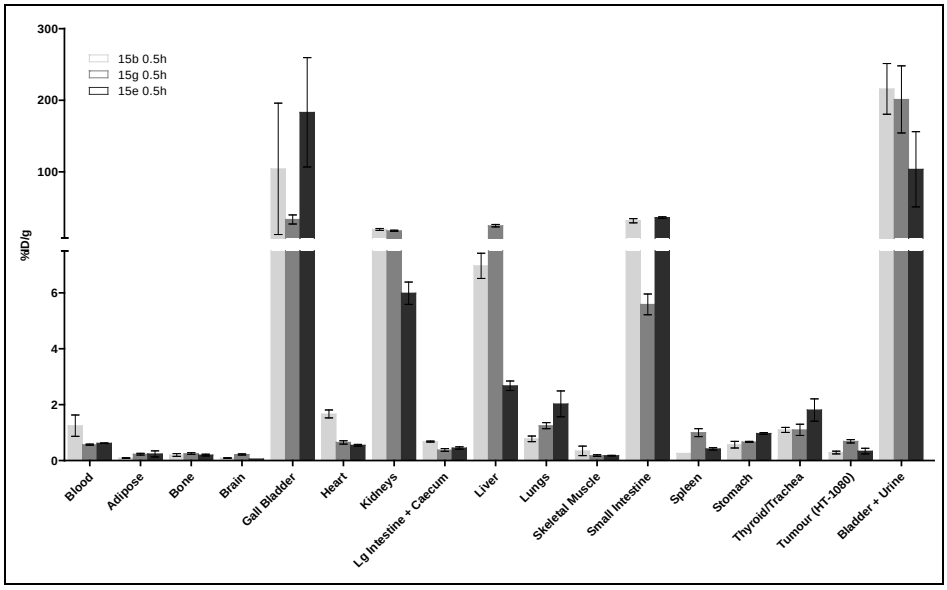

Figure 4.8. Comparative graphical analysis of percent injected dose per gram, in organs/tissues harvested for (**15b**), (**15e**) and (**15g**), at 0.5 h P.I .in HT-1080 tumour xenograft model.

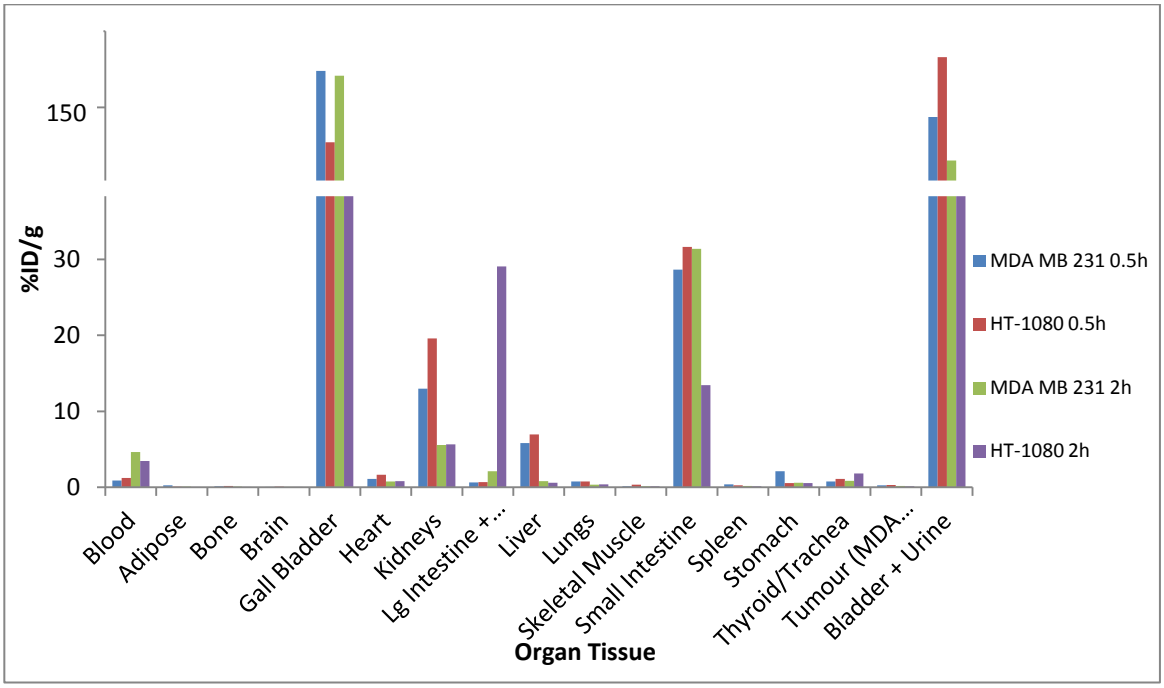

Figure 4.9. Graphical analysis of percent injected dose per gram, in organs/tissuesharvested for (**15b)** in both MDA-MB-231 and HT-1080 tumour xenograft models, 0.5h and 2h P.I.

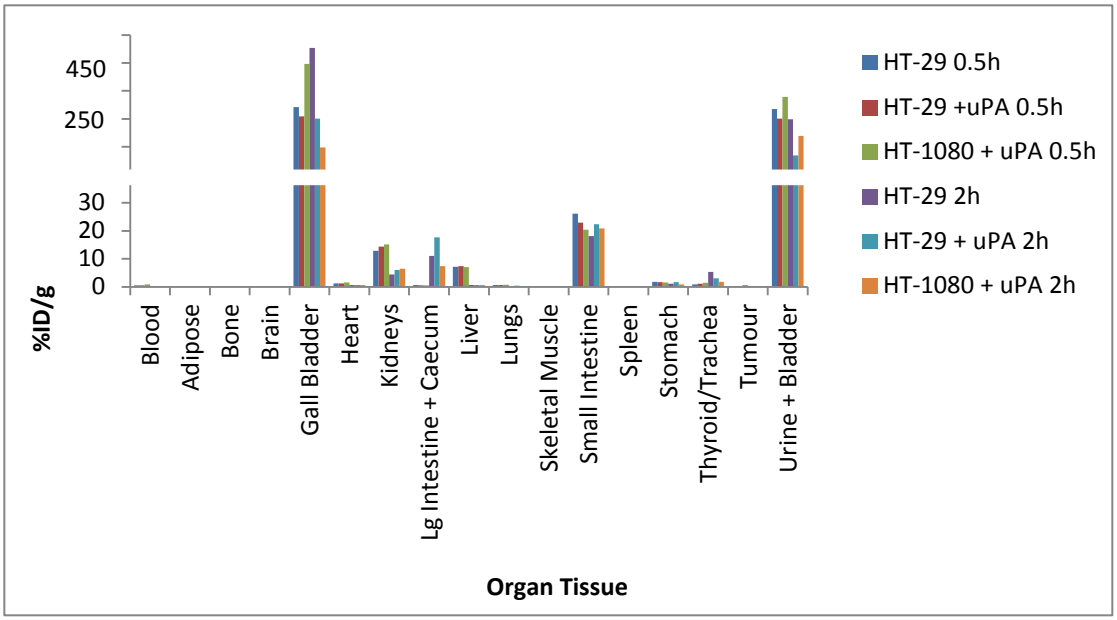

Figure 4.10. Graphical analysis of percent injected dose per gram, in organs/tissues harvested for (**15e**). Groups with uPA are indicative of groups that were pre- incubated with endogenous uPA for 0.5h at 37ºC.

Irrespective of the models used, all three radiotracers showed low tumour uptake (< 1% ID/g) and were rapidly eliminated *via* the hepatobiliary and renal systems at 0.5h P.I. The uptake showed minimal difference between the uPA positive models (HT-1080 and MDA-MB-231) and the negative control (HT29). In the liver, the uptake varied from 24 %ID/g for (**15g**), 6% %ID/g for (**15b**) to a low 2% D/g for (**15e**). These differences are likely due to the varying polarities of the compounds associated with the central amino acid.[4] Blood levels were low (< 1% ID/g) as was thyroid uptake which at 0.5h P.I was below 1.5 %ID/g and slightly increased (4.1% ID/g) at 2h P.I. These results sugest that the compounds tested are relatively stable towards *in vivo* dehalogenation.

One possible explanation for the low tumour uptake was the rapid excretion of the labeled compounds which is consistent with the pharmacokinetic data observed for the related amidine class of compound. Preincubation and coadministration with uPA was performed to assess the potential of using uPA as a carrier since the inhibitors are reported to not inhibit the ability of uPA to bind to uPAR. Following 0.5h and 2h uptake periods, groups of mice (n = 3 per time point, per cell line) were sacrificed and the tumours and organs were isolated by dissection. (Figure 4.10.). Unfortunately the addition of the protein had little impact on tumour uptake (0.69%ID/g).

4.2.6. Conclusions

A series of iodinated compounds were synthesized in an attempt to develop a radiotracer to monitor uPA expresion in tumours. Compounds were tested in *vitro* in a colorimetric assay where three leads demonstrated high affinity towards uPA. After successful preparation of the labeled compounds the biodistribution of (**15b**), (**15e**), and

(**15g**) was performed in three different mouse models showed only modest tumour uptake despite high affinity for the protein in vitro.

4.3. Experimental

Experimental Section General.

Unless otherwise stated, all chemicals reagents were purchased and used as received from Sigma-Aldrich without further purification. Solvents were purchased from Caledon. 1,3,5,7-Tetramethyl-2,4,8-trioxa-6-phenyl-6-phospha-adamantane(PA-Ph) was purchased from Cytec Canada (sold as CYTOP-292). Phenylmethanesulfonyl chloride (3, R_1= H) was purchased from Sigama Aldrich. (4-Iodophenyl)methanesulfonyl chloride (3, R_1=I)[24] and 3-(*tert*-butoxy)-2-(phenylmethylsulfonamido)propanoic acid (5, R_1=H) were synthesized according to the literature procedures.[24] Reactions were monitored using Alugram Sil G/UV254 thin layer chromatography (TLC) plates and visualized under ultraviolet light. Column chromatography was accomplished with Silica Flash P60 purchased from Silicycle. ^{125}I was obtained from the McMaster University Nuclear reactor as in a 0.1M NaOH solution (Na^{125}I). ^{1}H and ^{13}C NMR spectra were recorded on Bruker AV 700 or AV 700 spectrometer. ^{1}H Chemical shifts are reported in ppm relative to the residual proton signal of the NMR solvents. Coupling constants (*J*) are reported in Hertz (Hz). ^{13}C Chemical shifts are reported in ppm relative to the carbon signal of the NMR solvents. High resolution ES mass spectra were obtained on a Waters QToF Ultima Global spectrometer. Reverse phase analytical HPLC was performed using a Varian Prostar instrument equipped with a 355 UV detector or a Waters 2489 HPLC equipped

with a Waters 2489 UV/Vis (λ = 254 nm) and Bioscan flow count gamma detectors (model 106). Runs were performed using HPLC grade water containing 0.1 % TFA (solvent A) and ACN containing 0.08 % TFA (solvent B) as eluents, a 1 mL/min flow rate and a C18 reverse phase Phenomonex column (25 × 4.60 mm, 5 micron). Gradients consisted of 95 to 5% solvent A over 30 min (Method A) or 35 to 65% solvent A over 5 min followed by 65 to 100% solvent A over 18 min and then 35 to 65% solvent A over 5 min (Method B). Reactions requiring microwave irradiation were performed using a CEM Discover microwave (150W).

3-(Tert-butoxy)-2-((4-iodophenyl)methylsulfonamido) propanoic acid (5, R_1=I)

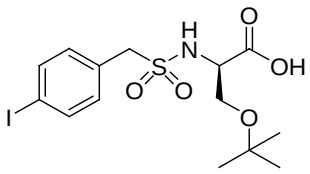

To a solution of (*R*)-2-amino-3-(*tert*-butoxy)propanoic acid (*D*-Ser(tBu)-*OH*, (**4**), 322 mg, 2 mmol) and TEA (0.562 ml, 4 mmol) in DCM (3 ml) under argon was added chlorotrimethylsilane (0.511 ml, 4 mmol) dropwise. The resultant solution was heated to reflux for 2h then cooled in an ice bath, treated with (4-iodophenyl)methanesulfonyl chloride (**3**, R_1 = I, 504 mg, 1.6 mmol) and stirred overnight. The solvent was removed *in vacuo*, the residue dissolved in ether (20 ml) and extracted with 5% aq. $NaHCO_3$ (20 ml). The combined aqueous extracts were acidified with 1M H_2SO_4 to pH = 2 and then extracted with ethyl acetate (2 x 20ml). The combined organic extracts were dried over Na_2SO_4, filtered and the solvent removed *via* evaporation under reduced pressure to afford the pure product in 76% yield (250 mg, 0.6 mmol). The compound showed:

^{1}H NMR (600 MHz, CD_3OD): δ = 7.71 (d, *J* = 8.2 Hz, 2H), 7.23 (d, *J* = 8.2 Hz, 2H), 4.35 (d, *J* = 13.7 Hz, 1H), 4.32 (d, *J* = 13.7 Hz, 1H), 4.03 (dd, *J* = 8.4 Hz, 1H), 3.70 (dd, *J* = 9.1 Hz, *J* = 4.4 Hz, 1H), 3.57 (dd, *J* = 9.1 Hz, *J* = 4.0 Hz, 1H), 1.18 (s, 9H);

^{13}C NMR (150 MHz, CD_3OD): δ = 173.5, 138.7, 134.1, 131.2, 94.8, 74.6, 64.4, 59.9, 58.4, 27.6;

HRMS (ES) for $C_{14}H_{19}NO_5SI$, calculated 440.0009 $[M + H]^+$ found 440.0029 $[M + H]^+$.

General procedure for the preparation of (8).

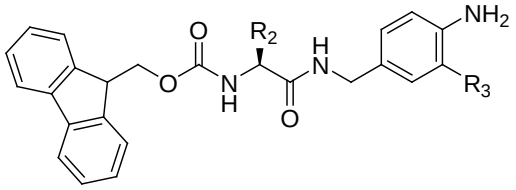

A solution of the Fmoc-protected amino acid (1 mmol), *i*Pr_2NEt (2 mmol) and PyBOP (1 mmol) in DMF (4 ml) was added dropwise to a solution of the 4-amino-benzylamine (1.5 mmol) in DMF (10ml) and the resultant solution was stirred for 3h. The reaction mixture was poured into water (20 ml) then extracted twice with 20 ml EtOAc. The combined organic extracts were washed with successively with water (3 x 20 ml) brine (20 ml) then dried over Na_2SO_4, filtered, and concentrated under a reduced pressure to provide a yellow solid. Purification by flash chromatography on silica gel using ethyl acetate in hexane yield the pure product. The free amine was converted to its hydrochloride salt by dissolving in methanol treated with 1M ethereal solution of HCl and precipitating upon the addition of cold ether.

Compound (8a)

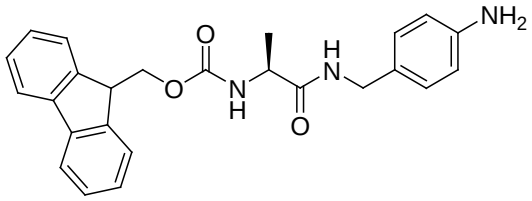

Using the general procedure for the synthesis of (**8**) with Fmoc-L-Ala-OH (311 mg, 1 mmol) and 4-(aminomethyl)aniline (183 mg,1.5 mmol) gave the title compound in 71% yield (340 mg). The compound showed:

^{1}H NMR (600 MHz, CD_3OD): δ = 7.79 (d, *J* = 7.5 Hz, 2H), 7.67–7.65 (m, 2H), 7.38 (dd, *J* = 7.5 Hz, 2H), 7.30 (ddd, *J* = 7.5 Hz, *J* = 0.9 Hz, 2H), 7.02 (d, *J* = 8.1 Hz, 2H), 6.67 (d, *J* = 8.1 Hz, 2H), 4.38–4.36 (m, 2H), 4.24–4.20 (m, 3H), 4.13–4.12 (m, 1H), 1.32 (d, *J* = 7.2 Hz, 3H);

^{13}C NMR (150 MHz, CD_3OD): δ = 175.4, 158.3, 147.9, 145.4, 145.2, 142.6, 129.6, 128.8, 128.2, 126.2, 126.1, 120.9, 116.7, 67.9, 52.1, 43.8, 18.4;

HRMS (ES) for $C_{25}H_{25}N_3O_3$, calculated 416.1974 $[M + H]^+$ found 416.1956 $[M + H]^+$.

Compound 8b

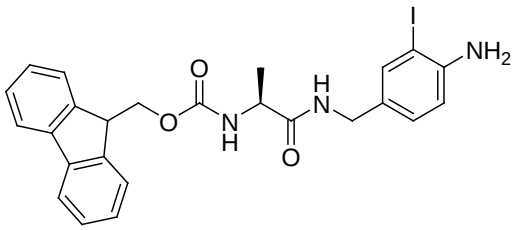

Using the general procedure for the synthesis of (**8)** with Fmoc-L-Ala-OH (311 mg, 1 mmol)) and 4-(aminomethyl)-2-iodoaniline (372 mg,1.5 mmol) gave the title compound in 66% yield (360 mg, 0.6 mmol). The compound showed:

^{1}H NMR (600 MHz, CD_3OD and DMSO): δ = 7.78 (d, *J* = 8.4 Hz, 2H), 7.66–7.64 (m, 2H), 7.52 (s, 1H), 7.37 (dd, *J* = 7.4 Hz, 2H), 7.28 (dd, *J* = 7.4 Hz, 2H), 7.03 (d, *J* = 8.3 Hz, 1H), 6.72 (d, *J* = 8.3 Hz, 1H), 4.39–4.35 (m, 2H), 4.21–4.18 (m, 3H), 4.11–4.10 (m, 1H), 1.32 (d, *J* = 7.0 Hz, 3H);

^{13}C NMR (150 MHz,DMSO): δ = 172.3, 155.7, 147.3, 143.9, 143.8, 140.7, 137.2, 128.3, 127.6, 127.0, 125.3, 120.0, 114.0, 82.9, 65.9, 50.1, 46.6, 40.8, 18.2; HRMS (ES) for $C_{25}H_{24}IN_3O_3$ calculated 542.0941 $[M + H]^+$ found 542.0950$[M + H]^+$.

Compound 8c

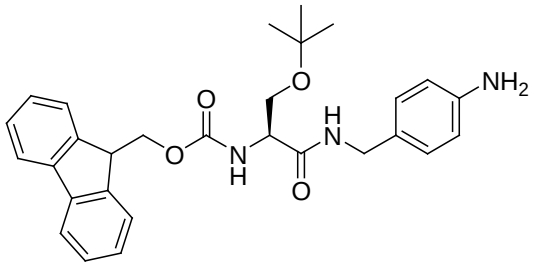

Using the general procedure for the synthesis of (**8**) with Fmoc-L-Ser(tBu)-OH (383 mg, 1 mmol)and 4-(aminomethyl)aniline (183 mg, 1.5 mmol) gave the compound in 70% yield (346 mg, 0.7 mmol). The compound showed:

^{1}H NMR (600 MHz, CD_3OD): δ 7.79 (d, *J* = 7.5 Hz, 2H), 7.66-7.65 (m, 2H), 7.39 (dd, *J* = 7.5 Hz, 2H), 7.30 (dd, *J* = 7.5 Hz, 2H), 7.04 (d, *J* = 7.9 Hz, 2H), 6.66 (d, *J* = 7.9 Hz,

2H), 4.42-4.36 (m, 2H), 4.30-4.21 (m, 4H), 3.65-3.63 (m, 1H), 3.58-3.55 (m, 1H), 1.15 (s, 9H);

^{13}C NMR (150 MHz, CD_3OD): δ = 172.7, 158.3, 147.9, 145.3, 145.2, 142.6, 129.6, 128.8, 128.2, 126.2, 121.0, 116.6, 74.7, 68.1, 63.2, 57.1, 48.4, 43.9, 27.7;

HRMS (ES) for $C_{29}H_{33}N_3O_4$ calculated 488.2549 $[M + H]^+$ found 488.2527 $[M + H]^+$.

Compound 8d

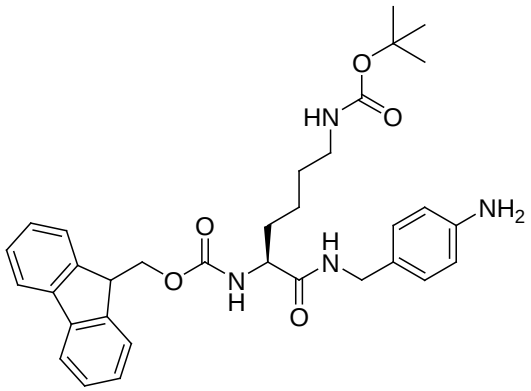

Using the general procedure for the synthesis of (**8**) with (*R*)-2-((((9*H*-fluoren-9-yl)methoxy)carbonyl)amino)-6-((*tert*-butoxycarbonyl)amino)hexanoic acid (468 mg, 1 mmol) and 4-(aminomethyl)aniline (183 mg, 1.5 mmol) gave the compound in 74% yield (425 mg). The compound showed:

^{1}H NMR (700 MHz, CD_3OD): δ = 7.79 (d, *J* = 7.4 Hz, 2H), 7.65 (m, 2H), 7.38 (dd, *J* = 7.4 Hz, 2H), 7.30 (dd, *J* = 7.4 Hz, 2H), 7.02 (d, *J* = 8.0 Hz, 2H), 6.66 (d, *J* = 8.0 Hz, 2 H), 4.38 (d, *J* = 6.8 Hz, 2H), 4.24 (d, *J* = 13.2 Hz, 1H), 4.22–4.19 (m, 2H), 4.05(dd, *J* = 8.4 Hz, *J* = 5.3 Hz, 1H), 3.01–3.00 (m, 2 H), 1.76–1.72 (m, 1H), 1.62–1.61 (m, 1H), 1.41–1.38 (m, 2H), 1.38 (s, 9H), 1.36–1.30 (m, 2H);

^{13}C NMR (175 MHz, $CDCl_3$): δ = 171.4, 162.7, 156.3, 146.0, 144.0, 143.9, 141.4, 129.2, 127.9, 127.3, 125.2, 120.1, 115.4, 67.2, 55.1, 47.3, 43.4, 40.0, 36.6, 32.3, 29.8, 28.6, 22.6; HRMS (ES) for $C_{33}H_{40}N_4O_5$ calculated 573.3077 [M + H^+] found 573.3080 [M + H^+].

Compound 8e

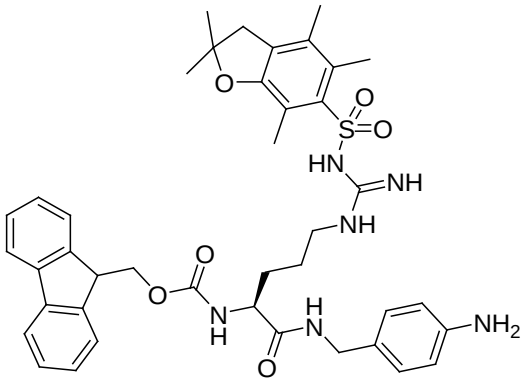

Using the general procedure for the synthesis of (**8**) with (*R*)-2-((((9*H*-fluoren-9-yl)methoxy)carbonyl)amino)-6-(3-((2,2,4,5,7-pentamethyl-2,3-dihydrobenzofuran-6-yl)sulfonyl)guanidino)hexanoic acid (648 mg, 1 mmol) and 4-(aminomethyl)aniline (183 mg, 1.5 mmol) gave the compound in 77% yield (580 mg). The compound showed:

^{1}H NMR (700 MHz, CD_3OD): δ = 7.77 (d, *J* = 7.4 Hz, 2H), 7.63 (dd, *J* = 7.0 Hz, 2H), 7.36 (dd, *J* = 7.4 Hz, 2H), 7.27 (dd, *J* = 7.0 Hz, 2H), 7.00 (d, *J* = 8.0 Hz, 2H), 6.65 (d, *J* = 8.0 Hz, 2H), 4.38–4.37 (m, 2H), 4.23–4.17 (m, 3H), 4.05 (dd, *J* = 8.4 Hz, *J* = 5.3 Hz, 1H), 3.13 (m, 2H), 2.95 (s, 2H), 2.57 (s, 3H), 2.50 (s, 3H), 2.06 (s, 3H), 1.74–1.72 (m, 1H), 1.58–1.57 (m, 1H), 1.50–1.47 (m, 2H), 1.41 (s, 6H);

^{13}C NMR (175 MHz, CD_3OD): δ = 174.3, 159.9, 158.4, 158.1, 147.9, 145.4, 145.1, 142.6, 142.6, 139.4, 134.4, 133.5, 129.7, 129.1, 128.8, 128.8, 128.2, 126.2, 126.2, 126.1, 120.9, 118.5, 116.6, 87.6, 67.8, 56.2, 43.9, 43.9, 30.6, 28.7, 19.6, 18.4, 12.5;

HRMS (ES^+) for $C_{41}H_{48}N_6O_6S$ calculated 753.3407 [M + H^+] found 753.3434 [M + H^+].

Compound 8f

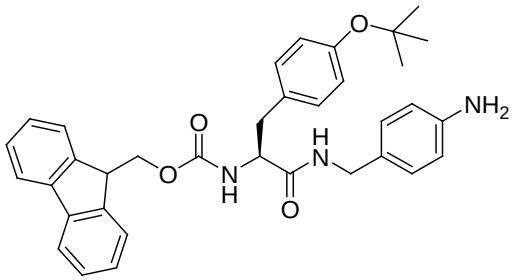

Using the general procedure for the synthesis of (**8**) with ((*R*)-2-((((9*H*-fluoren-9-yl)methoxy)carbonyl)amino)-3-(4-(*tert*-butoxy)phenyl)propanoic acid (460 mg, 1 mmol) and 4-(aminomethyl)aniline (183 mg, 1.5 mmol) gave the compound in 74% yield (422 mg). The compound showed:

^{1}H NMR (700 MHz, CD_3OD): δ = 7.78 (d, *J* = 7.4 Hz, 2H), 7.60 (dd, *J* = 7.4 Hz, 2H), 7.38 (dd, *J* = 7.4 Hz, 2H), 7.29 (dd, *J* = 7.4 Hz, 2H), 7.11 (d, *J* = 8.2 Hz, 2H), 6.96 (d, *J* = 8.1 Hz, 2H), 6.83 (d, *J* = 8.2 Hz, 2H), 6.65 (d, *J* = 8.1 Hz, 2H), 4.33–4.29 (m, 2H), 4.22–4.19 (m, 3H), 4.13–4.11 (m, 1H), 3.06 (dd, *J* = 13.8 Hz, *J* = 6.1 Hz, 1H), 2.81 (dd, *J* = 13.8 Hz, *J* = 8.5 Hz, 1H), 1.23 (s, 9H);

^{13}C NMR (175 MHz, CD_3OD): δ = 173.6, 158.2, 155.2, 147.9, 145.2, 145.1, 142.6, 142.5, 133.6, 130.9, 129.8, 128.9, 128.8, 128.2, 126.3, 126.2, 125.1, 120.9, 116.6, 79.5, 68.0, 58.0, 43.9, 38.9, 29.1;

HRMS (ES) for $C_{35}H_{37}N_3O_4$ calculated $[M + H]^+$ 564.2862 found 564.2875 [M + H^+].

Compound 8g

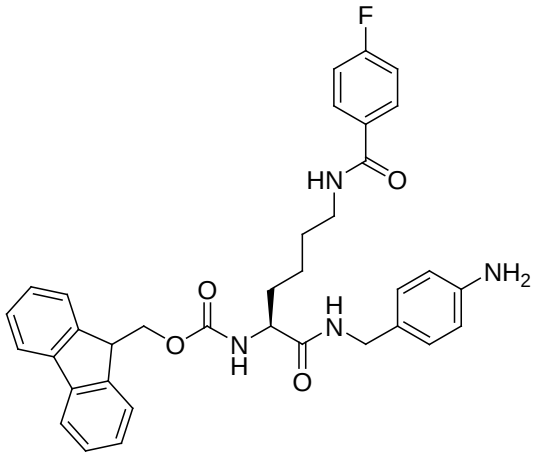

Using the general procedure for the synthesis of (**8**) with (S)-(9H-fluoren-9-yl)methyl1-(4-aminobenzylamino)-6-(4-fluorobenzamido)-1-oxohexan-2-ylcarbamate (490 mg, 1 mmol)and 4-(aminomethyl)aniline (183 mg, 1.5 mmol) gave the compound in 72% yield (430 mg). The compound showed: ^{1}H NMR (700 MHz, CD_3OD): δ = 7.85–7.83 (m, 2H), 7.78 (d, *J* = 7.5 Hz, 2H), 7.65– 7.62(m, 2H), 7.38– 7.36(m, 2H), 7.28–7.27(m, 2H), 7.14– 7.11(m, 2H), 7.02 (d, *J* = 7.8 Hz, 2H), 6.66 (d, *J* = 7.8 Hz, 2H), 4.37–4.35(m, 2H), 4.24 (d, *J* = 14.4 Hz, 1H), 4.20 (d, *J* = 14.4 Hz, 1H), 4.19–4.16 (m, 1H), 4.08(dd, *J* = 8.1 Hz, *J* = 5.3 Hz, 1H), 3.35–3.33 (m, 2H), 1.81–1.78 (m, 1H), 1.67–1.63 (m, 1H), 1.62–1.58 (m, 2H), 1.43–1.38 (m, 2H);

^{13}C NMR (175 MHz, $CDCl_3$): δ = 174.6, 169.0, 166.8, 165.4, 158.4, 147.7, 145.3, 145.2, 142.6, 132.1, 132.1, 130.8, 130.8, 129.6, 129.2, 128.8, 128.2, 128.2, 126.2, 126.2, 120.9, 116.7, 116.4, 116.3, 67.9, 56.6, 48.6, 43.8, 40.7, 33.0, 30.0, 24.3; HRMS (ES) for $C_{35}H_{35}FN_4O_4$ calculated 595.2721 [M + H^+] 595.2722 found [M + H^+].

General procedure for the preparation of (10)

Guanydilation was achieved by treating a solution of the hydrochloride salt of (**8**) (1 mmol) in MeOH (15 ml) with *tert*-butyl (1*H*-pyrazol-1-yl)methanediylidene-dicarbamate (N,N'-DiBoc-1H-pyrazole guanidine, 2 mmol) and allowing the reaction mixture to stir for 4h at room temperature. The solvent was evaporated under a reduced pressure and the crude product purified by flash chromatography on silica gel using a gradient of ethyl acetate in hexane.

Compound 10a

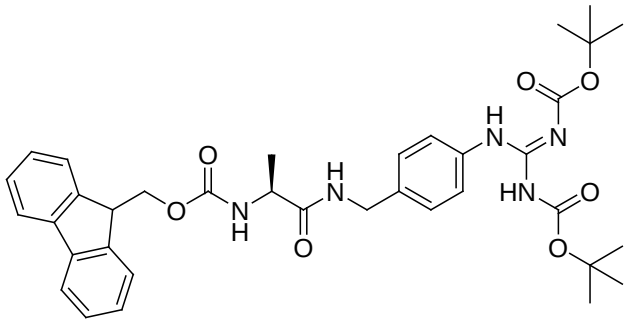

Using the general procedure and compound **8a** (416 mg, 1 mmol) the product was isolated in 76% yield (502 mg). The compound showed:

^{1}H NMR (600 MHz, CD_3OD): δ = 7.80 (d, *J* = 7.5 Hz, 2H), 7.67 (dd, *J* = 6.6 Hz, 2H), 7.47(d, *J* = 8.1 Hz), 7.40 (dd, *J* = 7.4 Hz, 2H), 7.31 (dd, *J* = 7.4 Hz, 2H), 7.27 (d, *J* = 8.1 Hz, 2H), 4.43–4.34 (m, 4H), 4.21–4.17 (m, 2H), 1.59 (s, 9H), 1.47 (s, 9H), 1.37 (d, *J* = 7.2Hz, 3H);

^{13}C NMR (150 MHz, CD_3OD): δ = 175.6, 164.6, 158.3, 155.2, 154.3, 145.4, 145.2, 142.6, 136.9, 128.9, 128.7, 128.2, 126.2, 126.1, 124.0, 120.9, 105.6, 85.0, 80.6, 67.9, 52.2, 43.5, 28.4, 28.2, 18.2;

HRMS (ES^+): for $C_{36}H_{43}N_5O_7$ calculated 658.3241 [M + H^+] found 658.3239 [M + H^+].

Compound 10b

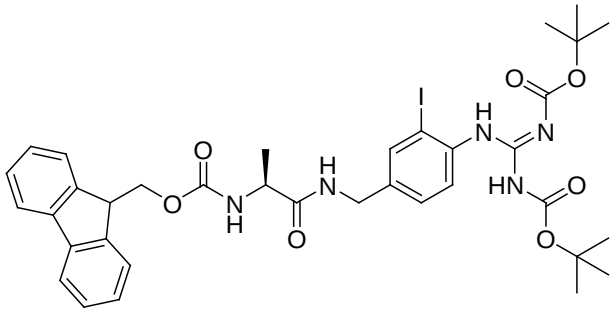

Using the general procedure and compound (**8b**) (542 mg, 1 mmol) the product was isolated in 75% yield (592 mg, 0.75 mmol). The compound showed:

^{1}H NMR (600 MHz, CD_3OD): δ = 7.78–7.76 (m, 3H), 7.64–7.61 (m, 3H), 7.37–7.34 (m, 2H), 7.37–7.34 (m, 3H), 7.28–7.26 (m, 3H), 4.39–4.32 (m, 4H), 4.18–4.08 (m, 2H), 1.57 (s, 9H), 1.39 (s, 9H), 1.40 (d, *J* = 7.2 Hz, 3H);

^{13}C NMR (150 MHz, CD_3OD): δ = 172.3, 163.4, 156.2, 154.0, 152.8, 143.8, 141.4, 138.2, 137.5, 136.8, 128.2, 127.8, 127.2, 126.4, 125.2, 120.8, 92.9, 83.9, 79.9, 67.1, 50.6, 47.2, 42.2, 28.2, 28.1, 18.7;

HRMS (ES^+): for $C_{36}H_{42}IN_5O_7$ calculated 784.2207[M + H^+] found 784.2224[M + H^+].

Compound 10c

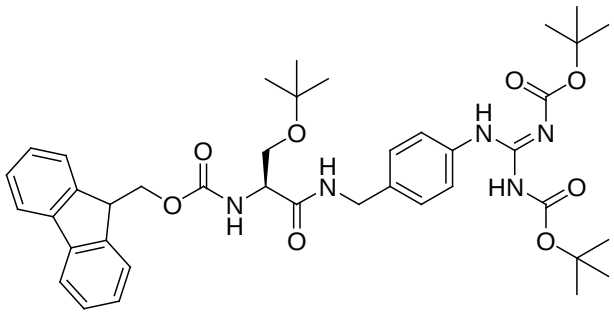

Using the general procedure and compound (**8c**) (488 mg, 1 mmol) the product was isolated in 73% yield (534 mg, 0.73 mmol). The compound showed:

^{1}H NMR (600 MHz, CD_3OD): δ = 7.76 (d, *J* = 7.4 Hz, 2H), 7.63-7.62(m, 2H), 7.45 (d, *J* = 8.0 Hz, 2H), 7.36 (dd, *J* = 7.3 Hz, 2H), 7.29–7.25 (m, 4H), 4.40–4.34 (m, 4H), 4.26–4.25 (m, 1H), 4.19–4.16 (m, 1H), 3.67-3.65 (m, 1H), 3.59-3.57 (m, 1H), 1.55 (s, 9H), 1.44 (s, 9H), 1.16 (s, 9H);

^{13}C NMR (150MHz, CD_3OD): δ = 172.9, 164.6, 158.3, 155.2, 154.4, 145.3, 145.1, 142.6, 136.7, 128.9, 128.8, 126.2, 123.9, 121.0, 85.0, 80.6, 74.7, 68.1, 63.1, 57.2, 48.4, 43.6, 28.5, 28.3, 27.8;

HRMS (ES^+): for $C_{40}H_{51}N_5O_8$ calculated 730.3816 [M + H^+] found 730.3795 [M + H^+].

Compound 10d

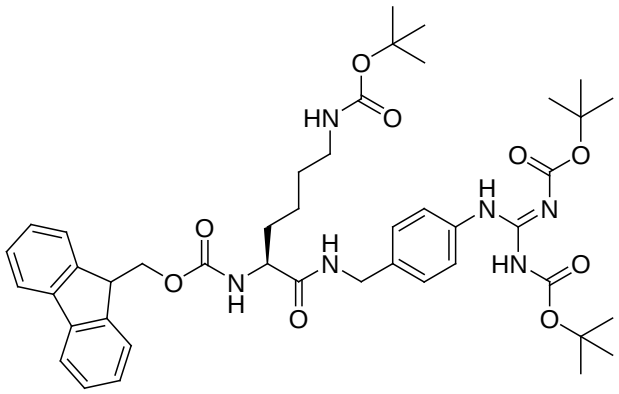

Using the general procedure and compound (**8d)** (573 mg, 1 mmol) the produc was isoleted in 75% yield (612 mg, 0.75 mmol). The compound showed:

^{1}H NMR (700 MHz, CD_3OD): δ = 7.79 (d, *J* = 7.4 Hz, 2H), 7.65 (m, 2H), 7.45 (d, *J* = 8.0 Hz, 2H), 7.38 (dd, *J* = 7.4 Hz, 2H), 7.29 (dd, *J* = 7.4 Hz, 2H), 7.25 (d, *J* = 8.0 Hz, 2 H), 4.41–4.32 (m, 4H), 4.18 (dd, *J* = 6.4 Hz, 1H), 4.07 (dd, *J* = 8.2 Hz, *J* = 5.3 Hz, 1H), 3.02–2.99 (m, 2H), 1.78–1.75 (m, 1H), 1.65–1.63 (m, 1H), 1.57 (s, 9H), 1.48–1.45 (m, 2H), 1.44 (s, 9H), 1.41 (s, 9H), 1.36–1.32 (m, 2H);

^{13}C NMR (175 MHz, CD_3OD): δ = 174.9, 164.6, 158.6, 158.5, 155.2, 154.3, 145.4, 145.1, 142.6, 142.5, 136.9, 129.0, 128.8, 128.2, 126.2, 126.2, 124.0, 120.9, 85.1, 80.6, 79.9, 67.9, 56.7, 43.5, 41.0, 32.8, 30.5, 28.8, 28.5, 28.2, 24.2;

HRMS (ES^+): for $C_{44}H_{58}N_6O_9$ calculated 815.4344 [M + H^+] found 815.4353 [M + H^+]

Compound 10e

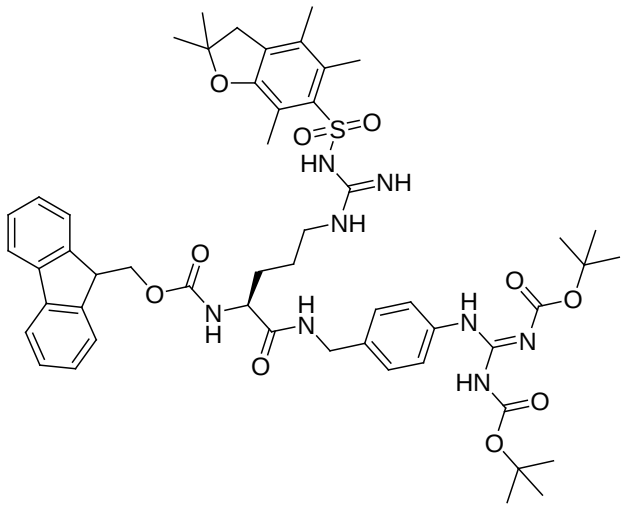

Using the general procedure and compound (**8e**) (376 mg, 0.5 mmol) the product was isolated in 79% yield (394 mg, 0.39 mmol). The compound showed:

^{1}H NMR (700 MHz, CD_3OD): δ = 7.77 (d, *J* = 7.4 Hz, 2H), 7.63 (dd, *J* = 7.0 Hz, 2H), 7.43 (d, *J* = 8.0 Hz, 2H), 7.35 (dd, *J* = 7.4 Hz, 2H), 7.28–7.26 (m, 2H), 7.22 (d, *J* = 8.0 Hz, 2H), 4.38 (d, *J* = 6.2, 2H), 4.35 (d, *J* = 14.8 Hz, 1H), 4.29 (d, *J* = 14.8 Hz, 1H), 4.17 (dd, *J* = 6.7 Hz, 1H), 4.08 (dd, *J* = 8.2 Hz, *J* = 5.7 Hz, 1H), 3.18–3.14 (m, 2H), 2.94 (s, 2H), 2.57 (s, 3H), 2.50 (s, 3H), 2.06 (s, 3H), 1.75–1.74 (m, 1H), 1.58–1.57 (m, 1H), 1 .57 (s, 9H), 1.50–1.43 (m, 2H), 1.43 (s, 9H), 1.40 (s, 3H), 1.40 (s, 3H);

^{13}C NMR (175 MHz, CD_3OD): δ = 174.5, 164.6, 159.9, 158.4, 158.1, 155.3, 154.3, 145.4, 145.1, 142.6, 142.6, 139.4, 136.9, 134.4, 133.5, 129.1, 128.8, 128.2, 126.2, 126.0, 124.1, 120.1, 118.5, 87.6, 85.0, 80.7, 79.9, 67.9, 56.2, 44.0, 43.6, 30.5, 28.7, 28.7, 28.5, 28.3, 28.2, 19.6, 18.4, 12.5;

HRMS (ES^+): for $C_{52}H_{66}N_8O_{10}$ calculated 995.4701 [M + H^+] found 995.4653 [M + H^+]

Compound 10f

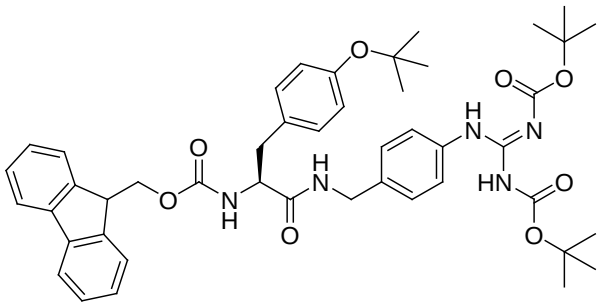

Using the general procedure and compound (**8f**) (564 mg, 1 mmol) the product was isolated in 77% yield (627 mg, 0.77 mmol). The compound showed:

^{1}H NMR (600 MHz, CD_3OD): δ = 7.78 (d, *J* = 7.5 Hz, 2H), 7.60 (dd, *J* = 6.9 Hz, 2H), 7.45 (d, *J* = 8.2 Hz, 2H), 7.38 (dd, *J* = 7.5 Hz, 2H), 7.29 (dd, *J* = 6.9 Hz, 2H), 7.15 (d, *J* = 8.3 Hz, 2H), 7.13 (d, *J* = 8.2 Hz, 2H), 6.85 (d, *J* = 8.3 Hz, 2H), 4.32–4.24 (m, 5H), 4.13–4.12 (m, 1H), 3.06 (dd, *J* = 13.7 Hz, *J* = 6.4 Hz, 1H), 2.85 (dd, *J* = 13.5 Hz, *J* = 8.6 Hz, 1H), 1.57 (s, 9 H), 1.44 (s, 9 H), 1.24 (s, 9 H);

^{13}C NMR (150 MHz, $CDCl_3$): δ = 170.8, 163.6, 156.0, 154.5, 153.6, 153.4, 143.9, 141.4, 136.2, 134.0, 131.2, 129.9, 128.4, 127.8, 127.2, 125.2, 124.3, 122.6, 120.0, 83.8, 79.7, 78.5, 67.1, 56.6, 47.2, 43.2, 38.2, 28.9, 28.3, 28.2;

HRMS (ES^+): for $C_{46}H_{55}N_5O_8$ calculated 806.4129 [M + H^+] found 806.4059 [M + H^+].

Compound 10g

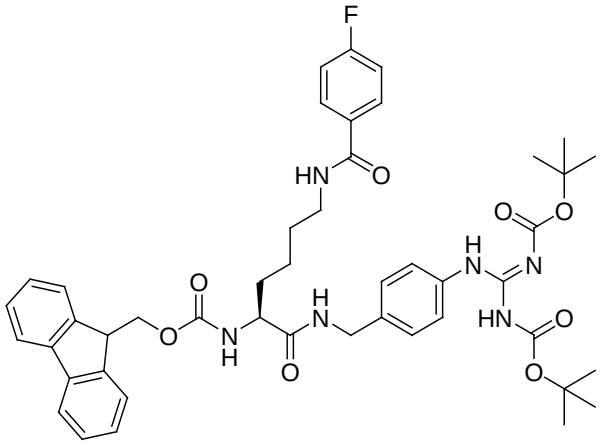

Using the general procedure and compound **8g** (595 mg, 1 mmol) the produc was isolated in 70% yield (578 mg, 0.70 mmol). The compound showed: ^{1}H NMR (700 MHz, CD_3OD): δ = 7.79 (dd, *J* = 7.9 Hz, *J* = 5.3 Hz, 2H), 7.78 (d, *J* = 7.5 Hz, 2H), 7.64–7.63 (m, 2H), 7.44 (d, *J* = 8.0 Hz, 2H), 7.38–7.36 (m, 2H), 7.29–7.28 (m, 2H), 7.25 (d, *J* = 8.0 Hz, 2H), 7.14–7.12 (m, 2H), 4.37–4.34 (m, 4H), 4.17–4.15 (m, 1H), 4.11–4.09 (m, 1H), 3.37–3.34 (m, 2H), 1.84–1.80 (m, 1H), 1.71–1.67 (m, 1H), 1.63–1.62 (m, 2H), 1.57 (s, 9H), 1.43 (s, 9H), 1.42–1.40 (m, 2H);

^{13}C NMR (175 MHz, CD_3OD): δ = 174.8, 169.0, 166.8, 165.4, 164.6, 158.5, 155.3, 154.3, 145.4, 145.2, 142.6, 136.9, 132.1, 132.1, 130.8, 130.8, 129.7, 129.0, 128.8, 128.2, 128.2, 126.2, 126.2, 124.0, 116.6, 116.4, 116.3, 85.0, 80.6, 67.9, 56.6, 43.6, 40.7, 32.9, 30.0, 28.5, 28.3, 24.4C;

HRMS (ES^+): for $C_{46}H_{53}FN_6O_8$ calculated 837.3973 [M + H^+] found 837.3987 [M + H^+].

General procedure for the preparation of protected Guanidinylated Dipeptides (11)

Removal of the Fmoc protecting group was achieved by dissolving (**10**) (1 mmol) in a 2:1 mixture DCM / diethylamine (6 ml total volume). The solution was stirred for 2h at room temperature at which time the solvent was removed via evaporation under a reduced pressure. The crude product was washed with a 4:1 mixture of hexane / ethyl acetate and used without further purification.

Deprotected (**10**) and (**5**) were coupled by taking a solution of the **5** (1 mmol), *i*Pr_2NEt (2 mmol) and PyBOP (1 mmol) in DMF (3 ml) and adding it to a solution of (**10**) (1 mmol) in DMF (1ml). The resultant solution was stirred overnight. The reaction mixture was poured into water (20 ml) then extracted EtOAc (2 x 20 ml). The combined organic extracts were washed with successively with water (3 x 20 ml) and brine (20 ml) then dried over Na_2SO_4, filtered, and concentrated under a reduced pressure. Purification by flash chromatography on silica gel using ethyl acetate in hexane yielded the pure product.

Compound 11a

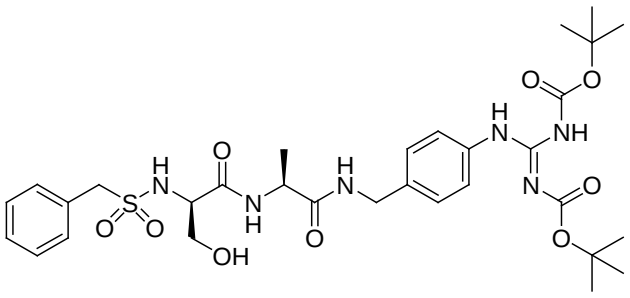

Using the general procedure for the preparation of protected guanidinylated dipeptides with compound (**10a**) (109 mg, 0.25 mmol) and compound (**5**) (R_1 = H, 79 mg, 0.25 mmol) yielded compound (**11a**) in 58% (107 mg) overall yield. The compound showed:

^{1}H NMR (600 MHz, CD_3OD): δ = 7.45 (d, *J* = 8.3 Hz, 2H), 7.42-7.40 (m, 3H), 7.25(d, *J* = 8.3 Hz, 2H), 4.40- 4.37 (m, 2H), 4.33- 4.31 (m, 3H), 3.94 (dd, *J* = 6.4 Hz, 1H), 3.56-3.51 (m, 2H), 1.51 (s, 18H), 1.39 (d, *J* = 7.2 Hz, 3H), 1.16 (s, 9H);

^{13}C NMR (150 MHz, CD_3OD): δ = 174.5, 172.4, 155.1, 137.0, 136.7, 132.1, 131.0, 129.5, 129.4, 129.0, 123.9, 74.9, 63.8, 60.0, 58.8, 50.7, 43.6, 38.9, 28.4, 27.7, 18.3;

HRMS (ES^+): for $C_{35}H_{52}N_6O_9S$ calculated 733.3721 [M + H^+] found 733.3677 [M + H^+].

Compound 11b

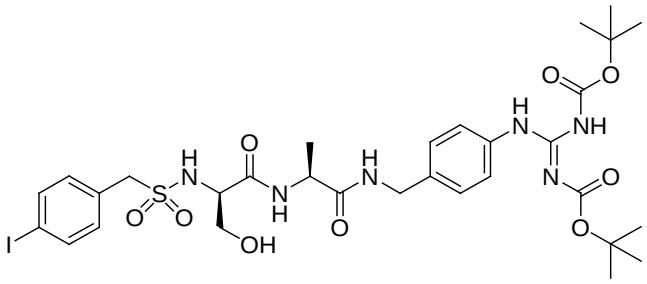

Using the general procedure for the preparation of protected guanidinylated dipeptides with compound (**10a**) (109 mg, 0.25 mmol) and compound (**5**) (R_1 = I, 110 mg, 0.25 mmol) yielded compound (**11b**) in 63% (136 mg) overall yield. The compound showed:

^{1}H NMR (600 MHz, CD_3OD): δ = 7.67 (d, *J* = 8.2 Hz, 2H), 7.45 (d, *J* = 8.4 Hz, 2H), 7.25(d, *J* = 8.4 Hz, 2H), 7.16 (d, *J* = 8.2 Hz, 2H), 4.41- 4.39 (m, 1H), 4.38 (d, *J* = 15.0 Hz, 1H), 4.32 (d, *J* = 15.0 Hz, 1H), 4.27 (d, *J* = 13.8 Hz, 1H), 4.24 (d, *J* = 13.8 Hz, 1H),

3.97 (dd, *J* = 6.4 Hz, 1H), 3.54 (dd, *J* = 9.0 Hz, *J* = 5.4 Hz, 1H), 3.52 (dd, *J* = 9.0 Hz, *J* = 6.4 Hz, 1H), 1.57 (s, 9H), 1.46 (s, 9H), 1.40 (d, *J* = 7.2 Hz, 3H), 1.18 (s, 9H);

^{13}C NMR (150 MHz, CD_3OD): δ = 174.6, 172.3, 164.6, 155.1, 154.4, 138.8, 137.0, 136.7, 134.1, 129.0, 123.9, 95.0, 85.1, 80.7, 75.0, 66.9, 63.8, 59.4, 58.7, 50.7, 43.6, 28.5, 28.3, 27.7, 18.2;

HRMS (ES^+): for $C_{35}H_{51}IN_6O_9S$ calculated 859.2528 [M + H^+] found 859.2542 [M + H^+].

Compound 11c

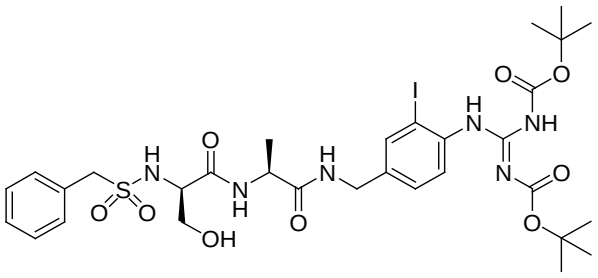

Using the general procedure for the preparation of protected guanidinylated dipeptides with compound (**10b**) (140 mg, 0.25 mmol) and compound (**5**) (R_1 = H, 79 mg, 0.25 mmol) yielded compound (**11c**) in 63% (136 mg) overall yield. The compound showed:

^{1}H NMR (600 MHz, CD_3OD): δ = 7.80 (m, 1H), 7.64 (d, *J* = 7.8 Hz, 1H), 7.41 (m, 2H), 7.33–7.30 (m, 3H), 7.29 (d, *J* = 8.4 Hz, 1H), 4.41–4.28 (m, 5H), 3.95–3.94 (m, 1H), 3.57–3.52 (m, 2H), 1.58 (s, 9H), 1.41 (s, 9H),1.40 (d, *J* = 7.2 Hz, 3H), 1.17 (s, 9H);

^{13}C NMR (101 MHz, CD_3OD): δ = 174.6, 172.4, 164.5, 156.0, 154.0, 139.8, 139.2, 138.5, 132.1, 131.0, 129.6, 129.5, 129.0, 128.3, 95.4, 85.1, 80.9, 74.9, 63.7, 60.0, 58.8, 50.6, 42.8, 28.5, 28.2, 27.7, 18.3;

HRMS (ES^+): for $C_{35}H_{51}IN_6O_9S$ calculated 859.2483[M + H^+] found 859.2488[M + H^+].

Compound 11d

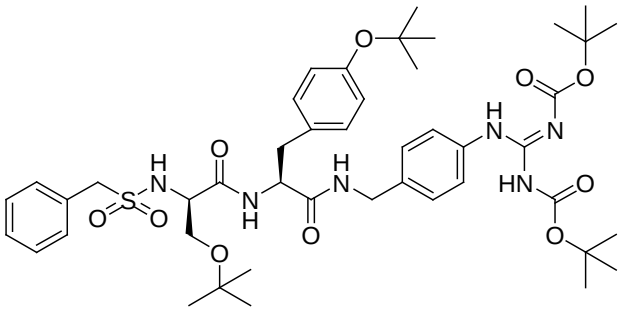

Using the general procedure for the preparation of protected guanidinylated dipeptides with compound (**10f**) (146 mg, 0.25 mmol) and compound (**5**) (R_1 = H, 79 mg, 0.25 mmol) yielded compound (**11d**) in 50% (110 mg) overall yield. The compound showed:

^{1}H NMR (600 MHz, $CDCl_3$): δ = 11.52 (s, 1H), 10.20 (s, 1H), 7.42 (d, *J* = 8.3 Hz, 2H), 7.30–7.29 (m, 2H), 7.28–7.26 (m, 3H), 7.19–7.18 (m, 1H), 7.00 (d, *J* = 8.3 Hz, 2H), 6.97 (d, *J* = 8.3 Hz, 2H), 6.79 (d, *J* = 8.3 Hz, 2H), 6.08 (t, *J* = 6.3 Hz, 1H), 5.32 (bs, 1H), 4.50 (dd, *J* = 14.3 Hz, *J* = 7.1 Hz, 1H), 4.20–4.14 (m, 4H), 3.69 (bs, 1H), 3.45 (dd, *J* = 9.1 Hz, *J* = 4.4 Hz, 2H), 3.20 (dd, *J* = 8.7 Hz, *J* = 7.3 Hz, 1H), 2.98(dd, *J* = 13.7 Hz, *J* = 6.3 Hz, 1H), 2.93 (dd, *J* = 13.7 Hz, *J* = 6.3 Hz, 1H), 1.45 (s, 9H), 1.40 (s, 9H), 1.22 (s, 9H), 1.00 (s, 9H);

^{13}C NMR (150 MHz, CD_3OD): δ = 170.2, 169.6, 163.6, 154.6, 153.5, 153.6, 136.3, 134.0, 131.1, 130.9, 129.9, 129.0, 128.9, 128.4, 124.4, 122.5, 83.8, 79.7, 78.4, 74.6, 62.7, 59.5, 57.0, 55.2, 43.2, 37.7, 28.9, 28.2, 28.1, 27.4;

HRMS (ES^+): for $C_{45}H_{64}N_6O_{10}S$ calculated [M + H+] 881.4450 found 881.4449[M + H+].

Compound 11e

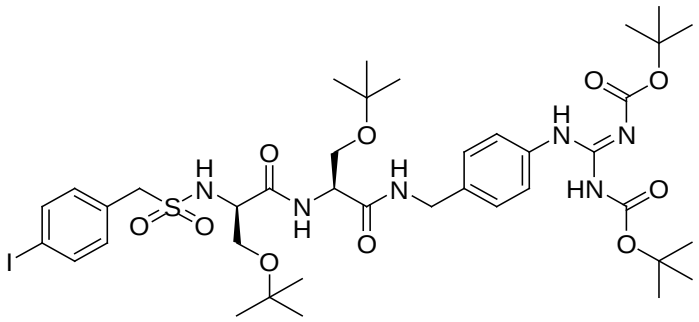

Using the general procedure for the preparation of protected guanidinylated dipeptides with compound (**10c**) (127 mg) and compound (**5**) (R_1 = I, 110 mg, 0.25 mmol) yielded compound (**11e**) in 53% (125 mg) overall yield. The compound showed:

^{1}H NMR (600 MHz, CD_3OD): δ = 7.69 (d, *J* = 8.3 Hz, 2H), 7.46 (d, *J* = 8.5 Hz, 2H), 7.27 (d, *J* = 8.5 Hz, 2H), 7.18 (d, *J* = 8.3 Hz, 2H), 4.49 (dd, *J* = 4.4 Hz, 1H), 4.42 (d, *J* = 15.2 Hz, 1H), 4.37 (d, *J* = 15.2 Hz, 1H), 4.31 (d, *J* = 13.8 Hz, 1H), 4.28 (d, *J* = 13.8 Hz, 1H), 4.05 (dd, *J* = 5.7 Hz, 1H), 3.80 (dd, *J* = 9.0 Hz, *J* = 4.0 Hz, 1H), 3.55 (dd, *J* = 9.0 Hz, *J* = 6.2 Hz, 1H), 1.57 (s, 9H), 1.46 (s, 9H), 1.20 (s, 9H), 1.19 (s, 9H);

^{13}C NMR (150MHz, CD_3OD): δ = 172.6, 172.3, 164.6, 155.1, 154.4, 138.8, 137.0, 136.6, 134.1, 131.0, 128.9, 123.8, 95.0, 85.0, 80.6, 75.1, 74.8, 63.8, 62.8, 59.3, 58.8, 55.7, 43.6, 28.5, 28.3, 27.8;

HRMS (ES^+): for $C_{35}H_{59}IN_6O_{10}S$ calculated 931.3078 [M + H^+] found 931.3103 [M + H^+].

Compound 11f

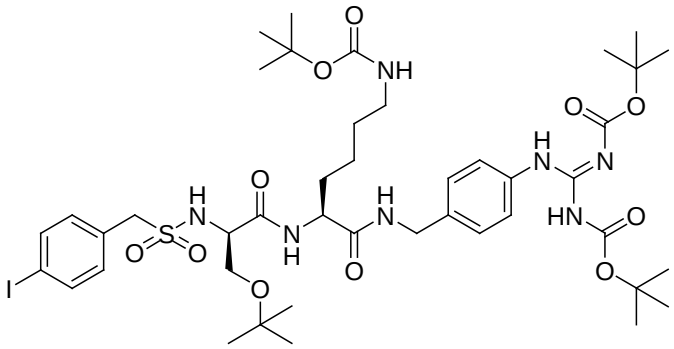

Using the general procedure for the preparation of protected guanidinylated dipeptides with compound (**10d**) (148 mg, 0.25mmol) and compound (**5**) (R_1 = I, 110 mg, 0.25 mmol) yielded compound (**11f**) in 57% (146 mg) overall yield. The compound showed:

^{1}H NMR (700 MHz, CD_3OD): δ = 7.66 (d, *J* = 8.2 Hz, 2H), 7.44(d, *J* = 8.4 Hz, 2H), 7.24 (d, *J* = 8.4 Hz, 2H), 7.15 (d, *J* = 8.2 Hz, 2H), 4.38 (d, *J* = 14.9 Hz, 1H), 4.33 (dd, *J* = 9.0 Hz, *J* = 5.0 Hz, 1H), 4.30 (d, *J* = 14.9 Hz, 1H), 4.24 (s, 2 H), 3.98 (d, *J* = 6.0 Hz, 1H), 3.52–3.51 (m, 2H), 3.04–2.97 (m, 2H), 1.87–1.82 (m, 1H), 1.69–1.64 (m, 1H), 1.56 (s, 9H), 1.47–1.46 (m, 12H), 1.41 (s, 9 H), 1.38–1.32 (m, 1H), 1.16 (s, 9H);

^{13}C NMR (175 MHz, CD_3OD): δ = 173.9, 172.7, 164.6, 158.5, 155.2, 154.4, 138.8, 137.0, 136.8, 134.1, 130.9, 129.0, 124.0, 95.0, 85.0, 80.7, 79.9, 74.9, 63.7, 59.3, 58.7, 55.0, 43.6, 41.1, 32.9, 30.5, 28.8, 28.5, 28.3, 27.7, 24.2;

HRMS (ES^+): for $C_{43}H_{66}IN_7O_{11}S$ calculated 1016.3664 [M + H^+] found 1016.3687 [M + H^+].

Compound 11g

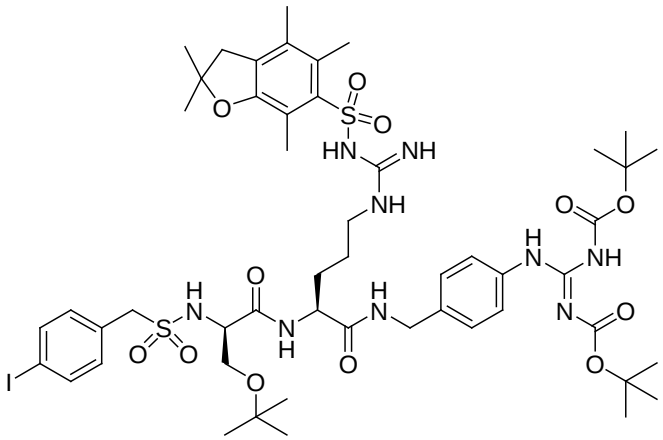

Using the general procedure for the preparation of protected guanidinylated dipeptides with compound (**10e**) (193 mg, 0.25 mmol) and compound (**5**) (R_1 = I, 110 mg, 0.25 mmol) yielded compound (**11g)** in 62% (187 mg) overall yield. The compound showed:

^{1}H NMR (700 MHz, CD_3OD): δ = 7.67 (d, *J* = 8.1 Hz, 2H), 7.43 (d, *J* = 8.2 Hz, 2H), 7.22 (d, *J* = 8.2 Hz, 2H), 7.16 (d, *J* = 8.1 Hz, 2H), 4.40 (dd, *J* = 8.9 Hz, *J* = 4.9 Hz, 1H), 4.34 (d, *J* = 14.8 Hz, 1H), 4.30 (d, *J* = 14.8 Hz, 1H), 4.25 (s, 2H), 3.95 (dd, *J* = 6.0 Hz, 1H), 3.53–3.49 (m, 2H), 3.16–3.13 (m, 2H), 2.97 (s, 2H), 2.50 (s, 3H), 2.07 (s, 3H), 2.07 (s, 3H), 1.87–1.85 (m, 1H), 1.65–1.64 (m, 1H), 1.57 (s, 9H), 1.56–1.46 (m, 2H), 1.45 (s, 9H), 1.44 (s, 3H), 1.43 (s, 3H), 1.14 (s, 9H);

^{13}C NMR (175 MHz, CD_3OD): δ = 173.6, 172.6, 164.6, 159.9, 158.1, 155.1, 154.4, 139.4, 138.8, 137.0, 136.7, 134.4, 134.1, 133.5, 130.9, 129.2, 126.0, 123.9, 118.5, 95.0, 87.6, 85.0, 80.7, 74.9, 63.6, 59.3, 58.7, 54.4, 44.0, 43.6, 28.7, 28.5, 28.3, 27.7, 19.6, 18.5, 12.5; HRMS (ES^+): for $C_{51}H_{74}IN_9O_{12}S_2$ calculated 1196.3988 [M + H^+] found 1196.3975 [M + H^+].

Compound 11h

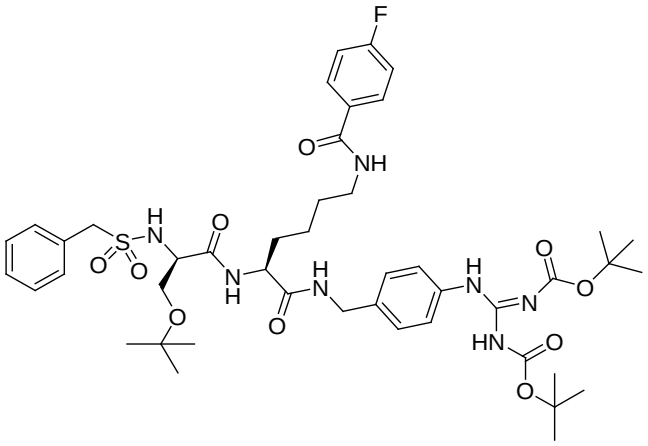

Using the general procedure for the preparation of protected guanidinylated dipeptides with compound **10g** (209 mg, 0.25mmol) and compound (**5**) (R_1 = H, 79 mg, 0.25 mmol) yielded Compound (**11g**) in 61% (140 mg) overall yield. The compound showed: ^{1}H NMR (700 MHz, CD_3OD): δ = 7.86 (dd, *J* = 8.6 Hz *J* = 5.4 Hz, 2H), 7.43(d, *J* = 8.3 Hz, 2H), 7.41–7.40 (m, 2H), 7.34–7.33 (m, 2H), 7.23 (d, *J* = 8.3 Hz, 2H), 7.15 (dd, *J* = 8.6 Hz, 2H), 4.41 (d, *J* = 14.9 Hz, 1H), 4.39–4.37 (m, 1H), 4.34–4.29 (m, 4H), 3.94–3.95 (m, 1H), 3.52–3.50 (m, 2H), 3.36–3.0 (m, 2H), 1.93–1.88 (m, 1H), 1.77–1.71 (m, 1H), 1.70–1.62 (m, 2H), 1.50 (s, 20H), 1.13 (s, 9 H);

^{13}C NMR (175 MHz, CD_3OD): δ = 173.8, 122.7, 169.0, 166.9, 165.3, 155.0, 137.0, 136.7, 132.1, 131.0, 130.9, 130.9, 129.6, 129.5, 129.0, 124.0, 116.4, 116.2, 74.9, 63.6, 60.0, 58.9, 54.9, 43.6, 40.7, 32.9, 30.0, 24.3;

HRMS (ES^+): for $C_{45}H_{62}FN_7O_{10}S$ calculated 912.4341 [M + H^+] found 912.4317 [M + H^+].

General procedure for the preparation of deprotected Guanidinylated Dipeptides (1)

Deprotection to give the guanidinylated dipeptides (**1**) was achieved by treating compound (**11**) with 2 ml of a solution of TFA (3.8 ml), H_2O (100 μL) and TIPS (100 μL). The mixture was stirred for 3h at RT at which time cold ether (15 ml) added to precipitate the product. The precipitate was collected, dissolved in a 1-3 mixture AcCN-H_2O (15 ml) then lyophilized.

Compound 1a

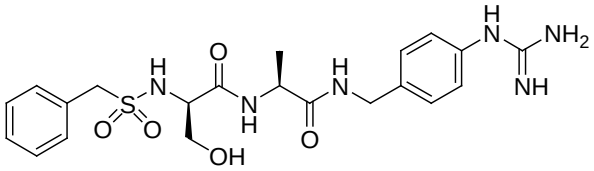

Using the general procedure for the deprotection of guanidinylated dipeptides with compound (**11a**) (73 mg, 0.1 mmol) yielded compound (**1a**) in 89% (42 mg) yield. The compound showed:

^{1}H NMR (700 MHz, CD_3OD): δ = 7.44–7.42 (m, 2H), 7.37–7.35 (m, 5H), 7.17 (d, *J* = 8.4 Hz, 2H), 4.41 (d, *J* = 15.4 Hz, 1H), 4.37–4.33 (m, 4H), 3.88 (dd, *J* = 5.5 Hz, 1H), 3.70 (d, *J* = 5.5 Hz, 2H), 1.40 (d, *J* = 7.2 Hz, 3H);

^{13}C NMR (150 MHz, CD_3OD): δ = 175.0, 172.8, 163.3, 163.1, 158.1, 139.7, 134.8, 132.2, 131.0, 130.0, 129.6, 126.7, 63.6, 60.3, 59.8, 51.0, 43.5, 17.8;

HRMS (ES^+): for $C_{21}H_{28}N_6O_5S$ calculated 477.1920 [M + H^+] found 477.1917 [M + H^+].

Compound 1b

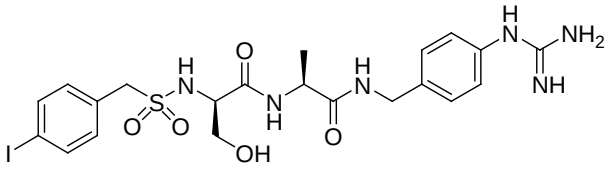

Using the general procedure for the deprotection of guanidinylated dipeptides with compound (**11b**) (86 mg, 0.1 mmol) yielded compound (**1b)** in 90 % (54 mg) yield. The compound showed:

^{1}H NMR (600 MHz, CD_3OD): δ = 7.71 (d, *J* = 8.2 Hz, 2H), 7.36 (d, *J* = 8.4 Hz, 2H), 7.21 (d, *J* = 8.2 Hz, 2H), 7.16 (d, *J* = 8.4 Hz, 2H), 4.41 (dd, *J* = 8.4 Hz, 2H), 4.42–4.30 (m, 3H), 4.31 (s, 2H), 3.93 (dd, *J* = 6.4 Hz, 1H), 3.72–3.71 (m, 2H), 1.41 (d, *J* = 7.2 Hz, 3H);

^{13}C NMR (150 MHz, CD_3OD): δ = 174.9, 172.6, 158.1, 139.7, 138.8, 134.8, 134.1, 130.9, 129.9, 126.7, 95.0, 63.6, 60.2, 59.2, 50.9, 43.4, 17.8;

HRMS (ES^+): for $C_{21}H_{27}IN_6O_5S$ calculated 603.0887 [M + H^+] found 603.0862 [M + H^+].

Compound 1c

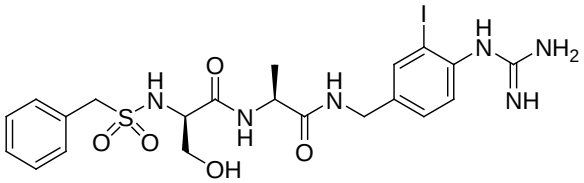

Using the general procedure for the deprotection of guanidinylated dipeptides with compound (**11c**) (86 mg, 0.1 mmol) yielded compound (**11c**) in 83% (50 mg) yield. The compound showed:

^{1}H NMR (700 MHz, CD_3OD): δ = 7.90 (d, *J* = 1.8 Hz, 1H), 7.44–7.43 (m, 2H), 7.39 (dd, *J* = 8.0 Hz, *J* = 1.8 Hz, 1H), 7.36–7.35 (m, 3H), 7.26 (d, *J* = 8.0 Hz, 1H), 4.39–4.31 (m, 5H), 3.89 (dd, *J* = 5.6 Hz, 1H), 3.71, (d, *J* = 11.0 Hz, 2H), 1.41 (d, *J* = 7.2 Hz, 3H);

^{13}C NMR (101 MHz, CD_3OD): δ = 175.1, 172.9, 163.2, 158.2, 143.0, 140.0, 136.6, 132.1, 131.0, 130.2, 130.0, 129.6, 129.5, 99.8, 63.7, 60.2, 59.8, 51.0, 42.8, 17.6;

HRMS (ES^+): for $C_{21}H_{27}IN_6O_5S$ calculated 603.0887[M + H^+] found 603.0882[M + H^+].

Compound 1d

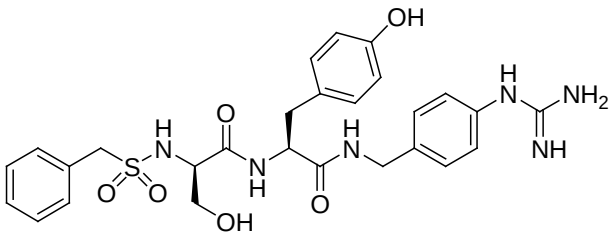

Using the general procedure for the deprotection of guanidinylated dipeptides with compound (**11d**) (88 mg, 0.1 mmol) yielded compound (**1d**) in 89% (50 mg) yield. The compound showed:

^{1}H NMR (700 MHz, CD_3OD): δ = 7.40–7.39 (m, 2H), 7.35–7.34 (m, 3H), 7.20 (d, *J* = 8.3 Hz, 2H), 7.14 (d, *J* = 8.3 Hz, 2H), 7.06 (d, *J* = 8.3 Hz, 2H), 6.69 (d, *J* = 8.3 Hz, 2H), 4.55 (dd, *J* = 14,4 Hz, 1H), 4.37 (d, *J* = 13,9 Hz, 1H), 4.33 (bs, 2H), 4.27 (d, *J* = 13,9 Hz, 1H), 3.87 (dd, *J* = 10.7 Hz, 1H), 3.63 (dd, *J* = 11.0 Hz, *J* = 5.5 Hz, 1H), 3.60 (dd, *J* = 11.0 Hz, *J* = 5.2 Hz, 1H), 3.04 (dd, *J* = 13.8 Hz, *J* = 7.8 Hz, 1H), 2.92 (dd, *J* = 13.8 Hz, *J* = 6.6 Hz, 1H);

^{13}C NMR (175 MHz, CD_3OD): δ = 173.4, 172.6, 158.1, 157.5, 139.4, 134.8, 132.2, 131.4, 130.9, 129.9, 129.6, 129.5, 128.6, 126.6, 116.4, 63.8, 60.3, 59.9, 56.6, 43.4, 37.8;

HRMS (ES^+): for $C_{27}H_{32}N_6O_6S$ calculated [M + H+] 569.2173 found 569.2182[M + H+].

Compound 1e

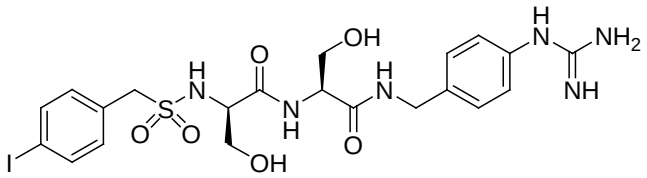

Using the general procedure for the deprotection of guanidinylated dipeptides with compound (**11e**) (93 mg, 0.1 mmol) yielded compound (**1e**) in 88% (54 mg) yield. The compound showed:

^{1}H NMR (700 MHz, CD_3OD): δ = 7.71 (d, *J* = 8.4 Hz, 2H), 7.37 (d, *J* = 8.4 Hz, 2H), 7.21 (d, *J* = 8.4 Hz, 2H), 7.17 (d, *J* = 8.4 Hz, 2H), 4.45 (d, *J* = 15.3 Hz, 1H), 4.40 (dd , *J* = 4.8Hz), 4.34 (d, *J* = 15.3 Hz, 1H), 4.33 (s, 2H), 3.98 (dd , *J* = 5.5Hz, 1H), 3.91 (dd, *J* = 5.0 Hz, *J* = 10.9 Hz, 1H), 3.81 (dd, *J* = 10.9 Hz, *J* = 4.6 Hz, 1H), 3.40 (d, *J* = 5.5 Hz, 2H);

^{13}C NMR (175 MHz, CD_3OD): δ = 173.0, 172.4, 158.1, 139.6, 138.8, 134.7, 134.1, 130.8, 129.9, 126.7, 95.1, 63.6, 62.6, 60.2, 59.1, 57.3, 43.5;

HRMS (ES^+): for $C_{21}H_{27}IN_6O_6S$ calculated 619.0836 [M + H^+] found 619.0864 [M + H^+].

Compound 1f

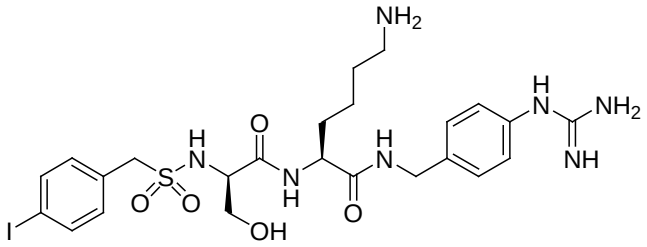

Using the general procedure for the deprotection of guanidinylated dipeptides with compound (**11f**) (101 mg, 0.1 mmol) yielded compound (**1f**) in 86% (57 mg) overall yield. The compound showed:

^{1}H NMR (700 MHz, CD_3OD): δ = 7.73 (d, *J* = 8.3 Hz, 2H), 7.36 (d, *J* = 8.3 Hz, 2H), 7.21 (d, *J* = 8.3 Hz, 2H), 7.19 (d, *J* = 8.3 Hz, 2H), 4.41–4.35 (m, 3H), 4.33 (s, 9H), 3.90–3.87 (m, 1H), 3.74–3.73 (m, 2H), 2.92–2.89 (m, 2H), 1.98–1.94 (m, 1H), 1.76–1.68 (m, 1H), 1.67–1.62 (m, 2H), 1.55–1.51 (m, 1H), 1.49–1.45 (m, 1H);

^{13}C NMR (175 MHz, CD_3OD): δ = 174.0, 173.4, 158.1, 139.5, 138.9, 134.9, 134.0, 130.8, 130.0, 126.7, 95.1, 63.4, 60.5, 59.0, 54.5, 43.5, 40.5, 31.9, 27.8, 23.7;

HRMS (ES^+): for $C_{24}H_{34}IN_7O_5S$ calculated 660.1431 [M + H^+] found 660.1435 [M + H^+]

Compound 1g

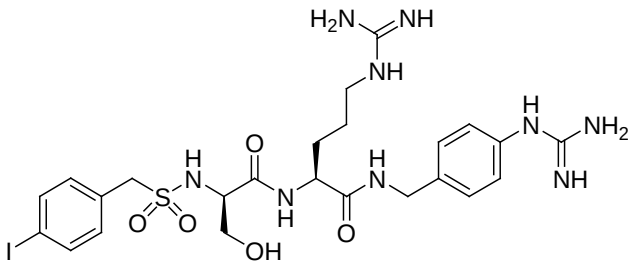

Using the general procedure for the deprotection of guanidinylated dipeptides with compound (**11g**) (119 mg, 0.1 mmol) yielded compound (**1g**) in 88% (60 mg) overall yield. The compound showed:

^{1}H NMR (700 MHz, CD_3OD): δ = 7.73 (d, *J* = 8.1 Hz, 2H), 7.36 (d, *J* = 8.2 Hz, 2H), 7.22 (d, *J* = 8.2 Hz, 2H), 7.19 (d, *J* = 8.1 Hz, 2H), 4.42–4.34 (m, 5H), 3.95 (dd, *J* = 5.3Hz, 1H), 3.74–3.72 (m, 2H), 3.22–3.17 (m, 2H), 2.05–1.97 (m, 1H), 1.77–1.71 (m, 2H), 1.67-164 (m, 1H);

^{13}C NMR (175 MHz, CD_3OD): δ = 173.8, 173.4, 158.6, 158.1, 139.5, 138.9, 134.9, 134.1, 130.8, 130.0, 126.7, 95.1, 63.5, 60.3, 58.9, 54.6, 43.5, 41.9, 29.7, 26.3;

HRMS (ES^+): for $C_{24}H_{34}IN_9O_5S$ calculated 688.1527 [M + H^+] found 688.1496 [M + H^+].

Compound 1h

Using the general procedure for the deprotection of guanidinylated dipeptides with compound (**11h**) (91 mg, 0.1 mmol) yielded compound (**1h**) in 66% (43 mg) overall yield. The compound showed:

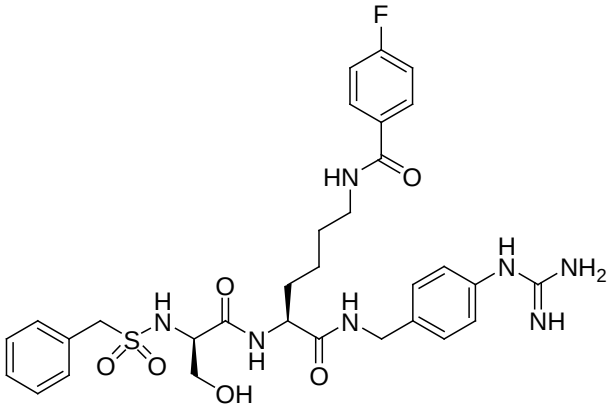

The compound showed: ^{1}H NMR (700 MHz, CD_3OD): δ =7.86–7.84 (m, 2H), 7.43–7.41 (m, 2H), 7.36–7.35 (m, 5H), 7.17–7.15 (m, 4H), 4.40 (d, *J* = 15.3 Hz, 2H), 4.34–4.32 (m, 4H), 3.89 (dd, *J* = 5.4Hz, 1H), 3.69 (dd, *J* = 5.4 Hz, 1H), 3.69 (d, *J* = 5.4 Hz, 2H), 3.36 (dd, *J* = 7.0 Hz, 2H), 1,96–1.91 (m, 1H), 1.78–1.72 (m, 1H), 1.67–1.60 (m, 2H), 1.54–1.42 (m, 2H);

^{13}C NMR (175 MHz, CD_3OD): δ = 172.3, 171.2, 167.2, 164.9, 163.5, 156.2, 137.8, 132.9, 130.2, 129.1, 129.0, 128.9, 128.1, 127.7, 127.7, 124.8, 114.5, 114.4, 61.7, 58.4, 57.9, 53.2, 47.5, 41.6, 38.8, 30.5, 28.1, 22.4;

HRMS (ES^+): for $C_{31}H_{39}N_7O_6SF$ calculated 656.2667 [M + H^+] found 656.2639 [M + H^+].

Compound 12 (R = $((CH_2)_2(CF_2))_5$-CF_3)

To a degassed suspension of 1,3,5,7-tetramethyl-2,4,8-trioxa-(2,4-dimethoxyphenyl)-6-phosphaadamantane (2.1 mg, 12 μmol) and palladium acetate (0.7 mg, 6 μmol) in THF (2 mL) a solution of tris(1*H*,1*H*,2*H*,2*H*-perfluorooctyl)tin hydride (232 mg, 200 μmol) in THF (1 mL) was added. The reaction mixture was stirred for 10 min and at which time compound (**5**) (R_1 = I ,18 mg, 90 μmol) in THF (1 mL) was added. The mixture was

heated in a microwave at 75° C for 15 min. The reaction was quenched by addition of aqueous saturated KF and extracted with ethyl acetate. The organic phase was washed twice with brine, dried over sodium sulfate and folowing filtration the solvent was removed by rotary evaporation. The product was used in next step without further purification.

Compound 13b

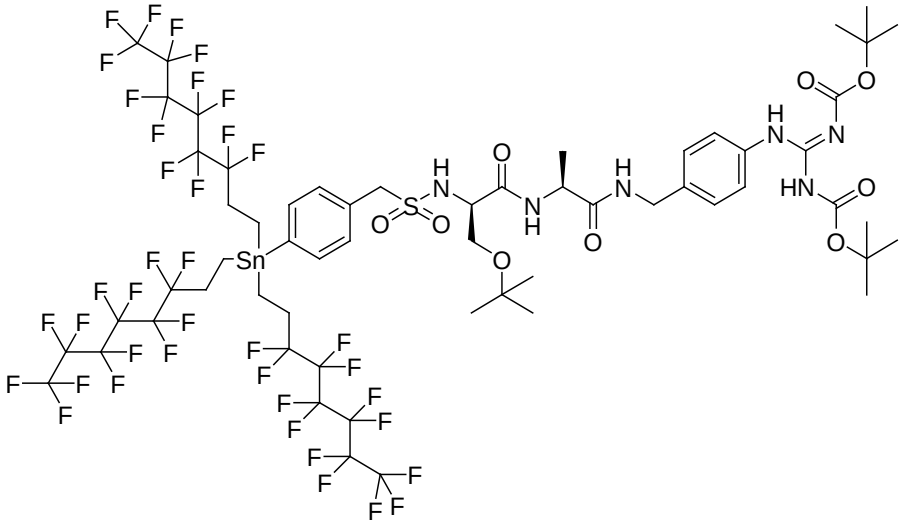

Using the general procedure for the preparation of protected guanidinylated dipeptides with compound (**10a**) (109 mg, 0.25 mmol) and compound (**12**) (368 mg, 0.25 mmol) yielded compound (**11a**) in 23% (108 mg) overall yield. The compound showed:

^{1}H NMR (600 MHz, CD_3OD): δ = 7.48 (s, 4H), 7.45 (d, *J* = 8.3 Hz, 2H), 7.25 (d, *J* = 8.5 Hz, 2H), 4.41–4.38 (m, 2H), 4.31 (s, 2H), 4.30 (d, *J* = 15.0 Hz, 1H), 3.99 (dd, *J* = 11.6 Hz, *J* = 5.4 Hz, 1H), 3.57 (dd, *J* = 9.0 Hz, *J* = 5.3 Hz, 1H), 3.54 (dd, *J* = 9.0 Hz, *J* = 6.3 Hz, 1H), 2.45–2.36 (m, 6H), 1.56 (s, 9H), 1.44 (s, 9H), 1.40 (d, *J* = 7.1 Hz, 3H), 1.34–1.32 (m, 6H), 1.16 (s, 9H);

^{13}C NMR (150 MHz, CD_3OD): δ = 174.6, 172.4, 164.5, 155.2, 154.4, 139.2, 137.3, 136.9, 136.7, 132.3, 132.0, 128.9, 123.9, 85.0, 80.6, 74.9, 63.7, 59.8, 58.7, 50.7, 43.5, 28.8, 28.7, 28.5, 28.4, 28.2, 28.6, 18.2, -0.49;

HRMS (ES^+): for $C_{59}H_{63}F_{39}N_6O_9SSn$ calculated 1893.2855 [M + H^+] found 1893.2738 [M + H^+].

Compound 13e

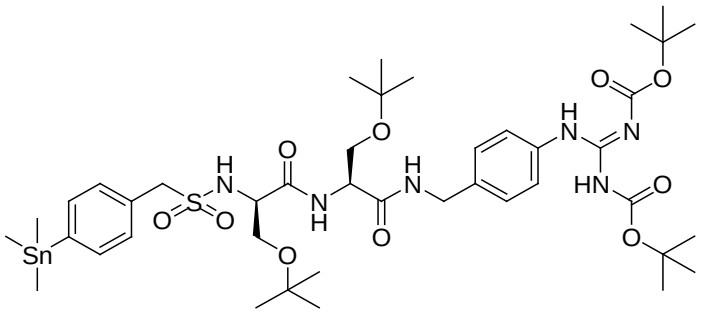

Using the general procedure for the preparation of protected guanidinylated dipeptides with compound (**10c**) (127 mg, 0.25 mmol) and compound (**12**) (R=Me) (119 mg, 0.25 mmol) yielded compound (**11a**) in 49% (120 mg) overall yield. The compound showed:

^{1}H NMR (600 MHz, CD_3OD): δ = 7.48–7.46 (m, 4H),7.39 (d, *J* = 7.7 Hz, 2H), 7.28 (d, *J* = 8.4 Hz, 2H), 4.49 (dd, *J* = 4.3 Hz, 1H), 4.43 (d, *J* = 15.1 Hz, 1H), 4.36 (d, *J* = 15.1 Hz, 1H), 4.34 (s, 2H), 4.00 (dd, *J* = 5.5 Hz, 1H), 3.82 (dd, *J* = 8.9 Hz, *J* = 3.9 Hz, 1H), 3.59 (dd, *J* = 8.9 Hz, *J* = 4.6 Hz, 1H), 3.57 (dd, *J* = 9.0 Hz, *J* = 6.0 Hz, 1H), 3.50 (dd, *J* = 5.0 Hz, *J* = 9.0 Hz, 1H), 1.57 (s, 9H), 1.45 (s, 9H) 1.20 (s, 9H), 1.16 (s, 9H), 0.27 (s, 9H);

^{13}C NMR (150MHz, CD_3OD): δ = 172.7, 172.3, 164.6, 155.2, 154.4, 143.8, 136.9, 136.6, 131.7, 130.9, 128.8, 105.6, 85.1, 80.6, 75.0, 74.8, 63.6, 62.8, 60.0, 58.9, 55.56, 43.5, 28.5, 28.3, 27.7, -9.9;

HRMS (ES^+): for $C_{42}H_{68}N_6O_{10}SSn$ calculated 969.3818 [M + H^+] found 969.3813 [M + H^+].

Compound 13g

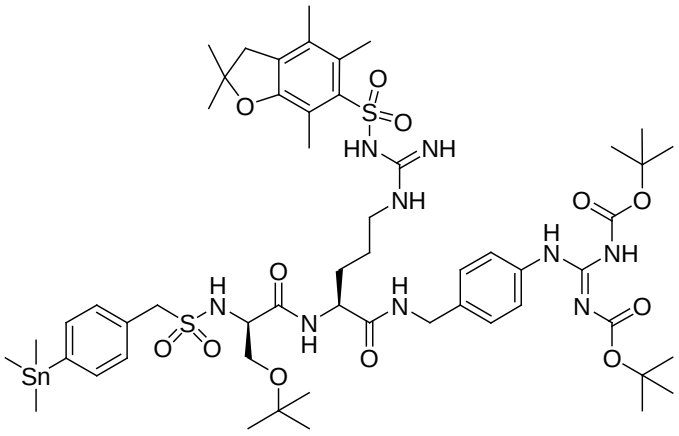

Using the general procedure for the preparation of protected guanidinylated dipeptides with compound (**10e)** (193 mg,0.25 mmol) and compound (**12**) **(**R = Me) (119 mg, 0.25 mmol) yielded compound (**11a**) in 59% (184 mg, 0.15 mmol) overall yield. The compound showed:

^{1}H NMR (700 MHz, CD_3OD): δ = 7.46 (d, *J* = 8.1 Hz, 2H), 7.42 (d, *J* = 7.8 Hz, 2H), 7.36 (d, *J* = 7.8 Hz, 2H), 7.21 (d, *J* = 8.1 Hz, 2H), 4.40 (dd, *J* = 9.2Hz, *J* = 4.8Hz, 1H), 4.33 (d, *J* = 14.8 Hz, 1H), 4.31 (s, 2H), 4.29 (d, *J* = 14.8 Hz, 1H), 3.92 (dd, *J* = 11.9Hz, *J* = 5.9 Hz, 1H), 3.51 (dd, *J* = 8.8 Hz, *J* = 5.1Hz, 1H), 3.47 (dd, *J* = 8.8 Hz, *J* = 6.8 Hz, 1H), 3.16–3.10 (m, 2H), 2.96 (s, 2H), 2.57 (s, 3H), 2.50 (s, 3H), 2.06 (s, 3H), 1.86–1.83 (m, 1H), 1.65–1.64 (m, 1H), 1.57 (s, 9H), 1.56–1.51 (m, 2H), 1.44 (s, 9H), 1.43 (s, 3H), 1.42 (s, 3H), 1.12 (s, 9H), 0.27 (s, 9H);

^{13}C NMR (175 MHz, CD_3OD): δ = 173.6, 172.8, 164.6, 159.9, 158.1, 155.2, 154.4, 143.8, 139.4, 137.0, 136.9, 136.8, 136.7, 134.4, 133.5, 131.8, 131.7, 131.6, 130.8, 129.2, 126.0, 124.0, 118.4, 87.6, 85.0, 80.7, 74.9, 63.5, 60.0, 58.8, 54.4, 44.0, 43.6, 30.4, 28.7, 28.5, 28.3, 27.7, 19.7, 18.5, 12.6, -9.9;

HRMS (ES^+): for $C_{54}H_{83}N_9O_{12}S_2Sn$ calculated 1234.4703 [M + H^+] found 1234.4720[M + H^+].

General procedure for radiolabeling

Eppendorf vials were coated with IodoGen (1,3,4,6-tetrachloro-3R,6R-diphenylglycouril) by concentrating a solution of the oxidant in chloroform (10 μL, 1 mg/mL) under a stream of argon. To an IodoGen coated vial was added a solution of the trialkylstannyl precursor in 5% glacial acetic acid in methanol (93μL, 5mg/mL), and aqueous sodium [^{125}I]iodide (7μL,12,6 MBq) which was obtained from a 0.1M NaOH solution. The reaction mixture was allowed to stand for 25 min with occasional swirling then quenched with aqueous sodium metabisulfite (100 μL, 0.01 mol/L). The reaction mixture containing compund (13b) was then loaded onto a FSPE cartridge that had been conditioned with DMF (5 mL) and washed with H_2O (10 mL). The reaction vial was rinsed with methanol (100 μL), which was added to the FSPE cartridge. The cartridge was then eluted with water (10 mL) followed by 80% MeOH-water (~80 mL, collected in 20 mL fractions). The respective activities of the collected fractions were measured using a dose calibrator. HPLC was used for assessing the purity (MethodB). The compounds (13e) and (13g) where purified using (Method B). The fractions which contained radioactivity were concentrated. TFA (2 mL) was added and the reaction mixture was left to stand for 4 hr. The excess of TFA

was removed by purging the vessel with nitrogen and the desired products were isolated in 63% RCY (8 MBq) for (**15b**) in 70% RCY (8.8 MBq) for (**15e**) and 66% RCY (8.4 MBq) for (**15g**). The purity was assessed using HPLC (MethodA)

uPA Inhibition – Colorimetric assay.[20]

The assay was performed in a 96 well polystyrene, flat bottom plate in a 50 mM Tris/0.15 M NaCl/0.5% Pluronic F-68 (Sigma), pH 7.4 buffer. The compounds were dissolved in DMSO at 20mM stock solution. Serial dilutions were performed with concentration ranging between 0.01-200 μM in a final reaction volume of 200µl. The hydrolysis reaction were initiated by the addition of substrate S2444 (final concentration of 200µM) with HMW human urokinase (3 nM final concentration).The reaction was monitored by the formation of *p*-nitroanaline at 405 nm at 37^{o}C and the absorbance readings were performed on a Bio-Rad EL 808 plate reader for 60 min. *K*i values were calculated using the previously established *K*m values for S-2444.

4.4. References

(1) Tamura, S. Y.; Weinhouse, M. I.; Roberts, C. A.; Goldman, E. A.; Masukawa, K.; Anderson, S. M.; Cohen, C. R.; Bradbury, A. E.; Bernardino, V. T.; Dixon, S. A.; Ma, M. G.; Nolan, T. G.; Brunck, T. K. *Bioorg Med Chem Lett* **2000**, *10*, 983.

(2) Levy, O.; Madison, E.; Semple, J.; Tamiz, A.; Weinhouse, M.; Google Patents: 2002; Vol. US20020037857 A1.

(3) Zeslawska, E.; Jacob, U.; Schweinitz, A.; Coombs, G.; Bode, W.; Madison, E. *J Mol Biol* **2003**, *328*, 109.

(4) Schweinitz, A.; Steinmetzer, T.; Banke, I. J.; Arlt, M. J.; Sturzebecher, A.; Schuster, O.; Geissler, A.; Giersiefen, H.; Zeslawska, E.; Jacob, U.; Kruger, A.; Sturzebecher, J. *J Biol Chem* **2004**, *279*, 33613.

(5) Zeslawska, E.; Jacob, U.; Schweinitz, A.; Coombs, G.; Bode, W.; Madison, E. *J. Biol. Chem.* **2003**, *328*, 109.

(6) Dass, K.; Ahmad, A.; Azmi, A. S.; Sarkar, S. H.; Sarkar, F. H. *Cancer Treat Rev* **2008**, *34*, 122.

(7) Look, M. P.; van Putten, W. L.; Duffy, M. J.; Harbeck, N.; Christensen, I. J.; Thomssen, C.; Kates, R.; Spyratos, F.; Ferno, M.; Eppenberger-Castori, S.; Sweep, C. G.; Ulm, K.; Peyrat, J. P.; Martin, P. M.; Magdelenat, H.; Brunner, N.; Duggan, C.; Lisboa, B. W.; Bendahl, P. O.; Quillien, V.; Daver, A.; Ricolleau, G.; Meijer-van Gelder, M. E.; Manders, P.; Fiets, W. E.; Blankenstein, M. A.; Broet, P.; Romain, S.; Daxenbichler, G.; Windbichler, G.; Cufer, T.; Borstnar, S.; Kueng, W.; Beex, L. V.; Klijn, J. G.; O'Higgins, N.; Eppenberger, U.; Janicke, F.; Schmitt, M.; Foekens, J. A. *J. Natl. Cancer Inst.* **2002**, *94*, 116.

(8) de Bock, C. E.; Wang, Y. *Med Res Rev* **2004**, *24*, 13.

(9) Law, B.; Curino, A.; Bugge, T. H.; Weissleder, R.; Tung, C. H. *Chem. Biol.* **2004**, *11*, 99.

(10) Al-Ejeh, F.; Croucher, D.; Ranson, M. *Exp. Cell. Res.* **2004**, *297*, 259.

(11) Kruithof, E.; Baker, M.; Bunn, C. *Blood* **1995**, *86*, 4007.

(12) Ranson, M.; Berghofer, P.; Vine, K. L.; Greguric, I.; Shepherd, R.; Katsifis, A. *Nucl. Med. Biol.* **2012**, *39*, 833.

(13) Look, M. P.; van Putten, W. L. J.; Duffy, M. J.; Harbeck, N.; Christensen, I. J.; Thomssen, C.; Kates, R.; Spyratos, F.; Fernö, M.; Eppenberger-Castori, S.; Sweep, C. G. J. F.; Ulm, K.; Peyrat, J.-P.; Martin, P.-M.; Magdelenat, H.; Brünner, N.; Duggan, C.; Lisboa, B. W.; Bendahl, P.-O.; Quillien, V.; Daver, A.; Ricolleau, G.; Meijer-van Gelder, M. E.; Manders, P.; Fiets, W. E.; Blankenstein, M. A.; Broët, P.; Romain, S.; Daxenbichler, G.; Windbichler, G.; Cufer, T.; Borstnar, S.; Kueng, W.; Beex, L. V. A. M.; Klijn, J. G. M.; O'Higgins, N.;

Eppenberger, U.; Jänicke, F.; Schmitt, M.; Foekens, J. A. *J. Natl. Cancer Inst.* **2002**, *94*, 116.

(14) Stutchbury, T. K.; Al-ejeh, F.; Stillfried, G. E.; Croucher, D. R.; Andrews, J.; Irving, D.; Links, M.; Ranson, M. *Mol. Cancer Ther.* **2007**, *6*, 203.

(15) Ides, J.; Thomae, D.; wyffels, L.; Vangestel, C.; Messagie, J.; Joossens, J.; Lardon, F.; Van der Veken, P.; Augustyns, K.; Stroobants, S.; Staelens, S. *Nucl. Med. Biol.* **2014**, *41*, 477.

(16) Augustyns, K. V. D. V., Pieter. Messagie, Jonas. Joossens, Jurgen. Malbeir, Anne-Marie; A61K 49/00 (2006.01) C07F 9/40 (2006.01) ed.; Organization, W. I. P., Ed. BE, 2012.

(17) Glaser, M.; Luthra, S.; Brady, F. *Int J Oncol.* **2003**, *22*, 253.

(18) Biersack, H. J.; Freeman, L. M. *Clinical nuclear medicine*; Berlin ; New York : Springer, c2007, 2007.

(19) Stürzebecher, J.; Prasa, D.; Hauptmann, J.; Vieweg, H.; Wikström, P. *J. Med. Chem.* **1997**, *40*, 3091.

(20) Wendt, M. D.; Rockway, T. W.; Geyer, A.; McClellan, W.; Weitzberg, M.; Zhao, X.; Mantei, R.; Nienaber, V. L.; Stewart, K.; Klinghofer, V.; Giranda, V. L. *J. Med. Chem.***2004**, *47*, 303.

(21) McIntee, J. W.; Sundararajan, C.; Donovan, A. C.; Kovacs, M. S.; Capretta, A.; Valliant, J. F. *J. Org. Chem.* **2008**, *73*, 8236.

(22) Adjabeng, G.; Brenstrum, T.; Frampton, C. S.; Robertson, A. J.; Hillhouse, J.; McNulty, J.; Capretta, A. *J. Org. Chem.* **2004**, *69*, 5082.

(23) Brenstrum, T.; Gerristma, D. A.; Adjabeng, G. M.; Frampton, C. S.; Britten, J.; Robertson, A. J.; McNulty, J.; Capretta, A. *J. Org. Chem.* **2004**, *69*, 7635.

(24) Liu, S.; Dockendorff, C.; Taylor, S. D. *Org. Lett.* **2001**, *3*, 1571.

Chapter 5 - The Synthesis and Evaluation of a Diaryl Phosphonate Inhibitor as a Molecular Imaging Agent for Urokinase Plasminogen Activator

5.1. Overview

Peptidyl diaryl phosphonates have been shown to be irreversible inhibitors of serine proteases (e.g. trypsin, chymotrypsin, and thrombin) acting as competitive transition state analogues.[1] These systems have been exploited as therapeutic agents and used in the treatment of cancer and metastasis, inflammatory diseases, hypertension, type 2 diabetes, immunological disorders and infections.[2]

Mechanistically, the phosphonate group reacts specifically with Ser195 present in the enzyme class and blocks the catalytic triad Asp102-His57-Ser195 which is responsible for the formation of an enzyme acyl intermediate involved in hydrolysis.[1,2] The transesterification-phosphonylation mechanism takes place through two tetrahedral transition states and starts with the addition of the Ser195 hydroxyl on the phosphorus atom and the release of one phenoxy group. The second step involves a nucleophilic attack of a water molecule accompanied by the release of the second phenoxy group (Scheme 5.1.).[1,2]

The synthesis, the initial radiolabelling and the initial screening procedures were performed by Silvia Albu. Subsequent labelling and screening was done by Alyssa Vitto while in-vivo biodistribution studies were completed by Alyssa Vitto and Nancy Janzen.

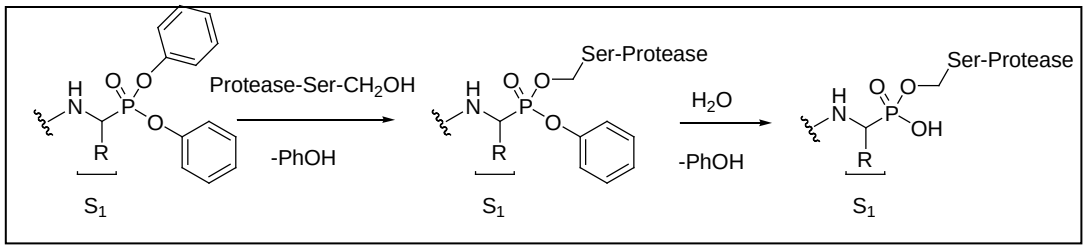

Figure 5.1. Mechanism of action of the diphenyl aminophosphonate inhibitors on serine proteases.[2]

A class of diphenyl phosphonates for inhibition of uPA was investigated by Jossens *et al* (Figure 5.2.).[3,4] SAR studies were performed on a series of tripeptidic diphenyl phosphonates where alkyl, cycloalkyl and aryl substituents were incorporated along with a terminal guanidine placed at the P_1 position.[4] The p-guanidinobenzyl group in compound (**2**) appears to fit best in the S1 subsite of uPA (IC_{50} = 57 nM). This compound also displays very good selectivity against other related proteases.[5] The P2 and P3 positions were also optimized and the most promising compounds from the series, (**3**) and (**4**), bind uPA with IC_{50} = 3.1 nM and IC_{50} = 7 nM, respectively. When the phenol leaving group was replaced with a paracetamol moeity, a less cytotoxic compound was obtained that maintained the binding affinity IC_{50} = 3.4 nM but showed less selectivity amongst related proteases. Compound (**3**) was used in preclinical studies and displayed a non-dose-dependent inhibition of tumor growth of roughly 10-18%. Furthermore, the number of lung foci (29-70%) and the weight of axillary lymph nodes (46-73%) decreased in a dose-dependent fashion.[5]

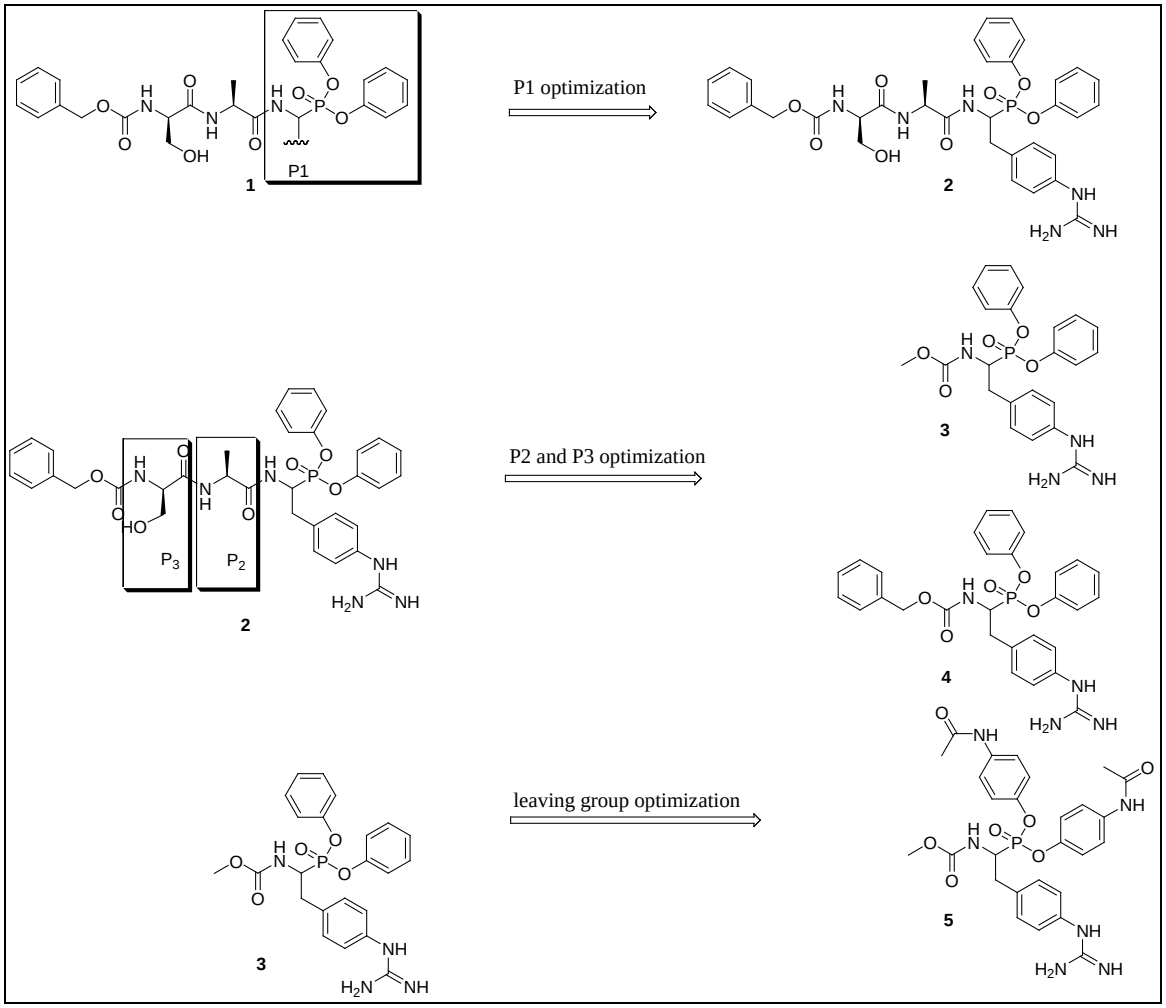

Figure 5.2. Optimization of the structure of diaryl phosphonate inhibitors of uPA.

During the course of this thesis work, a series of diaryl phosphonate activity-based MI probes for uPA were reported.[6] The lead compound (**3**) was connected to a series of different fluorophores (such as rhodamine, cyanine dyes and BODIPY) through a linker. The polarity of the ligands was optimized by replacing the alkyl linker with polyethylene glycol chains of different lengths. These constructs displayed fast kinetics and after 15 min. of incubation with the enzyme, IC_{50} values in low nM range were observed. Despite the promising results obtained *in vitro*, no *in vivo* studies were reported. A fluorine

derivative was also synthesized and its ^{18}F analogue was evaluated in *vivo*. Unfortunately, the biodistribution results showed a poor T/NT ratio.[7]

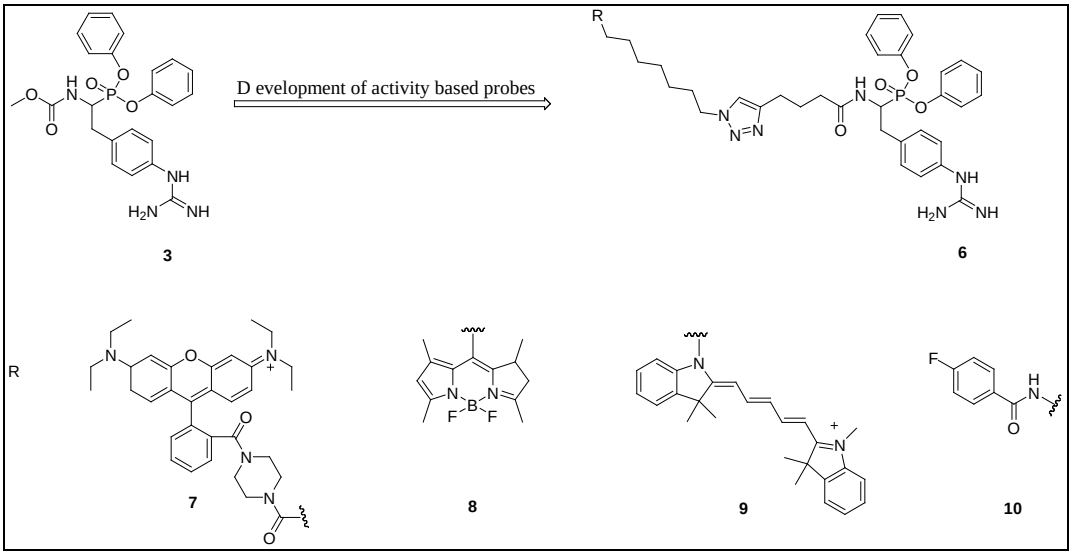

Figure 5.3. Diaryl phosphonate-derived activity based probes for uPA.

In keeping with our approach involving the tagging of suitable inhibitors of uPA with radionuclides for use as imaging agents, we developed a synthetic route for a derivative of compound (**4**) that would include an iodine tag (Figure 5.4.). This probe was evaluated *in vitro* and *in vivo* and is described in the following manuscript.

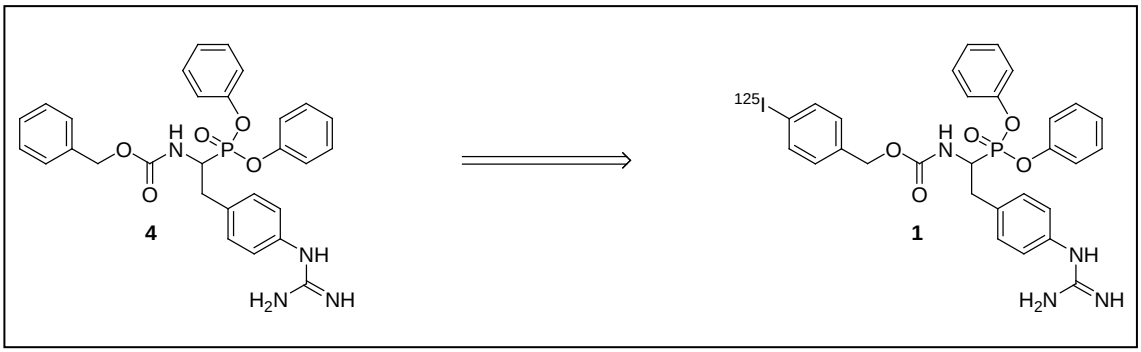

Figure 5.4. Development of ^{125}I Diaryl Phosphonate agents for uPA.

5.2. The Synthesis and Evaluation of an Iodinated Diaryl Phosphonate Inhibitor as Molecular Imaging Probe for Urokinase Plasminogen Activator

Silvia Albu, Alyssa Vito, Nancy Janzen, Alfredo Capretta and John Valliant

Department of Chemistry and Chemical Biology, McMaster University, Hamilton, Ontario, Canada, L8S 4M1

5.2.1. Introduction

Molecular Imaging (MI) plays an important role in oncology where techniques are routinely employed for early detection, tumour staging, assessment of response and to guide surgical resection.[8] MI requires the development and validation of probes that specifically target biochemical targets and processes.[8] Radiopharmaceutical based probes can provide insight into the unique biochemical aspects of tumours and they can be converted into therapeutic compounds by changing the nature of the isotope used.[9]

Urokinase plasminogen activator (uPA) is a serine protease of the trypsin family that plays an important role in cell adhesion, migration and proliferation.[10] Upon binding to its receptor uPAR, uPA activates plasminogen to plasmin which triggers an endogenous proteolytic cascade that enables tumour cell invasion.[10] Research studies have shown that elevated levels of uPA are associated with aggressiveness and likelihood of progression.[11] For this reason, uPA has become an attractive target[1] for both the development of new molecular imaging probes[6,12,13] as well as the synthesis of new

One approach to imaging uPA is to radiolabel non-covalent inhibitors of the protein.[14] In general the most potent inhibitors in this class contain a guanidine or amidine moiety that participates in specific ionic contacts with Asp189 present at the S1 site of the enzyme. Their inhibitory potency ranges from low nanomolar to micromolar but the compounds generally display poor selectivity against competitive proteases. Another drawback of the reversible inhibitors is their poor pharmacokinetic properties such as short plasma half-life following oral and subcutaneous administration.

An alternative approach is to build molecular imaging probes using irreversible inhibitors. A chloromethyl ketone derived peptide was first reported as an irreversible uPA inhibitor but was shown to lack selectivity.[15] Joossens *et al.*[3] developed an inhibitor *Z*-D-Ser-Ala-Arg diphenyl phosphonate which reacts with a serine in the uPA active site to give a covalent and stable phosphonylated complex. The tripeptide diphenyl phosphonate construct was optimized at P1 site followed by another report which developed compounds exploiting binding at the P2 and P3 positions.[4] Despite the removal of the peptide tail and replacement with smaller synthetic units, the binding affinities and selectivity were maintained. Based on its inhibitory and selectivity profile, compound (**4**) was selected as the starting point for our study and we developed a synthetic route for the preparation of an ^{125}I diphenyl phosphonate derivative as a potential molecular imaging probe for uPA.

5.2.2. Results and Discussion

5.2.2.1. Chemistry

The synthesis of the iodinated diphenyl phosphonate is outlined in Figure 5.5. and is based on the same synthetic protocol described previously for compound (**4**).[4] Commercially available amino-alcohol (**12**) was Boc-protected to give compound (**13**) that was subsequently oxidized using a Dess-Martin protocol to give the protected 4-aminophenylacetaldehyde (**14**).[4] The requisite iodocarbamate (**16**) was synthesized from commercially available alcohol (**15**) using sodium cyanate and TFA in toluene. An amidoalkylation reaction involving the iodo carbamate (**16**), the 4-aminophenylacetaldehyde (**14**) and triphenylphosphite, using copper triflate as catalyst, afforded the diphenyl phosphonate (**17**) in 43 % yield. After removal of the Boc protecting group (to give (**18**)), *N*,*N*′-bis(*tert*-butoxycarbonyl)-1-guanylpyrazole was used to introduce the protected guanidine group in compound (**19**). The desired iodinated diphenyl phosphonate (**20**) was obtained after deprotection with trifluoroacetic acid.

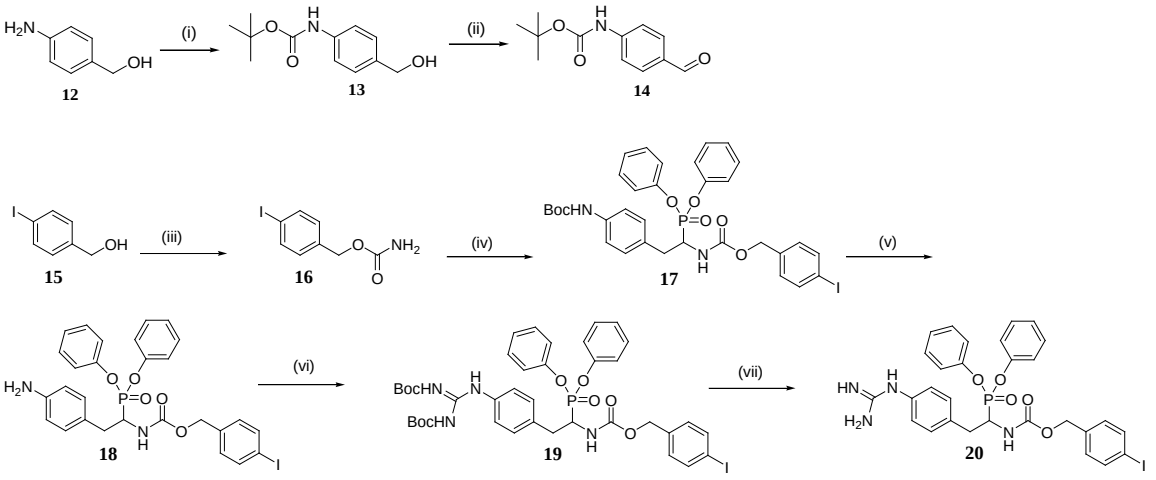

Figure 5.5. Synthesis of compound (**20**). Reagents: (i) Di-*tert*-butyl dicarbonate, TEA, DCM; (ii) Dess-Martin oxidation, compound (**13**), DCM; (iii) NaOCN, TFA, Toluene; (iv) Compound (**14**), Triphenyl phosphite, $Cu(OTf)_2$, DCM; (v) 4M HCl / dioxane; (vi) *N*,*N*'-bis(*tert*-butoxycarbonyl)-1-guanylpyrazole, DCM; (vii) TFA, ACN..

5.2.2.2. Screening

Compounds (**4)** and (**20**) were evaluated for their inhibitory activity against uPA in a colourimetric enzyme assay using Bio-Phen CS-61 substrate (Aniara, A2209061).[16] Each inhibitor, at various concentrations, was incubated in a 96-well microtitre plate with 50 µL of 694 nM stock of uPA (EMD Chemicals Millipore, 672081) for 15 min at 37°C. Upon addition of the substrate, the course of the hydrolysis reaction was monitored by detecting the formation of *p*-nitroaniline at 405 nm and 37° C for 30 min. The reaction rates obtained in the presence of compounds (**4**) and (**20**) were compared to those seen with substrate alone and the percent inhibition calculated. The reported K_m values of 90 µM were used for the K_i calculations and all experiments were done in triplicate. The results are presented in Table 5.1.

Table 5.1. Inhibitor structures and affinities

	Compound	K_i (nM)	95% CI	IC_{50} (nM)	95% CI	r^2	Std Error
4	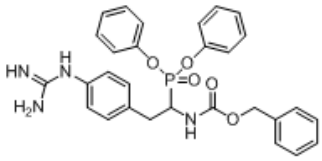	1.68	0.95 – 2.76	5.88	3.34 – 10.38	0.97	1.28
20	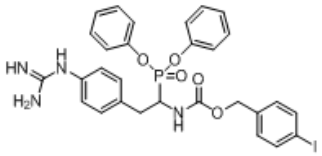	2.09	1.23 – 3.53	7.30	4.32 – 12.34	0.98	1.26

The K_i value is 1.70 nM of (**4**) reported by Joossens *et al* [4], matched the K_i value of 1.68 nM determined in our assay. The iodinated compound (**20**) was tested and was shown to have comparable *in vitro* binding with a K_i value of 2.09 nM.

5.2.3. Synthesis of Radiolabelled Derivatives

Based on the promising *in vitro* results, the preparation of ^{125}I diphenyl phosphonate (**11**) was undertaken. The synthesis, illustrated in Figure 5.6. utilized a Pd-catalyzed stannylation of the aryl iodide moiety with hexamethyldistannane in the presence of KOAc.[17] Treatment of the resultant (**21**) with IodoGen (1,3,4,6-tetrachloro-3R,6R-diphenylglycouril) and Na^{125}I allowed for introduction of the label and the formation

of (**22**). After purification on a silica gel cartridge, the Boc protected derivative (**22**) was treated with TFA in ACN to give the desire derivative (**11**). HPLC analysis of (**11**) co-injected along with its corresponding non-radioactive analogue (**20**) (Figure 5.7.) confirms the successful destannylation/iodination reaction sequence (RY 42%).

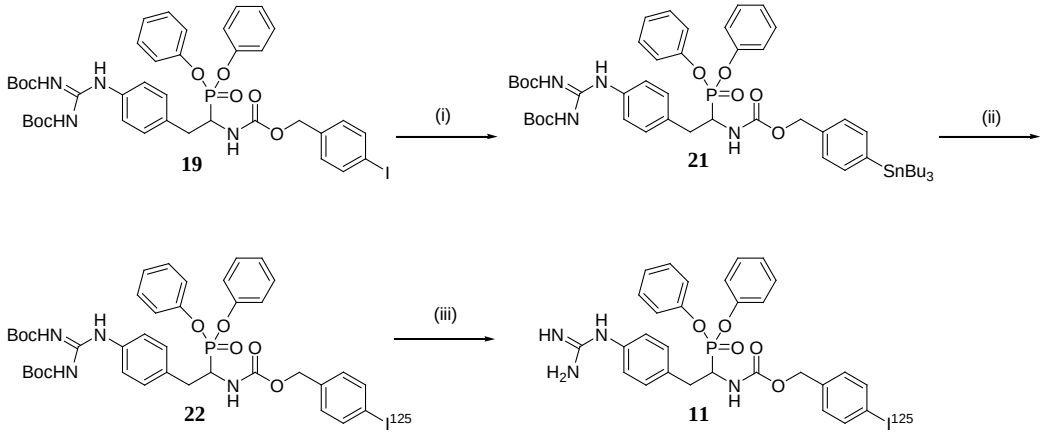

Figure 5.6. Synthesis of compound (**11**). Reagents: (i) $Bu_3Sn\text{-}SnBu_3$, PdOAc, KOAc, $PdCl_2(PPh_3)_2$,THF ; (ii) $Na^{125}I$, Iodogen, 5%AcOH/ACN; (iii) 90%TFA/CAN.

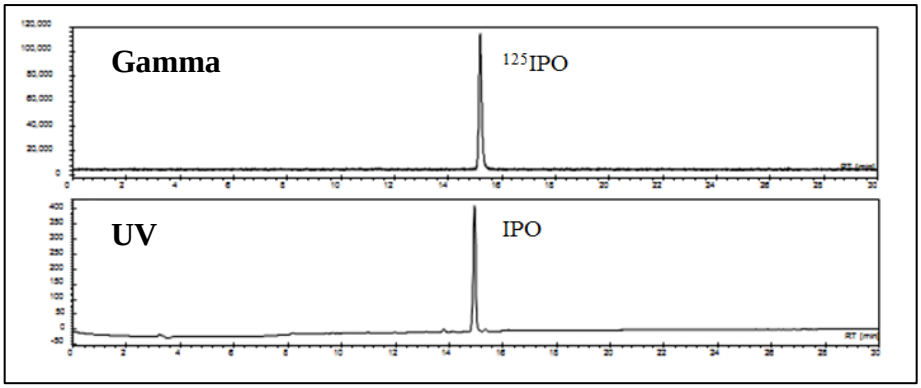

Figure 5.7. UV and γ-HPLC chromatograms of (**11**) co-injected with the nonradioactive standard (**20**).

5.2.4. SDS-PAGE Studies

After successful labeling, SDS-PAGE was conducted to confirm specific binding between the inhibitor and uPA. The gel showed a band that was consistent with uPA through comparison to MW reference standards. The appearance of double bands at higher concentrations of uPA could be due to cleavage of HMW-uPA to LMW-uPA by 2-mercaptoethanol. The band intensity increased with the amount of uPA added.

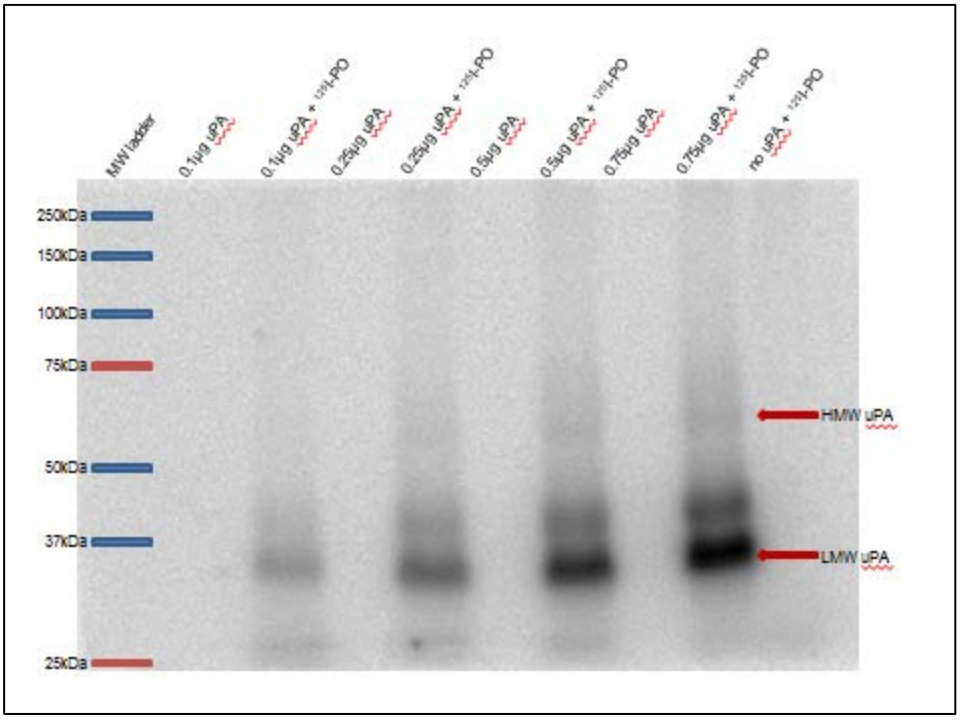

Figure 5.8: SDS-PAGE analysis of ^{125}IPO (**11**) binding to HMW uPA. The intense band around 37 kDa is consistent with a complex between LMW uPA and ^{125}IPO (**11**).

To test the specificity of (**11**), uPA was preincubated with two known inhibitors PAI-1 (endoegenous inhibitor of uPA) and compound (**4**) (Figure 5.9.). The gel successfully showed that (**11**) binds to uPA. It was also indicated that 2-mercaptoethanol does indeed

cleave HMW-uPA to LMW-uPA, although this has no effect on binding ability of the inhibitor. Both the positive control (**4**)[18] and PAI-1 are able to effectively block (**11**) from binding to uPA, when they are already bound to the protein. However, the covalent interaction of (**4**) proved to be a more effective than the endogenous PAI-1 which still allowed for a small amount of (**11**) to bind.

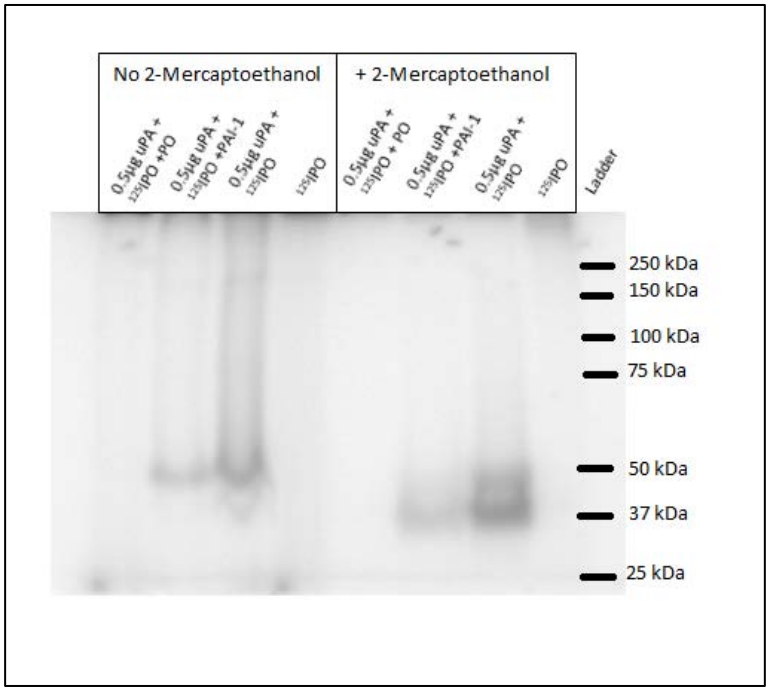

Figure 5.9. SDS-PAGE analysis of (**11**) binding to HMW uPA, with (**4**) and PAI-1 as competitive ligands. Lanes with no 2-mercaptoethanol only show bands indicative of a complex formed with HMW-uPA, whereas those with 2-mercaptoethanol show bands indicative of a complex formed with LMW-uPA. Complete inhibition of uPA is seen for compound (**4**). PAI-1 shows partial inhibition, and some (**11**) is still able to bind.

5.2.5. In Vivo Biodistribution Studies

The radiolabelled inhibitor (**11**) was assessed *in vivo* in biodistribution studies carried out using CD1 nude mice expressing HT-1080 human fibrosarcoma tumours. Tumour bearing mice were administered 37-185 kBq of the radiolabelled compound (**11**) *via* tail vein injection. Following 0.5 h, 2 h, 24 h, 48 h and 96 h groups of mice (n=3 per time point) were sacrificed and the tumours and organs isolated by dissection. Radiochemical uptake in tumour/organ samples was measured and expressed as the percent injected dose per gram (%ID/g, Figure 5.10.). The radioactivity in the blood circulation was relative high and decreased slowly over time indicating plasma protein binding. The compound displayed both renal and hepatic elimination; the latest could be explained by the fact that a fraction of the compound which was bound to plasma protein did not pass the glomeruli filtration. The uptake in gall bladder, kidney small intestine and large intestine decreased significantly after 24 h. There is not a significant uptake in the adipose tissue. The low thyroid levels found at 0.5 h, 2h and 24 h (2.3%ID/g, 2.5%ID/g and 4.8%ID/g respectively) point to a relative low deaiodination of the compound in vivo in the first 24 h. At later time points 48 h (12.9%ID/g) and 96 h (8.5%ID/g) the observed increased accumulation of radioactivity in the thyroid suggests that some free iodine cleaved from the compound. The biodistribution data for (**11**) showed retention in the tumour over time (peaking at 48 h post-injection with 1.95% ID/g) with increasing tumour-to-blood ratio up to 24 h and then slowly decreasing (0.65 at 24 h, 1.13 at 48 h and 1.09 at 96 h post-injection; Figure 5.11.).

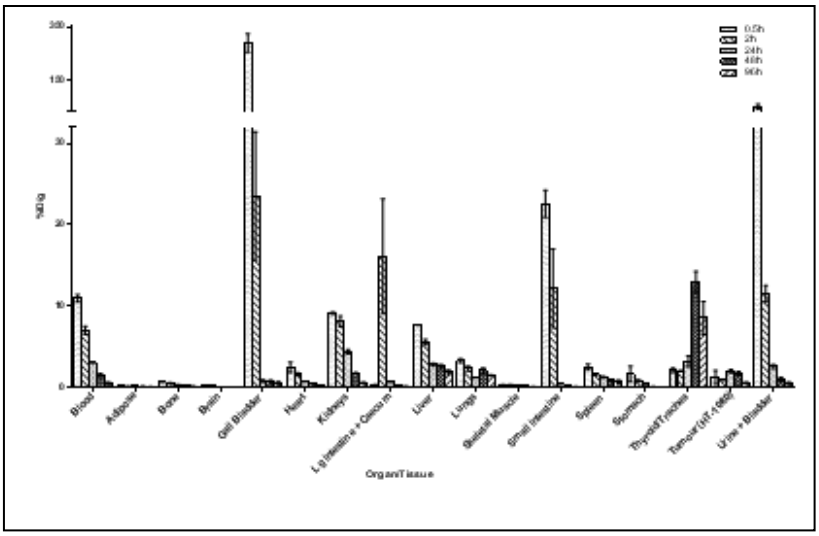

Figure 5.10. Graphical analysis of biodistribution data in relevant organs, expressed as % ID/g for ^{125}IPO (**11**) at 0.5 h, 2 h, 24 h, 48 h, and 96 h P.I. in nude mice bearing HT-1080 human fibrosarcoma tumours.

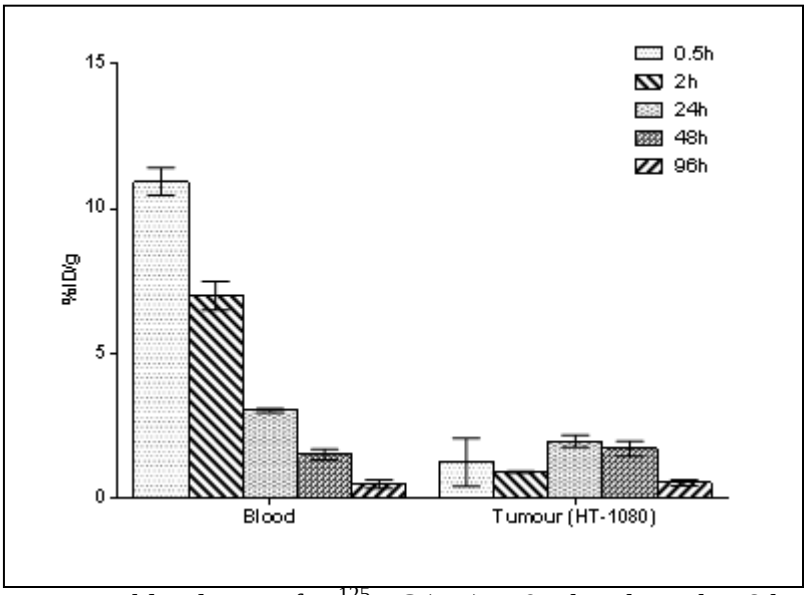

Figure 5.11. Tumor to blood ratios for ^{125}IPO(**11**) at 0.5 h, 2 h, 24 h, 48 h, and 96 h P.I. in nude mice bearing HT-1080 human fibrosarcoma tumours.

These results are comparable in terms of tumor uptake to those seen in biodistribution studies for ^{125}I-PAI-2.[12,19] In one study,[19] recombinant plasminogen activator inhibitor-2 (PAI-2) the endogenous inhibitor was radiolabelled with iodine-125

and biodistribution studies were performed in mice carrying a subcutaneous HCT116 human colon cancer xenograft. The results of this study showed rapid uptake in the tumor, with peak retention 60 minutes post-injection at 1.3% ID/g. Multiple i.v. injections of ^{125}I-PAI-2 resulted in an increase in tumor uptake to 1.6% ID/g. Our studies demonstrated that compound (**11**) after one i.v. injection it is accumulated in a specific manner in to the tumour peaking at 24 h post-injection with 1.95% ID/g while the best tumour to blood ratio with a value of 1.13 was achieved at 48 h P.I.

To test the specificity of (**11**), the radiolabelled inhibitor was assessed *in vivo* through a biodistribution blocking study. Biodistribution studies were carried out in CD1 nude mice expressing HT-1080 human fibrosarcoma tumours. Two groups of mice were utilized: the first set were administered 37-185 kBq of the radiolabelled compound alone, while the second set were administered 37-185 kBq of the radiolabelled compound + 2mg/kg of (**4**) as, *via* tail vein injection. Following a 48 h uptake period, groups of mice (n=3 per time point) were sacrificed and the tumours and organs isolated by dissection. Radiochemical uptake in tumour/organ samples was measured and used to generate an *in vivo* biodistribution pattern.

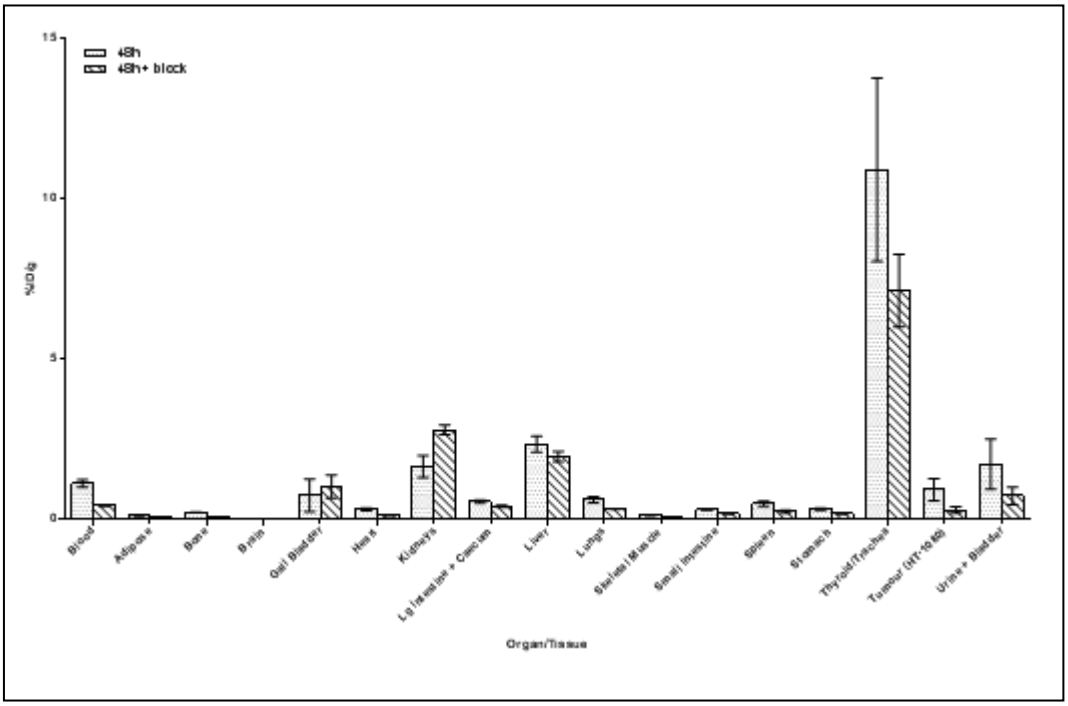

Figure 5.12. Biodistribution data in relevant organs, expressed as %ID/g for (**11**) in the absence or presence of inhibitor (**4**) at 48h P.I.

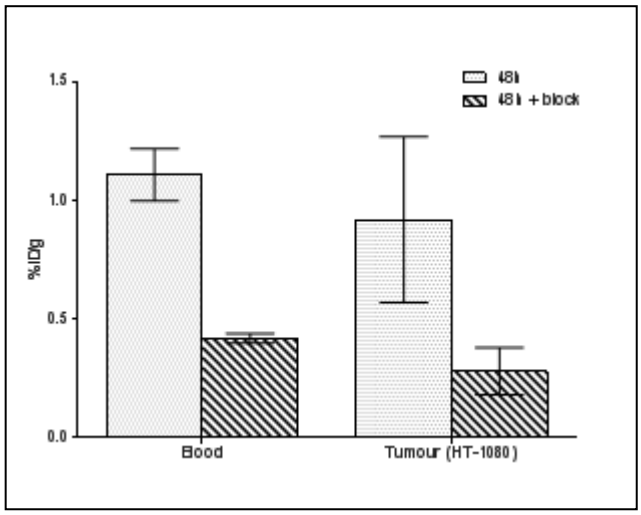

Figure 5.13. Tumor to blood ratios expressed as %ID/g for ^{125}IPO (**11**) in the absence or presence of inhibitor (**4**) at 48 h P.I.

.

Coinjection with the nonradioactive compound (**4**) reduced the blood uptake by 38% which might be due to the saturation of the nonspecific binding sites present in other

plasma proteins. There might be also a free circulating uPA which dissociated from the tumour site which could be responsible for binding with either compound (**4**) or radioactive compound (**11**)**.** The accumulation of (**11**) in the tumour was blocked by co-administration with (**4**) and the tumour uptake decreased by 30%. This result indicates specific accumulation of compound (**11**) in the tumour confirming the results from *in vitro* blocking study.

5.2.6. Conclusions

In an attempt to find a suitable uPA molecular imaging agent an ^{125} I irreversible inhibitor was successfully synthesized from its trybutil tin precursor. Results of in *vivo* biodistribution studies along with in *vitro* results suggest that compound (**11**) specifically accumulate to the tumour. The highest percentage of radioactivity in tumor was approximately 1-2%ID/g which is comparable to the previously published result of the radioaiodinated endogenous uPA inhibitor PAI-2. The undesirable nonspecific radioactive uptake observed in non targeted tissues required further optimization of the phosphonate structure or preincubation with uPA.

5.3. Experimental

Unless otherwise stated, all chemicals reagents were purchased and used as received from Sigma-Aldrich without further purification. Solvents were purchased from Caledon. Compound (**4**) and compound (**14**) were synthesized according to the literature procedures.[4] Reactions were monitored using Alugram Sil G/UV254 thin layer chromatography (TLC) plates and visualized under ultraviolet light. Column

chromatography was accomplished with Silica Flash P60 purchased from Silicycle. ^{125}I was obtained from the McMaster University Nuclear reactor as in a 0.1M NaOH solution ($Na^{125}I$). 1H and ^{13}C NMR spectra were recorded on Bruker AV 700 or AV 600 spectrometer. 1H Chemical shifts are reported in ppm relative to the residual proton signal of the NMR solvents. Coupling constants (*J*) are reported in Hertz (Hz). ^{13}C Chemical shifts are reported in ppm relative to the carbon signal of the NMR solvents. High resolution ES mass spectra were obtained on a Waters QToF Ultima Global spectrometer. Reverse phase analytical HPLC was performed using a Varian Prostar instrument equipped with a 355 UV detector or a Waters 2489 HPLC equipped with a Waters 2489 UV/Vis (λ = 254 nm) and / a Bioscan glow count gamma detector (model 106). Runs were performed using HPLC grade water containing 0.1 % TFA (solvent A) and acetonitrile containing 0.1 % TFA(solvent B) as eluents, a 1 mL/min flow rate and a C18 reverse phase Phenomonex column (25 x 4.60 mm, 5 micron). The desired products were eluted using a 95 to 5% gradient (Solvent A: Solvent B) over 30 min.

4-iodobenzyl carbamate (16)

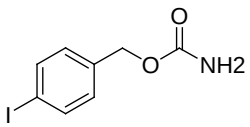

To a solution of 4-Iodobenzyl alcohol (234 mg, 1 mmol) in 25 ml toluene, sodium cyanate (130 mg, 2 mmol) is added. The suspension is stirred slowly (ca.120 r.p.m.) for 30 min. followed by the drop wise addition (3.1 ml, 0.4 mmol) of trifluoroacetic acid at a rapid rate. To prevent the overheating of the reaction mixture the flask is briefly

immersed in an ice-water bath. Slow stirring is continued for 24 h at room temperature. The mixture is treated with 15 ml. of water and stirred for 5 minutes. The impurities were extracted in hexane and the iodocarbamate was extracted with EtOAc and washed with 10 ml. of aqueous 5% sodium hydroxide and with 10 ml. of water. The organic extract was dried over anhydrous magnesium sulphate and filtered. The solvent was removed under reduced pressure. The product was washed with hexane and obtained as a white solid in 77% yield 215 mg. The compound showed:

^{1}H NMR (600 MHz, MeOD): 7.61 (d, *J* = 8.3 Hz, 2H), 7.14 (d, *J* = 8.3 Hz, 2H), 5.00 (s, 2H);

^{13}C NMR (150 MHz, MeOD): 159.6, 138.7, 138.3, 130.7, 94.0, 66.5;

HRMS (ES^+): for $C_8H_8NO_2NaI$ calculated 299.9498 [M + Na^+] found 299.9508 [M + Na^+].

4-iodobenzyl-2-(4-aminophenyl)-2-(4-(*tert*-butyloxycarbonylamino)phenyl)ethyl-carbamate (17)

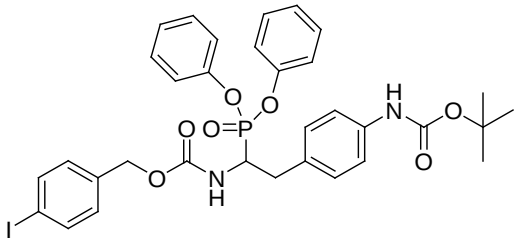

A solution of crude aldehyde **(14)**[4] (442 mg, 2 mmol), triphenyl phosphite (620 mg, 2 mmol) and iodo carbamate (**16**) (554 mg, 2 mmol) in 50 mL CH_2Cl_2 was treated with $Cu(OTf)_2$ (144 mg, 0.2 mmol). The solution was stirred at room temperature for 4 h. The solvent was removed in *vacuo* and the crude product was triturated with MeOH. The

crude reaction mixture was purified on silica gel (hexane, ethyl acetate) providing the desired compound as a white solid in 43% yield (628 mg). The compound showed:

^{1}H NMR (600 MHz, MeOD): 7.61 (d, *J* = 8.3 Hz, 1H), 7.37-7.33 (m, 4H), 7.24-7.19 (m, 4H), 7.22-7.14 (m, 4H), 7.15-7.13 (m, 4H), 6.92 (d, *J* = 8.3 Hz, 1H), 5.0 (d, *J* = 13.0 Hz, 1H), 4.89 (d, *J* = 13.0 Hz, 1H), 4.65- 4.60 (m, 1H), 3.35-3.34 (m, 1H), 3.01-2.95 (m, 1H), 1.54 (s, 9H);

^{13}C NMR (150 MHz, ($(CD_3)_2CO$)): 156.8, 153.8, 151.7, 151.5, 151.4, 139.4, 138.3, 138.2, 130.6, 130.5, 130.5, 130.2, 126.1, 125.9, 121.7, 121.6, 121.4, 121.3, 118.9, 93.5, 79.9, 66.0, 51.9, 50.8, 35.3;

HRMS (ES^+): for $C_{33}H_{35}N_2O_7IP$ calculated 729.1227 [M + H^+] found 729.1193 [M + H^+].

4-Iodobenzyl 2-(4-aminophenyl)-2-phenyl)ethyl-carbamate (18)

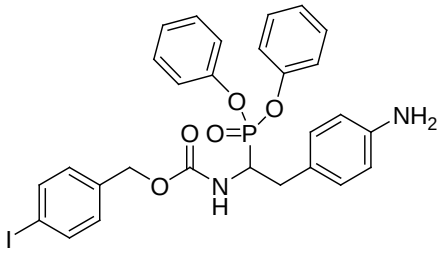

Compound (**17**) (728 mg, 1 mmol) was dissolved in 50% trifluoroacetic acid /CH_2Cl_2 (1ml). After stirring for 3h at room temperature, the solvent was evaporated under a stream of nitrogen. The crude oil was washed with cold ether and 500 mg precipitate of the TFA salt was isolated. And used in the next step without further purifications.

4-Iodobenzyl 2-(4-aminophenyl)-2-phenyl)ethyl-carbamate (19)

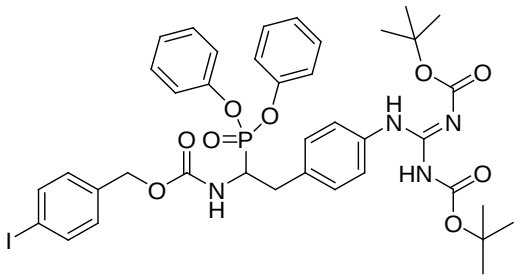

A mixture of the crude phosphonate (**18**) (314 mg, 0.5 mmol), *N*,*N*′- bis(*tert*-butyloxycarbonyl-1-guanyl-pyrazole (310 mg, 1 mmol), and triethylamine (208 μl, 1.5 mmol) in chloroform (20 mL) was stirred at room temperature for 24 h. The solvent was evaporated and the residue was dissolved in ethyl acetate and washed with 1 N HCl, saturated solution of $NaHCO_3$ and brine. The organic layer was dried over Na_2SO_4. The solvent was evaporated and the crude product was purified by silica gel (0–80% EtOAc in hexane) to obtain the protected guanidine as a white solid yield in 65% yield (287mg). The compound showed:

^{1}H NMR (700 MHz, MeOD): 7.58 (d, *J* = 8.4 Hz, 1H), 7.50 (d, *J* = 8.4 Hz, 1H), 7.37-7.33 (m, 4H), 7.26 (d, *J* = 8.4 Hz, 1H), 7.24-7.21 (m, 2H), 7.16-7.14 (m, 4H), 6.92 (d, *J* = 8.4 Hz, 1H), 5.20 (d, *J* = 7.7 Hz, 1H), 4.67-7.4.63 (m, 1H), 3.05-3.00 (m, 1H), 1.58 (s, 9H), 1.47 (s, 9H);

^{13}C NMR (150 MHz, MeOD): 164.6, 158.0, 158.0, 155.0, 138.9, 154.4, 138.6, 138.1, 136.9, 131.0, 130.9, 120.8, 130.4, 126.8, 126.7, 123.6, 121.8, 121.8, 121.6, 121.6, 93.9, 85.0, 80.7, 66.9, 28.5, 28.3;

HRMS (ES^+): for $C_{39}H_{45}N_4O_9PI$ calculated 871.1969 [M + H^+] found 871.1962 [M + H^+].

4-Iodobenzyl-methyl-1-(di)ethylcarbamate-phenoxyphosphoryl)-2-(4-guanidinophenyl Trifluoroacetate (20)

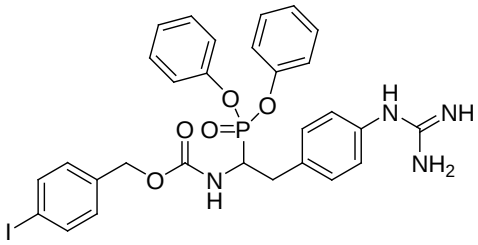

Compound (**19**) (217 mg, 0.25 mmol) was dissolved in a 50/% TFA/AcCN (1 ml) The mixture was stirred for 3h at r.t. then evaporated under stream of nitrogen. The resulting sticky compound was dissolved in a 1:3 v/v mixture AcCN-H_2O (15 ml) then lyophilized. The crude mixture was purified on a CombiFlash using a C18 cartridge and a gradient H_2O/AcCN from 90 to 10%. The desired product was obtained as a white solid in 52% yield 88 mg). The compound showed:

^{1}H NMR (700 MHz, MeOD): 7.64 (d, *J* = 8.4 Hz, 1H), 7.38 (d, *J* = 8.4 Hz, 1H), 7.36-7.34 (m, 4H), 7.24-7.21 (m, 2H), 7.16-7.14 (m, 4H), 7.13 (d, *J* = 8.4 Hz, 1H), 7.04 (d, *J* = 8.4 Hz, 1H), 4.95 (q, *J* = 13.3Hz, 1H), 4.62-.4.57 (m, 1H), 3.41-3.38 (m, 1H), 3.09-3.04 (m, 1H);

^{13}C NMR (150 MHz, MeOD): 158.3, 158.2, 158.0, 151.6, 151.5, 151.4, 151.3, 138.7, 137.9, 134.9, 131.8, 131.0, 130.9, 130.8, 126.9, 126.8, 126.6, 121.8, 121.7, 121.6, 121.6, 94.2, 67.1, 51.9, 50.9;

HRMS (ES^+): for $C_{29}H_{29}N_4O_5IP$ calculated 671.0920 [M + H^+] found 671.0928 [M + H^+].

-4-(tributylstannyl)2-(4-aminophenyl)-2-phenyl)ethyl-carbamate (21)

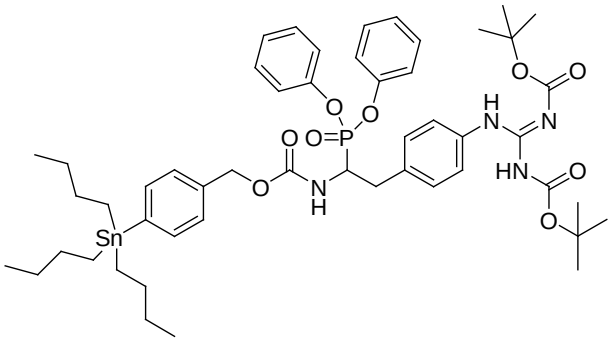

A 25 mL round bottom flask was charged with $PdCl_2(PPh_3)_2$ (11 mg, 0.0015 mmol) degassed and 5ml of NMP was added through a syringe while the degassing was still maintained. KOAc (74 mg, 3.0 mmol) was added, followed by of hexabutylditin (189 µl, 0.37 mmol) and compound (**19**) (217 mg, 0.25 mmol). The reaction mixture was stirred for 3h at rt. or until all starting material had been consumed as determined by TLC. The crude reaction mixture was quenched with a saturated aqueos solution of KF (2 ml) and extracted with DCM (3 x 15 ml). The solvent was removed in *vacuo* and the desired product was purified by flash column chromatography using a gradient 100-60% (hexane-ethylacetate). The desired product was obtained as an oil in 68 % yield (175 mg). The compound showed:

^{1}H NMR (700 MHz, MeOD): 7.55 (d, *J* = 8.4 Hz, 1H), 7.46 (d, *J* = 8.4 Hz, 1H), 7.32-7.29 (m, 2H), 7.24-7.21 (m, 5H), 7.18-7.14 (m, 5H), 7.06 (d, *J* = 8.4 Hz, 1H), 5.14 (d, *J* = 10.5 Hz, 1H), 5.08 (d, *J* = 10.5 Hz, 1H), 4.92 (d, *J* = 12.6 Hz, 1H), 4.81-4.75 (m, 1H),

3.39-3.34 (m, 1H), 3.05-3.01 (m, 1H), 1.53 (s, 9H), 1.50 (s, 9H), 1.33-1.29 (m, 6H), 1.04-1.02 (m, 6H), 0.88 (t, J = 7 Hz, 9H);

^{13}C NMR (150 MHz, MeOD): 163.7, 153.6, 153.4, 150.3, 150.1, 142.4, 136.8, 136.7, 135.9, 135.7, 130.0, 129.9, 129.8, 127.9, 127.8, 127.8, 125.6, 125.4, 122.4, 120.8, 120.8, 120.6, 120.5, 83.9, 79.7, 67.6, 67.2, 35.6, 35.5, 29.2, 28.3, 28.2, 27.5,17.6, 13.8, 9.7;

HRMS (ES$^+$): for $C_{51}H_{72}N_4O_9PSn$ calculated 1035.4059[M + H$^+$] found 1035.4038 [M + H$^+$].

General procedure for radiolabeling

A solution of Iodo-gen (1,3,4,6-tetrachloro-3R,6R-diphenylglycouril) was prepared by concentrating the oxidant in acetonitrile (1 mg/mL). To an Eppendorf vial was added a solution of the trialkylstannyl precursor (**21**) in 5% glacial acetic acid in acetonitrile (93 μL, 5 mg/mL), and aqueous sodium [^{125}I] iodide (7μL, 12.6 MBq) which was obtained from a 0.1M NaOH solution. The reaction mixture was allowed to stand for 6 min with occasional swirling then quenched with aqueous sodium metabisulfite (100 μL, 0.01 mol/L). The reaction mixture was concentrated down to remove excess acetonitrile under a stream of air and then loaded onto a silica gel column that had been conditioned with hexanes (10 mL). The cartridge was eluted with a gradient of 100- 60% hexanes: ether. The respective activities of the collected fractions were measured using a dose calibrator. HPLC was used for assessing the purity. The desired compound (**22**) eluted with 40:60 ether: hexane. The fractions which contained radioactivity were concentrated using a stream of air. TFA (2 mL) was added and the reaction mixture was left to stand

for 4 hr. The excess of TFA was removed by purging the vessel with air and the desired product (**11**) was isolated in 42% RCY (5.3 MBq).

5.4. References

(1) Sampson, N. S.; Bartlett, P. A. *Biochemistry* **1991**, *30*, 2255.
(2) Mucha, A.; Kafarski, P.; Berlicki, Ł. *J. Med. Chem.* **2011**, *54*, 5955.
(3) Joossens, J.; Van der Veken, P.; Lambeir, A. M.; Augustyns, K.; Haemers, A. *J. Med. Chem.* **2004**, *47*, 2411.
(4) Joossens, J.; Ali, O. M.; El-Sayed, I.; Surpateanu, G.; Van der Veken, P.; Lambeir, A.-M.; Setyono-Han, B.; Foekens, J. A.; Schneider, A.; Schmalix, W.; Haemers, A.; Augustyns, K. *J. Med. Chem.* **2007**, *50*, 6638.
(5) Sieńczyk, M.; Oleksyszyn, J. *Bioorg. Med. Chem. Lett* **2006**, *16*, 2886.
(6) Augustyns, K.; . Joossens, J., Lambeir, A. M., MESSAGIE, J., Van, D. V. P., Eds.; Google Patents: 2012.
(7) Ides, J.; Thomae, D.; wyffels, L.; Vangestel, C.; Messagie, J.; Joossens, J.; Lardon, F.; Van der Veken, P.; Augustyns, K.; Stroobants, S.; Staelens, S. *Nucl. Med. Biol.* **2014**, *41*, 477.
(8) James, M. L.; Gambhir, S. S. *Physiol Rev.* **2012**, *92*, 897.
(9) Wild, D.; Frischknecht, M.; Zhang, H.; Morgenstern, A.; Bruchertseifer, F.; Boisclair, J.; Provencher-Bolliger, A.; Reubi, J. C.; Maecke, H. R. *Cancer Res.* **2011**, *71*, 1009.
(10) Ulisse, S.; Baldini, E.; Sorrenti, S.; D'Armiento, M. *Curr. Cancer Drug Targets* **2009**, *9*, 32.
(11) Harris, L.; Fritsche, H.; Mennel, R.; Norton, L.; Ravdin, P.; Taube, S.; Somerfield, M. R.; Hayes, D. F.; Bast, R. C., Jr. *J. Clin. Oncol.* **2007**, *25*, 5287.
(12) Ranson, M.; Berghofer, P.; Vine, K. L.; Greguric, I.; Shepherd, R.; Katsifis, A. *Nucl. Med. Biol.* **2012**, *39*, 833.
(13) Hsiao, J. K.; Law, B.; Weissleder, R.; Tung, C. H. *J. Biomed. Opt.* **2006**, *11*, 34013.
(14) Rockway, T. W. *Exp. Opin. Med. Diagnost.* **2003**, *13*, 773.
(15) Kettner, C.; Shaw, E. *Methods Enzymol* **1981**, *80 Pt C*, 826.
(16) Schweinitz, A.; Steinmetzer, T.; Banke, I. J.; Arlt, M. J. E.; Stürzebecher, A.; Schuster, O.; Geissler, A.; Giersiefen, H.; Zeslawska, E.; Jacob, U.; Krüger, A.; Stürzebecher, J. *J. Biol. Chem.* **2004**, *279*, 33613.
(17) Murata, M.; Watanabe, S.; Masuda, Y. *Synlett* **2000**, *2000*, 1043.
(18) Helenius, M. A.; Savinainen, K. J.; Bova, G. S.; Visakorpi, T. *BJU international* **2006**, *97*, 404.

(19) Hang, M. T. N.; Ranson, M.; Saunders, D. N.; Liang, X. M.; Bunn, C. L.; Baker, M. S. *Fibrinol Proteol* **1998**, *12*, 145.

Chapter 6 - Development of a ^{125}I-labeled tetrazine for radioiodination via rapid inverse-electron-demand Diels-Alder ligation

6.1. Overview

Given the poor tumour uptake of the uPA probes and a poor target to nontarget ratio reported here a pre targeting approach was explored. Maximizing background is key to developing effective imaging probes.

For pre-targeting approaches[1-3] several biorthogonal ligations has been shown to enhance tumour to blood ratios and overall tumour uptake. In principle[1] an unlabeled bifunctional construct with affinity for the tumour and for a radiolabeled compound is administered as the first component. After the construct has cleared from the circulation and non-targeted tissues the radiolabeled components are administered. Irreversible chemoselective coupling reactions such as the Staudinger ligation[4] and azide-alkyne cycloadditions[5] have been used for biorthogonal ligations but their poor kinetics ($k < 1$ $M^{-1}sec^{-1}$) can limit their applications.[6] A rapid inverse-electron-demand Diels–Alder reaction between electron-deficient tetrazines (Tz) and strained trans-cyclooctene (TCO) has been reported to be more effective.[7] Tetrazines react through a [4+2] Diels-Alder cycloaddition with various dienophiles (norbornene, cyclooctyne and *trans*-cyclooctene) and the adduct which is formed undergoes an irreversible retro Diels-Alder step, with release of nitrogen[7]. (Figure 6.1.)

Silvia Albu synthesized all the compounds and performed the radiolabelling procedures. Subsequent experiments were performed by Salma Al-Karmi and Dr.Ramesh Patel

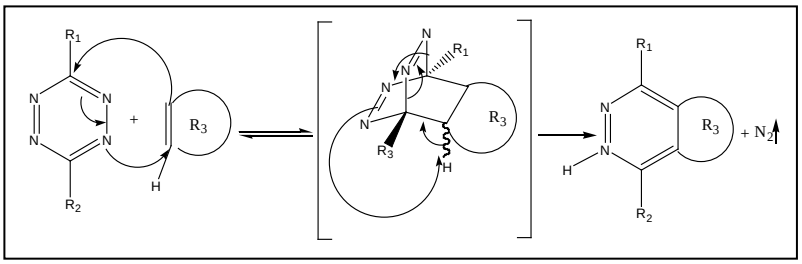

Figure 6.1. The mechanism of The Diels-Alder-Reaction with inverse electron demand.[7]

The fast kinetics ($k_2 \approx 2000\ M^{-1}s^{-1}$) of the reaction will allow for in *vivo* coupling at low concentration. The stability of tetrazine- trans-cyclooctene reaction towards the amino, thiols and hydroxide nucleophiles that are present in biological system, the compatibility with water media and the catalyst free conditions makes this reaction suitable for in *vivo* applications.[8] Consequently, this reaction has been applied used in the incorporation of ^{18}F, ^{111}In ^{64}Cu ^{11}C and ^{177}Lu. A successful in *vivo* labeling of antibody using an In^{111} DOTA derivative was reported by Robillard.[3] The antibody TCO was allowed to clear for 24 h from circulation and then the indium-111 labeled tetrazine was injected. Imaging and analysis were performed three hours p.i. of the indium-111 labeled tetrazine and tumor to muscle ratio of 13 was reported.

In order to reduce the background radiation and to improve the tumour uptake we decided to explore and extend the pretargeted approach discussed above. In the next chapter we describe a generic platform for radioiodination of tetrazine and its reaction with TCO.

Rather than using existing tetrazine, an iodinated tetrazine was developed for use with uPA targeted probes. The following work is reported as a draft manuscript which is focused on the synthesis labelling and reactivity of the tetrazine.

6.2. Development of a ^{125I}-labeled tetrazine for radioiodination via rapid inverse-electron-demand Diels-Alder ligation

Silvia A. Albu, Salma A. Al-Karmi, Ramesh M. Patel, Alfredo Capretta and John F. Valliant

Department of Chemistry and Chemical Biology, McMaster University, Hamilton, Ontario, Canada, L8S 4M1

6.2.1. Introduction

A new radioiodine containing tetrazine suitable for *in vitro* and *in vivo* ligation reactions using inverse electron demand Diels-Alder type reactions was developed. The synthesis employed a high-yielding oxidative destannylation reaction which concomitantly oxidized the dihydrotetrazine precursor. The product reacts quickly and efficiently with *trans*-cyclooctene and the product distribution matched standards characterized by MS and 2-D NMR.

The traditional approach for the preparation of nuclear molecular imaging and therapy probes involves the radiolabeling of a targeting vector with a suitable radionuclide prior to administration.[9] More recently, owing to the development of bioorthoganal coupling strategies, it is possible to administer the targeting vector first, allowing time for optimal

target accumulation and clearance from non-target organs, prior to administration of a labeled coupling partner.[10,11] This approach creates the opportunity to use short-half-life isotopes with macromolecular targeting vectors, can potentially reduce the dose burden for patients and has produced images with exquisite target-to-non-target ratios.[2,3,12]

One particularly attractive approach is the inverse electron demand Diels-Alder reaction involving derivatized tetrazines and *trans*-cyclooctenes (TCO's).[8,13,14] The system offers a number of advantages including biocompatibility and rapid coupling rates. Given the widespread use of radioiodine in nuclear medicine and for labeling proteins for *in vitro* screening studies[15] it was surprising to note the absence of a tetrazine-based system suitable for use with isotopes of iodine. One of the major advantages of developing radiopharmaceuticals from iodine is that agents for imaging using positron emission tomography (PET),[16,17] or single photon emission computed tomography (SPECT)[18] and for Auger[19] and β^- therapy applications[20] can be created from a single construct.

Given the commercial availability of trans-cyclooctene derivatives for tagging biovectors, which include succinimidyl carbonate functionalized cyclooct-4-enol for labeling amine containing compounds, our approach focused on the development of a convenient method to produce an iodinated tetrazine. The synthetic strategy involves a facile oxidative destannylation type reaction and a study of the product distribution where the product was evaluated through reaction with TCO in direct comparison to reactions run using cold standards. The approach was designed to be scaleable and based on methods that are commonly used to produce iodine radiopharmaceuticals for clinical use.

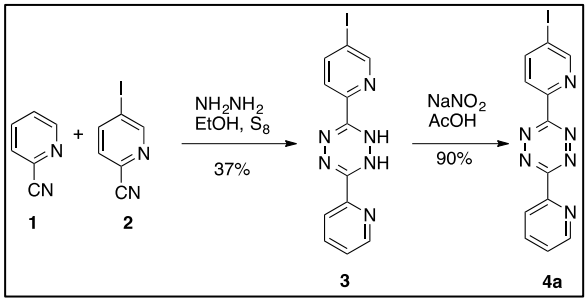

Scheme 6.1. Synthesis of I tetrazine **4a**.

An iodine containing 1,2-dihydrotetrazine (**3**, Scheme 6.1.) was prepared taking advantage of differential reaction rates between 2-cyanopyridine **1** and the iodinated pyridine **2**.[21] The highest yield of **3** (37%) was realized when a 4-fold excess of **1** was coupled with 5-iodopicolinonitrile in the presence of ethanolic hydrazine. Oxidation of **3** using $NaNO_2$ in acetic acid gave the desired tetrazine **4a** in 90% yield. This compound served as an important reference standard for the radiochemical work.

Direct production of the tin precursor from **4a** was unsuccessful and gave a mixture of products. As a result, the tin precursor **5** was prepared in 76% yield by treating **3** with hexamethyldistannane (Scheme 6.2) in the presence of palladium acetate and 1,3,5,7-tetramethyl-2,4,8-trioxa-6-phenyl-6-phospha-adamantane (PA-Ph).[22] This alternative approach is feasible as iodination reactions are done in the presence of excess oxidant, which not only promotes the substitution of tin but can also generate the desired tetrazine concomitantly. The practical advantage of this strategy is that compound **4b** was found to be stable as a solid in the freezer indefinitely.

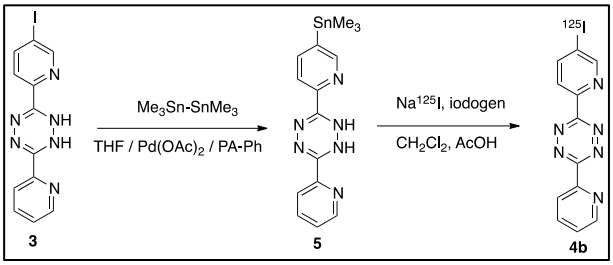

Scheme 6.2. Synthesis of ^{125}I tetrazine **4b.**

Radiolabeling was performed by treating **5** with $Na^{125}I$ and iodogen and allowing the reaction to proceed for 15 min. at room temperature. Overall compound **4b** could be synthesized and isolated by separated by semi-preparative HPLC in 80% radiochemical yield where the retention time of the product matched that for the authentic standard **4a** (Figure 6.2.). The iodotetrazine has a log P of 1.29[23] and was stable for at least 24 hours in solution. The latter feature provides the opportunity to use **4b** for multiple labeling experiments from a single batch of labeled tetrazine.

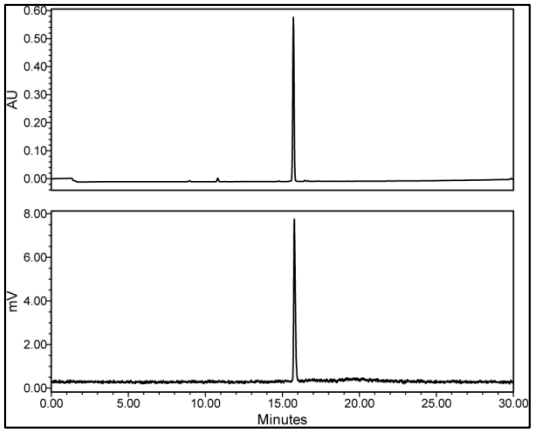

Figure 6.2. (Top) UV-HPLC-chromatogram of a mixture of **4a**/**4b** (bottom) **γ**-HPLC trace of the same reaction sample.

Initial studies of the Diels-Alder ligation were carried out with the non-radioactive tetrazine **4a** and *trans*-cyclooctene (Scheme 6.3.) in ethanol and PBS buffer[24,25]. The reaction mixture showed an immediate change from purple to colourless. Analytical HPLC analysis of the crude reaction mixture revealed three major peaks and no evidence of residual starting materials, which is consistent with literature reports on other [8]analogous ligation reactions. HRMS followed by 2-D NMR studies of the isolated products allowed us to assign the peaks observed in the HPLC. The peak eluting at *ca.* 20 min. was a mixture of **7a** and **8a** while the peak at 24 min. was the oxidized product **9a**. We were unable to isolate sufficient quantities of the early eluting product for NMR analysis as it rearranged to the other products during purification. This peak did show a m/z value comparable to **7a** and **8a** suggesting that it is a related isomer. One additional note was that the relative amounts of the different products is sensitive to the reaction conditions and times as has been observed by others. After 2 hours under the reaction conditions reported ^{1}H NMR indicated the relative ratios of **7a**:**8a** was 88:12 while after 12 hours the ratio was 65:35.

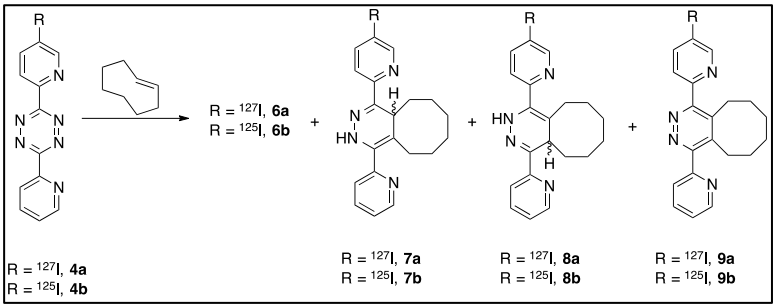

Scheme 6.3. ^{125}I tetrazine and I tetrazine reaction with cyclooctene.

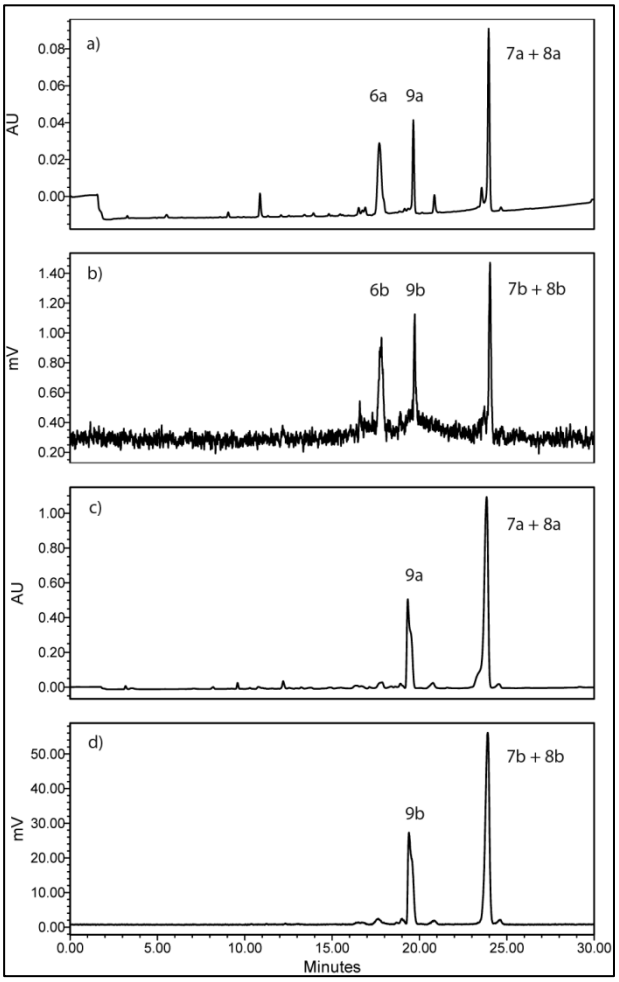

Figure 6.3. a) UV-HPLC- chromatogram of the reaction mixture containing **4a**/**4b** and transcyclooctene injected immediately after the reaction initialization b) **γ**-HPLC- traces of the same reaction mixture c) UV-HPLC chromatogram of the reaction mixture after an additional 45 min. d) **γ** –HPLC chromatogram corresponding to c).

For the radiochemical synthesis, 3.7 MBq (100 μCi) of **4b** was added to TCO where the reaction proceeded to completion quickly in ethanol and PBS buffer. To ensure consistency and generate the reference standards, a reaction with **4a** was run in parallel. The HPLC of a mixture of the cold and hot reactions run in parallel (Figure 6.3.) after 4

min. revealed 3 peaks in both the UV (panel a) and gamma (panel b) traces corresponding to the retention times for compounds **6a**/**b**, **7a**/**b** and **8a**/**b**, and **9a**/**b**. After an additional 45 min. compounds **6a** and **6b** underwent similar rearrangement to generate **7a/b**, **8a/b** and **9a/9b**. These experiments demonstrates that the tracer level work matches that of the fully characterized standards and validates the use of **4b** as a synthon for labeling TCO derived targeting vectors.

6.2.2. Conclusions

A new iodine-125 tetrazine derivative was prepared and characterized. The product is stable for 24 hours and reacts with trans-cyclooctene in a manner that is consistent with other radiolabeled tetrazines. With **4b** in hand its utility for creating new radiopharmaceuticals derived from TCO-modified vectors *in vitro* and *in vivo* will be assessed along with the development of ^{123}I, ^{124}I and ^{131}I analogues for use in SPECT, PET and radiotherapy applications.

6.3. Experimental Section

General. Unless otherwise stated, all chemicals reagents were purchased and used as received from Sigma-Aldrich without further purification. Solvents were purchased from Caledon. 1,3,5,7-Tetramethyl-2,4,8-trioxa-6-phenyl-6-phospha-adamantane (PA-Ph) was purchased from Cytec Canada (sold as CYTOP-292). Reactions were monitored using Alugram Sil G/UV$_{254}$ thin layer chromatography (TLC) plates and visualized under ultra-violet light. Column chromatography was accomplished with Silica Flash P60 purchased

from Silicycle. ^{125}I was obtained from the McMaster University Nuclear reactor as in a 0.1M NaOH solution ($Na^{125}I$).

^{1}H and ^{13}C NMR spectra were recorded on Bruker AV 700 spectrometer. ^{1}H Chemical shifts are reported in ppm relative to the residual proton signal of the NMR solvents. Coupling constants (*J*) are reported in Hertz (Hz). ^{13}C Chemical shifts are reported in ppm relative to the carbon signal of the NMR solvents. High resolution ES mass spectra were obtained on a Waters QToF Ultima Global spectrometer. Reverse phase analytical HPLC was performed using a Varian Prostar instrument equipped with a 355UV detector or a Waters 2489 HPLC equipped with a Waters 2489 UV/Vis (λ = 254 nm) and / a Bioscan glow count gamma detector (model 106). Runs were performed using HPLC grade water containing 0.08% TFA (solvent A) and acetonitrile containing 0.08 % TFA (solvent B) as eluents, a 1 mL/min flow rate and a C18 reverse phase Phenomonex column (25 x 4.60 mm, 5 micron). The desired products were eluted using a 95 to 5% gradient (Solvent A: Solvent B) over 30 min. Reactions requiring microwave irradiation were performed using a CEM Discover microwave at 150W.

Experimental Procedures

3-(5-Iodopyridin-2-yl)-6-(pyridin-2-yl)-1,2-dihydro-1,2,4,5-tetrazine (**3**)

A vial was charged with picolinonitrile (**1**, 0.21 g, 2.02 mmol), 2-cyano-5-iodopyridine (**2**, 0.11 g, 0.48 mmol) and sulfur (0.03 g, 0.93 mmol) and purged with argon. A solution of 64% hydrazine monohydrate (600 µL, 7.89 mmol) and absolute ethanol (2 mL) were added to the vial which was then sealed and heated at 125^{o}C for 2

hours behind a blast shield. The reaction mixture was cooled to room temperature, the solvent evaporated and the mixture was suspended in water (10 mL) and extracted with dichloromethane (2 x 10 mL). The organic phase was dried over anhydrous magnesium sulfate, filtered and the desired product was isolated by silica gel flash chromatography (using 20% EtOAc in hexanes as the eluent) as an orange solid (0.064 g, 37%). Compound **3** showed: m.p 158-160 ^{o}C; R_f 0.38 (20% EtOAc/hexanes); ^{1}H NMR (700 MHz, $CDCl_3$): δ 8.79 (d, *J* = 1.40 Hz, 1 H), 8.59 (s, 1H), 8.59-8.56 (m, 1H), 8.39 (s, 1H), 8.07 (dd, *J* = 1.68 Hz, 7.63 Hz, 1H), 8.04 (d, *J* = 7.98 Hz, 1H), 7.83 (dd, *J* = 0.49 Hz, 8.40 Hz, 1H), 7.76 (dt, *J* = 1.68 Hz, 7.63 Hz, 1H,), 7.36 (ddd, *J* = 0.98 Hz, 4.90 Hz, 7.42 Hz, 1H,); ^{13}C NMR (150 MHz, $CDCl_3$), 154.63, 148.52, 147.48, 146.67, 146.54, 146.23, 145.18, 136.94, 125.12, 122.92, 121.48, 95.04; HRMS (m/z-ESI^{+}) for $C_{12}H_{10}IN_6^{+}$ calculated:365.0012 found: 365.0009.

3-(5-Iodopyridin-2-yl)-6-(pyridin-2-yl)-1,2,4,5-tetrazine (4a)

Compound **3** (0.054 g, 0.15 mmol) was dissolved in glacial acetic acid (2 mL) and the solution was cooled to 0^{o}C. A solution of sodium nitrite (0.068 g, 0.98 mmol) in water (2 mL) was added dropwise resulting in a colour change from orange to purple. The mixture was stirred for an additional 10 min. at room temperature. The pH was adjusted to 11 via the addition of aqueous saturated sodium bicarbonate (10 mL) and the solution extracted with dichloromethane (2 x 15 mL). The organic layers were combines and dried over anhydrous magnesium sulphate and the solvent removed by rotary evaporation. The desired product was isolated by silica gel chromatography (using 65% EtOAc in hexanes as the eluent) and concentrated to afford a bright purple solid (0.049 g, 90%).

Compound **4a** showed: m.p. 223-225 ^{o}C; R_f = 0.52 (5% MeOH/DCM); ^{1}H NMR (700 MHz, $CDCl_3$): δ 9.19 (dd, *J* = 0.35 Hz, 1.89 Hz, 1H,), 9.01-8.97 (m, 1H,) 8.75 (d, *J* = 7.91 Hz, 1H,), 8.52 (dd, *J* = 0.56 Hz, 8.26 Hz, 1H,), 8.35 (dd, *J* = 2.10 Hz, 8.26 Hz, 1H), 8.02 (dt, *J* = 1.68 Hz, 7.70 Hz, 1H), 7.59 (ddd, *J* = 1.05 Hz, 4.69 Hz, 7.56 Hz, 1 H); ^{13}C NMR (150 MHz, $CDCl_3$): δ 164.03, 163.92, 157.34, 151.25, 150.10, 148.97, 146.13, 137.66, 126.84, 125.79, 124.75, 98.32; HRMS (m/z-ESI^{+}) for $C_{12}H_8IN_6^{+}$ calculated: 362.9855 found: 362.9856.

3-(Pyridin-2-yl)-6-(5-(trimethylstannyl)pyridin-2-yl)-1,2-dihydro-1,2,4,5-tetrazine (5)

A solution of 1,1,1,2,2,2-hexamethyldistannane (0.085 g, 0.26 mmol) in dry THF (1 mL) was added to a microwave vial which was evacuated and purged with argon. 1,3,5,7-Tetramethyl-2,4,8-trioxa-(2,4-dimethoxyphenyl)-6-phosphaadamantane (PA-Ph, 4.4 mg, 0.015 mmol) and palladium acetate (1.60 mg, 7.13 μmol) were added to the reaction vessel which was sealed and stirred at room temperature for 5 min. A solution of **3** (0.049 g 0.13 mmol) in THF (0.5 mL) was added under argon. The reaction vessel was heated in the microwave for 30 min. at 70^{o}C. The vessel was cooled to room temperature and the solution treated with saturated aqueous potassium fluoride (1 mL) to quench the reaction. The mixture was extracted with dichloromethane (2 x 10 mL). The organic layers were combine, dried over anhydrous magnesium sulfate, filtered and the solvent removed by rotary evaporation. The desired product was obtained by silica gel chromatography (using 90% ether in pentane as the eluent) and concentrated to afford a yellow solid (0.039 g, 76%). Compound **5** showed: m.p. 73-75 ^{o}C; R_f = 0.50 (50% EtOAc/hexanes); ^{1}H NMR

(700 MHz, $CDCl_3$):δ 8.56-8.60 (m, 2H), 8.57 (s, 1H), 8.54 (s, 1H), 8.05 (d, *J* = 7.98 Hz, 1H), 7.97 (dd, *J* = 0.91 Hz, 7.70 Hz, 1H), 7.84 (dd, *J* = 1.47 Hz, *J* = 7.70 Hz, 1H), 7.75 (dt, *J* = 1.68 Hz, 7.70 Hz, 1H), 7.34 (ddd, *J* = 1.05 Hz, 4.90 Hz, 7.42, 1H), 0.36 (s, 9H); ^{13}C NMR (150 MHz, $CDCl_3$): δ 154.36 (sat), 154.25, 154.12 (sat), 148.53, 147.71, 147.15, 147.12, 146.83, 144.33 (sat), 144.25, 144.16 (sat), 139.79, 136.85, 124.97, 121.42, 121.11 (sat), 121.02, 120.92 (sat), - 8.31 (sat), -8.35 (sat), -9.33, -10.32 (sat), -10.36 (sat); HRMS (m/z-ESI$^+$) for $C_{15}H_{19}N_6Sn^+$ calculated: 397.0532 Found: 397.0544

Tetrazine-*trans* Cyclooctene Ligation Procedure

Tetrazine **4a** (0.014 g, 0.04 mmol) was dissolved in 5% ethanol in 0.05 M PBS buffer (2 mL, pH 7.4) and added to a vial containing *trans*-cyclooctene (8.8 mg, 0.088 mmol) which brought about a colour change (from purple to colourless). The solution was extracted with ethyl acetate (2 x 5 mL) and the organic solvents combined and removed by rotary evaporation. The desired products were obtained by silica gel chromatography (using 10-15% pentane in EtOAc as the eleunt) and concentrated to afford one sample containing a mixture of isomers **7a** and **8a** and another containing the oxidized product **9a**.

4-(5-Iodopyridin-2-yl)-1-(pyridin-2-yl)-2,4a,5,6,7,8,9,10 octahydrocycloocta[d]pyridazine (7a) showed: m.p 92-97 ^oC; R_f = 0.45 (20% EtOAc/hexanes); ^1H NMR (700 MHz, $CDCl_3$): δ 8.89 (s, 0.88H), 8.88 (d, *J* = 2.03 Hz, 0.12H), 8.80 (d, J = 1.47 Hz, 0.88 H), 8.73(s, 0.1H), 8.73 (s, 0.12H), 8.67-8.62 (m, 0.88H), 8.58-8.55 (m, 0.12 H), 8.17 (dd, J = 2.10, 8.26, 0.12 H), 8.05 (dd, *J* = 2.10 Hz, *J*

= 8.47 Hz, 0.88 H), 8.05-8.01 (m, 0.12 H), 7.87 (dd, *J* = 0.49 Hz, 8.47 Hz, 0.88 H), 7.84 (dt, *J* = 1.82 Hz, 7.70 Hz, 0.88 H), 7.73 (dt, *J* = 1.61 Hz, 7.74 Hz, 0.12 H) , 7.59 (d, *J*= 8.75, 0.88 H), 7.41 (d, *J* = 8.40 Hz, 0.12 H), 7.34, (ddd, *J* = 0.91 Hz, 4.83 Hz, 7.49 Hz, 0.88 H), 7.27 (ddd *J* = 0.84 Hz, 7.70 Hz, 5.11 Hz,7.28 Hz, 0.12 H), 4.43- 4.38 (m, 0.12 H), 4.26-4.36 (m, 0.88H), 2.84 (ddd, *J* = 2.59 Hz, 8.89 Hz, 15.26 Hz, 0.88 H), 2.79 (ddd, *J* = 2.73 Hz, 9.03 Hz, 15.26 Hz, 0.12 H), 2.10-2.02 (m, 1H), 2.00-1.97 (m, 1H), 1.93-1.87 (m, 1H), 1.78-1.64 (m, 5H), 1.51-1.40 (m, 3H); ^{13}C NMR (150 MHz, CDCN): δ 155.52, 154.61, 153.17, 150.48, 145.43, 142.63, 137.82, 134.94, 125.27, 124.02, 123.38, 112.52, 92.62, 35.51, 31.92, 29.82, 28.23, 27.73, 25.35, 23.25; HRMS (m/z-ESI$^+$) for $C_{20}H_{22}IN_4^+$ calculated: 445.0889 found: 445.0904.

1-(5-iodopyridin-2-yl)-4-(pyridin-2-yl)-2,4a,5,6,7,8,9,10 octahydrocycloocta[d]pyridazine (8a) showed: m.p 92-97 ^{o}C; R_f = 0.45 (20% EtOAc/hexanes); ^{1}H NMR (700 MHz, CDCN) : δ 8.90 (s, 0.65H), 8.87 (d, *J* = 1.47 Hz, 0.35H), 8.79 (d, J = 1.47 Hz, 0.65 H), 8.74 (s, 0.35H), 8.67-8.60 (m, 0.65 H), 8.58-8.54 (m, 0.35 H), 8.16 (dd, *J* = 2.17 Hz, 8.33 Hz, 0.35H), 8.04 (dd, *J* = 2.17 Hz, 8.47 Hz, 0.65H), 8.03 (d, *J* = 7.91 Hz, 0.35 H), 7.86 (dd, *J* = 0.49 Hz, 8.54, 0.65 H), 7.84 (dt, *J* = 1.75 Hz, 0.65 H), 7.40 (dd, *J* = 0.28 Hz, 8.26 Hz, 0.35 H), 7.33 (ddd, *J* = 0.91 Hz, 4.83 Hz, 7.49 Hz, 0.65H), 7.26 (ddd, *J* = 1.05 Hz, 4.90 Hz, 7.35 Hz, 0.35H), 4.44-4.36 (m, 0.35 H), 4.34-4.27 (m, 0.65 H), 2.83 (ddd, *J* = 2.59 Hz, 8.89 Hz, 15.19 Hz, 0.65 H), 2.79 (ddd, *J* = 2.73 Hz, 8.96 Hz, 15.30 Hz, 0.35 H), 2.11-2.02 (m, 1H), 2.02-1.95 (m, 1H), 1.93-1.85 (m, 1H), 1.79-1.61 (m, 5H), 1.51-1.40 (m, 3H); ^{13}C NMR (150 MHz, CDCN): δ 156.37, 155.51, 155.40, 154.60, 153.17, 152.24, 150.47, 149.64, 146.05, 145.43,

143.65, 142.60, 137.82, 137.23, 134.93, 134.26, 126.88, 125.27, 124.02, 123.78, 123.39, 121.57, 113.49, 112.52, 92.63, 35.90, 35.50, 31.95, 31.92, 29.82, 29.68, 28.24, 28.22, 27.72, 25.34, 25.32, 23.35, 23.24; HRMS (m/z-ESI$^+$) for $C_{20}H_{22}IN_4^+$ calculated: 445.0889 found: 445.0904

1-(5-Iodopyridin-2-yl)-4-(pyridin-2-yl)-5,6,7,8,9,10 hexahydrocycloocta[d]pyridazine (9a) showed: m.p 105-110^{o}C; R_f = 0.68 (EtOAc); ^{1}H NMR (700 MHz, CDCN): δ 8.96 (d, *J* = 2.12 Hz, 1H), 8.74-8.68 (m, 1H) 8.31 (dd, *J* = 2.17 Hz, 8.26 Hz, 1H), 7.95 (dt, *J* = 1.82 Hz, 7.77 Hz, 1H), 7.79 (d, *J* = 7.77 Hz, 1H), 7.67 (d, *J* = 8.19 Hz, 1H), 7.47 (ddd, *J* = 1.05 Hz, 4.83 Hz, 7.77 Hz, 1H), 3.01-2.94 (m, 4 H), 1.77-1.68 (m, 4H), 1.45-1.38 (m, 4H); ^{13}C NMR (150 MHz, CD_3CN): δ 160.44, 159.34, 158.02, 156.99, 155.58, 149.65, 146.35, 141.93, 141.87, 137.93, 127.60, 125.70, 124.50, 94.22, 31.17, 31.06, 27.30, 27.23, 26.75, 26.72; HRMS (m/z-ESI$^+$) for $C_{20}H_{19}IN_4^+$ calculated: 443.0733 found: 443.0745

Radiolabeling procedure

A 5 mg/mL solution (5 µL) containing iodogen in 5% acetic acid/ acetonitrile was added to a vial containing **5** (10 µL from a 10 mg/mL in acetonitrile). The mixture was combined with aqueous [^{125}I]NaI (7 µL, 12.6 MBq) which was obtained from a 0.1M NaOH solution. The mixture was agitated for several seconds by hand and allowed to stand for 5 min. To this was added an additional aliquot (28 µL) of the iodogen solution and the solution left to stand for a further 15 min. The reaction mixture was quenched with aqueous sodium metabisulfite (100 µL, 0.1 M) and extracted with dichloromethane

(100 µL). The organic solvent was separated and evaporated by purging the vessel with nitrogen. The resulting residue was dissolved in ethanol or acetonitrile for analysis and purification by HPLC. The desired product was isolated in 80% RCY (10 MBq, 270 µCi).

Radioactive tetrazine ligation procedure

3.7 MBq (100 µCi) of **4b** was dissolved in a mixture of 95% ethanol (5 µL) and PBS buffer (85 µL, pH 7.4) in a micro-centrifuge tube. A freshly prepared solution of *trans*-cyclooctene (10 µL) in ethanol (2 µM) was added to the vial and the mixture agitated by hand for several seconds. The mixture was immediately analyzed by HPLC initially giving rise to three distinct peaks. After approximately 20 min. HPLC analysis showed two major peaks corresponding to a mixture of isomers **7b** and **8b** and a peak associated with **9b**.

Specific Activity

A 0.37 MBq solution of **4b** in 100 µL acetonitrile: water (1:1) was prepared and the entire solution analyzed by HPLC. The mass was determined using a linear calibration curve derived from 50 µL injections of various concentrations of **4a** ranging from 0.00- 0.49 mM. The specific activity was calculated using the linear regression function of the calibration curve and was found to be 7.5 µCi/mmol.

log P determination

A 100 µL of solution of **4b** (0.33 MBq) in 20 mM phosphate buffer (pH 7.4) was added to a mixture of n-octanol and phosphate buffer (100 µL of each). The mixture was

vortexed for 30 min. and centrifuged at 6000 rpm for 10 min. The organic and aqueous phases were separated and 20 µL of each phase were pipetted into 12 x75 mm RIA tubes. The counts per minute were determined using a Wallac Wizard 1470 automatic γ counter. The experiment was performed in triplicate giving an average log P of 1.29 ± 0.05.

6.4. References:

(1) Boerman, O. C.; van Schaijk, F. G.; Oyen, W. J.; Corstens, F. H. *J. Nucl. Med.* **2003**, *44*, 400.

(2) Rossin, R.; Lappchen, T.; van den Bosch, S. M.; Laforest, R.; Robillard, M. S. *J. Nucl. Med.:* **2013**, *54*, 1989.

(3) Rossin, R.; Verkerk, P. R.; van den Bosch, S. M.; Vulders, R. C.; Verel, I.; Lub, J.; Robillard, M. S. *Angew. Chem. Int. Ed. (English),* **2010**, *49*, 3375.

(4) Saxon, E.; Bertozzi, C. R. *Science* **2000**, *287*, 2007.

(5) Rostovtsev, V. V.; Green, L. G.; Fokin, V. V.; Sharpless, K. B. *Angew. Chem. Int. Ed. (English),***2002**, *41*, 2596.

(6) Kolb, H. C.; Finn, M. G.; Sharpless, K. B. *Angew. Chem. Int. Ed. (English),* **2001**, *40*, 2004.

(7) Wiessler, M.; Waldeck, W.; Kliem, C.; Pipkorn, R.; Braun, K. *Int. J. Med. Sci.* **2009**, *7*, 19.

(8) Devaraj, N. K.; Weissleder, R. *Acc. Chem. Res.* **2011**, *44*, 816.

(9) Kassis, A. I.; Adelstein, S. J. In *Handbook of Radiopharmaceuticals*; John Wiley & Sons, Ltd: 2005, p 767.

(10) Jewett, J. C.; Bertozzi, C. R. *Chem. Soc. Rev.* **2010**, *39*, 1272.

(11) Bertozzi, C. R. *Acc Chem Res* **2011**, *44*, 651.

(12) Zeglis, B. M.; Mohindra, P.; Weissmann, G. I.; Divilov, V.; Hilderbrand, S. A.; Weissleder, R.; Lewis, J. S. *Bioconjugate. Chem.* **2011**, *22*, 2048.

(13) Li, Z.; Cai, H.; Hassink, M.; Blackman, M. L.; Brown, R. C. D.; Conti, P. S.; Fox, J. M. *Chem. Commun.* **2010**, *46*, 8043.

(14) Herth, M. M.; Andersen, V. L.; Lehel, S.; Madsen, J.; Knudsen, G. M.; Kristensen, J. L. *Chem. Commun.***2013**, *49*, 3805.

(15) Adam, M. J.; Wilbur, D. S. *Chem. Soc. Rev.* **2005**, *34*, 153.

(16) Koehler, L.; Gagnon, K.; McQuarrie, S.; Wuest, F. *Molecules (Basel, Switzerland)* **2010**, *15*, 2686.

(17) Belov, V. V.; Bonab, A. A.; Fischman, A. J.; Heartlein, M.; Calias, P.; Papisov, M. I. *Mol. Pharm.* **2011**, *8*, 736.

(18) Bourguignon, M. H.; Pauwels, E. K.; Loc'h, C.; Maziere, B. *Eur. J. Nucl. Med. Mol. Imaging* **1997**, *24*, 331.
(19) Bodei, L.; Kassis, A. I.; Adelstein, S. J.; Mariani, G. *Cancer Biother. Radiopharm.* **2003**, *18*, 861.
(20) Wyszomirska, A. *Nucl Med Rev Cent East Eur* . **2012**, *15*, 120.
(21) Abdel, N. O.; Kira, M. A.; Tolba, M. N. *Tetrahedron Lett.* **1968**, *9*, 3871.
(22) McIntee, J. W.; Sundararajan, C.; Donovan, A. C.; Kovacs, M. S.; Capretta, A.; Valliant, J. F. *J. Org. Chem.* **2008**, *73*, 8236.
(23) Wilson, A. A.; Jin, L.; Garcia, A.; DaSilva, J. N.; Houle, S. *Appl. Radia.t Isot* **.2001**, *54*, 203.
(24) Karver, M. R.; Weissleder, R.; Hilderbrand, S. A. *Bioconjugate Chem.* **2011**, *22*, 2263.
(25) Blackman, M. L.; Royzen, M.; Fox, J. M. *J. Am. Chem. Soc.* **2008**, *130*, 13518.

Chapter 7 – Conclusions and Future work

The understanding of the biological and molecular events will impact the development of more efficient drugs and provide more precise ways to monitor the disease progression. Early detection of both primary tumors and metastatic potential is a key goal on managing cancer. The role of protease is not limited to cancer they are also involved in diseases such as arthritis, atherosclerosis, and myocardial infarction.[1] In recent years efforts were under way on the development of protease imaging probes with optimal in *vivo* properties.[1] Many of these probes although are target specific they have a low target to background ratios.[2] Ultimately generation of probes with desirable pharmacokinetical properties and in *vivo* stability will be amenable for clinical settings and will provide data sets with higher sensitivity and specificity. Innovations in chemistry lead to development of new fast bio orthogonal reactions that found applications in the pretargeted strategy.[3] Such probes once optimized may not only be used for several targets but may also result in improved efficiencies with regard to tumor to background ratios.

Over the course of this study, three classes of reversible and one class of irreversible uPA inhibitors have been modified and investigated for their applicability as molecular imaging agents. In addition, a new radioiodinated tetrazine has been synthesized and evaluated as a potential synthon for use in pre-targeting imaging strategies.

Seven new guanidinyl dipeptides (Scheme **4.1.**, Chapter **4**) were synthesized and tested for their binding affinities towards uPA. Iodinated peptides **1b**, **1e** and **1g** were found to have high binding affinities (in the low nanomolar range). The position of the iodine in the ring was shown to affect the binding affinities towards uPA. The optimized synthetic strategy employed in preparing the naphthamidine class generated additional iodinated derivatives (Figure **3.26.**, Chapter **3**) that have not yet been evaluated. In Chapter **5**, irreversible phosphonates were synthesized, radiolabelled and tested in an uPA bioassay and quantitative biodistribution studies performed. The preliminary study demonstrates the superiority of ^{125}I phosphonates over existing uPA probes in terms of tumour-to-blood ratio.

The preparation of the first ^{125}I-labelled tetrazine (Chapter **6**) led to the development and evaluation of a new prosthetic group that can be used in a pre-targeting strategy (as opposed to conventional active targeting methods). The newly created synton reacts with *trans*-octene rapidly in high yields. The one-pot oxidation-radiolabeling procedure represents an efficient method for the preparation of iodinated tetrazine using a convergent synthetic method. The reported compound represents a new and highly versatile reagent in that it can be used to develop novel imaging probes and for in vitro screening of new targeting vectors.

7.1. Future work and preliminary results

There is a need to exploit the general utility of the tetrazine derivative including using it to develop an uPA/uPAR probe. This should begin by studying the properties of the radioiodinated tetrazine (Chapter **6**) *in vivo* in order to characterize the pharmacokinetics and to assess binding to non-target organs. One potential concern is that the compound is too hydrophobic. Consequently future work should focus on preparing variants containing polar groups such as carboxylic acids, alcohols or on introduction of a polyethelyene glycol substituent. More specifically the tetrazine derivative (**3b**) bearing an amine can be further derivatized with polar groups such as succinic anhydride, for example, which would generate the hydrophilic construct (**4b**).

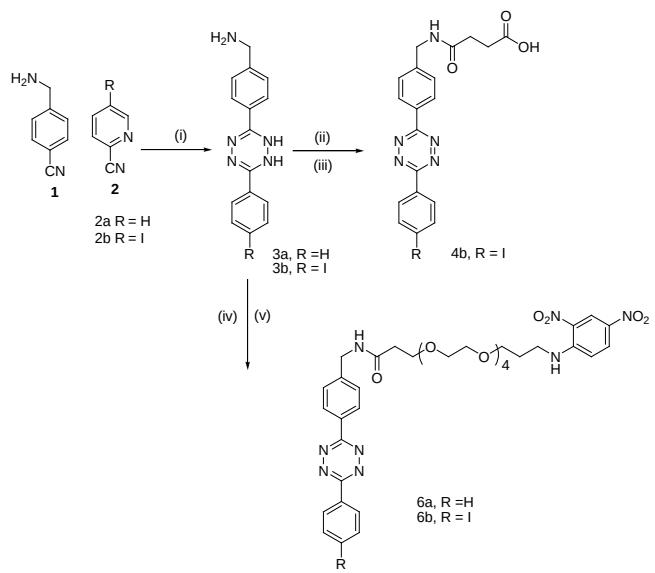

Scheme 7.1. Synthesis of modified tetrazines. Reagents: (i) Hydrazine , S_8 EtOH; (ii);$NaNO_2$,AcOH, (iii) succinic anhydride, ACN (iv) compound (**5)** PEG_8-DNP, THF, DIPEA, PyBop,(v) $NaNO_2$,AcOH.

Further derivatization of the tetrazine core with a 2, 4-dinitrophenyl (DNP) group (**5**) could potentially be used as a bioorthogonal reagent for immunomediated destruction of cancer cells. Jakobsche[4] and coworkers reported that endogenous and exogenous antibodies can be recruited to destroy cancer cells through presence of (DNP) antigens. A DNP derivative of the tetrazine would allow for localization of DNP groups through coupling to TCO modified targeting vectors. In the case of uPA/uPAR this could include TCO modified inhibitors like those presented or antibodies. In this way an antibody-dependent immune response can be directed against uPAR expressing cancer cells. Based on these results, it was envisioned that adding an ^{131}I could potentially have a cumulative and efficient effect on destroying cancer cells.

The tetrazine construct or its precursor (**8**) could also be used generate a new class of turn-on fluorophores. Turn on probes are described by the ability of the fluorophore to

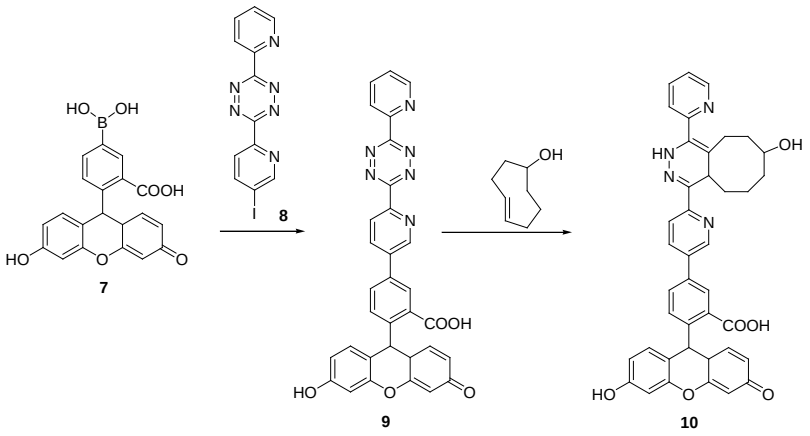

Scheme 7.2. Suzuki reaction using the iodotetrazine precursor and fluorescein.

have an increase emission upon reaction with its biorthogonal complement part.[5] One potential approach is to couple compound (**8**) to a fluorescein modified scaffold, since

recent publications suggest that directly connected tetrazine to a fluorophore[6] such as BODIPY[5] and coumarine[7] enables efficient energy transfer and quenching. Subsequent studies would involve evaluating fluorogenic activation upon reaction with trans cycloctyne in *vitro* and in *vivo*. Preliminary studies undertaken during this research showed (Scheme **7.2.**) that the iodotetrazine or its precursor could be employed in Suzuki type reaction although the product was never isolated and further purification was required.

7.2 Experimental

Compound (**6b**)

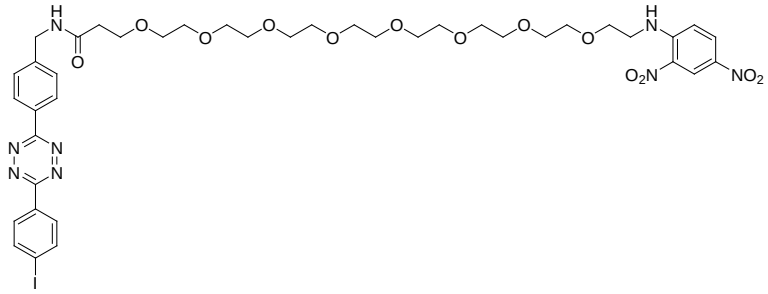

A vial was charged with 4-aminomethylbenzonitrile (**1**, 0.26 g, 2.0 mmol), 2-cyano-5-iodopyridine (**2**, 0.11 g, 0.48 mmol) and sulfur (0.03 g, 0.93 mmol) and purged with argon. A solution of 64% hydrazine monohydrate (600 µL, 7.89 mmol) and absolute ethanol (2 mL) were added to the vial which was then sealed and heated at 125^{o}C for 2 hours behind a blast shield. The reaction mixture was cooled to room temperature and suspended in water (10 mL) upon which a precipitates was formed. The desired product was isolated by filtration, dried in the vacuum and used in the next step without further purification. Compound **3b (**0.95 g, 0.25 mmol) was coupled in THF (5ml) with

compound (**5)** PEG_8-DNP (0.151g, 0.25mmol) in the presence of DIPEA (64mg, 0.5mmol) and PyBop(130mg, 0.25mmol). The reaction mixture was stirred overnight at r.t , suspended in water (10 mL) and extracted with DCM (3x50ml).The organic phase was concentrated in *vacuo* and then dissolved in glacial acetic acid (2 mL). The reaction was cooled to 0^oC and a solution of sodium nitrite (0.068 g, 0.98 mmol) in water (2 mL) was added dropwise resulting in a colour change from orange to purple. The mixture was stirred for an additional 10 min. at room temperature. The pH was adjusted to 11 via the addition of aqueous saturated sodium bicarbonate (10 mL and the solution extracted with dichloromethane (2 x 50 mL) and ethyl acetate (2 x 50 mL).The desired product was isolated on Combi -Flash reverse phase C18 colum chromatography (using gradient AcCN in water as the eluent) and concentrated to afford a bright purple solid (0.029 g, 12% overall yield). Compound **6b** showed: m.p. ^{1}H NMR (700 MHz, $CDCl_3$): δ 9.14 (s, 1H), 9.11 (d, *J* = 2.8 Hz, 1H), 8.61 (d, *J* = 8.4 Hz, 1H), 8.44 (d, *J* = 8.4 Hz, 1H), 8.32 (dd, *J* = 8.4 Hz, *J* = 2.1 Hz, 1H), 8.23 (dd, *J* = 9.1 Hz, *J* = 2.8 Hz, 1H), 7.55 (d, *J* = 8.4 Hz, 1H), 6.94 (d, *J* = 8.4 Hz, 1H), 4.58 (s, 1H), 3.80-3.78 (m, 4H), 3.68-3.54 (m, 28H), 2.58 (t, *J* = 4.9 Hz, 2H);^{13}C NMR (150 MHz, $CDCl_3$): δ 172.3, 164.4, 163.4, 157.1, 149.1, 148.4, 146.1, 144.7, 136.2, 130.4, 128.8, 128.5, 125.2, 124.4, 114.2, 97.8, 70.8, 70.7, 70.6, 70.5, 70.4, 68.7, 67.4, 50.0, 49.9, 49.8, 49.7, 43.3, 43.0, 36.9;

HRMS (m/z-ESI$^+$) for $C_{40}H_{51}IN_8O_{13}^+$ calculated: 979.7849 found: 979.7856.

7.3. References

(1) Yang, Y.; Hong, H.; Zhang, Y.; Cai, W. *Cancer growth and metastasis* **2009**, *2*, 13.

(2) Kobayashi, H.; Longmire, M. R.; Ogawa, M.; Choyke, P. L. *Chem. Soc. Rev.* **2011**, *40*, 4626.

(3) Blackman, M. L.; Royzen, M.; Fox, J. M. *J. Am. Chem. Soc.* **2008**, *130*, 13518.

(4) Jakobsche, C. E.; McEnaney, P. J.; Zhang, A. X.; Spiegel, D. A. *ACS Chem. Biol.* **2011**, *7*, 316.

(5) Carlson, J. C. T.; Meimetis, L. G.; Hilderbrand, S. A.; Weissleder, R. *Angew. Chem. Int. Ed. (English)* **2013**, *52*, 6917.

(6) Wu, H.; Yang, J.; Šečkutė, J.; Devaraj, N. K. *Angew. Chem. Int. Ed. (English)* **2014**, *126*, 5915.

(7) Meimetis, L. G.; Carlson, J. C.; Giedt, R. J.; Kohler, R. H.; Weissleder, R. *Angew. Chem. Int. Ed. (English)* **2014**, *53*, 7531.